Design and testing of an integrated catalytic membrane reactor for deoxygenating water using hydrogen for down-hole injection and process applications.

ORAKWE, I.R.

2018

Design and Testing of an Integrated Catalytic Membrane Reactor for Deoxygenating Water using Hydrogen for Down-hole Injection and Process Applications

Ifeyinwa Regina Orakwe

A thesis submitted in partial fulfilment of the requirements of the Robert Gordon University for the degree of Doctor of Philosophy

This research programme was carried out in collaboration with the Centre for Process Integration and Membrane Technology

October 2018

ABSTRACT

Water obtained from the sea contains dissolved oxygen (DO) and is considered to be undesirable for use in down-hole water injection or other process applications. The presence of DO leads to corrosion and other related problems and hence the need for its removal. Various methods are in place for sea water deoxygenation, but with requirements of floating facilities to meet smaller footprint, compact deoxygenating methods have been proposed. Presently, Minox and Seaject processes are the most compact deoxygenating methods in place, but research is still ongoing on devising even more compact means.

One attractive method for water deoxygenation is the reaction of hydrogen and dissolved oxygen over a wider highly catalytic dispersed surface area, and this can be seen to be achievable by employing membrane technology. Membrane technology is seen to provide compactness and are already applicable in other water treatments like reverse osmosis.

In this study, inorganic tubular ceramic membranes with highly dispersed catalytic metals: palladium and platinum were produced on both meso and macro porous membranes. They were characterised and tested in membrane reactors by feeding hydrogen saturated water under varying operating conditions and the results compared to that of a fixed-bed reactor.

The catalytic activities of the different membranes resulted in different deoxygenating efficiencies. The 6000nm palladium membrane was found to give the highest oxygen conversion of over 80% on the range of the saturated feed flow rate of 200 -1000 mL/min, with a 97% DO reduction at the lowest flow rate of 200 mL/min.

Increase in hydrogen gas flow rate and catalytic loading were observed to lead to improved removal of DO. Reaction run time was found to play an important role in the DO removal rate efficiency. Only when the reaction time of a flowrate was longer than 30 minutes under the experimental condition did a very low DO level be attained.

The reaction order for reactant oxygen was found to follow a pseudo-first order kinetics for both the fixed-bed and membrane reactor. The effect rate of reaction

of oxygen showed a strong dependence on the hydrogen total pressure to the power of 3 albeit with a low rate constant. The values for the rate constant k for the rate of reaction of oxygen were calculated to be $2.6\,X\,10^{-6}$ (mol.s^{-1}.g$_{catalyst}^{-1}$.mg^{-1}.L) for fixed-bed (k_1) and $1.3\,x\,10^{-4}$ (mol.s^{-1}.g$_{catalyst}^{-1}$.mg^{-1}.L) for CMR (k_2) respectively. The value of k for the dependency on hydrogen pressure for the fixed-bed reactor (k_3) was calculated to be $8.4\,X\,10^{-6}$ (mol.s^{-1}.g$^{-1}_{catalyst}$.atm^{-3}).

Keywords: Ceramic alumina membrane, platinum, palladium, dissolved oxygen, water deoxygenation, catalytic membrane reactor, fixed bed reactor, chemical kinetics, plug flow model

DEDICATION

I dedicate this work to my dearest and most loving husband, Sir Martin Orakwe (KSC) for his countless support, love, assistance, patience and encouragement with every step and decision I made through this program. I will remain ever grateful.

ACKNOWLEDGEMENT

I would like to thank God Almighty for sustaining me throughout this research. I also wish to express my sincere gratitude to my supervisor, Professor Edward Gobina for his encouragement, input, support, understanding, patience and guidance throughout the period of my studies. I appreciate and will remain ever grateful.

My appreciation also goes to all my colleagues at the Centre for Process Integration and Membrane Technology, RGU: Habiba Shehu, Oluwademilade Ogunsesan, Ofasa Abunumah, Edidiong Okon, Ngozi Nwogu, Mohammed Kajama and Abubakar Alkali for their wonderful support and contributions through the course of my studies.

I would also like to extend my appreciation to Iain Tough for his time spent in training and analysing my samples at the scanning electron microscopic section of the School of Pharmacy and Life sciences.

I am grateful to Robert Nicol Grant for their financial support.

To all my wonderful friends, for their encouragement in so many ways I cannot mention: Engr Ogochukwu Ikenwilo and Engr & Pharm Emeka Onu amongst others. I would not forget you all and may God grant all your heart desires.

I owe a lot to my wonderful children: Ifunanya, Chibuikem and Somtochukwu who prayed endlessly for my successful completion. I love and cherish you all. Also, to my mother (Beatrice K. Ezugwu) and parents in-law (Mr and Mrs Mathew Orakwe Abugu) for their prayers and support with babysitting my kids at various times of my program.

And finally, to my dad (of blessed memory) who would have loved to witness this day. Am glad I fulfilled one of your last wishes.

TABLE OF CONTENT

ABSTRACT i
DEDICATION iii
ACKNOWLEDGEMENT iv
TABLE OF CONTENT v
List of Figures xi
List of Tables xvii
Nomenclature xix
Abbreviations xxi
Conversions xxiii

CHAPTER ONE 1
Chapter 1 2
1 INTRODUCTION 2
1.1 Background of the work 2
1.2 Scope of this work 6
1.3 Aim and Objectives 7
1.4 Methodology 8
1.5 Publications/Conferences attended 9
1.6 Thesis Outline 11

CHAPTER TWO 13
Chapter 2 14
2 LITERATURE REVIEW 14
2.1 Dissolved Oxygen (DO) in Water 14
2.2 Problems Resulting from the Presence of DO 14
2.3 Deoxygenating Methods 17
2.3.1 Physical methods 17
2.3.1.1 Thermal degassing 17
2.3.1.2 Vacuum degassing 17
2.3.1.3 Gas stripping method 18
2.3.2 Chemical methods 18
2.3.3 Compact deoxygenating methods 19
2.3.3.1 Minox technology 19
2.3.3.2 Seaject Technology 21
2.3.4 Reviews on laboratory-based Deoxygenating methods 22
2.4 Membrane Technology 24
2.4.1 Ceramic membranes 25

2.4.2 Transport mechanisms in a Membrane 28
2.4.2.1 Knudsen flow mechanism.....28
2.4.2.2 Viscous flow 29
2.4.2.3 Surface diffusion.....29
2.4.2.4 Molecular sieving 30
2.4.2.5 Solution diffusion mechanism 30
2.5 Membrane Reactor Concepts 31
2.5.1 An extractor 31
2.5.2 A Distributor 31
2.5.3 A Contactor 31
2.5.4 Other Functions.....32
2.6 Catalytic Membrane Reactor Technology in Water Deoxygenation 33
2.6.1 Catalysts for CMR Water Deoxygenation.....33
2.6.2 Source of hydrogen supply in a hybrid water deoxygenating process37
2.7 Catalytic Membrane Preparation 38
2.7.1 Palladium Membrane preparation 38
2.7.1.1 Chemical vapour deposition (CVD) 39
2.7.1.2 Electroless plating (ELP) 39
2.7.1.3 Magnetron sputtering 39
2.7.1.4 Electroplating 39
2.7.2 Platinum Membrane preparation.....40
2.7.2.1 Evaporation-crystallization impregnation.....40
2.7.2.2 Anionic impregnation.....40
2.8 Alumina Ceramic supports for CMR process in water deoxygenation 40
2.9 Reaction Mechanism and Kinetic models for Catalytic Water Deoxygenation.....41
2.9.1 Thermodynamics of the H_2/DO reaction.....41
2.9.1.1 Half reactions 42
2.9.2 Reaction Mechanism: Langmuir-Hinshelwood Model 42
2.9.3 Modified Langmuir-Hinshelwood model: Hougen – Watson (H-W) equation.....44
2.10 Principles governing Catalysts in water deoxygenation 45
2.11 Factors affecting operation of the CMR in water deoxygenating process46
2.11.1 Effect of Variables.....46
2.11.2 Fouling 47
2.11.2.1 Catalytic site fouling 47
2.11.2.2 Membrane fouling 47
2.12 Operating and capital cost of CMR in water deoxygenating process....48

2.13 Advantages of CMR in water deoxygenating process 50
2.14 Contribution to knowledge.....51

CHAPTER THREE 56
Chapter 3.....57
3 METHODS.....57
3.1 Method No 1: Catalytic fixed-bed (Platinum on alumina) 57
3.1.1 Catalyst Characterization.....58
3.2 Method No 2: Platinum Impregnation 58
3.3 Method No. 3: Palladium membrane.....62
3.3.1 Sensitization and activation steps 63
3.3.2 Plating step 65
3.4 Membrane Catalyst Reduction/Activation 67
3.5 Characterization 69
3.5.1 Gas permeation.....69
3.5.1.1 Feed delivery section.....69
3.5.1.2 Gas permeation analysis 70
3.5.2 Scanning electron microscopy (SEM) coupled with Energy Dispersive Analytical X-ray (EDAX) 71
3.5.3 Nitrogen Adsorption Desorption analysis.....72
3.5.3.1 Degassing stage 74
3.5.3.2 Analysis Stage.....74

CHAPTER FOUR 76
Chapter 4.....77
4 REACTOR DESIGN 77
4.1 Membrane Reactor design 77
4.2 Ceramic Support design.....80
4.3 Catalytic membrane and process design 81
4.4 Fixed-Bed Reactor Design 82

CHAPTER FIVE 85
Chapter 5.....86
5 CATALYTIC FIXED-BED REACTOR FOR WATER DEOXYGENATING PROCESS (METHOD No 1) 86
5.1 Introduction 86
5.2 Equipment and Apparatus 86
5.3 Materials.....87
5.4 Health and safety.....87

5.5 Experimental Procedure 87
5.5.1 Feed delivery Section 90
5.5.2 Fixed-bed catalytic reactor section 90
5.5.3 Analytical Section 90
5.5.4 Kinetic Experimental runs 90

CHAPTER SIX 92
Chapter 6 93
6 CATALYTIC MEMBRANE REACTOR WATER DEOXYGENATING PROCESS (Method No 2 & 3) 93
6.1 Introduction 93
6.2 Equipment and Apparatus 93
6.3 Materials 95
6.4 Health and safety 95
6.5 Experimental Procedure 95
6.5.1 Feed delivery Section 97
6.5.2 Catalytic Membrane Reaction Section 98
6.5.3 Analytical Section 99
6.5.4 Kinetic Experimental Runs 100

CHAPTER SEVEN 103
Chapter 7 104
7 REACTOR ENGINEERING 104
7.1 Kinetic analysis 104
7.1.1 Mole balance and stoichiometry 104
7.1.2 Rate law 107

CHAPTER EIGHT 110
Chapter 8 111
8 RESULTS AND DISCUSSIONS 111
8.1 Catalytic Loading on Membranes 111
8.2 Membrane characterisation 112
8.2.1 Gas Permeation 112
8.2.1.1 Gas permeation through supports 113
8.2.1.2 Gas permeation through support and catalytic membranes 115
8.2.2 Scanning electron microscopy coupled with Energy Dispersive Analytical X-ray analysis 117
8.2.2.1 Method No 1 117

8.2.2.2 Methods No 2 and No 3 119
8.2.3 BET Liquid nitrogen analysis 126
8.3 Catalytic performance measurement/ Efficiency and evaluation in water deoxygenating process 132
8.3.1 Fixed-bed reactor experiment 132
8.3.1.1 Effect of varying the amount of catalyst and hydrogen pressure 132
8.3.1.2 Effect of varying feed water flowrate 133
8.3.2 Membrane Reactor Experiments 135
8.3.2.1 Effect of membrane pore size on outlet DO level using palladium membranes 135
8.3.2.2 Effect of membrane area on outlet DO level using platinum membrane 137
8.3.2.3 Effect of feed water flow rate on the outlet DO level 139
8.3.2.4 Percentage efficiency of the catalytic membranes 140
8.3.2.5 Effect of time on DO concentration 141
8.3.2.6 Effect of the hydrogen gas flow rate on water deoxygenation in catalytic membrane 142
8.3.2.7 Effect of blanket gases in DO measurement 143
8.3.3 Comparison of Fixed-Bed and Membrane Catalytic Deoxygenation 144
8.3.3.1 Catalyst weight and efficiency 144
8.3.3.2 Rate of reaction 145

CHAPTER NINE 150
Chapter 9 151
9 CONCLUSION AND RECOMMENDATION FOR FUTURE WORK 151
9.1 Conclusion and significance 151
9.2 Recommendations for future work 154

CHAPTER TEN 156
Chapter 10 157
REFERENCES 157

CHAPTER ELEVEN 169
Chapter 11 170

APPENDIX I: Experimental 170
APPENDIX II: Materials 176
APPENDIX III: Health and Safety 180

APPENDIX IV: Calculation 183
APPENDIX V: Results for Fixed-bed Deoxygenating Processes..... 184
APPENDIX VI: Results for Catalytic Membrane Deoxygenating Process..... 185
APPENDIX VII: Results used for rate of reaction..... 187
APPENDIX VIII: Other Conferences 188

List of Figures

Figure 1: Dispersion of active catalytic metal over an alumina support material with flow-through pores forming a catalytic membrane (CM) 5
Figure 2: Schematic diagram representation of the methodological steps carried out in the catalytic water deoxygenating process 9
Figure 3: Picture showing the presence of DO molecule in water [25]. 14
Figure 4: Corroded pipe [3].....15
Figure 5: Minox Compact tower (one-stage process) [37] 20
Figure 6: Ultra Minox compact Stage 2 (two-staged process) [37]. 21
Figure 7: Flow diagram of a Seaject deoxygenating process [9] 22
Figure 8: A schematic diagram of a composite membrane 25
Figure 9: Schematic representation of a separation process between two phases using a membrane as a perm selective device/barrier [56].....26
Figure 10: Schematic diagram illustrating Knudsen flow mechanism.....29
Figure 11: Schematic diagram illustrating viscous flow mechanism.....29
Figure 12: Schematic diagram illustrating Surface diffusion 30
Figure 13: Schematic diagram illustrating Molecular sieving 30
Figure 14: Schematic diagram illustrating Solution diffusion mechanism 31
Figure 15: Concepts of a membrane reactor [44] 32
Figure 16: Flow-through membrane reactor 33
Figure 17: The reaction path of water formation [57] 34
Figure 18: Main heterogeneous catalytic coupling methods (a) Bed of catalyst on an inert membrane; (b) catalyst dispersed in an inert membrane and (c) catalytic membrane due to composition of the membrane material [65]. 34
Figure 19: Periodic table showing group VIII metals [76] 36
Figure 20: Hydrogen generation through electrolysis [78] 38
Figure 21: Postulated reaction pathway for the synthesis of $\boldsymbol{H2O}$ on Pd/Pt catalyst.....44
Figure 22: Reaction pathway of equations (i) to (iii) described by H-W 45
Figure 23: Showing the concentration profile in the fixed-bed reactor 51
Figure 24: Heterogeneously catalysed steps in chemical reactions involving a porous pelletised catalyst 52
Figure 25: Scheme of catalytic consecutive reaction in (a) pore flow-through membrane (b) and traditional fixed bed reactor with pelletized catalyst 55

Figure 26: Fixed-bed catalyst set up.....58
Figure 27: Picture showing the weighing of a ceramic support 59
Figure 28: Fresh support dipped in water 59
Figure 29: Picture showing the ends of a membrane covered in Teflon tapes, (a) uncovered and Teflon covered support end, (b) side view of the Teflon covered support with an extra cap cover, (c) front view of b. 60
Figure 30: Pictures showing the processes of platinum impregnation, (a) platinum solution undergoing proper mixing in deionised water, (b) membrane dipped in platinum solution with stirring.....60
Figure 31: Air drying of the membrane at room temperature.....61
Figure 32: Oven drying of the membrane at 65^{o}C (a) Picture of the oven showing the operating temperature, (b) Picture showing the membrane placed inside the oven for drying 61
Figure 33: Platinum impregnated membrane 62
Figure 34: A schematic diagram for the conventional Pd-Sn procedure 63
Figure 35: Pictorial representation of the Pd-Sn membrane seeding process, (a) in $SnCl_2$ solution, (b) in deionised water and (c) in $PdCl_2$ solution 64
Figure 36: (a) Picture showing the fresh support and Pd activated membrane, (b) witness sample.....65
Figure 37: Electroless plating process of the palladium membrane 66
Figure 38: Showing pictures of thinly coated palladium membranes A and B 67
Figure 39: Pictorial representation of the hydrogen reduction activation process/gas permeation experimental rig (1. Gas bottle, 2. Gas gauge control On/Off, 3. Pressure gauge, 4. Membrane holder, 5. Wrapped heating tape, 6. Hydrogen safety monitor, 7. Thermometer).....67
Figure 40: Picture showing the reduction activation process using helium gas...68
Figure 41: Picture showing the fresh support and activated platinum and palladium membranes 68
Figure 42: Schematic experimental diagram showing the catalytic membrane reactor process for gas permeation analysis (1. Gas bottle, 2. Gas gauge control On/Off, 3. Pressure gauge, 4. Membrane holder, 5. Heating tape, 6. Catalytic membrane, 7. Thermocouple attached to a thermometer, 8. Flowmeter, 9. Waste) 70
Figure 43: Picture of the SEM-EDAX setting.....71

Figure 44: Picture showing fragments of the witness samples going in for SEM-EDAX analysis 72
Figure 45: Types of Physisorption isotherms [49].....73
Figure 46: Picture showing samples undergoing degassing stage 74
Figure 47: Picture showing sample analysis taking place inside the liquid nitrogen.....75
Figure 48: Stainless steel reactor housing 77
Figure 49: (a) Picture showing the hollow space in a membrane holder, (b) Picture of a membrane sealed inside a membrane holder using graphite rings ..78
Figure 50: (a) Plain reactor, (b) reactor wrapped with heating tape and thermocouples, (c) heating tapes covered with a fibre material.....79
Figure 51: Thermally insulated reactor mounted on rig ready for experiment....80
Figure 52: Cross-sectional view of a catalytically impregnated membrane showing its different layers.....81
Figure 53: Cross section of the catalytic membrane undergoing chemical reaction82
Figure 54: Longitudinal catalytic packed-bed for a fixed bed reactor.....83
Figure 55: Schematic diagram of a fixed-bed reactor.....83
Figure 56: DO analyser.....87
Figure 57: Schematic diagram of the fixed-bed experiment (1. Hydrogen gas, 2. Control valve, 3. Digital gauge pressure, 4. H_2 inlet port, 5. Inlet feed water source, 6. Catalyst bed, 7. Stainless-steel reactor, 8. Beaker containing water, 9. DO probe, 10. DO analyser 88
Figure 58: Pictorial diagram of the fixed-bed experiment: (1. Hydrogen gas, 2. Control valve, 3. Digital gauge pressure, 4. H_2 inlet port, 5. Inlet feed water source, 6. Stainless-steel reactor, 7. Beaker containing water, 8. DO probe, 9. DO analyser 89
Figure 59: Electric water pump 94
Figure 60: Stainless steel gas sparger 94
Figure 61: Schematic experimental diagram for the removal of DO in water using a catalytic membrane reactor process (1. Hydrogen cylinder, 2. Water source, 3. Flow meter, 4. Pyrex glass reactor, 5. Sparger, 6. Stirrer, 7. Magnetic stirrer plate, 8. Water pump, 9. Catalytic membrane reactor, 10. Catalytic membrane, 11. DO analyser, 12. Waste.....95
Figure 62: Pictorial representation of the experimental setup for the catalytic membrane water deoxygenating process (1. N_2 cylinder, 2, H_2 cylinder, 3. H_2

safety monitor, 4. Flowmeter for H_2 and N_2, 5. Round bottom flask, 6. H_2 sparger, 7. Cole palmer pump, 8. Stirrer, 9. DO analyser, 10. Catalytic membrane reactor, 11. Water supply, 12.DO probe, 13. Water beaker with N_2 as a blanket gas, 14. Water beaker with air as a blanket gas 96
Figure 63: Connection of the gas sparger to a stainless tube and cork seal.....97
Figure 64: Pictorial representation of a Catalytic impregnated membrane inserted into the membrane holder. 98
Figure 65: Picture showing the reactor clamped to a retort stand 98
Figure 66: Process showing measuring of DO level in water.....100
Figure 67: Schematic diagram of the reactor module (a) catalytic membrane reactor illustrating the working principle, (b) section showing the arrangement of the catalytic active phase on the tubular membrane, (c) showing a pore and how the catalyst is impregnated 102
Figure 68: Schematic diagram showing the flow of water through a pore of a catalytic membrane.....105
Figure 69: Cross sectional slice of the pore showing the direction of flow 105
Figure 70: Effect of flow rate on the feed gauge pressure of support material (a) 15nm-support A and (b) 6000nm-support B at 298 K 114
Figure 71: A plot of kinetic diameter of permeating gases against flow rate at 0.5 bar.....115
Figure 72: A graph showing the effect of hydrogen feed gauge pressure against flow rate of support, palladium and platinum deposited membranes at 573 K .116
Figure 73: A plot of kinetic diameter of permeating gases through a Pt deposited membrane at 0.5 bar 117
Figure 74: Micrograph showing the outer surface of the catalyst pellet 118
Figure 75: Micrograph showing the edge of the catalyst pellet 118
Figure 76: EDAX showing the chemical compositions of the outer surface 119
Figure 77: Micrographs for 15 nm α-Al_2O_3 support: (a) inner surface, (b) outer surface and (c) EDAX showing the chemical compositions of the outer surface.120
Figure 78 : Micrographs for 6000 nm α-Al_2O_3 support: (a) inner surface, (b) outer surface and (c) EDAX showing the chemical compositions of the outer surface. 121
Figure 79: Micrographs for the 15 nm γ-Pd/Al_2O_3 membrane: (a) inner surface, (b) outer surface and (c) EDAX showing the chemical compositions of the outer surface. 123

Figure 80: Micrographs for the 6000 nm γ-Pd/Al_2O_3 membrane (a) inner surface, (b) outer surface, and (c) EDAX showing its elemental composition ... 124
Figure 81: Micrographs for the 15 nm γ-Pt/Al_2O_3 membrane: (a) inner surface, (b) outer surface and (c) EDAX showing the chemical compositions of the outer surface. ... 125
Figure 82: Micrographs for the 6000 nm γ-Pt/Al_2O_3 membrane: (a) inner surface, (b) outer surface and (c) EDAX showing the chemical compositions of the outer surface. ... 126
Figure 83: Physisorption isotherm of the 15nm support ... 127
Figure 84: Physisorption isotherm of the 6000nm support ... 127
Figure 85: T-plot for a 15 nm pore sized support ... 128
Figure 86: BJH graph showing the pore size distribution and pore diameter for 15nm support ... 129
Figure 87: T-plot for a 6000 nm pore sized support ... 130
Figure 88: BJH graph showing the pore size distribution and pore diameter for 6000nm support ... 131
Figure 89: Graph showing the effects of catalyst weight and hydrogen pressure on the removal of DO in the fixed-bed ... 133
Figure 90: Graph showing the effect of water flowrate on the outlet DO concentration ... 134
Figure 91: A plot of DO removal efficiency against water flow rate of the 3.0g fixed–bed reactor ... 134
Figure 92: Graph showing the effects of membrane pore size on outlet DO concentration using palladium coated membranes ... 136
Figure 93: Graph showing the effects of membrane pore size on outlet DO concentration using platinum deposited membranes ... 137
Figure 94: Effect of water flowrate on the outlet DO concentration comparing membrane areas ... 138
Figure 95: Effect of liquid phase resistance on the DO removal ... 139
Figure 96: Effect of feed water flow rate on the DO removal ... 140
Figure 97: A plot of DO removal efficiency against water flow rate for the different catalytic deposited membranes. H_2 flow rate was 1.55 L/min. Membrane areas: Memb A= 0.0008m^2, Memb B=0.023m^2, Memb C=0.045m^2 ... 141
Figure 98: Effect of time on the removal of DO on 6000nm Pd coated membrane 142

Figure 99: Effect of H_2 gas flow rate and H_2 pressure on water deoxygenation in catalytic membranes 143
Figure 100: Effect of air and N_2 being used as blanket gases 144
Figure 101: A plot of DO removal efficiency comparing % wt of Pt catalyst on fixed-bed and catalytic membrane reactor..... 145
Figure 102: A plot of $In[XO_2/(W/FAi)]$ against $In[O_2]$ for oxygen reaction in the fixed-bed reactor 146
Figure 103: A plot of $In[XO_2/(W/FAi)]$ against $In[O_2]$ in the catalytic membrane reactor 147
Figure 104: A plot of In(Rate of reaction of oxygen) against In(feed pressure of H_2) in the fixed-bed reactor..... 148
Figure 105: Graphite "O" rings..... 170
Figure 106: Picture showing a Cole-Parmer gas flow meter 172
Figure 107: Picture of a H_2 safety monitor..... 173
Figure 108: Picture of a pressure gauge..... 174
Figure 109: Deionised water dispenser 175
Figure 110: Measurement of the outer diameter of the 3 different supports.... 176
Figure 111: Measurement of the inner diameter of the 3 different supports.... 177
Figure 112 Pictures of the 3 different supports used showing their variation in length and width..... 177

List of Tables

Table 1: Examples of studies carried out by ceramic catalytic membrane reactors6
Table 2: The chemical compositions of the sensitization and activation solutions64
Table 3: Composition of the electroless plating bath 66
Table 4: List the experimental conditions and system parameters used in the study.....91
Table 5: List the experimental conditions and system parameters used in the study.....101
Table 6: Showing the catalyst loading of the palladium metal 111
Table 7: Showing the catalyst loading of the platinum metal 112
Table 8: Shows the molecular weights and kinetic diameter of gases.....113
Table 9: Details obtained from the BJH method on the 15nm support.....129
Table 10: Results showing parameters obtained for 15nm support and catalytic deposited membranes 129
Table 11: Details obtained from the BJH method on the 6000nm support.....130
Table 12: Results showing parameters obtained for 6000nm support and catalytic deposited membranes.....131
Table 13: Ceramic supports used and their parameters.....176
Table 14: List of gases with their risk and safely measures.....180
Table 15: show the chemicals and their health and safety measures 182
Table 16: results showing effects of catalyst loading and hydrogen pressure in the removal of DO in the fixed-bed reactor.....184
Table 17: Results for water deoxygenation using 3.0g of catalyst pellet in the fixed-bed reactor 184
Table 18: Results showing the effects of membrane pore size on outlet DO concentration using platinum deposited membranes.....185
Table 19: Results showing the effects of membrane pore size on outlet DO concentration using platinum deposited membranes.....185
Table 20: Table showing the DO removal efficiency against water flow rate for the different catalytic deposited membranes. H_2 flow rate was 1.55 L/min. Membrane areas: Memb A= 0.0008m^2, Memb B=0.023m^2, Memb C=0.045m^2 185
Table 21: Results showing the effect of time on the removal of DO concentration in Pd coated 6000nm membrane.....186

Table 22: Extrapolated values for the effect of H_2 gas flow rate and H_2 pressure on water deoxygenation in catalytic membranes 186
Table 23: Showing the values drawn for rate of reaction for oxygen in the fixed-bed reactor 187
Table 24: Showing the values drawn for rate of reaction for oxygen in for CMR187
Table 25: Results drawn from the dependency of hydrogen pressure on the rate of reaction of oxygen in the fixed-bed reactor 187

Nomenclature

Symbol	Meaning	Units
A	Membrane surface area	m^2
[ ]	concentration	$mg.L^{-1}$/ppm
d	Molecular diameter	m
F	Flow rate	$mols^{-1}$
F_A	Flow rate of gas A	$mols^{-1}$
J	Permeance	$mol.m^{-2}.s^{-1}.Pa^{-1}$
J_A	Permeance of gas A	$mol.m^{-2}.s^{-1}.Pa^{-1}$
J_B	Permeance of gas B	$mol.m^{-2}.s^{-1}.Pa^{-1}$
k_1	Rate constant for the rate of reaction of oxygen in fixed-bed reactor	$mol.s^{-1}.g_{catalyst}^{-1}.mg^{-1}.L$
k_2	Rate constant for the rate of reaction of oxygen in catalytic membrane reactor	$mol.s^{-1}.g_{catalyst}^{-1}.mg^{-1}.L$
k_3	Rate constant for the dependency on hydrogen pressure for the fixed-bed	$mol.s^{-1}.g^{-1}_{catalyst}.atm^{-1}$
M_A	Molecular weight of gas A	$gmol^{-1}$
M_B	Molecular weight of gas B	$gmol^{-1}$
N	Avogadro's number	mol^{-1}
$\overline{P}$	Average pressure across the membrane	Pa
Pm	Mean pressure	bar
ΔP	Pressure drop across the	bar

	membrane	
Q	Permeability	$mol.m^{-1}.s^{-1}.Pa^{-1}$
R	Gas constant	$m^3Pa.mol^{-1}\ K^{-1}$
r	Pore radius	m
T	Temperature	K, ^oC
W	weight of catalyst	g
wt. %	weight percentage	-
X	Conversion	-
x	Value corresponding to Knudsen diffusion	-
y	Value corresponding to Viscous constant	-
	Greek Symbols	
α	Selectivity factor, permselectivity	-
$\alpha_{A/B}$	Permselectivity of gas A to gas B	-
$\alpha_{B/A}$	Permselectivity of gas B to gas A	-
λ	Mean free path	m
π	Pi	-
ϑ	Viscosity	Pa.s

Abbreviations

Al_2O_3	Aluminium Oxide
atm	Atmosphere
BET	Brunauer Emmett and Teller
BJH	Barrett, Joyner and Halenda
CAS	Chemical Abstracts Service number
CM	Catalytic Membrane
CMR	Catalytic Membrane Reactor
DO	Dissolved oxygen
EDXA/EDAX	Energy dispersive X-ray Analysis
H_2	Hydrogen
H_2O	Water
KBr	Potassium Bromide
KCl	Potassium Chloride
N_2	Nitrogen
Na_2EDTA	Disodium ethylenediaminetatraacetate
NH_4OH	Ammonium hydroxide
N_2H_2	Hydrazine
O_2	Oxygen
Pd	Palladium
P_{avg}	Average pressure
$PdCl_2$	Palladium II Chloride
ppb	Part per billion
ppm	Part per million

Pt	Platinum
PVC	Polyvinyl Chloride Piping
SEM	Scanning electron microscope
$SnCl_2$	Stannous Chloride or Tin (II) Chloride
SiO_2	Silicon II oxide
Ti	Titanium
TiO_2	Titanium II oxide
ZrO_2	Zirconium dioxide

Conversions

1 ounce = 28.3495 g

1 mol = 22.4 L

1 min = 60 s

1000 mL = 1 L

1°C = 273 K

1 bar = 10,000 Pa

1 bar = 0.99 atm

CHAPTER ONE

Chapter 1

1 INTRODUCTION

1.1 Background of the work

Water, which could be sourced from sea, lake or river is required for enhanced petroleum recovery and for several other process applications such as in microelectronics, food industry, atomic and thermal power plants [1]. This need stems from its use either during production or manufacturing of components/products. The quality of this water is highly paramount for an efficient production to occur. In the oil and gas industry for example, it is the norm for the reservoir pressure of an oil well to be maintained by seawater injection during water-flooding operations (the process of sweeping the oil to the producers) [2]. This process is called improved and enhanced oil recovery [3, 4].

The advantages of the use of sea compared to other surface water sources is therefore enormous, but majorly, it is readily available, abundant in nature and creates little or no environmental impact by its use. Sea water properties vary from one location to another, but the downside of using untreated seawater is that it contains contaminants: dissolved oxygen (DO), suspended solids, dissolved solids, planktons and bacteria) which are undesirable depending on the application, hence the need for its treatment prior to use [5, 6]. For the purpose of this study, the contaminant of interest is DO because without its removal it can lead to corrosion of wellheads and subsea structures.

In the process industry, corrosion of steam generators of power reactors and water-cooled stator windings in turbine generators is also a major problem and suffer from various forms of corrosion induced by the presence of DO in water [7]. Reduction in the concentration of DO to extremely low levels can significantly eliminate the problems associated with corrosion [8, 9]. Depending on the type of process application involved, some may need very stringent low acceptable DO levels. A typical example where very low concentration of DO in the water stream is required are in atomic power plants and microelectronics (semiconductor) industries. The DO required in these industries should ideally not exceed 1 part per billion (ppb). Meanwhile, under normal conditions, the

concentration of DO in water is about 8 part per million (ppm) which is the same as 8 milligram per litre (mg/L) [1].

Removal of DO contaminant in water for the various applications require specially designed systems [6]. Cost, efficiency, weight, bulkiness, environmental impacts are some of the major factors that are being considered presently while designing a water deoxygenating equipment. In the offshore industry, the facilities involved in water deoxygenating processes are usually located on floating platforms and presently there are requirements for these platforms to meet smaller footprints and weights [4].

There are various forms of deoxygenation processes currently being employed. In 1992 in the oil and gas sector, a compact seawater deoxygenating system using regenerated nitrogen gas was introduced for water deoxygenation purposes. The flow of nitrogen was either done co-currently with the flow of seawater or counter-currently against the flow of seawater respectively. The co-current flow of nitrogen with serpentine tubes as a mixing zone was utilized by first generation units, while second generation units utilized a structured packing as a mixing zone with counter-current nitrogen flow. These second-generation units used vacuum towers that were less in height compared to the first-generation ones. In a nutshell, the first and second generation units employed vacuum pumps, towers and gas stripping equipment which were bulky and non-compact, thus leading to the third generation units which looked at more simplified control strategies and this has consequently led to further research and innovations [4].

Studies have mentioned Minox and Seaject as the two most recent compact deoxygenation technologies, with Seaject having a 75% reduction in terms of the unit size when compared to other deoxygenating systems present on offshore platform decks [9]. There are still downsides with these two though. The Minox process seems cumbersome while Seaject has limitations caused by effects of mass transfer as a result of the use of catalyst pellets. These disadvantages have therefore motivated the on-going innovative research focusing on the design of catalytically active membranes that can be used in membrane reactors specifically to remove DO from water for deoxygenated

water production for use in various industrial process applications and in down-hole water injection processes.

This research has been undertaken with the view of developing a more compact and integrated modular process for the reduction of DO in water employing membrane technology. The idea behind this method suggests the provision of a large reaction surface area where the catalytic reaction of the DO present in water and supplied hydrogen will be enhanced thereby forming water as the only product. The catalyst is not consumed during a chemical reaction therefore, the catalyst can be used over and over again. Catalytic membrane reactors (CMR) was therefore designed and tested for the removal of DO in water and the benefits of using membrane reactors in this application is that they facilitate the intimate contact of the reactants and enhance the contact of the reactants on the catalyst surface while limiting the production of any side products by reducing mass transfer processes [10].

Different catalytic membranes (CM) were fabricated taking note of effects of membrane pore size, type of catalyst and catalytic membrane area in testing for the DO process. The methods of catalytic deposition in the membranes was carried out such that high distributions of catalyst are achieved over and inside the pores of the permeable length of the membrane material as shown in Figure 1, such that the activity per unit mass of the catalyst is maximised in as much assessable surface as possible. An inactive material with a large surface area, in this case, a ceramic alumina (Al_2O_3) support is chosen and it is deposited with highly dispersed active components, in this case, catalyst. This therefore created a wider surface area of active sites for chemical reaction to occur between the reactants [11]. These active sites can be defined as sites on the pore surface that have the ability of creating strong chemical bonds with the reactant species. It is also worth noting that in such catalytic membrane process, the catalyst is not consumed in the reaction, therefore it can be reused repeatedly in a continuous flow of reactants [11].

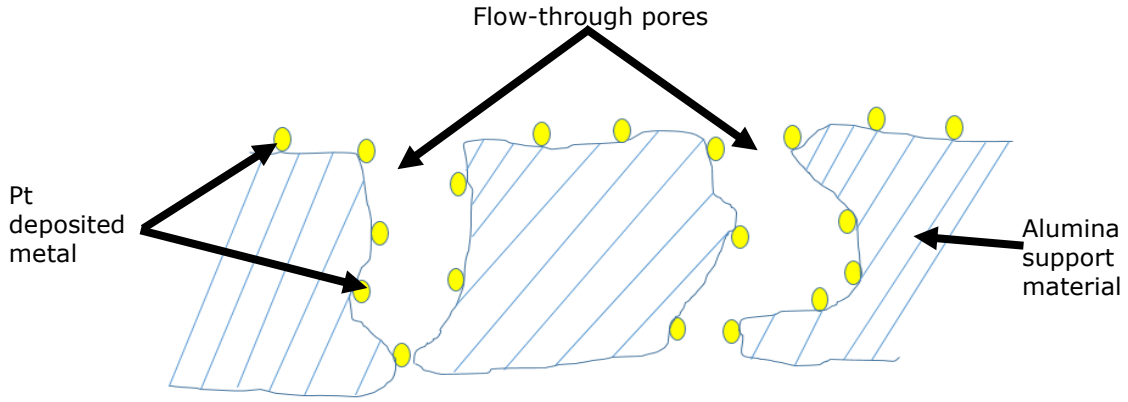

Figure 1: Dispersion of active catalytic metal over an alumina support material with flow-through pores forming a catalytic membrane (CM)

The catalytic membrane reactor was also focused on the idea of combining porous ceramic material with nanoparticles (catalyst) thereby addressing the concerns of the amount of catalyst required in a fixed-bed reactor being that the method developed during this PhD research tends to use minimal amount of catalyst in the process.

Applications involving porous ceramic membranes in catalytic membrane reactors are well reported in the scientific literature [12] and arise due to the need for integrating reaction and separation and also to carry out reactions at high temperatures since polymeric membranes are not thermally stable under harsh reaction conditions. This combination of catalysts and reactions has also been reported by various researches in different areas of study and some of these are summarized in Table 1.

Table 1: Examples of studies carried out by ceramic catalytic membrane reactors

Authors	**Reaction**	**Ceramic materials/ Configuration**	**Catalyst/ deposition method**
Zhang et al. [13]	Hydrogenation and CO oxidation	Al_2O_3 ceramics/ Tube	Pt/ Al_2O_3 Sol gel solvent vapourization
Kajama et al. [14]	VOC oxidation	Al_2O_3 ceramics/ Tube	Pt/ Al_2O_3 Wet impregnation
Uzio et al. [15]	Gas-liquid application	Al_2O_3 ceramics/ Tube	Pt/ Al_2O_3 Ionic and wet impregnation
Kajama et al. [16]	Hydrogen separation	Al_2O_3 ceramics/ Tube	Pt/ Al_2O_3 Wet impregnation
Melendez et al. [17]	Hydrogen separation	Al_2O_3 ceramics/ Tube	Pd-Ag/ Al_2O_3 Electroless plating
Li et al. [18]	Hydrogen separation	Al_2O_3 ceramics/ Tube	Pd/ Al_2O_3 Electroless plating
Abate et al. [19]	H_2O_2 synthesis	Al_2O_3 ceramics/ Tube	Pd/ Al_2O_3 Electroless plating
Yuranov et al. [20]	Methane combustion	SiO_2 ceramics/ Tube	Pd/SiO_2 Ion exchange
Wand et al. [21]	CO_2 reforming of methane	Al_2O_3 ceramics/ Tube	Rh/ Al_2O_3 Wet impregnation

1.2 Scope of this work

The scope of this work focuses majorly on experimental research involving the design and testing of fixed-bed catalytic reactors and membrane reactor processes. In the case of the membrane reactor it involves the deposition of two types of catalysts, namely: palladium and platinum metals into the tiny fine pores of commercially purchased tubular ceramic alumina supports and then evaluating the catalyst's performance in water deoxygenation process. In the case of the fixed-bed, the catalyst were purchased from Sigma Aldrich and used as received.

Catalytic membrane reactors having highly dispersed metallic particles along and around the porous tubular ceramic supports have been used and compared with the performance of fixed bed reactors such as those used in the Seaject process discussed earlier. The tubular shaped alumina supports in this instance, creates a medium which has a wider contact surface area where the reactions can take place in the presence of impregnated catalyst.

1.3 Aim and Objectives

The aim of this study is to design, test and evaluate the use of a tubular catalytic membrane reactor in comparison to a fixed-bed process for the purpose of water deoxygenation for down-hole water injection and process applications.

Based on the aim above, the objectives of the research are:

1. To fabricate a non-dense palladium layer on different pore sized ceramic alumina supports using the electroless plating method.
2. To impregnate low platinum metal loading into the tiny pores of different pore sized ceramic alumina membranes using wet impregnation method.
3. To characterize the catalytic ceramic membranes using gas permeation test, scanning electron microscopy (SEM) coupled with Energy Dispersive X-ray analyser (EDX or EDA), and liquid nitrogen adsorption desorption analyser.
4. To study the gas transport mechanisms on both the commercially supplied alumina supports and catalytic deposited membranes to understand gas transport mechanisms.
5. To characterize the catalytic membrane deoxygenating performance as a function of metal loading, membrane pore size, pore size distribution, liquid flux and molar ratio of oxygen to hydrogen.
6. To evaluate the percentage conversion of dissolved oxygen by using an on-line dissolved oxygen analyser to monitor the levels of dissolved oxygen both at the feed and permeate ends of the catalytic membrane reactor unit.
7. To compare the performance of the membrane process with that of the traditional fixed-bed reactor.

8. To postulate a chemical reaction mechanism for the deoxygenating process.
9. To evaluate the rate of reaction for predicting this type of chemical reaction using the kinetic parameters obtained in the study.

1.4 Methodology

The catalytic tests carried out in this study comprised of three methods. The first was on a commercially purchased platinum on alumina pellets, while the other two methods involved catalytic membranes prepared from fresh supports.

The methods which involved deposition of platinum and palladium catalyst on fresh supports are selected based on cost and simplicity of the processes. Deionised water was used for sample preparations in all the cases. Both platinum and palladium deposition methods involved a dipping process. This dipping process results in the catalyst being highly dispersed in the outer surface and pore surface of the ceramic material. The presence of the catalyst on the surface and in the pores of the ceramic material helps the catalyst attain a very high degree of efficiency because the reactants can easily access the active sites [22].

The method of the catalytic coating tend to reduce the effect of mass transfer usually found in catalytic pellets and also optimise the performance of the catalyst because the amount of catalyst used will also be significantly reduced. It should also be noted that this would not affect its effectiveness.

A summary of the methodology used is schematically presented in Figure 2.

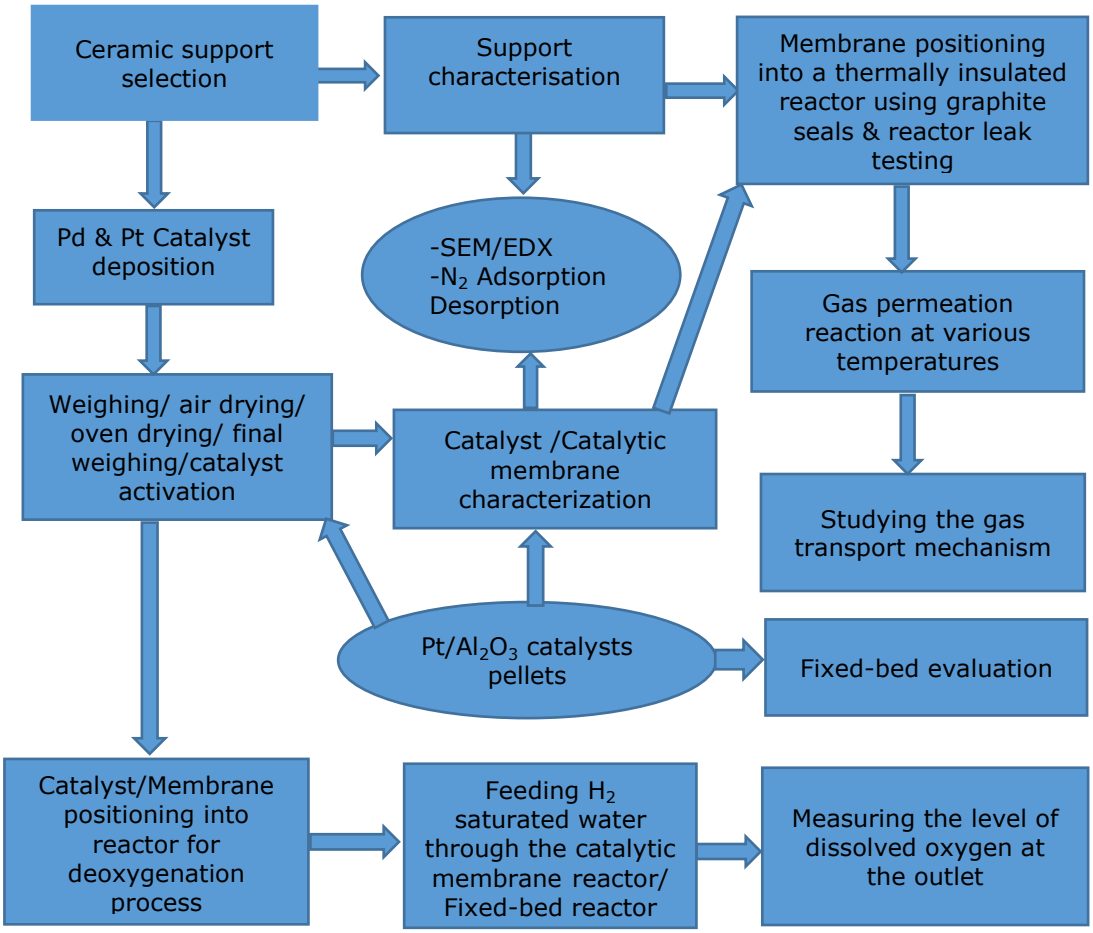

Figure 2: Schematic diagram representation of the methodological steps carried out in the catalytic water deoxygenating process

1.5 Publications/Conferences attended

2017

Orakwe, I., Shehu, H., Okon, E. and Gobina, E "Surface analysis of Pt-modified ceramic membrane using N_2 adsorption desorption and application for process of water deoxygenation". International Conference & Exhibition on Advanced & Nano Materials 2017 Proceeding August 7-9, 2017, Toronto, Canada. Pp 67-72. *http://iaemm.com*.

Orakwe, **I. R**, Nwogu N.C, Gobina, E. "Characterization of Gamma-alumina Ceramic Membrane". In Transactions on Engineering Technologies. 2017, (pp.563-572). Springer (Book Chapter). *http://link.springer.com/chapter/10.1007/978-981-10-2717-8 40*

Orakwe Ifeyinwa, Habiba Shehu, Edidiong Okon and Edward Gobina "Application of highly dispersed metallic membrane in the removal of dissolved oxygen in water". International Conference on Catalysis and Chemical Engineering 22nd to 24th February 2017 Baltimore, USA.

Orakwe Ifeyinwa and Edward Gobina "Removal of dissolved oxygen using a platinum impregnated catalytic membrane". International Conference on Catalysis and Chemical Engineering 22nd to 24th February 2017 Baltimore, USA.

2016

Orakwe Ifeyinwa, Edidiong Okon and Edward Gobina, "Development of Catalytic Membrane Reactors for Esterification of Lactic Acid and Hydrogenation of Water for Oxygen Removal" International Journal of Scientific Engineering and Technology ISSN:2277-1581 Volume No.5 Issue No.6, pp: 335-338 2016. *doi : 10.17950/ijset/v5s6/603 Page 335*

Orakwe, I., Nwogu, N. and Gobina, E. "Characterization of an alumina membrane using single gas permeation". In Transactions on engineering technologies 2016, pages 179-189. Springer. (Book chapter) *https://doi.org/10.1007/978-981-10-1088-0_14*.

Orakwe, Ifeyinwa R., Mohammed Kajama, Ngozi C. Nwogu, Edward Gobina. **"**Gas permeation of single gases on a platinum impregnated alumina membrane", 1st Green and Sustainable Chemistry Conference 3 - 6 April 2016, Intercontinental Hotel, Berlin, Germany.

Orakwe, Ifeyinwa and Edward Gobina. "Preparation and Characterization of Ultra-thin Palladium membrane for deoxygenation purposes in water", Conference on "Emerging and Hybrid Membrane Technologies" organized by institution of chemical engineers (IChemE) advancing chemical engineering worldwide, 10 June 2016, Swansea University, UK.

2015

Orakwe, Ifeyinwa R., Ngozi C. Nwogu, Mohammed Kajama, Habiba Shehu, Edidiong Okon & Edward Gobina, "Effect of temperature on gas transfer through alumina membrane". 3rd International conference on Mechanical and Aerospace Engineering October 2015

Orakwe, Ifeyinwa, Ngozi C. Nwogu, and Edward Gobina, "Morphological Characterization and Gas Permeation of Commercially Available Ceramic Membrane," Lecture Notes in Engineering and Computer Science: Proceedings of The World Congress on Engineering and Computer Science 2015, 21-23 October 2015, San Francisco, USA, pp607-610.

Orakwe, I.R., Nwogu, N.C., Kajama, M., Shehu, H., Okon, E. and Gobina, E., 2015. An Initial Study of Single Gas Permeation using a Commercial Alumina Membrane. Proceedings of the World Congress on Engineering 2015; Vol II WCE 2015, July 1 - 3, 2015, London, UK, pp737-739
http://www.iaeng.org/publication/WCE2015/WCE2015_pp737-739.pdf.

1.6 Thesis Outline

This thesis comprises of 9 chapters, followed by references and appendices. Below is a brief summary of each chapter.

Chapter 1 presents an introduction of the research and how it was conceived. The aim and objectives of the study are also presented and discussed as well as the summary of the methodology employed. Publications/conferences made/attended on the research findings are also provided.

Chapter 2 presents literature review on dissolved oxygen and its implications, deoxygenating methods, membrane technology, types of catalyst chosen for the study, different methods of catalyst deposition, catalytic membrane reactor and reaction kinetic mechanism for the process. It also presents the research's contribution to knowledge.

Chapter 3 presents the experimental procedures carried out in the preparations of fixed-bed catalyst, palladium-coated membrane and platinum impregnated

membrane. Characterization methods carried out on both the catalyst pellet and catalytic membranes were also discussed.

Chapter 4 gives an overview on the reactor design for both the catalytic membrane and fixed-bed reactors.

Chapter 5 details the materials and methodology/kinetic runs carried out on the fixed-bed reactor for water deoxygenating processes.

Chapter 6 details the materials, methodology/kinetic runs carried out on the catalytic membrane reactor water deoxygenating processes.

Chapter 7 presents a kinetic analysis, mole balance and rate law governing the chemical process involved in deoxygenation of water.

Chapter 8 discusses most of the results obtained from the various experiments done, the gas transport mechanism and the gas permeation results. Morphological features of the catalyst pellet and catalytic membranes using scanning electron microscopy coupled with energy dispersive X-ray analyser, specific surface areas and pore diameters of the catalytic membranes using the liquid nitrogen analyser and evaluations of the effectiveness of the fixed-bed and catalytic membrane reactor process are discussed. Comparisons between the fixed-bed reactor and catalytic membrane reactor's performance were evaluated and the rate of reaction calculated. An order for the influence of hydrogen pressure was also proposed.

Chapter 9 presents the conclusion of the study, findings and its significance. A recommendation for future work is also presented.

Reference section outlines all the references used in the study.

Appendices present detailed outlines on all the equipment, chemical and materials used, risk and safety measures for the chemical and gases used. Some other calculations and results relating to the membranes are also presented here.

CHAPTER TWO

Chapter 2

2 LITERATURE REVIEW

2.1 Dissolved Oxygen (DO) in Water

DO is one of the many dissolved gases found in water [23]. It is the level or volume of gaseous oxygen dissolved in water or could be explained as the measure of gaseous oxygen in water media [24]. This oxygen in water is usually non-bonded as shown in Figure 3. The DO usually gets into the water from the atmosphere and from plant photosynthesis [25]. The presence of DO in hydrogen sulphide containing water and water free from hydrogen sulphide in concentration of 0.01 and 0.5 ppm respectively are more than enough to cause problems in water injection units or other process applications [6].

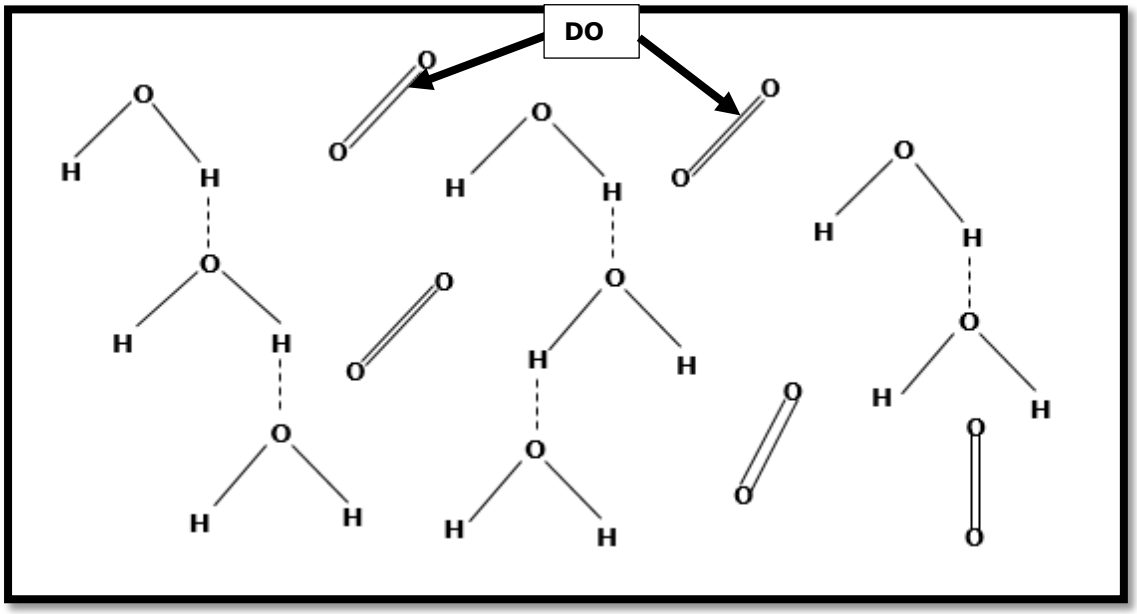

Figure 3: Picture showing the presence of DO molecule in water [25].

2.2 Problems Resulting from the Presence of DO

DO is highly corrosive in water and its level depending on the process application can result in serious problems. Without a proper and efficient water deoxygenation system in place, corrosion of metals which is a major problem caused by the presence of dissolved oxygen in water occurs. This corrosion leads to the formation of galvanic cells in water thereby promoting the rate of

corrosion in various industrial sectors, such as steam and energy producing companies [26]. In the steam generating industries, problems as a result of corrosion occurring on the boiler system cost the industry billions of pounds annually and is the main cause of reduced reliability in the steam producing industries [27]. Corrosion of iron and metal alloys also occurs in the marine steel infrastructures where corrosion of pipeline and offshore oil and gas installation units can occur. This consequently leads to huge revenue losses because affected producing units are shut down for repairs and also the high cost involved in replacing corroded pipelines or units [28]. The greater the oxygen concentration in the water the higher the rate of corrosion. There are also some factors that facilitate the oxygen attack in a system. These are: temperature of the feed water, flow rate, dissolved solids and system's physical conditions. In relation to the feed water temperature, the concentration of dissolved oxygen is usually around 8ppm at ambient temperature. It was also suggested that higher feed water temperature favours the occurrence of severe corrosion on metal surfaces because this temperature leads to an accelerated oxygen reaction [27].

Pitting is the most common type of corrosion and is caused by the presence of DO in water. Figure 4 shows a corroded pipe as a result of pitting. Pitting is very destructive, difficult to detect and has the ability of penetrating deep into the metallic structures, causing perforation which can lead to failure of production units [27].

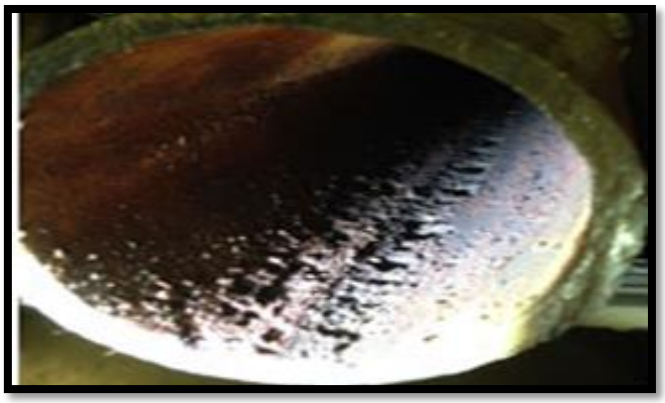

Figure 4: Corroded pipe [3]

Oxygen related corrosion can be explained as an electrochemical process involving anodic and cathodic reactions as described in equations 1 to 3 below and this usually occurs on any metallic surface. The oxygen rich water on

contact with the metallic surface represents the cathode, while below the metallic surface is the anode.

At the anode, the metal dissociates into an ion and two free electrons forming the pit site.

$$Fe \rightarrow Fe^{2+} + 2e^{-} \quad (1)$$

At the cathode, the two free electrons are absorbed by the water molecule and hydroxyl ions are formed.

$$^{1}/_{2}\, O_2 + H_2O + 2e^{-} \rightarrow 2OH^{-} \quad (2)$$

The overall reaction then involves the ion (Fe^{2+}) travelling to the oxygen rich environment and reacting with oxygen and water to form hydroxyl ions as shown in equation 3. Fe^{2+} also reacts with hydroxyl ions to form Fe_2O_3 which are rust solid debris that can form in the system and usually results in blocking or clogging of the system.

$$Fe + {}^{1}/_{2}\, O_2 + H_2O \rightarrow Fe(OH)_2 \quad (3)$$

Corrosion in the oil and gas industry may not be the only problem of DO in water. Its removal is also necessary for production of food (for better food taste and beer making) [3, 29], nuclear and biotechnological industries, pharmaceuticals and semiconductors [5, 26, 30]. An example of DO problem in the semiconductor industry is in silicon wafer production. Ultrapure water is one of the requirements needed for this production and the presence of DO leads to formation of native oxide layer on the silicon wafer surface, thereby hindering high performance of the production process [31]. In the production of beverages, ultra-pure water is required to prevent the oxidation of organic components which may lead to an alteration in their qualitative and quantitative values [8].

Due to the problems resulting from the presence of DO in water, it leads to high economic costs of fixing corroded units and loss of production. Control of DO in feed water is therefore an important process and corrosion and other problems can therefore be minimized through a proper process design that target the reduction of the level of DO present in the water source [27].

2.3 Deoxygenating Methods

So many methods have been proposed for deoxygenation purposes. These methods can be divided into physical and chemical techniques. Drawbacks from each of these two categories have led to efforts into developing newer technologies that can reduce the oxygen content in water to a substantial level [8] and are generally referred to as compact deoxygenation methods. They sometimes combine simultaneously physical and chemical methods [26].

2.3.1 Physical methods

Physical methods include thermal degassing, vacuum degassing and gas stripping [32].

2.3.1.1 Thermal degassing

Thermal degassing achieves removal of DO by mixing water with high temperature steam [30]. The major disadvantage of this method is that it is only applicable in power stations where there is availability of low cost steam. It is also not capable of reducing the DO level to very low levels [30]. This method involves high operation cost mostly as a result of heating. It is also stated that with the physical methods, achieving a reduction of DO in ppb from ppm is very difficult [23].

2.3.1.2 Vacuum degassing

In the vacuum degassing method, an assumption is made in which the partial pressure of oxygen present in a water system is a function of the entire pressure of the unit system. So the process of water deoxygenation is achieved by applying a vacuum to the unit and consequently results in the reduction of the oxygen concentration in the system, by reducing the partial pressure of oxygen. This reduction in partial pressure results in oxygen coming out of the water to re-establish equilibrium. Vacuum degassers are usually used where stripping

gases are scarce. It has some disadvantages, such as its inability to achieve very low DO levels. However, it costs a lot to install and maintain. It uses high towers that may be affected by wind movement [6]. In general, physical methods have drawbacks as a result of their bulkiness.

2.3.1.3 Gas stripping method

In gas stripping, Henry's law applies and is based on the relationship between the amount of a given gas and its solubility in water with the partial pressure of the gas at constant temperature [33]. In this case, water deoxygenation is based on the fact that, the amount of DO in water is directly proportional to the partial pressure of oxygen gas in the gas phase in contact with the water. The removal of DO by gas stripping method can be achieved by both co-current and counter-current flow of the water in the direction of the stripping gas through a column of beads. By stripping the system with other gases, the partial pressure of oxygen will therefore be reduced. Nitrogen is the most used stripping gas in this method [6]. Advantages of this system include the fact that it is not bulky and the waste gas at the top of the tower can be re-used by some other industries. The disadvantage is the waste gas if not channelled properly may lead to environmental pollution [34].

2.3.2 Chemical methods

Deoxygenation of water by chemical method refers to the addition of chemicals into water. Secondary compounds are thus formed as a result of reaction between the dissolved oxygen and the chemicals. An example is the addition of sulphite-based chemical. Sulphates are thereby formed when the sulphites chemically reacts with the DO [27] as illustrated in equation 4.

$$2Na_2SO_3 + O_2 \rightarrow 2Na_2SO_4 \quad (4)$$

The chemicals added for the purpose of removal of DO are termed "oxygen scavengers" and examples include hydrazine and sulphite-based chemicals for example; ammonium bisulphate, potassium bisulphite and sodium bisulphite [5, 35]. Organic oxygen scavengers such as hydroquinone and ascorbates, and catalysed forms of hydrazine and sulphites are also used as chemical oxygen

scavengers. The hydrazine related chemical reaction on DO is shown in equation 5.

$$N_2H_4 + O_2 \rightarrow 2H_2O + N_2 \quad (5)$$

The downside of using chemicals like the sulphites is that they increase the total dissolved solids present in the water and chemicals such as hydrazine are very toxic in nature and a suspected carcinogen and should therefore be handled with extreme caution [22]. There could also be issues arising from shortage of supplies in the case of deep-water operations and remote industrial locations [9]. The use of sulphites in high pressure boilers tend to form sulphur dioxide and hydrogen sulphide which can lead to further corrosion of the systems. These chemical scavengers are also not robust; the type of process application determines the applicable chemicals [27]. Too much or too less of these chemicals can also lead to various forms of corrosion [36].

Chemical methods are usually used in scenarios where mechanical deaerators fail to remove or lower the concentration of DO to the required level needed for the specific process application or where an immediate action is necessary to prevent pitting**-**type corrosion from occurring [27].

2.3.3 Compact deoxygenating methods

The compact deoxygenating methods are usually a combination of physical and chemical processes using a catalyst. Minox and Seaject deoxygenating processes are the two major compact systems in place at present.

2.3.3.1 Minox technology

In Minox technology, the DO is removed by the principle of high gas/water ratio stripping process. Nitrogen gas is usually used as the stripping gas and the column is packed with palladium coated alumina spherical balls [37]. The Minox process uses nitrogen gas in either one-stage (counter-current) or two-stage (co-current) process for water deoxygenation [6]. Figure 5 shows the schematic flow diagram of a one-stage process in which the nitrogen gas is introduced in a counter-flow to the water inlet stream. The oxygen saturated water is feed into

the mixing unit through the upstream, while the nitrogen flows through the downstream. The water and nitrogen mixes so well that a simultaneous reduction of DO occurs as a result of the stripping action of nitrogen [37].

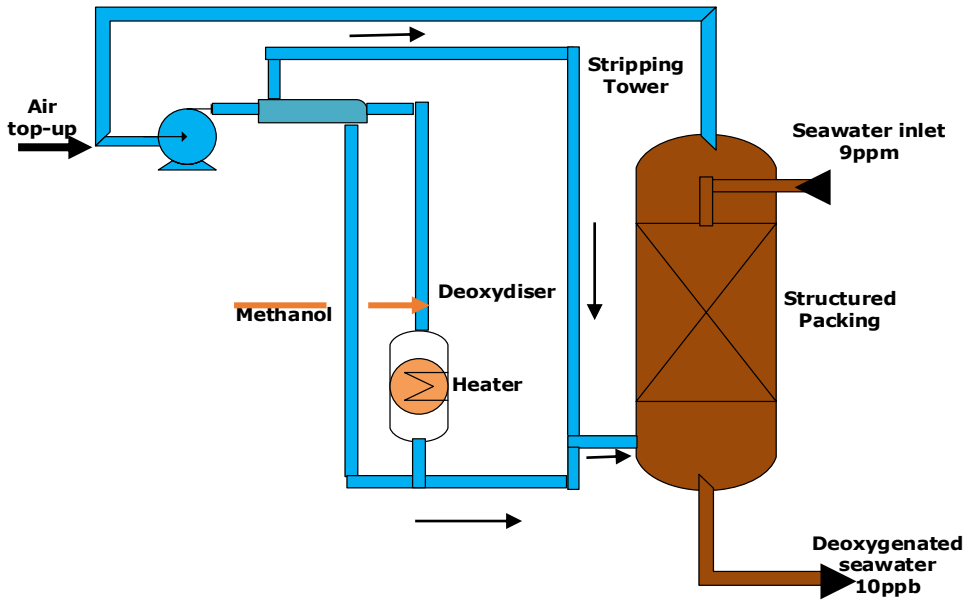

Figure 5: Minox Compact tower (one-stage process) [37]

Figure 6 shows the schematic flow diagram of a co-current process which is carried out in a two-stage process of the static mixer [6]. The difference between the 1st and 2nd stage process is that, nitrogen gas is regenerated in the 2nd stage in a closed looped system and the nitrogen and water are introduced into the static mixing unit co-currently [37].

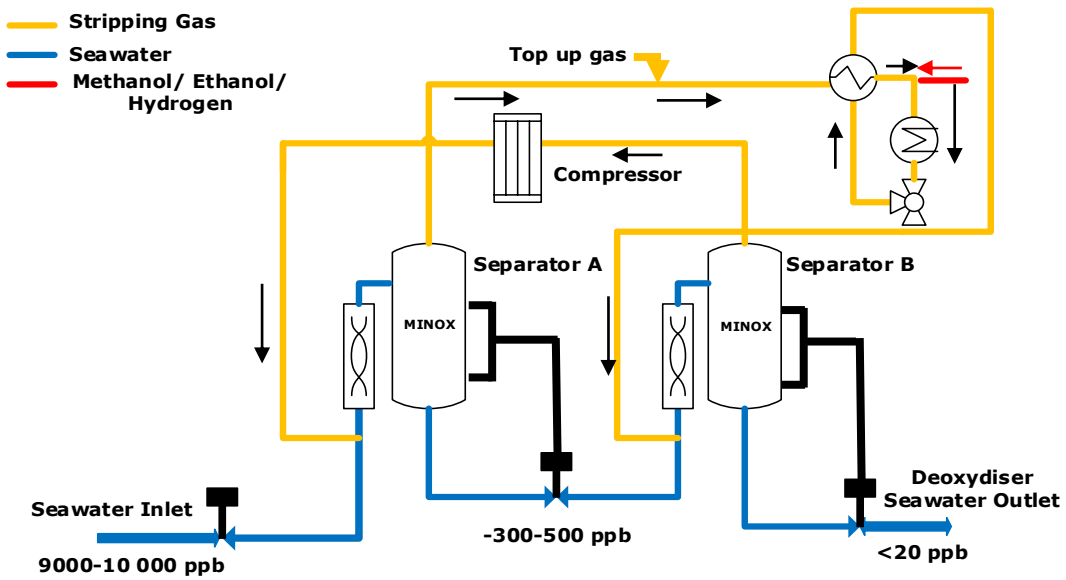

Figure 6: Ultra Minox compact Stage 2 (two-staged process) [37].

Advantages of the Minox systems are compactness, small foot print to fit in a small space, lower energy consumption and no need for chemicals [3, 37]. A major disadvantage is that it introduces nitrogen component into the water [30].

2.3.3.2 Seaject Technology

An example of wet combustion catalytic process is the Seaject deoxygenation process shown in Figure 7. In this process, hydrogen is being added into the water stream and mixed thoroughly with the help of a mixing unit. This mixture is then passed through a bed containing palladium catalyst (in the form of coarse spherical beads, of diameter in the range between 0.3 to 1 mm), where the DO reacts with the hydrogen, thereby producing only water as a by-product. This process involves a controlled scenario where the inlet water is channelled into the mixing unit thus avoiding further contaminations which may affect the proposed chemical reaction. The advantage of this system is that it needs no vacuum or deaerators and it is more compact than the Minox process. The catalyst beads require a backwash quarterly, and this does not affect its production as there are normally two beds. The downside of this process is linked to high operational cost probably as a result of large amount of precious metal catalyst needed for the process to take place [9].

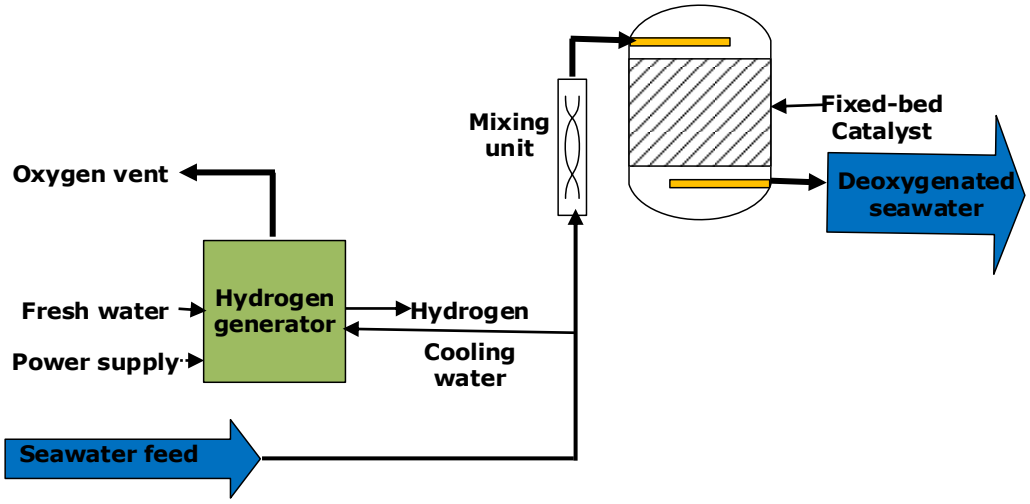

Figure 7: Flow diagram of a Seaject deoxygenating process [9]

2.3.4 Reviews on laboratory-based Deoxygenating methods

Several applications of membrane reactor processes in dissolve oxygen reduction have been reported in literatures [30]. These processes utilize a heterogeneous catalytic method involving the reduction of DO with the application of hydrogen. Most commonly reported is the hybrid concept which involves deoxygenation by dissolving hydrogen in water and passing it over a palladium catalyst [8, 29]. Literatures have reported different ways this process is being carried out, but are majorly focused on the use of palladium catalyst.

Sinha et al. [30] used a membrane reactor in water deoxygenation experiment where his method used a dual principle of both physical and chemical methods. A hollow-fibre membrane packed with catalyst in the shell-side of the reactor using palladium doped anion-exchange resin based on styrene and divinyl benzene was employed. The hydrogen in this principle served simultaneously both as a purging gas (physical stripping) and as a reducing agent (chemical reaction).

Studies also report on the use of polymeric membranes [29, 38]. Lebedeva et al. [29] used porous polypropylene hollow fibre membranes in a catalytic membrane reactor. This membrane was coated with a palladium catalyst. Two studies were simultaneously carried out looking at the amount of palladium deposited employing different deposition methods. This resulted in membranes

having palladium metal >20% wt Pd in one and the others had a range of 0.3-0.73 wt Pd. They also used hydrogen as a reducing agent, where it was feed co-currently with water into the hollow-fibre membranes. They used a magnetic stirrer in the reactor while the process was a batch process. A DO reduction from 8.8 ppm down to 0.76 ppm was achieved.

Li et al [23] tried developing membrane ultra-violet (UV) reactor, where they used silicone rubber hollow fibre membrane to surround a UV light. Hydrogen was also used in this process as a reducing agent, but was feed into the reactor shell while the dissolved oxygen saturated water was feed into the hollow fibre lumen. Hydrogen gas in this case was used for both physical stripping and chemical reduction. The percentage dissolved oxygen level was not stated to show how effective it was.

Ito et al [39] reported the removal of DO using non porous hollow-fibre membrane. A theoretical study on oxygen permeation was carried out on the non-hollow membrane to evaluate the oxygen's permeability considering gas phase driving force [39]. They suggested measuring the permeabilities of individual permeating gases in the gas of vapour state. Nitrogen, oxygen and water vapour were measured. This also contributed to the carrying out of permeation studies of some single gases in this study.

Gross et al carried out a similar research employing same principle used by Seaject technology. Palladium catalyst was deposited on a weak anion exchange resin by ionic exchange method on a fixed bed reactor. A DO concentration of less than 10 ppb was achieved at ambient temperature. The method involves the introduction of hydrogen into a water stream which is then mixed with the help of a static mixer to enable the dissolution of hydrogen into the water. After which the mixture is passed through the fixed bed reactor [8]. In the membrane process, periodic cleaning of the catalyst with sodium hydroxide at 60^{o}C is encouraged because of microbial growth and organic contamination that may occur hindering the effectiveness of the catalytic activity [8].

2.4 Membrane Technology

Membrane technology has drawn much interest as well as being competitive to other conventional methods particularly in areas such as gas separation, wastewater treatment and also as integrated reactors in applications where space is a major issue [40-43]. In water purification technology, membrane technology has dominated based on efficiency [44]. They are also energy efficient and environmental friendly as their use poses little or no risk to human or aquatic life [45].

There are three main types of membrane materials: polymeric (organic membrane), metallic (inorganic membrane) and ceramic (inorganic membrane) [46, 47]. Polymeric membranes are most commonly used due to being cost effective, but the down sides are that they are restricted to operations where mild thermal, chemical and mechanical applications are required. They can only be applicable to operations in temperature range between 90^{o}C to 100^{o}C [48]. Metallic and ceramics on the other hand are more robust and can operate in harsh conditions and are known to provide reliable results over a long period of operation. They have unique physical and chemical properties (can withstand high pressure drop, controllable pore size distribution, good scalability) thereby providing great potentials for catalytic applications [48]. Metallic membranes are stable at temperature ranging from 500 to 800^{o}C while ceramic membranes are stable at temperatures well above 1000^{o}C [46]. Ceramic membranes are known to be far more expensive than the polymeric membranes. However, sustainable development have made the ceramics now more affordable, effective and even more compact and are reported to be an alternative material in water treatment applications [44].

Membranes can also be classified as dense or porous membranes, with the porous further classified based on their pore sizes [49, 50]. They are termed macroporous if their pore size is >50 nm, mesoporous if the pore size falls within the range >2< 50nm, and microporous if pore size <2nm [49].

2.4.1 Ceramic membranes

Ceramic membranes have actually drawn keen interest in the last couple of years to researchers due to their enormous advantages in various applications [51-54]. In the industrial sector, porous ceramic membranes have great advantages in that, they are thermally stable and can withstand a wide range of temperature, chemically stable which allows applicability in any pH and organic solvent, have low thermal conductivity and have high amount of hardness and compressive in strength. They are also easy to clean when fouled in cases where application causes great foulness. They also possess a greater lifetime when compared to organic membranes [55, 56]. As a result of these properties, the porous ceramic materials are used variously as supports for catalyst, filters, insulators, membranes and biomaterials [55]. Some disadvantages of the use of ceramic membranes is that they are brittle, hence the need to handle with extra care. As a result of their brittleness, care is also made in the choice of ceramic holders (housing) and seals so as not to damage the ceramic membranes [44].

There are three factors that govern the applicability of a porous ceramic material, these are: its pore size, wall thickness and its porosity. These ceramic membranes are usually composites, that is, they are made up of one or more different layers of materials which serve a number of purposes as shown in Figure 8. A membrane structure is comprised of a support having bigger pore sizes (macroporous) and this provides mechanical support; intermediate layer(s) having a much smaller pore sizes structure (mesoporous) which serves as an intermediate between the top and the bottom layers, thereby providing a bridge as a result of the great pore size difference; and then a top layer which has tiny pore (microporous) where the actual membrane activity takes place [49].

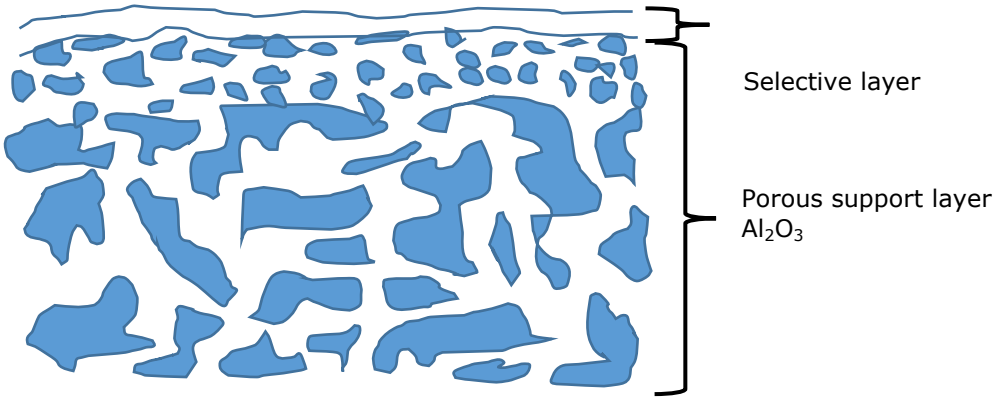

Figure 8: A schematic diagram of a composite membrane

Ceramic membranes can be defined as semi permeable materials, barriers or even as an interphase between two phases [49, 56]. A schematic diagram showing the membrane being used as a semi-permeable material between two interphases is shown in Figure 9. Ceramic membranes can be made from oxides of different metals like such as alumina (Al_2O_3), silica (SiO_2), zirconia (ZrO_2) and titania (TiO_2) or even a combination of these metals. The type of ceramic material chosen are usually based on the specific requirement of the industrial application [44].

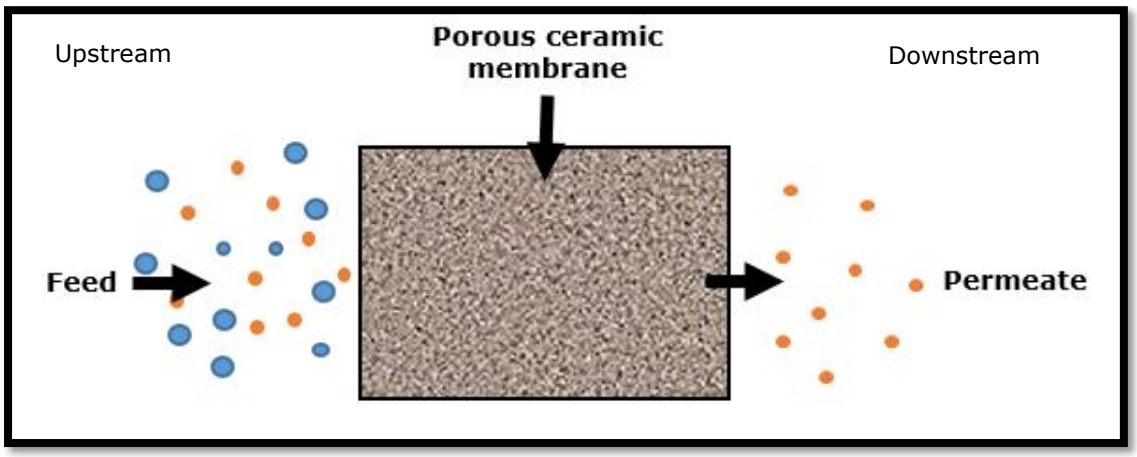

Figure 9: Schematic representation of a separation process between two phases using a membrane as a perm selective device/barrier [56].

The ceramic materials/membranes could be in different forms or shapes such as tubular, plate or disc structure [49]. The support being tubular has an advantage such that it enhances the separation area per unit volume of a reaction process [49, 57].

Kang 2007 [49] stated that the permeability/permeance and separation factor are the two important performance indicators of a membrane quality while Mulder M. [56] stated that a membrane's performance is dependent on its selectivity and flow through a membrane per unit area (flux). Looking at the above statements, the following performance indicators will be further explained for a better understanding as they are intertwined.

A flow through a membrane is given by the volume of the component flowing through the membrane per unit area per unit time [56]. The ideal selectivity

performance of a membrane over one or more components is explained in relation to a mixture of either liquids or gases and is given by the permeance of component (a) over component (b) or the flow rate of component (a) over flow rate of component (b). The symbol α is used to denote the separation factor and it is used in defining the selectivity equation. The equation is therefore illustrated in equation 6. Separation is said to have not taken place in cases where $\alpha_{a/b} = \alpha_{b/a} = 1$ [58, 59]

$$\propto_{a/b} = \frac{J_a}{J_b} = \frac{F_a}{F_b} \quad (6)$$

Where $\propto_{a/b}$ is the perm-selectivity of component a to component b, J_a & J_b are the permeances, F_a and F_b are the flow rates of components a and b respectively.

The permeance of a gas can be defined by equation 7 [59], which is the flowrate of the particular gas per unit area of the membrane divided by its pressure difference.

$$J = \frac{F}{A\Delta P} \quad (7)$$

Where J is permeance ($mol.m^{-2}.s^{-1}.Pa^{-1}$), F is the flowrate, A is the surface area of the membrane (m^2) and ΔP is the pressure drop of the gas across the membrane. If a membrane's thickness is taken into account, the permeance then becomes permeability ($mol.m^{-1}.s^{-1}.Pa^{-1}$) [60] as shown in equation 8.

$$J = \frac{F}{A\Delta P} x\ l \quad (8)$$

Where l is the thickness of the membrane (m)

Flux Q ($mol.s^{-1}.m^{-2}$) of a membrane is calculated from equation 9

$$Q = \frac{F}{A} \quad (9)$$

2.4.2 Transport mechanisms in a Membrane

There are various transport mechanisms that takes place during a membrane process. Though in the traditional sense this membrane acts as a semipermeable barrier in a two phased system, the membrane has the ability to transport selected specie over the others from the upstream to the downstream. This is usually as a result of the differences which could either be physical or chemical or even both, existing between the membrane and the permeate (selected specie). This selectivity is termed separation and the principle governing this can be explained by the gas transport mechanisms [56]. The assumption associated with the principle linked to transport of gases, is that, each pore represents a capillary tube and this serves as a passage for permeating species [49]. This is in respect to Knudsen, slip and viscous flow mechanisms [49]. Some of these gas transport mechanism also takes into considerations the molecular mass of the gases and their atomic sizes [49].

2.4.2.1 Knudsen flow mechanism

In this case, the mean free path (λ) of the diffusing gas molecule is greater than the membrane's pore size (r_p), that is: (r_p/λ) < 0.05, and this leads to a situation where the collision between molecule-pore wall is greater than that between molecule-molecule collision as shown in Figure 10 [49]. The Knudsen flow mechanism is predominant in the macro and meso porous membranes and equation 10 defines the Knudsen number [49, 59].

$$Kn = \frac{\lambda}{r_p} = \frac{16\mu}{5\pi\bar{P}}\sqrt{\frac{\pi RT}{2M}} \tag{10}$$

Where Kn is the Knudsen number, λ is the mean free path, r_p is pore radius (m), μ is viscousity (Pa.s), $\bar{P}$ is average pressure across the membrane (Pa), R is gas constant (8.314 m^3Pa/mol K), T is absolute temperature (K) and M is the molar mass of the gas (g/mol).

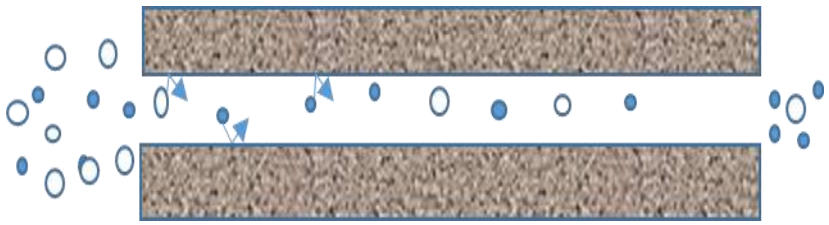

Figure 10: Schematic diagram illustrating Knudsen flow mechanism

2.4.2.2 Viscous flow

In the viscous flow mechanism, the membrane's pore size (r_p) is greater than the mean free path (λ) of the diffusing gas molecule, that is, (r_p/λ) > 3, and this leads to a situation where molecule-molecule collisions predominates over molecule-wall collisions as shown in Figure 11 [49]. This mechanism does not lead to any meaningful separation because the viscousities of gases are relatively close to one another.

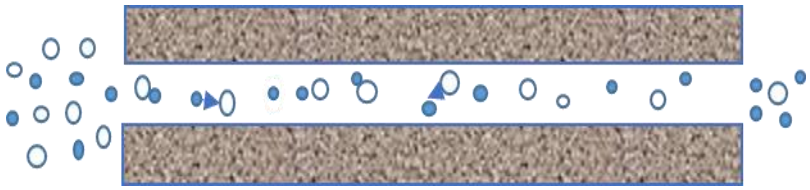

Figure 11: Schematic diagram illustrating viscous flow mechanism

2.4.2.3 Surface diffusion

Surface diffusion is a type of transport that relies on the relationship between the nature of the membrane's surface and that of the permeating component. In a case where the permeating component shows a strong affinity for the membrane surface, the components tend to get adsorbed along the pore walls and the diffusion or flow of this permeating component along the pore's surface is called surface diffusion and this takes place at either low temperature or high pressure or both. The properties of the membrane's pore surface determines the surface type of diffusion and it is illustrated in Figure 12 [49, 59].

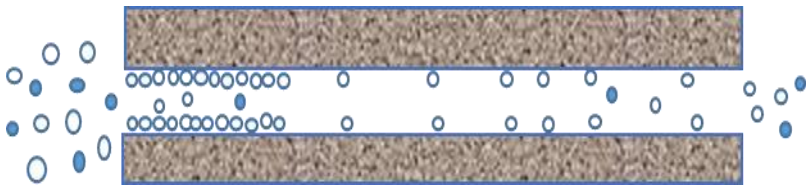

Figure 12: Schematic diagram illustrating Surface diffusion

2.4.2.4 Molecular sieving

Molecular sieving is a type of transport that takes into consideration the pore sizes of the membrane material and the permeating species respectively. A membrane exhibiting molecular sieving in a process of separating a mixture of gases will favour the transport of gases with same or smaller size than the larger sized gases (Figure 13), there by achieving a high separation [61]. For example, a scenario where the gas to be separated in a mixture is known, a membrane with a smaller pore size than that gas diameter should be used to achieve this separation.

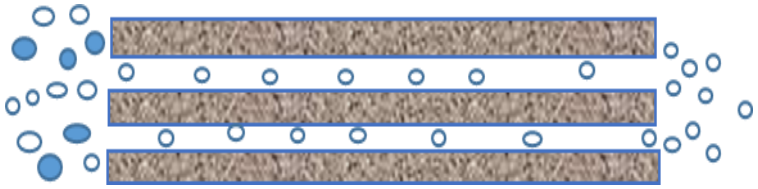

Figure 13: Schematic diagram illustrating Molecular sieving

2.4.2.5 Solution diffusion mechanism

Solution diffusion type of mechanism is usually achieved by non-porous membranes which could be termed as dense. In this case, the permeating species will have to dissolve into the membrane's material and then diffuse through it down the concentration gradient (Figure 14). In a mixture of gases undergoing solution diffusion, separation is achieved by the highest amount of permeating gas that could dissolve and diffuse most [61].

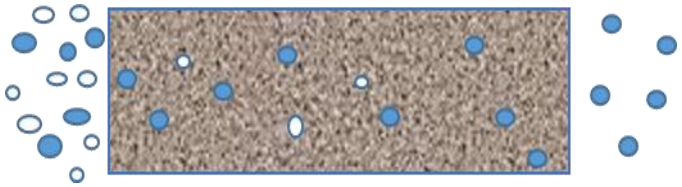

Figure 14: Schematic diagram illustrating Solution diffusion mechanism

2.5 Membrane Reactor Concepts

The membrane reactor concept is an integrated technology, it combines chemical reaction and/or membrane separation in a single unit [29, 62]. The membrane reactor could also be viewed as a reaction chamber which contains a membrane serving as a reaction contact for reactants and also as a removal system for the products that are formed [14, 62].

A membrane can serve 3 main functions, namely, as an extractor, distributor and a contactor [1, 47]. Figure 15 shows schematic representation of these functions.

2.5.1 An extractor

In the extractor, the membrane has the ability to selectively extract the reaction products from the reaction area. In other words, readily permits the permeation of products from reaction side to product side [47].

2.5.2 A Distributor

In the distributor, the membrane has the ability of controlling the addition of one or more of the reactants into the reaction side [1].

2.5.3 A Contactor

In the contactor, the membrane has a unique ability to be used as a contact medium for reactants and catalyst leading to an effective catalytic reaction zone [1]. It therefore intensifies the reactant-catalyst contact [47].

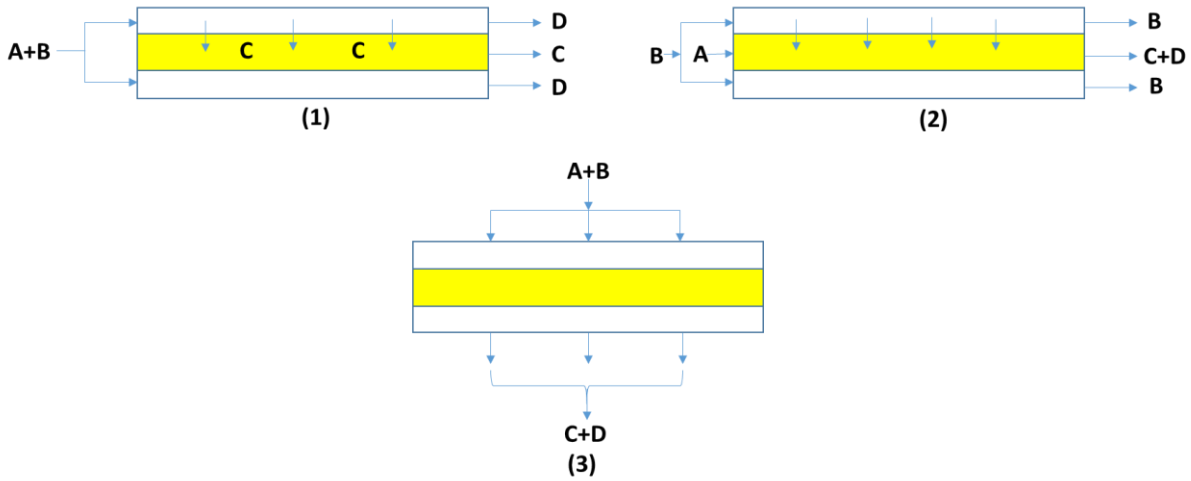

Figure 15: Concepts of a membrane reactor [44]

2.5.4 Other Functions

The above functions can be said of a typical membrane concept, but there exist some membrane configurations that deviate from those mentioned above. An example is the flow-through membrane concept where selective permeation does not occur, instead, the entire feed is allowed to permeate through. Volkov et al [1] further stated that there are two types of three-phase catalytic membrane concept: flow-through and interfacial type of contractors. The flow-through membrane concept is usually expected in a catalytic membrane reactor, where the reactants are made to converge on the membrane surface, react as a result of intensive contact, then permeate through with negligible mass transport resistance [12, 47].

For the purpose of this study and the nature of the delivery of the reactants into the membrane surface, flow-through contactor approach has been selected and applied for achieving reduction in the concentration of DO in water as shown in Figure 16. In other words, the catalytic membrane reactor is designed to favour a flow-through concept and this involves the application of a porous catalytic membrane [1]. The catalyst is deposited into the pores of the membrane and the reactants are forced to flow-through the pores of the membrane because the membranes are sealed at both ends making the pores the only exit of the reaction product. With this happening, the reaction residence time is short with a high catalytic activity taking place over the highly dispersed catalysts in the pores of the membrane.

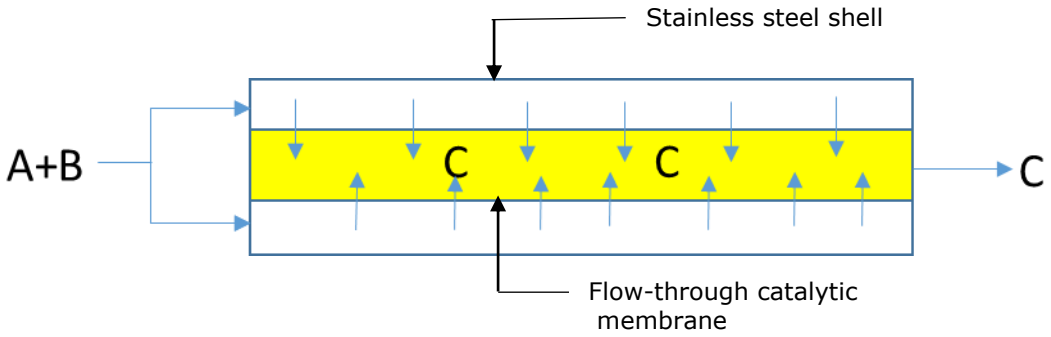

Figure 16: Flow-through membrane reactor

The aim of applying flow-through concept of the catalytic membrane reactor process containing palladium or platinum impregnated catalytic porous ceramic membranes is mainly to perform and achieve complete conversion in the shortest possible time making efficient use of the highly active catalytic site (efficiency) in a single stage.

2.6 Catalytic Membrane Reactor Technology in Water Deoxygenation

2.6.1 Catalysts for CMR Water Deoxygenation

A catalyst can be defined as a substance either liquid, gas or solid that can assist or facilitate the rate of a chemical reaction without itself being consumed in that process. The type of catalyst needed for a reaction is highly dependent on the nature of the reaction in question. A catalyst works by lowering the pathway required by the reactants towards achieving a product as seen in Figure 17 [63].

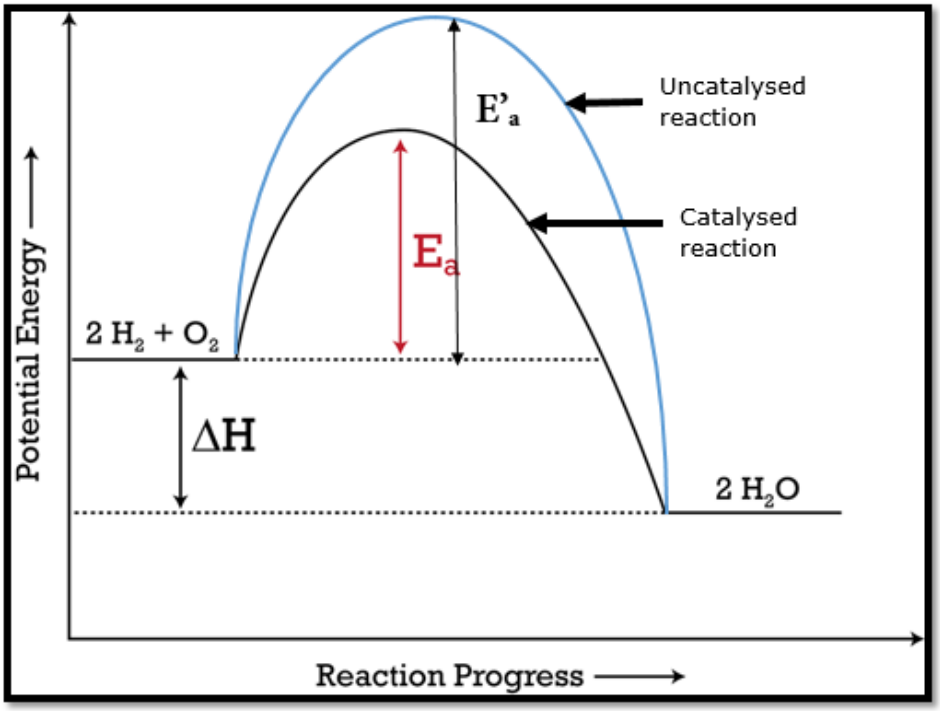

Figure 17: The reaction path of water formation [57]

Catalysts are widely used in environmental, pharmaceuticals, petroleum and energy industries for various applications [44]. A catalyst could either be homogenous or heterogeneous depending on whether it is in the same phase or not as the reactants [63]. In a reaction that involves a heterogeneous catalyst, the nature of its coupling to the support is of importance to the researcher. There are three main heterogeneous catalytic coupling methods which are applicable in catalytic membrane reactors. As shown in Figure 18, the catalyst could be deployed as conventional pellets on the support's surface as seen in Figure 18(a), impregnated into the pores of a support (18b), or deposited as a thin layer on the top of the membrane as seen in Figure 18(c) [49].

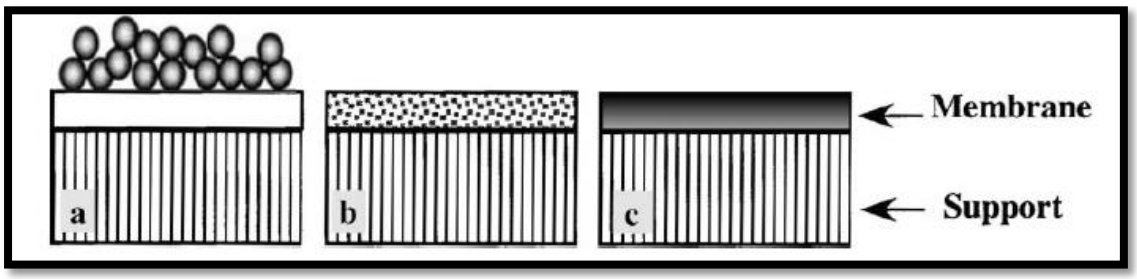

Figure 18: Main heterogeneous catalytic coupling methods (a) Bed of catalyst on an inert membrane; (b) catalyst dispersed in an inert membrane and (c) catalytic membrane due to composition of the membrane material [65].

For the purpose of this study, a heterogeneous catalyst is employed and coupled to the ceramic material as seen in the method shown in Figure 18b. This will be done in a way so as to achieve a porous catalytic medium, thereby providing a wider catalytic surface area for the reactions to take place.

The choice of the types of heterogeneous catalyst made in this study were motivated by four factors, namely; selectivity, activity (the ability to promote the reaction rate), stability and regenerability [11]. Based on these four factors, palladium and platinum which are known to catalyse the activation of hydrogen and reaction involving hydrogen were chosen. These noble metals belong to group VIIIB metals of the periodic table shown in Figure 19 and are used for removal of DO in water [66]. Palladium and platinum metals are also classified as platinum group metals, and they are known to be very efficient and effective in hydrogenation reactions. This is attributed to their ability in dissolving a huge amount of hydrogen in hydrogen related reactions [1]. Both catalysts have also proven to be selective in DO reactions for the production of water [22, 67].

Palladium metal shows a strong and outstanding ability in aiding hydrogen dissociation/ dissolution in any hydrogen transport reaction [68]. Catalytic membrane reactor applications involving palladium as a catalyst has also been reported for reactions such as hydrogenation, dehydrogenation, hydrogen peroxide synthesis and water-gas shift reactions [68, 69]. Studies have also shown that palladium metal is highly selective in the separation of hydrogen gas [18, 70, 71].

Platinum catalysts are as well highly recommended in reactions involving hydrogen oxidation, oxygen reduction reactions [72] and hydrogen evolution [73]. These reactions tend to occur on the platinum's surface [74].

Literature has extensively reported on the use of palladium in water deoxygenation [22, 38], but these studies were executed on catalyst beds where pellets were used (packed bed reactors). Most researchers [67, 74, 75] who carried out water deoxygenation using platinum catalyst were more of theoretical and modelling nature and little was said on the experimental/methodological aspect. The current work thereby investigates both

palladium and platinum metals for both membrane and fixed-bed reactors bearing in mind the amount of catalyst needed as a result of its cost implications.

Zhang et al [13] discussed the fears associated with the use of platinum group metals. They stated that these metals are scarce and therefore very expensive, and hence minimising the amount of precious metal would be ideal because just a little amount of these catalyst is necessary for a reaction to occur. They went ahead and suggested low-content loading of precious metals on supports as a means of reducing the amount needed for a reaction. They also stated that these metals have no adequate alternatives, hence the need for innovative methods of loading and dispersing the active metal.

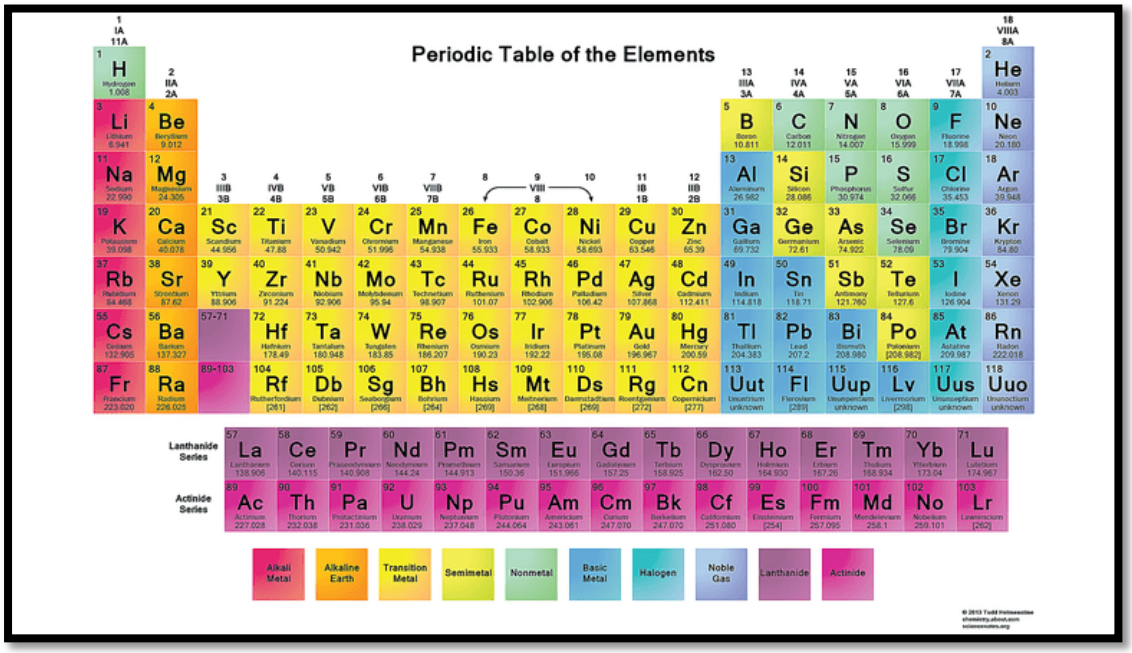

Figure 19: Periodic table showing group VIII metals [76]

The preferred methods for catalytic membrane preparations will determine the amount of catalytic materials needed and subsequently impacts on the cost. In terms of durability, studies have shown that palladium-based composite membranes can be stable for up to 10 months according to a national energy technology laboratory (NETL) report [68].

As a result of the advantages and features of the alumina ceramic material and noble metals chosen for this work, the production of composite membranes that

have a low metal loading and high reactivity property is a major objective in this study. The porous alumina ceramic support provides a suitable surface for the impregnation of the metals in a highly dispersed fashion. During the catalytic membrane preparation, defect sites could occur on catalytic surfaces as a result of their complex geometry and the reaction mechanism may become difficult to be reliably predicted. The nature of particle size as well as the pore shape are all taken into account. The defect sites are actually seen as an advantage in DO removal in that they are considered to be more active sites and help in adsorption and desorption of reactants and products respectively [77].

2.6.2 Source of hydrogen supply in a hybrid water deoxygenating process

The source of hydrogen needed for the water deoxygenating process is very crucial due to its high flammability and possibility of an explosion if there is a leak. In a laboratory scale deoxygenating experiment, hydrogen cylinders could be used to supply the required hydrogen gas. In the case of offshore industries, where the storage of hydrogen cylinders at platforms are highly discouraged due to their high flammability property, other options of hydrogen supply have to be considered. An example is the Seaject process where the water electrolysis method is used to generate the hydrogen required for the DO process [9]. Analysis were however made considering two factors: water temperature and water salinity. At higher water temperatures and water salinity, the concentration of dissolve oxygen in water reduces respectively and vice versa. Therefore depending on the water temperature and salinity level, about 22 litres of hydrogen will be needed for a Seaject operation for every cubic meter of water requiring deoxygenation [9]. In the electrolysis method shown in Figure 20, water is charged with an electric current which leads to the water molecule splitting into hydrogen and oxygen components. The electric current produces a charge that breaks up the chemical bond existing between the hydrogen and oxygen molecules and consequently produces molecular oxygen and hydrogen ions. At the anode, reaction also occurs and oxygen gas is produced as shown in equation 11 [78] but it is vented off. The oxygen can also be used by divers.

$$2H_2O \rightarrow O_2 + 4H^+ + 4e^- \quad (11)$$

The hydrogen ions migrate through the semi-permeable membrane into the cathode where they react with electrons to generate hydrogen gas as shown in equation 12. This hydrogen gas produced is subsequently directed into the reactor section of the water deoxygenating process.

$$4H^+ + 4e^- \rightarrow 2H_2 \quad (12)$$

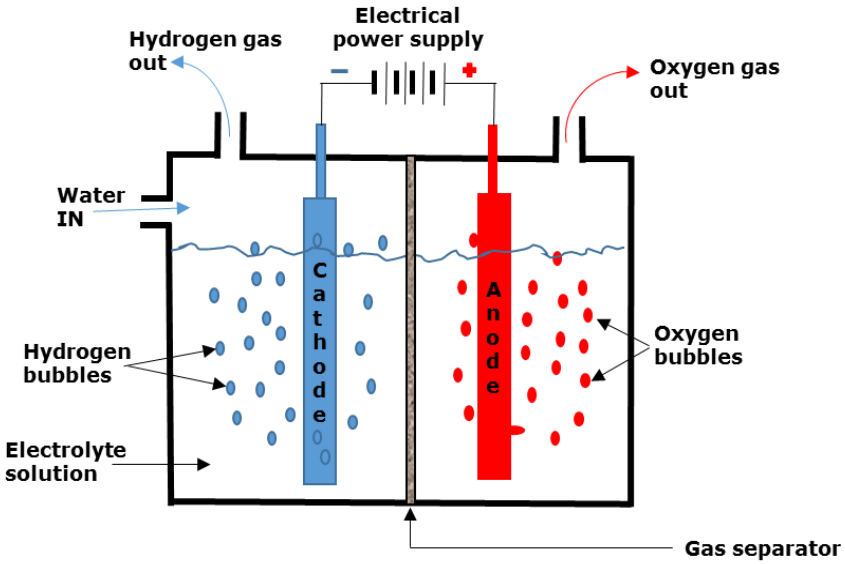

Figure 20: Hydrogen generation through electrolysis [78]

2.7 Catalytic Membrane Preparation

The following sections discuss the various ways in which the catalytic membranes can be prepared.

2.7.1 Palladium Membrane preparation

Several methods have been developed for the fabrication of palladium based membranes. These includes: chemical vapour deposition, spray pyrolysis, magnetron sputtering, electroplating and electroless plating techniques [18].

2.7.1.1 Chemical vapour deposition (CVD)

This method involves the thermal decomposition of volatile precursors on the near surface of substrates to obtain a thin film on a support material [62]. The method allows for controlled palladium deposition thereby capable of controlling the thickness of the film [68]. The downside of the CVD process is that the rate of palladium deposition is not high and the chemicals required are very toxic and are also required in large quantities and therefore, not very cost effective. This method could be difficult if carried out in a larger scale so it is mostly applicable in a small scale arrangement [79].

2.7.1.2 Electroless plating (ELP)

This technique focuses on the target surfaces and controls autocatalytic reduction of the metastable metallic salt complexes. It is an oxidation-reduction reaction, that is, anodic oxidation of the reductant and cathodic reduction of the metal occur simultaneously [62, 80]. Advantages of ELP technique includes; simplicity of the deposition process with the use of simple equipment, low cost, high deposition achievable, uniformity of deposition on complex shapes and applicability in a larger scale [18]. A limitation is that plating of only very few metals has been documented and the process of co-plating is not usually very successful [79, 80].

2.7.1.3 Magnetron sputtering

Magnetron sputtering is a type of technique used in coating thin films on materials of different shapes [79]. An advantage of this method is that, it is applicable in a large scale process. The downside to the process lies in the difficulty of controlling the sputtering composition [79].

2.7.1.4 Electroplating

This technique involves coating of a conductive material by electrical current involving the reduction of cations from the plating solution. An advantage of this method is that deposition of palladium metal can be high. The limitation of the process is that it is only applicable to materials that are conductive in nature, thus, cannot be carried out on ceramics as they are not conductive. It is also a complex method [79].

2.7.2 Platinum Membrane preparation

Two types of platinum deposition methods will be discussed. These are evaporation-crystallization and anionic impregnation methods [15, 81].

2.7.2.1 Evaporation-crystallization impregnation

This type of catalytic deposition method aims at impregnating the platinum metal into the pores of the support, and this is achieved by dipping the ceramic support into a platinum precursor solution for some hours. It could also be referred to as "wet impregnation" [82] which is the simplest method of preparing a platinum impregnated membrane. The principle of wet impregnation involves an adsorption mechanism which draws the metal precursor into the pores of the support [83]. Example of this process is given by Uzio et al 2003 in which the ceramic material is initially dipped in water for 2 hours, then in a platinum solution (0.1 – 10 g Pt/L) for about 5 to 10 hours under stirred condition. This method is also referred to as "reserviour method" [15]. Advantages of this technique include simplicity and thus requires simple equipment and a highly dispersed catalytic material is achievable.

2.7.2.2 Anionic impregnation

The mechanism governing this type of impregnation is that of an electrostatic interaction between the platinum containing specie $(PtCl)^{2-}$ and the hydroxyl group present in the support surface (OH_2^+) [15]. In this method, the ceramic material is also soaked in water, and then in the platinum precursor for some hours, after which it is washed in 0.1 N nitric acid as many as three times. The number of washings are dependent on the concentration of the platinum specie being reduced to almost zero in the wash solution [81]. This method also involves the use of a simple equipment.

2.8 Alumina Ceramic supports for CMR process in water deoxygenation

There are several types of commercially available support materials. The ceramic supports used in this study were selected based on their porosity, pore size and shape. Li et al [18] suggested that a support's pore size and its surface

smoothness are the two key factors that should be considered when choosing a support material for catalytic deposition. This is because an effective deposition depends solely on these factors. A support should also have the ability to give shape, strength and size to the catalyst [11].

The supports chosen for the study therefore have a combination of alumina and titania oxides. This combination was preferred because, alumina is a type of a ceramic material that has a compact crystal structure and this gives it a unique ability to possess strong chemical bonds which are thermally and chemically stable. Titania (TiO_2) on the other hand are neither too coarse nor to smooth and was applied as a wash-coat on the alumina surface. The essence of the TiO_2 wash-coat on the alumina was therefore to create a rough surface and increase tortuosity and adhesiveness of the catalyst. This will enhance mixing of the reactants and improve mass transfer of the limiting reactant to the catalytic active site [84]. TiO_2 also has good stability and possible catalytic properties [85]. TiO_2 has also been reported to be commercially available and are used in polymeric membranes as it has characteristics of reducing fouling from occurring [44].

Zhang also reported the suitability of choosing alumina (Al_2O_3) supports for Pt impregnation in environmental and industrial applications for example, in hydrogenation and carbon monoxide oxidation [13].

For the purpose of this study, a tubular shaped alumina ceramic material with a TiO_2 wash-coat was chosen to act as a support due to its ability in creating a wider surface area to volume ratio and sized to fit into the reactors available in the laboratory [57].

2.9 Reaction Mechanism and Kinetic models for Catalytic Water Deoxygenation

2.9.1 Thermodynamics of the H_2/DO reaction

The reaction between hydrogen and oxygen molecules happens with a heat of reaction and water molecule is formed as a product. The thermodynamic process

is explained by using redox half equations 13, 14 and 15 respectively. The hydrogen molecules are oxidized while the oxygen molecules are reduced.

2.9.1.1 Half reactions

Oxidation: $2H_2 \rightarrow 4e^- + 4H^+$ (13)

Reduction: $4e^- + 4H^+ + O_2 \rightarrow 2H_2O$ (14)

Overall equation: $2H_2 + O_2 \rightarrow 2H_2O$ (15)

Equation 16 shows the complete reduction of oxygen molecule and this is possible because the DO is carried out in the presence of noble metals (platinum and Palladium) and in a controlled reaction zone [86].

The stoichiometric chemical equation for the synthetic reaction is given by equations 16 or 17 depending on the number of molecules of water formed. Their corresponding enthalpy changes are also presented along with their equations. The reaction is an exothermic reaction hence the negative sign [87].

$H_{2(g)} + \frac{1}{2}O_{2(g)} \rightarrow H_2O(l)$ ΔH°_{298K}= -285.8 kJ/mol (16)

$2H_{2(g)} + O_{2\,(g)} \rightarrow 2H_2O(l)$ ΔH°_{298K}= -571.6 kJ/mol (17)

Taking a look at the stoichiometric equations in 16 and 17, they look so straight forward. However, the mechanism of water formation is unclear even though water formation from the reaction has been extensively studied in literature [67, 74, 75]. The pathways to water formation can be extremely complex and remains imprecise [74]. In section 2.9.2, the mathematical reaction pathways to the water formation using the Langmuir-Hinshelwood and Hougen-Watson models have been demonstrated.

2.9.2 Reaction Mechanism: Langmuir-Hinshelwood Model

When hydrogen and oxygen molecules contact the catalytic surface, they tend to undergo various steps which include reactant adsorption, surface chemical reaction and product desorption. The mechanism of water formation from hydrogen and oxygen have been reported by Hellsing et al [67] and they

suggested that the reaction path to the formation of water could either be through equations 18, 19 or 20 shown below, where the index "ads" refers to adsorbed species. This is in agreement with the Langmuir-Hinshelwood type of model.

$$OH(ads) + OH(ads) \rightarrow H_2O(ads) + O(ads) \quad (18)$$

$$H(ads) + OH(ads) \rightarrow H_2O(ads) \quad (19)$$

$$H(ads) + H(ads) + O(ads) \rightarrow H_2O(ads) \quad (20)$$

The reaction of hydrogen and oxygen on the catalytic surface of either platinum or palladium is usually a very fast reaction even at ambient temperature. There are experimental conditions that could also determine which is the most appropriate reaction mechanism. The reaction path in equation 20 is usually negligible and therefore mostly overlooked.

For the purpose of this study, equation 18 will be the preferred reaction mechanism considering the experimental conditions and equations 21 to 26 will be the likely path. Figure 21 shows the probable pathways that explains the equations.

$$H_{2(gas)} \leftrightarrow 2H\ (ads) \quad (21)$$

$$O_{2(gas)} \leftrightarrow 2O\ (ads) \quad (22)$$

$$\mathrm{H}_{(ads)} + O(ads) \leftrightarrow OH(ads) \quad (23)$$

$$OH(ads) + OH(ads) \leftrightarrow H_2O(ads) + O(ads) \quad (24)$$

$$H_2O(ads) \rightarrow H_2O(gas) \quad (25)$$

$$H_2O(gas) \rightarrow H_2O(liquid) \quad (26)$$

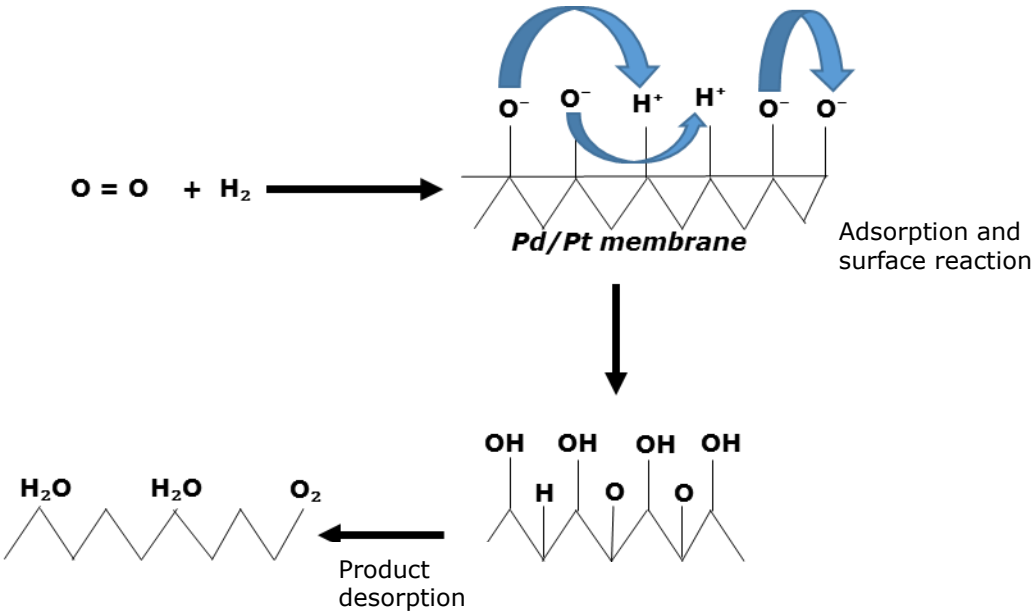

Figure 21: Postulated reaction pathway for the synthesis of H_2O on Pd/Pt catalyst

2.9.3 Modified Langmuir-Hinshelwood model: Hougen – Watson (H-W) equation

The modified Langmuir-Hinshelwood model is identical to the Hougen - Watson (H-W) equation and simplifies the surface reaction into 3 steps: (i) chemisorption of reactants, (ii) surface reaction of chemisorbed reactants and reverse reaction of chemisorbed products and (iii) chemidesorption of products. This model is based on the fact that internal and external diffusions are either removed or reduced and so the reaction mechanism is based on intrinsic kinetics [11].

In a reaction being represented in equation 27 and taking place on a catalytic Pd or Pt surface, and its active sites represented as "S", the H-W model demonstrates the reaction in equations 28 to 31. The reaction pathway is described in Figure 22.

$$A + B \rightarrow C \qquad (27)$$

i. Chemisorption of reactants

$$A + S \leftrightarrow AS \quad (28)$$

$$B + S \leftrightarrow BS \quad (29)$$

ii. Surface reaction

$$AS + BS \rightarrow CS \quad (30)$$

iii. Chemidesorption of product

$$CS \rightarrow C + S \quad (31)$$

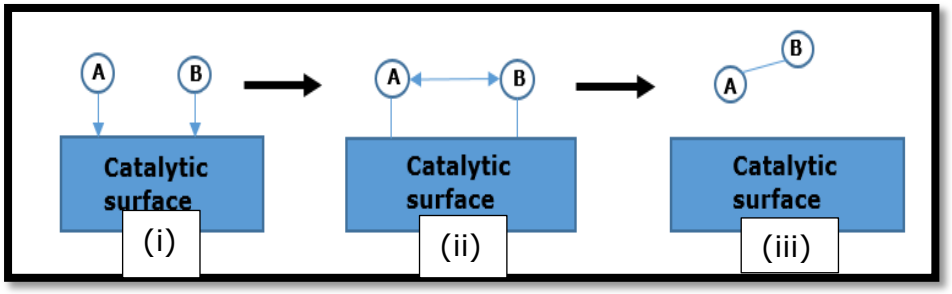

Figure 22: Reaction pathway of equations (i) to (iii) described by H-W

2.10 Principles governing Catalysts in water deoxygenation

The first hypothesis of this work is that the CMR will increase the conversion of DO by lowering the mass-transfer resistance [82] when compared with other deoxygenating processes carried out in packed bed reactors. In the CMR, the direction of the flow of feed is perpendicular to the membrane walls, thereby reducing the external mass transfer to a great limit, while in the packed bed reactors, the reactants will first of all have to diffuse through the external film surrounding the catalyst beads, then into the stagnant gas that fills the pores before reaching the reaction sites [82]. After reaction, the products too will have to overcome these resistance as they leave the reaction sites.

The principle of catalytic deoxygenation of water through hydrogenation reaction involves two major stages: the absorption of hydrogen gas into water and the controlled channelling of the mixture (water containing saturated hydrogen and

DO) through the catalytic membrane reactor [1]. The catalytic impregnated membranes on the other hand allows for the reaction of hydrogen and DO in water. The catalytic impregnated membrane reactor arrangement serves four important roles:

- Provides a well-defined surface area for hydrogen and DO reaction to take place,
- It provides easy accessibility of the catalyst sites to the reactants (hydrogen and DO)
- As a result of the geometry of the membranes, mass transfer limitations are highly minimised.
- The positioning and loading of the active sites within the membrane walls play a major role in the catalytic membrane deoxygenating process

In summary, the stages involved in the removal of DO in water can be explained in 4 levels.

1. The catalytic membrane has to display high permeance and flux with respect to the hydrogen gas which in this study is the limiting reactant.
2. There has to be a way of enabling the introduction and dissolution of hydrogen gas in water.
3. It is able to channel the properly mixed mixture (water and hydrogen) into the reaction chamber that has the catalytic membrane for reaction to take place in the presence of a catalyst in the membrane pores.
4. The membrane has to be permeable to water, so as to have a product exiting the catalytic membrane which can then be analysed with a DO analyser at the permeate end.

2.11 Factors affecting operation of the CMR in water deoxygenating process

2.11.1 Effect of Variables

There are some factors that may affect the efficiency of the catalytic method in this process. Parameters such as: variation in inlet water flowrate, catalytic membrane area, membrane pore size, water temperature, inlet DO concentration [88], type of catalyst, contact time [88] and partial pressure of

hydrogen [5] are all thought to affect the efficiency of the catalytic process and some of these parameters will be discussed in detail in chapter 8 where the results has been presented.

Another very important factor is the reaction temperature of the process. The reaction temperature is highly influenced by the nature of the gas used in the deoxygenating process. At a temperature range of 10–20^{o}C, deoxygenation reaction can be achieved using hydrogen gas, and water is the only product formed with no by product(s). If methanol or methane was to be used for the same purpose, the reaction temperature will have to be raised to a minimum of 75^{o}C and 400^{o}C respectively, and by-products such as CO_2 will be produced respectively [89].

2.11.2 Fouling

2.11.2.1 Catalytic site fouling

Fouling is a process whereby the active sites of the catalytic surface is covered by impurities leading to deactivation. These substances could either be salts or inorganic deposits, and tend to inhibit the activity of the catalyst over time. Fouling could be severe or mild depending on the type of impurity and the decline in activity of the catalyst can be immediate or over a long period of operation [11].

In the case of water deoxygenating processes, inorganic deposits could be of concern. Some sources of inorganic deposits include precipitates from the reaction of salts present in the feed. This type of fouling can be prevented by constructing a guard bed containing already partially deactivated catalysts in which the inorganic deposits will be deposited. In that way, the deposits will not get to the main reactor process [11].

2.11.2.2 Membrane fouling

Membrane fouling occurs as a result deposition and accumulation of feed components within the pores and/or on the membrane surface [100]. Types of fouling that could affect the functioning of my catalytic membrane includes pore

blocking/clogging, which is caused by small molecules getting stuck within the pores of the membrane and gel layer or cake formation, which is adhesion of bigger molecules on the membrane's surface forming a cake layer.

Fouling can reduce the efficiency of membranes thereby greatly limiting the use of the membrane in the catalytic water deoxygenating process. As an example, membrane permeability drops over time [101, 102], leading to an increase in operational and maintenance cost [103, 104]. Membrane systems are usually operated in either constant permeate flux with variable transmembrane pressure or vice versa, and this is related to the broadly classified membranes used in water treatment [102]. Depending on the type of membrane used, Seidel 2002 [103] stated that the extent of membrane fouling can be influenced by the system's operating conditions such as applied pressure, crossflow velocity, pH and ionic composition of the nature of the reactant. Membrane fouling can therefore occur during an increase or decrease in transmembrane pressure to maintain a particular working system flux [102].

Fouling of membrane can be significantly reduced by optimizing operational parameters such as: decreasing the initial flux or ionic strength and increasing the cross-flow velocity [103, 104]. Backwash and surface cleaning should also be done quarterly, this can be used to address a reversible type of membrane fouling [101, 102]. In the case of irreversible membrane fouling where backwash cannot restore the transmembrane flux, an extensive chemical cleaning is required [102]. Another option for preventing membrane fouling is pre-treatment of the feed water such as coagulation, adsorption and peroxidation [100].

2.12 Operating and capital cost of CMR in water deoxygenating process

Installation of every new deoxygenating process system can be very expensive, but they are usually a one-off. In designing a new process, feasibility studies are carried out on both the preliminary design and the cost/economic estimation. The preliminary design in this case gives an idea of the project operations and

technical requirements while the cost evaluates the total capital investment [105].

2.12.1 Preliminary design

Preliminary design includes

- Installation of a catalytic membrane reactor deoxygenating system which requires housing unit that will serve as the catalytic membrane reactor unit.
- Multi-channelled ceramic membrane which are industrial alternatives to single-channelled ones on account of economic cost and footprint [105].
- Preparation of catalytic membranes which involves dipping and metal reduction achieved by hydrogen gas activation.
- An installation of a compact hydrogen generator to supply the feed water with the required amount of hydrogen.
- An electric pump to supply the feed water mixture into the reactor. This will be connected to a mixing unit with polyvinyl chloride (PVC) piping.
- Full process design of the above points is shown in Figure 62, chapter 6.

2.12.2 Economic evaluation

The economic evaluation involves fixed and working capital investments [105].

2.12.2.1 Fixed capital investment

The fixed capital investment can be further divided into direct and indirect costs. Direct cost includes investment on: purchase of alumina ceramic supports, production of catalytic membrane (main operating system), installation of the main system, electrical, installation space, instrumentation and controls. While indirect cost investment includes: construction expenses, supervision and engineering, payment of contractors and other contingencies [105].

2.12.2.2 Working capital investment

The working capital investment includes: energy consumption (4% of the fixed capital investment), operation, performance and maintenance (6% of the fixed capital investment). Maintenance will probably be mostly on the replacement of catalyst in situations that the level of DO is not effectively reduced as expected and man power labour (3% of the fixed capital investment) [105].

Once the process design is installed and running, alterations to the injection pump power, in terms of pressure or flowrate can be easily done [2]. As of today's economy, the cost of catalyst palladium and platinum are given as follows [90]: an ounce of palladium is expected to cost £659.86, while platinum is £653.74. With the idea of depositing these catalyst in low catalytic loading, and being that they have a life span of about 10 months, this catalytic approach is workable. The alumina supports are also reusable and durable. The duration of membranes has been estimated to last for about 3 years or more [107].

For a more accurate costing, an economic cost model may probably have to be set up having a real scenario as a guide [2].

2.13 Advantages of CMR in water deoxygenating process

The advantages of this proposed system are:

1. Being an integrated design of plug flow model, it could be tailored in shape to fit into any process space requirement by either offshore installation or process industries.

2. Advantages of this system is that the only power required will be to power the electric pump and mixing unit, no need to heat up water. Hence these systems have lower operating costs compared to conventional systems where steam or vacuum is required. Though the initial cost of setting up the system may be high due to expenditure involved in membrane and catalyst. Long term operation are definitely economical and have ease of operation.

3. The catalytic reduction of DO using hydrogen gas does not increase the total dissolved solids unlike chemical methods involving addition of chemicals to reduce the DO.

4. The method was proposed bearing in mind the cost of the catalyst, thereby, low catalytic loading was of an option.

5. The method is a safe as long as a vent is created for the excess undissolved hydrogen gas to vent off. That way, there are no gaseous mixtures inside the mixing tank that could lead to explosion.

2.14 Contribution to knowledge

Figure 23 shows the concentration profile of the DO in a fixed bed reactor [22] and the mass transfer and reaction steps are illustrated in Figure 24. In a heterogeneously catalysed pelleted multiphase reaction, mass transfer phenomena plays important roles and can be used to determine the rate determining step depending on the process parameters under consideration. In the theory of this experiment, the reaction involving a heterogeneous catalytic reaction involves two general mass transfer phenomena.

1. Mass transfer in the bulk phase, that is, to and from the external surface of the catalyst, and
2. Mass transfer into and out of the catalytic deposited pores.

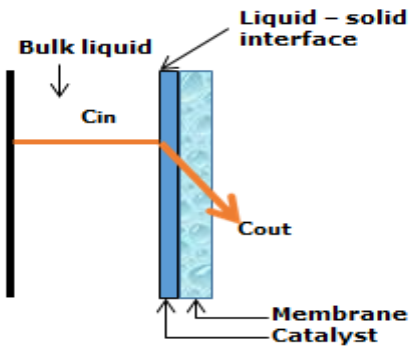

Figure 23: Showing the concentration profile in the fixed-bed reactor

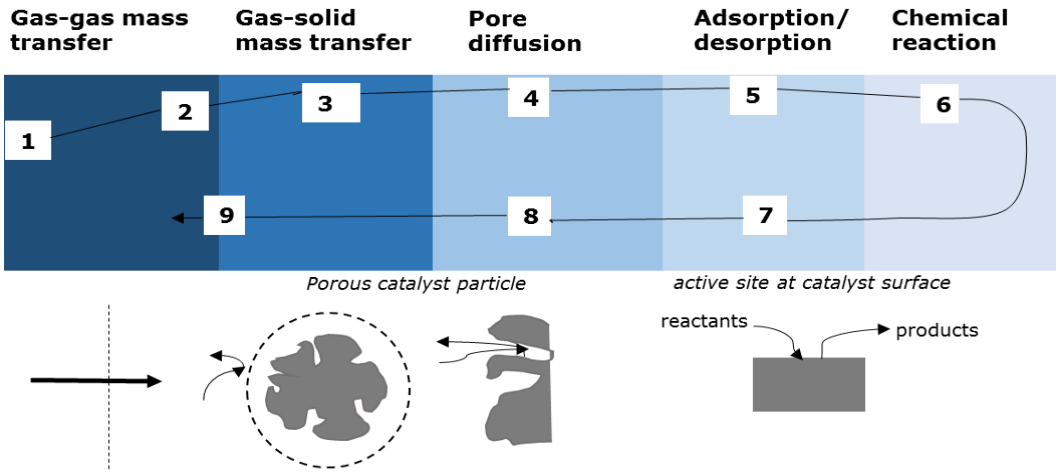

Figure 24: Heterogeneously catalysed steps in chemical reactions involving a porous pelletised catalyst

The following describes what happens at each of the steps identified in Figure 24.

1. Transfer of mass of gaseous reactant from the free gas stream to the interface of the gas-film interface;
2. Transfer of mass by diffusion of the gaseous reactant specie in the bulk of the film of the gas;
3. The gaseous reactant diffusion through the gas-solid-interface to the solid catalyst;
4. Pore diffusion-reactants diffusion within the pores of the catalyst to the catalytic sites;
5. Chemisorption-dissolved reactants adsorption on the catalytic active surface;
6. Chemical reaction occurring at the catalytic surface;
7. Desorption of the specie product from the catalytic surface;
8. Diffusion of the specie product out of the active pores to the external surface of the catalytic particles and
9. Product diffusion through the external gas interface to the bulk gas stream.

With the steps described above occuring in conventional reactor systems, the two main limitations are: primarily, internal pore diffusion which occurs when the diameter of the catalyst particles are too large in a fixed bed reactor and

secondly, the difficulty in separating the products from the catalyst due to very small diameter of the catalyst as in the case with slurry reactors.

In an attempt to solve the problems mentioned above, the flow-through membrane reactor concept has been used in this work.

Figure 25 compares the process of consecutive reaction in a conventional fixed-bed reactor having porous catalyst pellets and in a membrane operating in pore-flow-through (PFT) reactor. In the fixed bed reactor, the catalyst pellets are usually spherically shaped and in the pores of these spherical structures, the residence time of reactants and products is usually long due to the internal diffusion limitations which results in a concentration profile of the reactants in the pores of the catalyst pellets. As the fast reactions occurs across the pellet, the concentration of the reactants (A and B) decreases from the shell side to the catalyst pellet core with an increase in the concentration of the product C and resulting in the formation of by-product D consecutively leading to the selectivity of product C decreasing. Meanwhile in a pore flow-through membrane reactor, both the reactants are forced-through the pores of the membrane as thus, having a very short residence time, which reduces the internal diffusion limitations. As a result, the pore-flow through membrane reactor concept can be said to have some great advantages over the fixed-bed reactor and these are:

- Because the catalysts are highly dispersed as nanoparticles in the membrane pores, pore diffusion can be reduced/eliminated
- No need for catalyst-product separation
- Because the catalyst are highly dispersed, there is easy accessibility to the active sites as well as wider reaction catalytic area for the reactants
- Higher product selectivity due to a reduction of consecutive reactions

There are however some limitations:

- The possibility of pore blockage happening
- An increase in pressure drop of the membrane which occurs when there is an increased flow of velocity with a decrease in the membrane's pore diameter.

If the benefits of the PFT membrane reactor such as higher reaction rates, better product quality and improved selectivity to mention but a few, can compensate these limitations, it offers exciting viewpoints for industrial applications.

The membrane reactor process therefore considered in this work for deoxygenating reactions functions in pore-flow through way (Figure 25a) using a porous membrane which acts as a support for the catalyst and not as a selective membrane separator, with the catalyst impregnated as nanoparticles in the membrane pore structures. Hydrogen (A) is dissolved by a gas-inducing stirrer at high rotational speed in the water (B) phase in a saturation container. This is then connected to the actual membrane reactor. The reactants which are then in liquid phase are forced by pumping it through the pores of the membrane where the highly dispersed nano catalyst particles induce the reaction to take place. With the membrane reactor process, internal diffusion limitations as a result of fast convective flow are reduced. This is because the products are immediately removed from the membrane pore which avoids product build-up within the membrane. The effective reaction rate hence is not influenced by mass transfer limitations and the selectivity for the desired product (H_2O) can thereby be increased. In a summary, the membrane works as a contact zone for the reactants and the catalyst. The research on this work aims at also advancing the improvement and utilization of such a flow-through membrane reactor concept for other hydrogenation reactions.

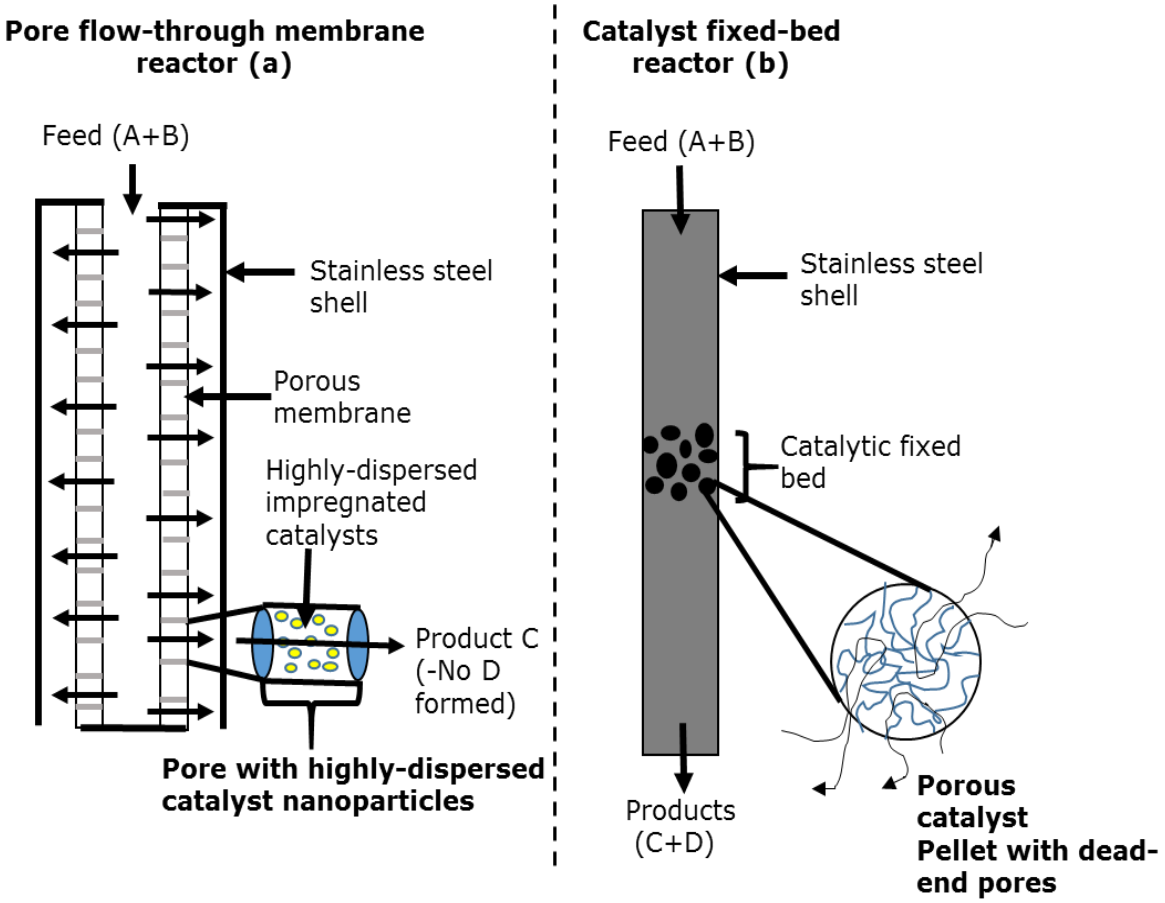

Figure 25: Scheme of catalytic consecutive reaction in (a) pore flow-through membrane (b) and traditional fixed bed reactor with pelletized catalyst

CHAPTER THREE

Chapter 3

3 METHODS

The first part of the study involves developing a catalyst fixed-bed using pelletised catalyst. Therefore, commercially purchased platinum on alumina pellets were used for this purpose (Method No 1). These pellets were characterised using scanning electron microscopy (SEM).

The second part develops catalytic membranes using platinum and palladium catalyst on ceramic alumina supports for the formation of catalytic membranes. This was achieved by adding platinum and palladium metals onto the internal porous surface of commercially purchased ceramic supports. These commercial supports were initially characterised prior to the metal deposition. Metal deposition on the supports lead to the provision of method No 2 (platinum membrane) and method No 3 (palladium coated membrane). The highly dispersed catalytic membranes were both obtained using wet impregnation and electroless plating methods respectively. These two deposition techniques have been reported to involve simple processes in achieving metallic deposition. These catalytic membranes were further characterized using gas permeation analysis, scanning electron microscopy and liquid nitrogen analysis respectively.

3.1 Method No 1: Catalytic fixed-bed (Platinum on alumina)

For the catalytic fixed-bed, the catalyst bed was created by folding and moulding a flat stainless steel mesh (Figure 26a) into a cone-shaped structure (Figure 26b) to enable it house the catalytic pellets as shown in Figure 26c. The cone-shaped mesh was zeroed on the weighing scale to enable the weighing of the pellets. 0.8g and 3g of platinum on alumina pellets were then taken out of the catalyst container, weighed and suspended inside the reactor as shown in Figure 26d. It should also be noted that these pellets were solid cylindrical in shape coated with activated platinum. Though 0.8g and 3g of pellets were weighed, their equivalent wt % of platinum metal are 16% and 60% respectively (see Appendix IV for the % Pt weight calculations).

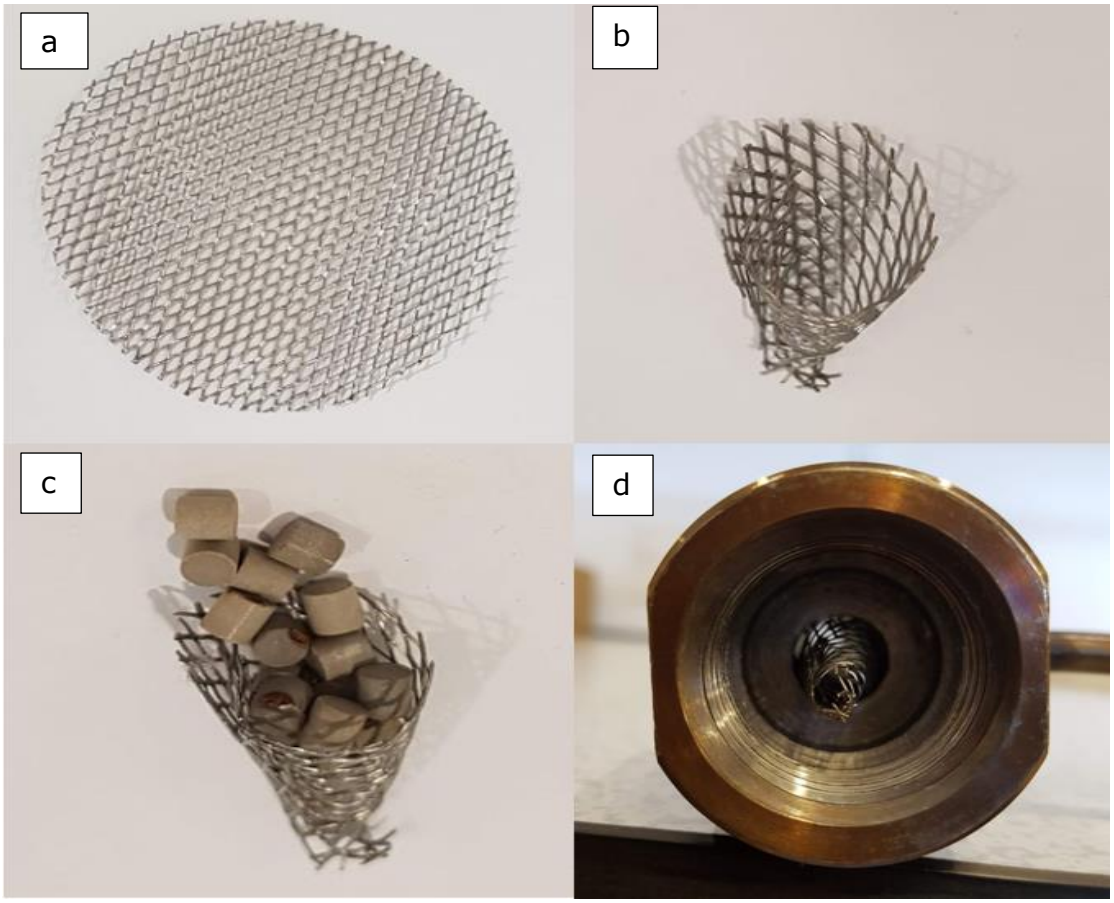

Figure 26: Fixed-bed catalyst set up

3.1.1 Catalyst Characterization

The morphology of the catalyst pellet was characterised using a scanning electron microscopy equipped with an energy dispersive analytical system which is further explained in section 3.5.2. The outer surface and cross-section images as well as the metal distribution of the platinum catalyst were measured. During the SEM-EDAX characterization, one of the pellets was halved and positioned firmly on a stainless steel disc using suitable adhesive. The sample was then loaded on a sample carousel and then analysed in the SEM-EDAX instrument. The SEM micrographs of the outer and edge areas were obtained at a number of different magnifications.

3.2 Method No 2: Platinum Impregnation

The platinum impregnation technique was used in this process to deposit the catalyst on the fresh porous ceramic support and was based on the "reservoir" method which is an evaporation-crystallization deposition technique [15]. In the

first instance, the fresh supports were initially washed with deionised water and dried in an oven for 24 hours at 65^{o}C so as to remove any dirt and moisture impurity that may be present. It was then weighed as shown in Figure 27 and its initial weight noted. After weighing of the supports, they are then initially dipped in a glass measuring cylinder containing deionised water for 2 hours as shown in Figure 28, after which both ends of the supports were covered with Teflon tapes to avoid the solution coming into contact with the supports' inner surface as shown in Figure 29a-c. The support is then immersed into another measuring cylinder containing platinum precursor solution for 24 hours under stirred condition as shown in Figure 30b.

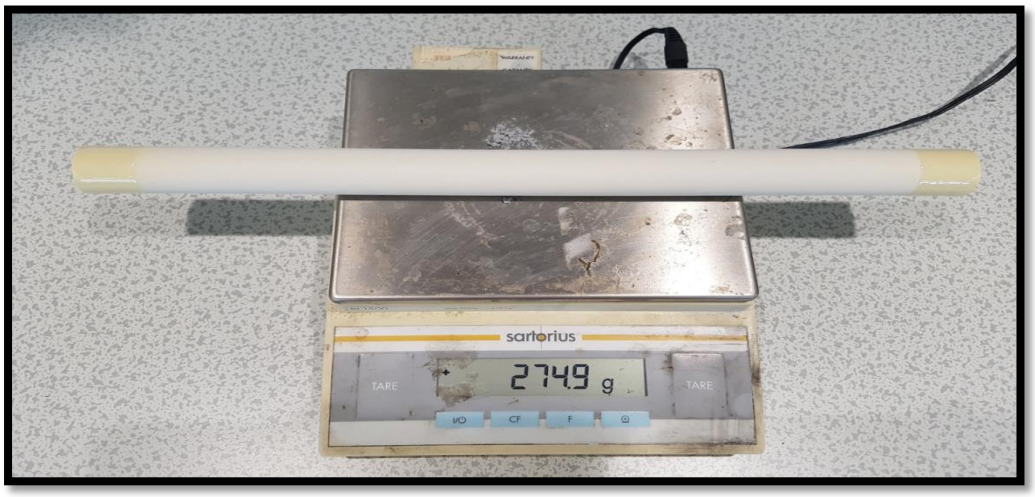

Figure 27: Picture showing the weighing of a ceramic support

Figure 28: Fresh support dipped in water

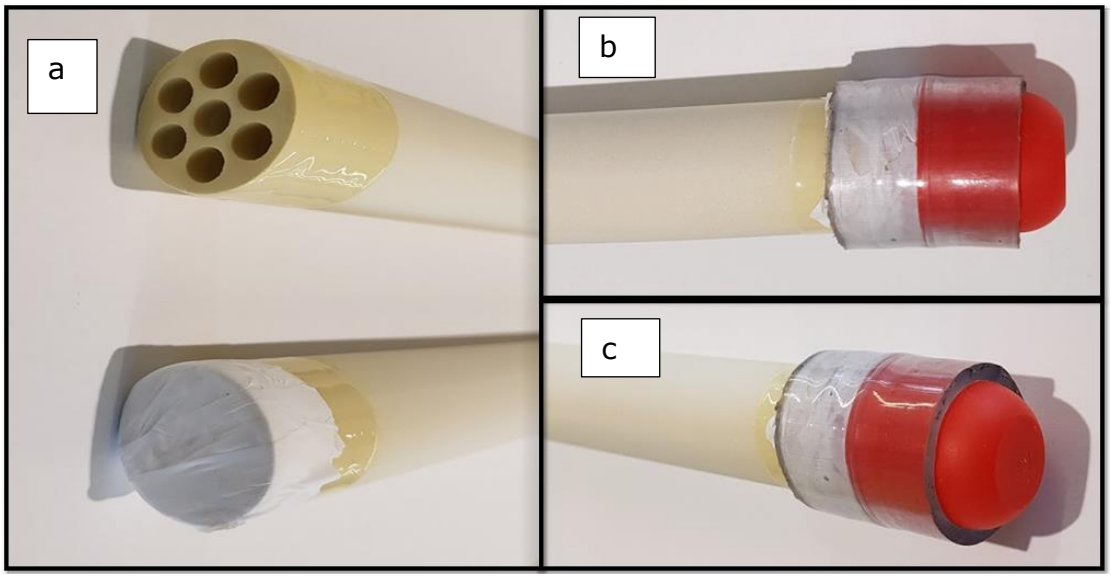

Figure 29: Picture showing the ends of a membrane covered in Teflon tapes, (a) uncovered and Teflon covered support end, (b) side view of the Teflon covered support with an extra cap cover, (c) front view of b.

Figure 30 shows the process of platinum deposition. The chemical composition of the platinum precursor used is 30g of H_2PtCl_6 solution in 500 mL of deionised water. To ensure complete mixing of the solution in deionised water, it was left stirring for 24 hours as shown in 30a.

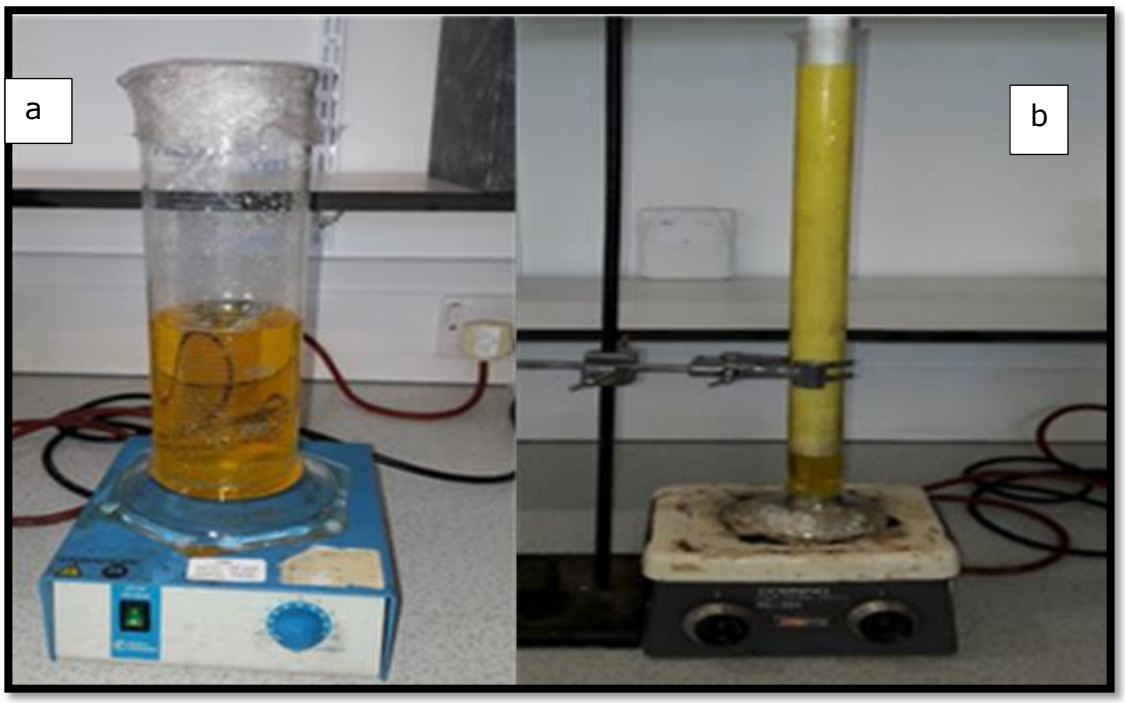

Figure 30: Pictures showing the processes of platinum impregnation, (a) platinum solution undergoing proper mixing in deionised water, (b) membrane dipped in platinum solution with stirring

After this immersion, the membrane along with the witness sample are taken out and are allowed to dry under room temperature for 24 hours as shown in Figure 31. The membrane are also put in an oven of 65°C for 4 hours to ensure complete drying as shown in Figure 32.

Figure 31: Air drying of the membrane at room temperature

Figure 32: Oven drying of the membrane at 65°C (a) Picture of the oven showing the operating temperature, (b) Picture showing the membrane placed inside the oven for drying

For the platinum impregnation, fresh support materials A, B and C were all deposited. Please refer to Appendix II for full details on the support dimensions. Figure 33 shows both the fresh support and platinum impregnated membrane placed side by side. The difference can be seen by the colour change after impregnation. It changes from whitish colour to yellowish.

Figure 33: Platinum impregnated membrane

This method which involves deposition of platinum catalyst was chosen based on cost and simplicity of the process. Deionised water was used for sample preparations in all the cases. This method basically involves a dipping process and this process results in the catalyst being highly dispersed in the outer surface and pores of the ceramic material. The presence of the catalyst on the surface and in the pores of the ceramic material helps the catalyst attain a very high degree of efficiency because the reactants easily access the active sites [22]. The method of the catalytic coating tend to reduce the effect of mass transfer usually found in the use of catalytic pellets and also optimise the performance of the catalyst. The amount of catalyst used will also be significantly reduced. It should also be noted that this would not affect its effectiveness.

3.3 Method No. 3: Palladium membrane

The method used for the palladium coating as mentioned earlier is the "Electroless plating" method. This method is a better option when compared to other methods such as chemical vapour deposition, thermal decomposition and sputtering. These other methods tend to produce a thicker palladium coating and are also not cost effective [91].

The electroless plating method comprises of 3 steps, of which the first two steps, sensitization and activation are done together at room temperature to produce a seeded palladium sites; this procedure is also referred to as the conventional Pd-Sn activation procedure [80]. The third step, which is the plating, is the final step in producing a thinly coated palladium membrane. It should also be noted

that the plating step could be done once or multiple times depending on the thickness required.

3.3.1 Sensitization and activation steps

Prior to the catalyst deposition, the ceramic supports were washed carefully with deionised water and dried in an oven at 65°C for 12 hours to remove dirt and moisture which could inhibit catalytic sites formation. The supports were then weighed to determine their initial weight as shown in Figure 27. This was then followed by covering both ends of the supports with Teflon tapes as shown in Figure 29 to prevent the solution coming in contact with the inner surfaces of the supports. The sensitization solution was made up of 0.005M $SnCl_2$ while the activation solution consisted of 0.005M $PdCl_2$. Table 2 shows the solution composition to this.

The process of sensitization and activation steps involved dipping the supports with their witness samples into the cylinder containing 0.005M $SnCl_2$ solution for 5 minutes, take it out then rinse immediately in deionised water for about 2 minutes, followed by an immediate dipping in the 0.005M $PdCl_2$ solution for another 5 minutes as shown schematically in Figure 34. This was done in a continuous process and at room temperature.

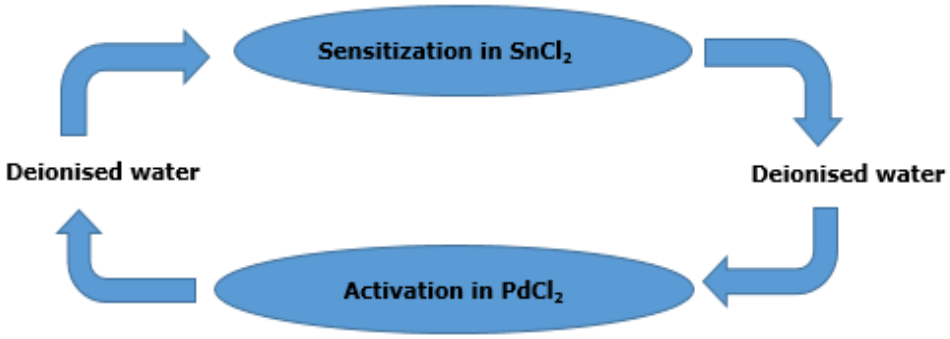

Figure 34: A schematic diagram for the conventional Pd-Sn procedure

The sensitization and activation steps are compulsory steps in an electroless plating technique. The $SnCl_2$ solution enters the pores of the ceramic material and reduces the palladium ions thereby leading to the formation of auto-catalytic sites which will favour palladium plating [92].

Table 2: The chemical compositions of the sensitization and activation solutions

Chemical	**Amount of deionised water needed**	**Percentage composition of the solution**
Sensitization 0.90g of $PdCl_2$	1000 mL of deionised water	0.005M
Activation 0.95g of $SnCl_2$	1000 mL of deionised water	0.005M

Figures 35(a-c) show the pictorial process of sensitization and activation steps. This process was repeated 10 times with fresh deionised water obtained at each rinse. The essence of the repeated dipping is to have a uniform autocatalytic site on the surface of the support, without which, the palladium deposition plating process will be poor [92]. This sensitization and activation steps took about 1 hr, 30 min to give a dark uniformly coloured membrane (Figure 36a bottom). The membrane is allowed to dry under room temperature before the final plating step.

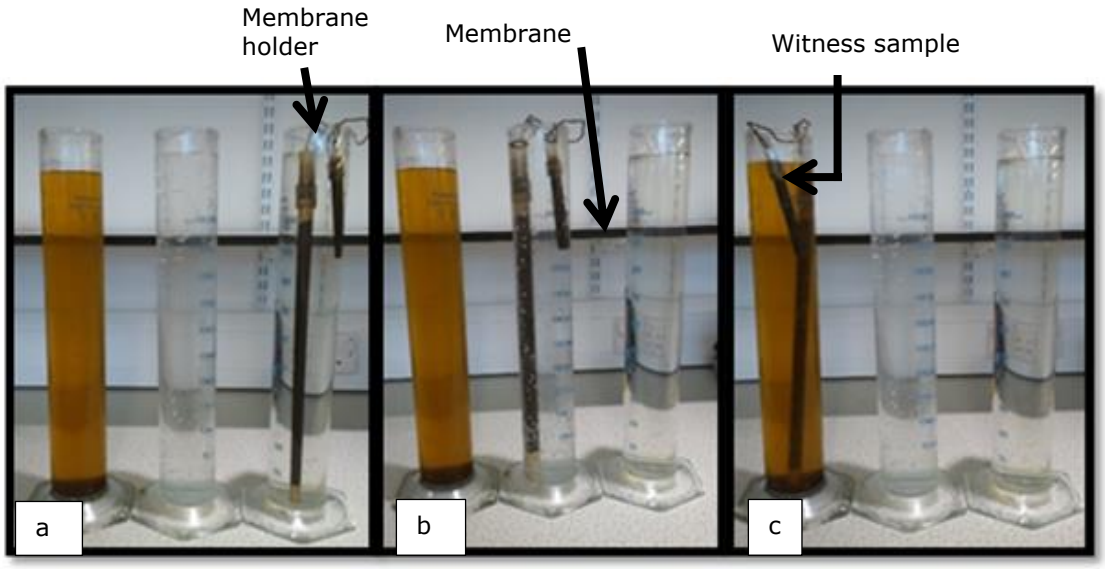

Figure 35: Pictorial representation of the Pd-Sn membrane seeding process, (a) in $SnCl_2$ solution, (b) in deionised water and (c) in $PdCl_2$ solution

The process of rinsing in deionised water as shown in Figure 35b is necessitated to prevent the deposition or adsorption of the products of $SnCl_2$ hydrolysis on the surface of the support [92]. The initial colour of the support is white after the Pd-Sn procedure it changes to a dark colour as shown in Figure 36a.

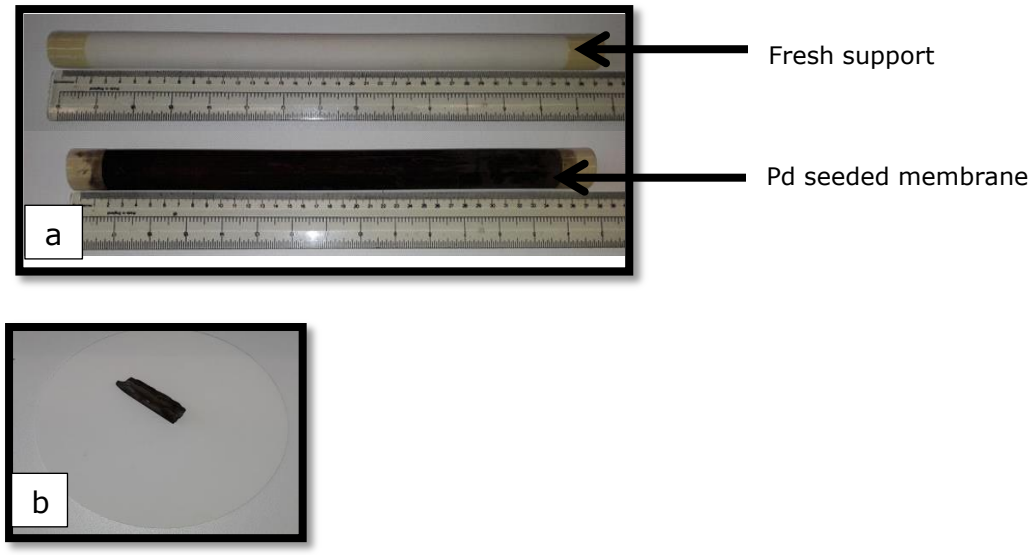

Figure 36: (a) Picture showing the fresh support and Pd activated membrane, (b) witness sample

3.3.2 Plating step

This step consists of a plating solution comprising of $PdCl_2$, Na_2EDTA and ammonium oxide (controls the pH of the solution) solution properly mixed and heated to a temperature of 60°C with the help of a water bath. The composition of the plating bath is given in Table 3.

The plating procedure involves placing the activated membrane in the plating solution and heating it up to 60°C. 10 mls of hydrazine solution was then added to it and left to plate for 30 minutes. The plating actually starts the moment the hydrazine is added and then timed for 30 minutes. The hydrazine is a reducing agent mostly used in electroless plating of palladium membranes. Figure 37 shows the plating solution being heated in a water bath. After deposition of the palladium through the plating solution, the palladium plated membrane was rinsed in deionised water and dried at room temperature for 24 hours after which it was placed in an oven for 12 hours at 65°C to ensure complete drying.

Table 3: Composition of the electroless plating bath

Component	Composition
$PdCl_2$	2.7 g
Na_2EDTA	70 g
NH_4OH	440 mL
$N_2H_2.H_2O$	10 mL
pH	10-11

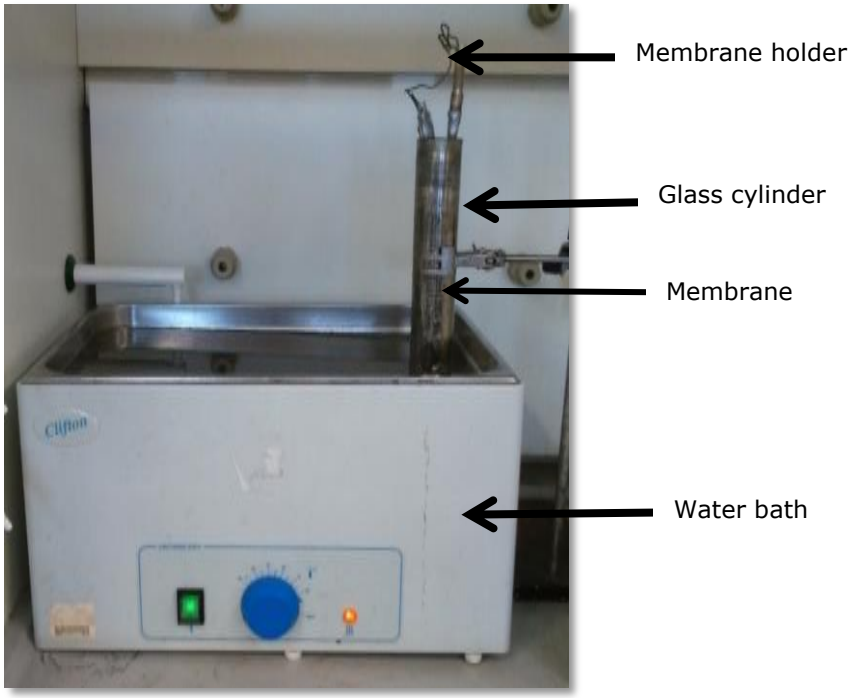

Figure 37: Electroless plating process of the palladium membrane

The process of palladium deposition was done only once to avoid a dense layer forming. The dense layer would not be appropriate for the purpose of deoxygenation of water for which this membrane is being prepared for. Figure 38 shows the picture of the thinly coated palladium membranes. It appeared to have had a good adherent film of palladium on the surface of the tube. For the palladium plating, only membranes A and B were fabricated for this study. Fabrication of Membrane C was not feasible due to its length (650mm) and the apparatus was not available at the time of the research.

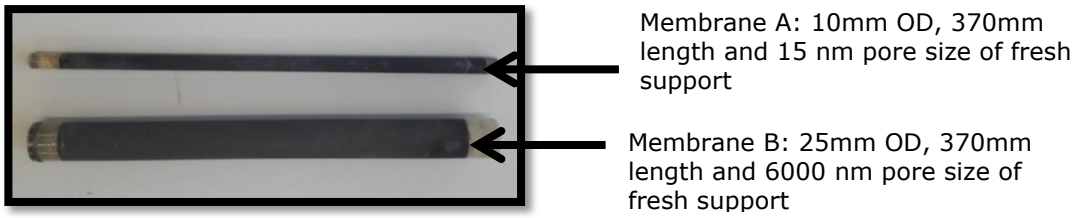

Figure 38: Showing pictures of thinly coated palladium membranes A and B

3.4 Membrane Catalyst Reduction/Activation

After the catalytic deposition of the precursor as explained in sections 3.2 and 3.3 on the membranes, the metallic elements of membranes in methods No 2 and No 3 needed to be activated. This process involves reducing $PdCl_2$ and H_2PtCl_2 and activating Pd and Pt metals. This was done by flowing hydrogen gas through the membranes at 573 K for 30 minutes as shown in Figure 39, and then flowing helium gas through them for another 30 min (Figure 40). The reactor is usually allowed to cool down before the membrane is taken out. The witness samples too were also reduced/activated at the same time as the whole membranes.

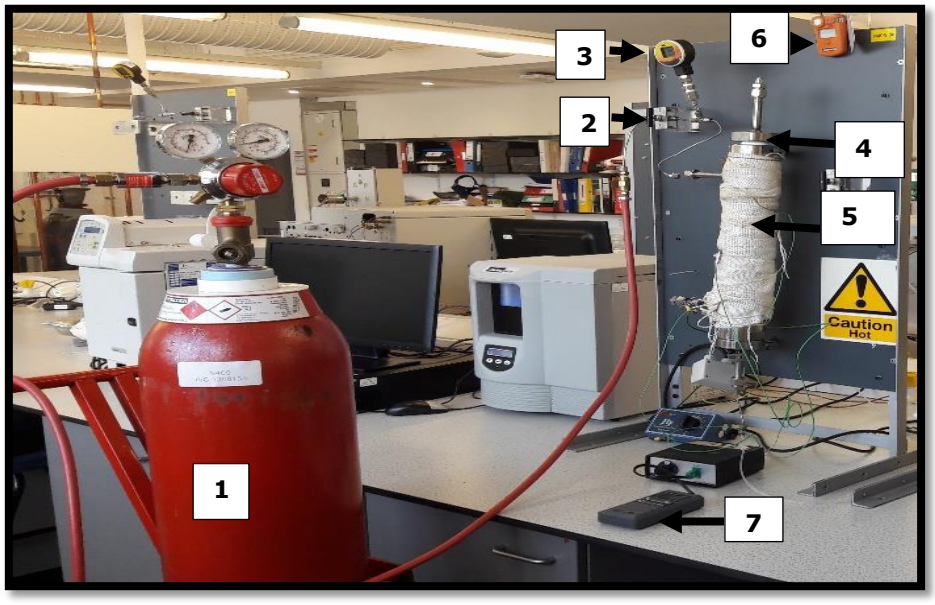

Figure 39: Pictorial representation of the hydrogen reduction activation process/gas permeation experimental rig (1. Gas bottle, 2. Gas gauge control On/Off, 3. Pressure gauge, 4. Membrane holder, 5. Wrapped heating tape, 6. Hydrogen safety monitor, 7. Thermometer)

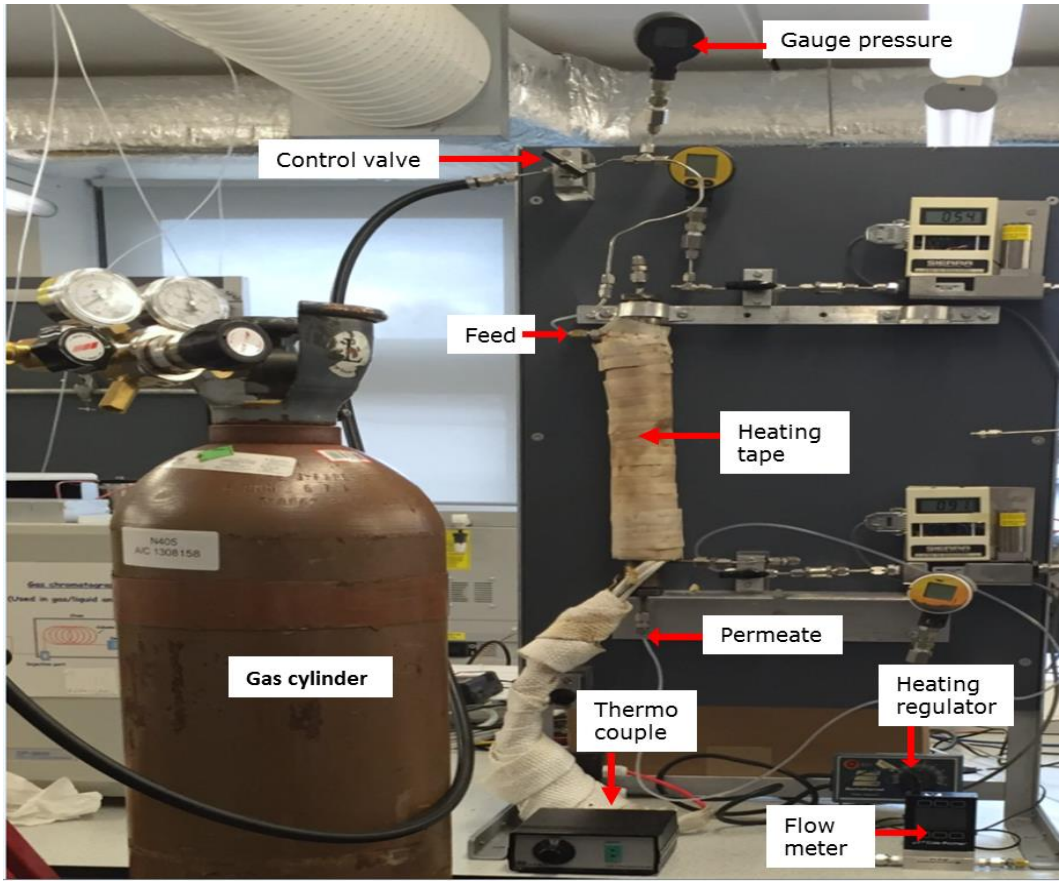

Figure 40: Picture showing the reduction activation process using helium gas

After the membranes were activated, the colour of the membranes changed and appeared darker in colour. It is even more noticeable on the platinum membrane as shown in Figure 41.

Figure 41: Picture showing the fresh support and activated platinum and palladium membranes

3.5 Characterization

Characterization of a membrane is a necessitated aspect of study for both the producers and end users of it. This is a process whereby a membrane is analysed, thereby determining its futures which will help in predicting its application for various industrial use [49]. The characterization methods employed in this study are described below:

3.5.1 Gas permeation

The experimental arrangement for gas permeation test comprise of two sections: 3.5.1.1 (feed delivery) and section 4.1 (membrane reactor design). Section 3.5.1.2 then details the method carried out for the gas permeation analysis.

3.5.1.1 Feed delivery section

The feed in this process can be any of the gases used in the study. These gas cylinders are connected to approve and individually specified regulators that is used to control the gas flow from the cylinders. The gas flow is directed through the control valve which is also a gas control apparatus and this controls the amount of gas entering the reactor. The pressure gauge located just after the control valve and before the reactor is used to monitor the variations of the feed gases as it flows through into the membrane reactor where the permeation occurs. The schematic diagram showing the arrangement of apparatus used in the gas permeation test is presented in Figure 42, while the pictorial representation of the process taken from the laboratory is shown in Figure 39. It should be noted that all connections were made with stainless steel tubes and screws. This method was adopted from Gobina E. [93].

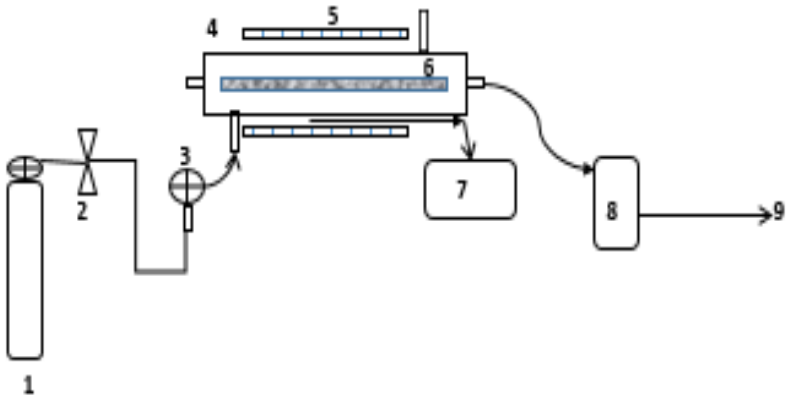

Figure 42: Schematic experimental diagram showing the catalytic membrane reactor process for gas permeation analysis (1. Gas bottle, 2. Gas gauge control On/Off, 3. Pressure gauge, 4. Membrane holder, 5. Heating tape, 6. Catalytic membrane, 7. Thermocouple attached to a thermometer, 8. Flowmeter, 9. Waste)

3.5.1.2 Gas permeation analysis

Gas permeation is the process whereby a flowmeter is used to measure the flowrate of gases flowing through the membrane in a membrane reactor at different operating temperatures and pressures. Section 4.1 describes the shell and tube membrane module in details so this will not be repeated.

Various permeation gases including pure hydrogen, oxygen, helium and nitrogen were used. These gases were fed through the feed port using digital pressure gauge at pressure range between 0.05 to 1 gauge pressures (bar), with an increment of 0.05 bar at each measurement. To ensure the pressure readings remained constant on the digital pressure gauge, the control valve located between the gas cylinder and pressure gauge is usually turned off. The pressure at the gas cylinder is also raised and maintained at 2 pressure bar mostly throughout the experiment, with exception of cases where the pressure on the digital reading does not get to 1, an increase in the gas cylinder will then be necessitated. The gases were introduced into the membrane tube from the outer shell through the pressure control valve and the permeate gases were subsequently led to a Cole-Parmer flow meter to determine the flowrate.

It is also important to note that the pressure difference across the membrane were obtained using the digital pressure gauge at the upstream and the permeate end (downstream) is kept constantly at atmospheric pressure of 1 atm

(1.0 bar). Measurements of these gases were made at different temperature ranges (523 – 623 K). The fresh support were tested at room temperature (298K).

3.5.2 Scanning electron microscopy (SEM) coupled with Energy Dispersive Analytical X-ray (EDAX)

Scanning electron microscopy is a morphological technique used to characterize the surface of a sample. It produces detailed high-resolution images of a sample and this is achieved when its electron beams are focussed across the sample's surface. The SEM allows one to examine the topography of the membrane or catalyst surface and can detect any defeat or surface irregularities, cracks, surface smoothness, grain structures (size or shape) or any segregation effects and can also use for measuring the thickness of a coating on a material's surface [11, 50, 94].

The SEM (Zeiss EVO LS10 Variable Pressure scanning electron microscope) used in this study was equipped with an Energy Dispersive X-Ray Analyser (EDX or EDA) which was used to provide elemental composition by identifying and quantifying the elements present [94]. Figure 43 shows the pictorial representation of the microscope used. The SEM-EDAX is capable of analysing a sample from different angles (outer, inner, edge and cross sectional area) depending on the required information.

Figure 43: Picture of the SEM-EDAX setting

During the SEM-EDAX characterization, witness samples of the membranes obtained from methods No 2 and 3 (Figure 44) were positioned firmly on a stub (stainless steel disc) using suitable adhesive. The samples are then loaded on a sample carousel and then analysed in the SEM-EDAX instrument. The SEM photographs of the outer and inner areas were obtained at a number of different magnifications.

Figure 44: Picture showing fragments of the witness samples going in for SEM-EDAX analysis

3.5.3 Nitrogen Adsorption Desorption analysis

The nitrogen adsorption desorption analysis is actually one of the most common analysis carried out to obtain parameters such as the pore size, pore size distribution and specific surface area for a porous membrane [50]. It is widely used for characterization of porous materials.

Figure 45 shows the different types of isotherms that could occur during a gas adsorption and desorption process. Type I is dominant with microporous solids, type II is observed with non-porous solids, types III and V are common for vapour adsorption, types IV and V are common with mesoporous solids, in which a hysteresis loop caused by the desorption occurring at a lower pressure than the adsorption can be observed. This is usually as a result of capillary condensation. Type VI is uncommon and is seen in special types of carbon materials [49].

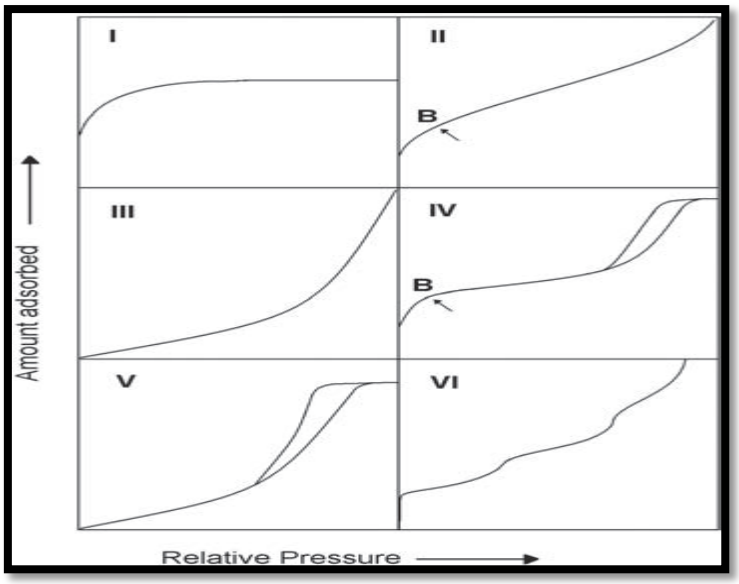

Figure 45: Types of Physisorption isotherms [49]

Figure 46 shows the Quantachrome®ASiQwin™ nitrogen adsorption-desorption analyser used in obtaining BET and BJH results. The Barrett, Joyner and Halenda (BJH) method is used for calculating average pore size and pore size distribution, while the Brunauer, Emmett and Teller (BET) method calculates the specific surface area by measuring how much of the gas is adsorbed per gram of a material [95]. The pore size distribution is a quantitative measure of the pore volume over a range of pore radii. It is usually represented as a plot of pore volume against pore radius [11]. The BET and BJH methods were used to analyse results on both the support and catalyst impregnated membranes and their results were compared.

The analysis of samples on the liquid nitrogen analyser comprises of two stages: degassing and main analysis, and it's based on the adsorption desorption principle. Samples need to be in either powdered or coarse forms to be able to be analysed with the Quantachrome analyzer. Small fragments of the witness samples of both fresh support and catalytic impregnated membrane were ground into coarse forms using a pestle and mortar. The sample cells which have been washed and dried in an oven were initially weighed to note down the weight of the empty cell as this is required when filling in the details for analysis. After the empty cell is weight, it is then zeroed to enable the weighing of the samples. The weight of samples can actually be varied from 0.1 to 1g depending on the nature

of the material. 0.1g was chosen for the catalytic membranes, while that of the fresh support varied but in most cases less than 1g.

3.5.3.1 Degassing stage

A sample needs to be degassed prior to any analysis on the Quantachrome analyser. This is necessary so as to remove any moisture that could be present in the sample. The process of degassing involves attaching the sample containing cell into the degassing stations as shown in Figure 46 and following the procedure on the manual. This powered samples were degassed for about 4 to 5 hours at a temperature of 338K. Helium and nitrogen pure gases are used as inert gases in this process.

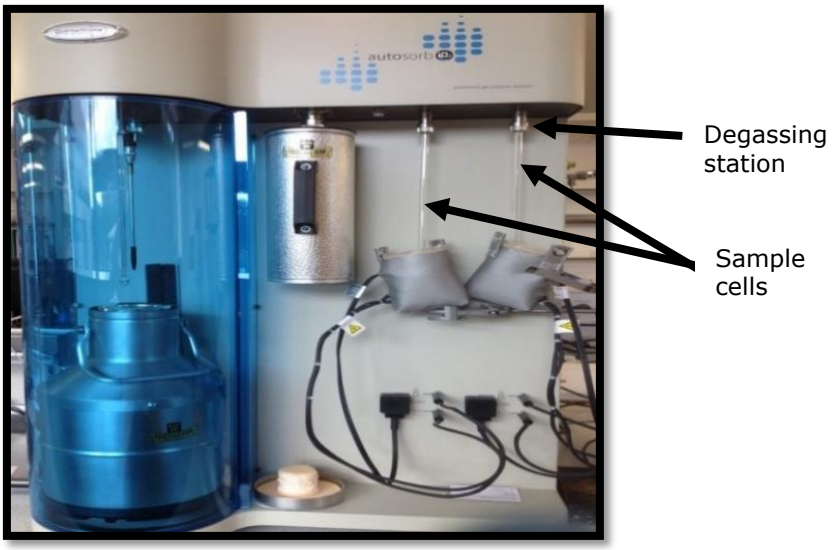

Figure 46: Picture showing samples undergoing degassing stage

3.5.3.2 Analysis Stage

The degassed samples are then removed from the degassing station and transferred to the analysis station where analysis is carried out by liquid nitrogen. The analysis is initiated and the Dewar containing the liquid nitrogen lifts up and the cell containing samples which were directly under it are immersed into the liquid nitrogen and analysed at a temperature of 77K (-196^{o}C). The samples undergoing analysis is shown in Figure 47. The results are then interpreted through the computer attached to the analyser.

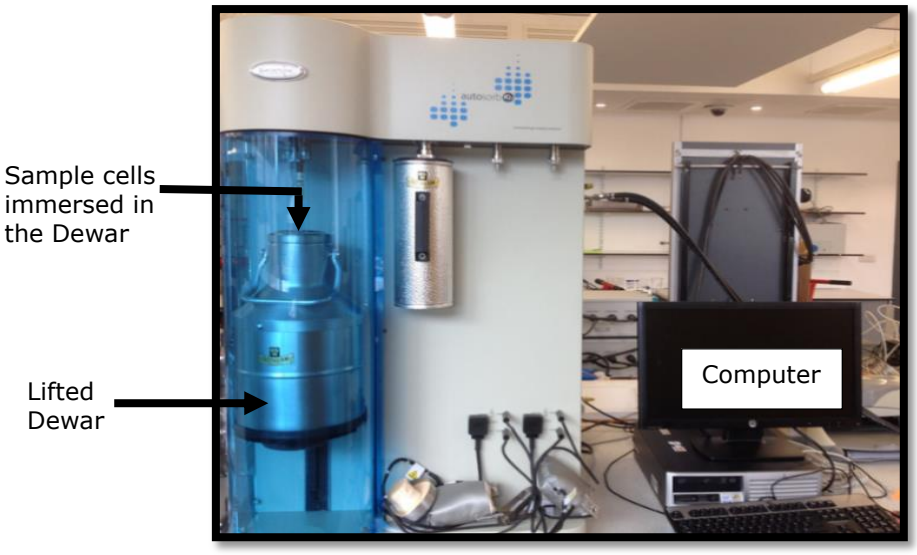

Figure 47: Picture showing sample analysis taking place inside the liquid nitrogen

CHAPTER FOUR

Chapter 4

4 REACTOR DESIGN

4.1 Membrane Reactor design

Three different reactor holders used in the study were designed by Professor Edward Gobina, school of engineering, RGU. Figure 48 shows the different sized holders for the fixed-bed catalysts and membranes used in the water deoxygenating experiments. These reactors are made of stainless steel materials and differ in length and width. These reactors have a shell and tube module arrangement in the case of the catalytic membrane. In the fixed-bed case, the catalysts is located in the empty void spaces meant to house the tubular ceramic membranes. They are basically structured in a circular pipe like shape with two flat ends. At these flat ends, there is void space for the insertion of the membrane or catalyst basket so as to align axially to the shell. These reactors are usually welded, pressure tested up to 50 bar and tested for leaks by accredited companies. They are characterised by having three basic sections: feed, retentate and permeate sections. They can be heated up to temperatures around 450^{o}C without any significant structural deformation of the shell material.

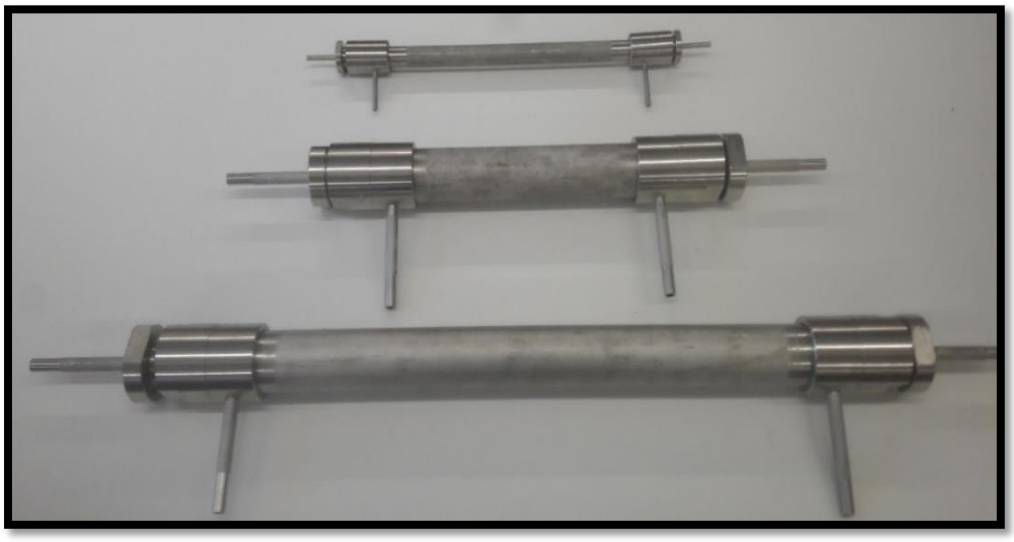

Figure 48: Stainless steel reactor housing

The reactor itself consists of the catalytic membrane and the stainless steel housing. The membrane is inserted into the hollow space of the housing (Figure

49a) and sealed with graphite seals so as to prevent the leakage of gas during any experiment. An example of a membrane with the seal in place is shown in Figure 49b. In the reactor chamber, reaction is expected to take place in the catalytically impregnated membrane. In other cases, the membrane may act as a selective semi-permeable device favouring the passage of one type of gas over another. This is an important aspect in determining the transport mechanism of gases through these membranes.

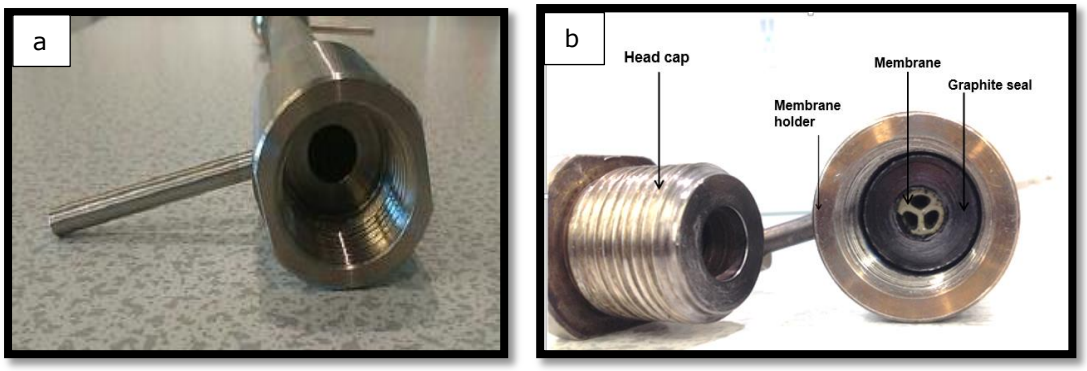

Figure 49: (a) Picture showing the hollow space in a membrane holder, (b) Picture of a membrane sealed inside a membrane holder using graphite rings

Once the membrane is sealed and certified that there are no leaks (Figure 50), the outer shell is wrapped in heating tape as shown in Figure 50b with three to four thermocouples strategically positioned at the top, middle and bottom of the reactor's length so as to monitor the temperature in the reactor. The heating tape is usually connected to a temperature controller, which is then connected to a thermocouple selector switch where the thermocouples are also connected. A digital thermometer is connected to this thermocouple selector switch which can monitor as well as regulate the desired temperature. Figure 50(c) shows the heating tape covered with a fire resistant glass fibre insulating material. This is done so as to confine the heat within the reactor system, thereby maintaining a uniform temperature and also to protect researchers from the high temperature.

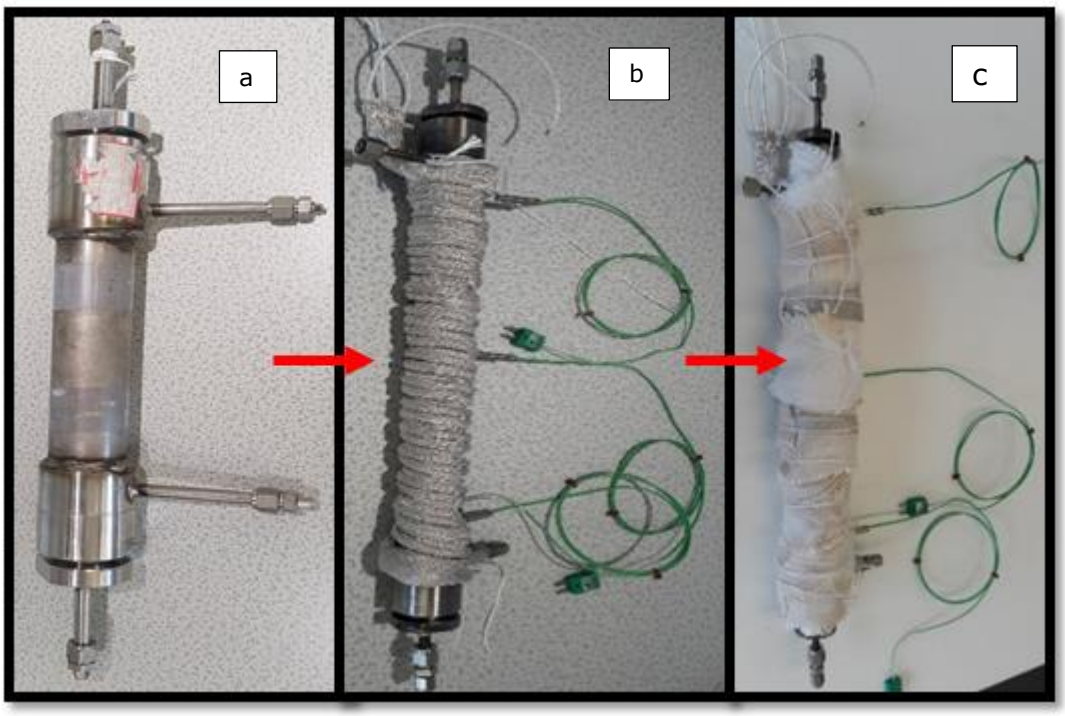

Figure 50: (a) Plain reactor, (b) reactor wrapped with heating tape and thermocouples, (c) heating tapes covered with a fibre material

Figure 51 shows the thermally insulated reactor mounted on an experimental rig ready for analysis. A flow meter is connected at the reactor's permeate end, and its purpose is to read off the flowrate at which the gas is permeating through the membrane reactor at each pressure as indicated on the pressure gauge.

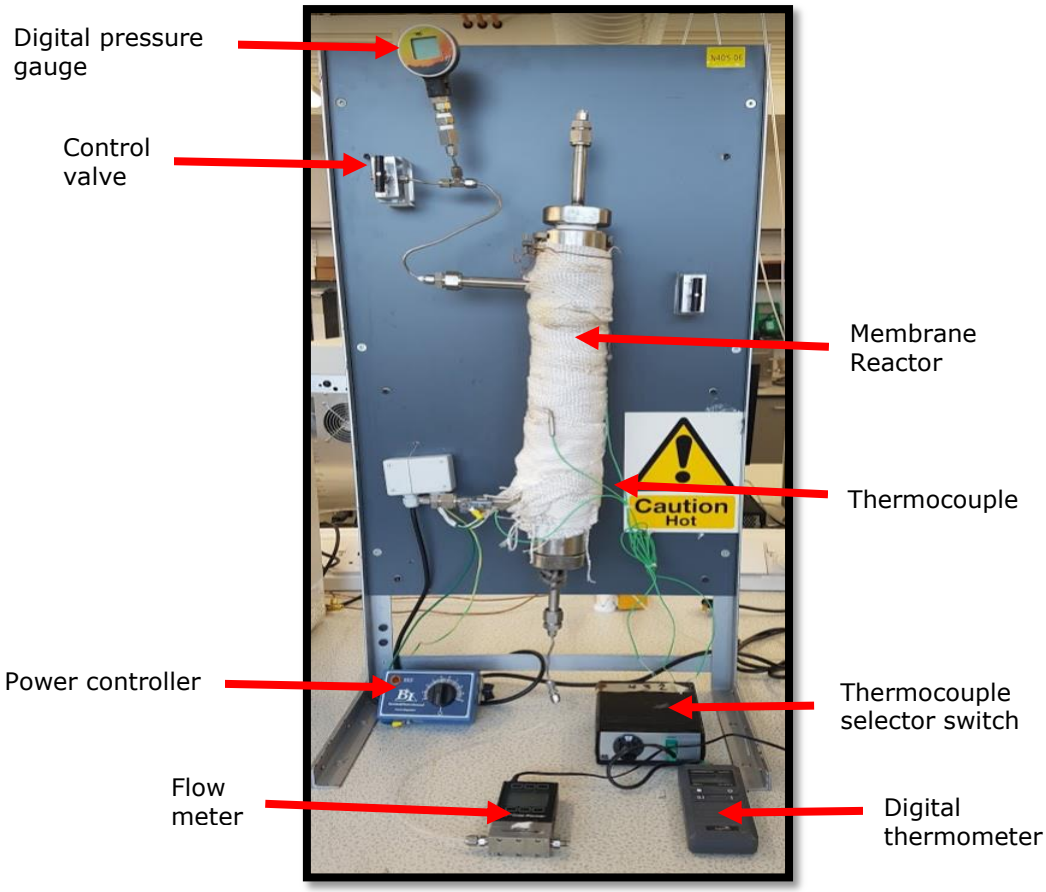

Figure 51: Thermally insulated reactor mounted on rig ready for experiment

4.2 Ceramic Support design

Request was made to Ceramiques Techniques et Industrielles (CTI SA) France for the design and production of the porous tubular ceramic supports (see Appendix II). This is because, with their porous nature when impregnated with catalyst best suited the purpose of the research. The tubular shape was also preferred because when inserted into the stainless steel housing units available in the laboratory, a dead-end mode was achieved. This therefore allows the reactants to be forced through the catalytic pores. Also, the tubular structure is an added advantage in mass transfer limitations, it provides a wider surface area for reaction to take place.

4.3 Catalytic membrane and process design

Figure 52 illustrates the design and arrangement of membrane layers on the catalytic membrane for its utilization in the water deoxygenating process. Figure 8 in section 2.4.1 illustrates the arrangement of layers to support the catalytic top layer surface. The catalysts were chosen because they have high affinity for hydrogen molecules as previously discussed.

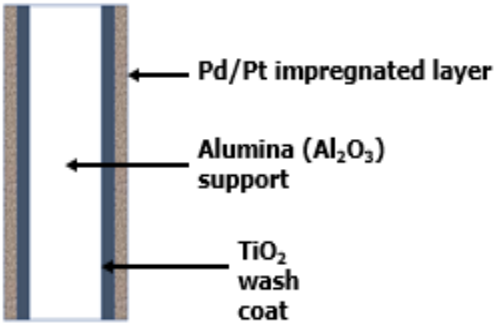

Figure 52: Cross-sectional view of a catalytically impregnated membrane showing its different layers

A hydrogen saturated water with chemical compositions: H_2 and H_2O/O_2 are feed at the upstream of the reactor to and perpendicular to the membrane as described in Figure 53. On contact with the catalytic surface, there exist diffusion of the reactant to the external surface of the catalyst particle, the reactants then diffuse with in the pores of the catalytic active site, here adsorption of the dissolved reactants take place. This is then followed by complete or partially hydrogenation reactions between the adsorbed species. The product of the reaction then desorbs from the active site. Diffusion of the product then occurs through the pores towards the permeate end at the downstream. The chemical reaction involves in a summary: adsorption of reactants, catalytic surface reaction, desorption of products formed and then diffusion of products.

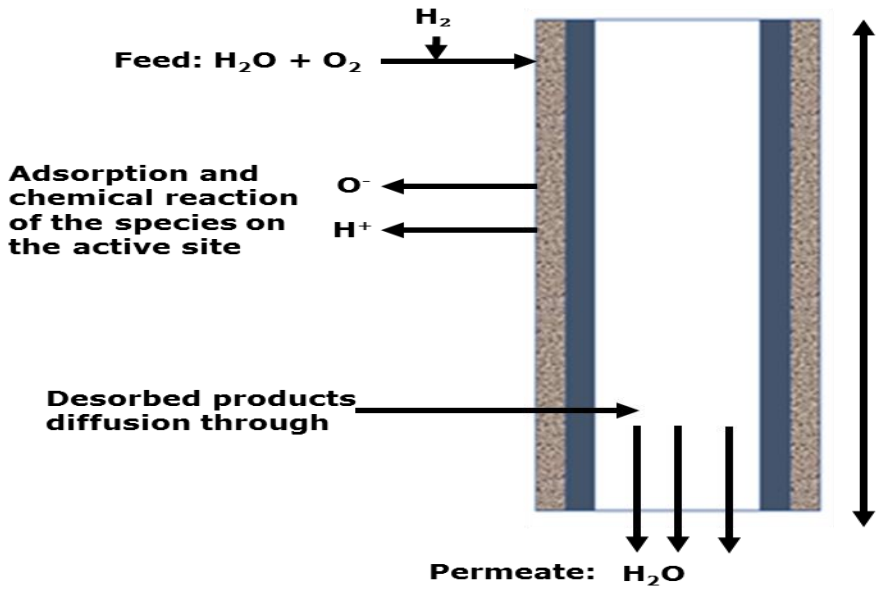

Figure 53: Cross section of the catalytic membrane undergoing chemical reaction

4.4 Fixed-Bed Reactor Design

Afandizadeh et al [96] stated that the packing of catalyst pellets in a reactor generates wide interest on reaction engineering as the design of the catalyst bed from the shape configuration, internal pores and available surface area leads to the efficiency of a catalytic process and also determines the mass transfer properties in the reactor [96]. Figure 54 therefore illustrates the design and controlled arrangement of the packed catalyst pellets in a fixed-bed reactor and details the many phenomena that has to be taken into account inorder to model it accurately.

For an effective pellet arrangement, some variables are considered such as: the shape of the reactor, the shape and surface properties of the catalyst pellet and the method of installation [96, 97]. It is also assumed while in the controlled packing process that the catalyst pellets are of same size and that the packing will be done to avoid void spaces. This is an assumption in an ideal scenerio, but usually not the case and the presence of void spaces can also affect the efficiency and transport properties in a system [96].

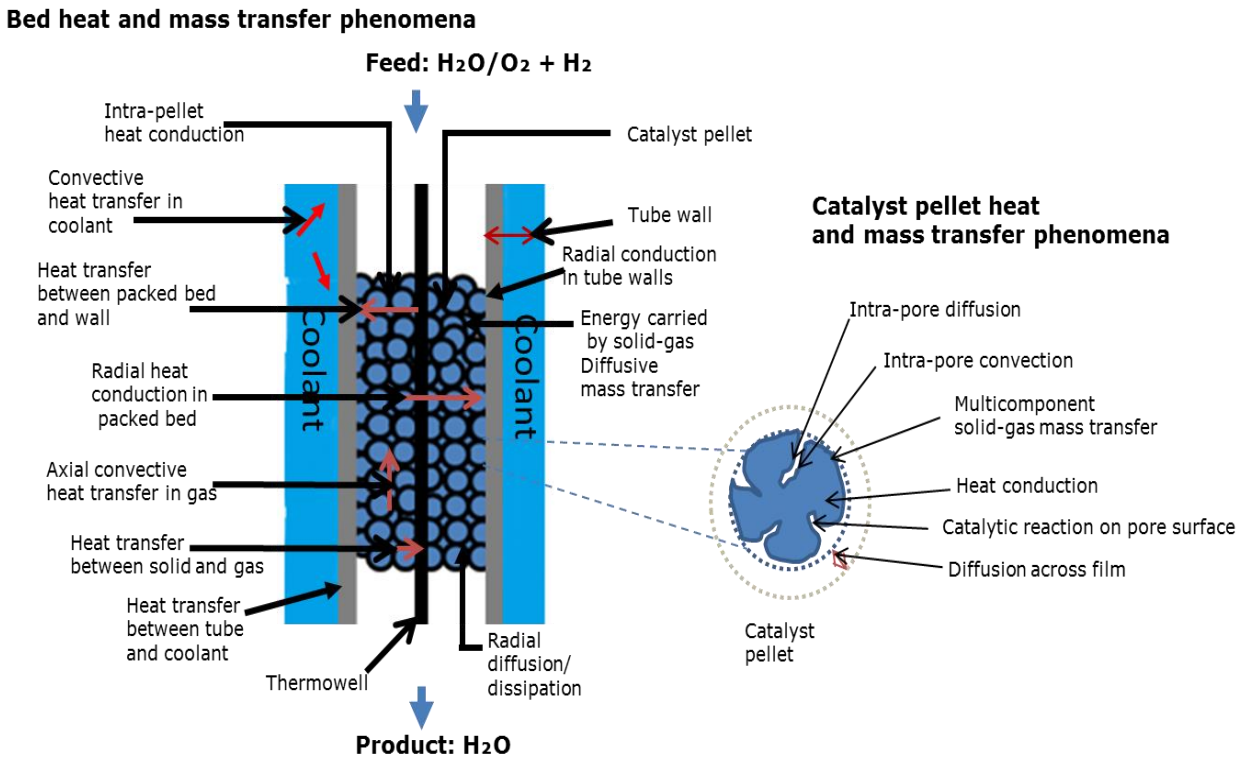

Figure 54: Longitudinal catalytic packed-bed for a fixed bed reactor

Figure 55 shows a slice of the fixed-bed reactor and from which a design equation is proposed.

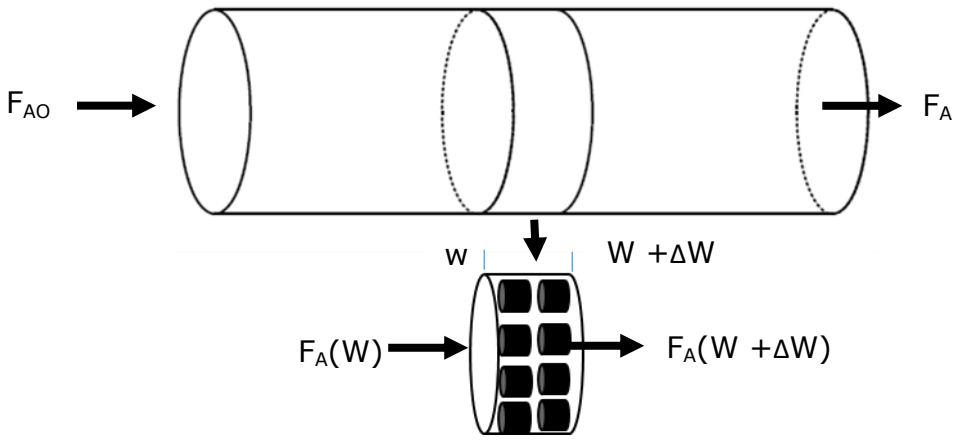

Figure 55: Schematic diagram of a fixed-bed reactor

The design equation for the fixed-bed reactor will be developed based on a reactor volume equation but considering the mass (weight) of the catalyst pellet being that the weight of the catalyst is of primary importance [98]. The equations are given below assuming there is no radial gradients in

concentration, reaction rate or temperature. The generalized mole balance equation is also applicable here as shown in equation 32.

Input(In) – Output(out) + generation(G) = Accumulation (32)

And the generalized mole balance on specie A over the weight of catalyst pellet ΔW results in the following equations

$$F_{A(W)} - F_{A\,(W+\Delta W)} + r'_A \Delta W = 0 \quad (33)$$

$$(r'_A)\,\Delta W \equiv \left(\frac{Moles\ of\ A}{time\ X\ mass\ of\ catalyst}\right) X\ (mass\ of\ catalyst) \equiv \frac{Moles\ of\ A}{time} \quad (34)$$

Dividing equation 34 by ΔW and taking the limits as ΔW⟶ 1, equation 35 is generated and it represents the mole balance of specie "A".

$$\frac{dF_A}{dW} = -r_A \quad (35)$$

CHAPTER FIVE

Chapter 5

5 CATALYTIC FIXED-BED REACTOR FOR WATER DEOXYGENATING PROCESS (METHOD No 1)

5.1 Introduction

First part of this work was carried out exploring fixed bed reactor experiment using pelletised catalyst and its catalytic performance was evaluated in the removal of DO. The removal of DO was carried out experimentally using the fixed-bed catalyst prepared as described in chapter 3, section 3.1. The experiment was carried out in a continuous flow system at ambient pressure and temperature. Various operating conditions were also applied in the study.

5.2 Equipment and Apparatus

A stainless steel reactor was used and it was held in place using a rig on which the reactor was clamped. A hydrogen detector and monitoring system was used to comply with the health and safety regulations. A stop watch which was used to note the time it took to reach a certain volume in the beaker was required. A plastic tubing used for feeding in the water into the reactor system, a 500 mL glass beaker for collecting the product, a digital pressure gauge connected on the rig was used to enable the reading of the hydrogen gas flowing into the reactor, hydrogen gas cylinder, tap water supply and DO analyser were all required. The DO analyser used was a digital HQ 30D portable DO meter with field luminescent DO sensor and a 100 cm cable purchased from HACH, UK. This instrument is designed to be used solely in water media. As shown in Figure 56, the analyser has an oxygen probe connected to it which has a sensor that is protected by a shroud. The sensor sends the readings to the analyser, which in turn has a digital screen that displays the results with details of the temperature at the point of measurement. The DO analyser can measure reading up to 20 mg/L and it is a reliable means to measure the amount of DO present in water and user friendly.

Figure 56: DO analyser

5.3 Materials

Materials used for this part of the work includes the catalyst fixed-bed (method No 1), gases (hydrogen and helium) at 99% purity and tap supplied water.

5.4 Health and safety

The experiment was conducted inside the fume cupboard at all times. A hydrogen safety monitor was activated at all times due to the long duration of hydrogen gas supply. Personal protective clothing were also worn at all times. See appendix III for other health and safety measures undertaken.

5.5 Experimental Procedure

An experimental test rig for the fixed-bed reactor process was assembled as shown schematically in Figure 57, while Figure 58 shows the pictorial arrangement. In designing the fixed-bed test rig, 3 sections were involved: the feed, the fixed-bed reactor and the analytical sections.

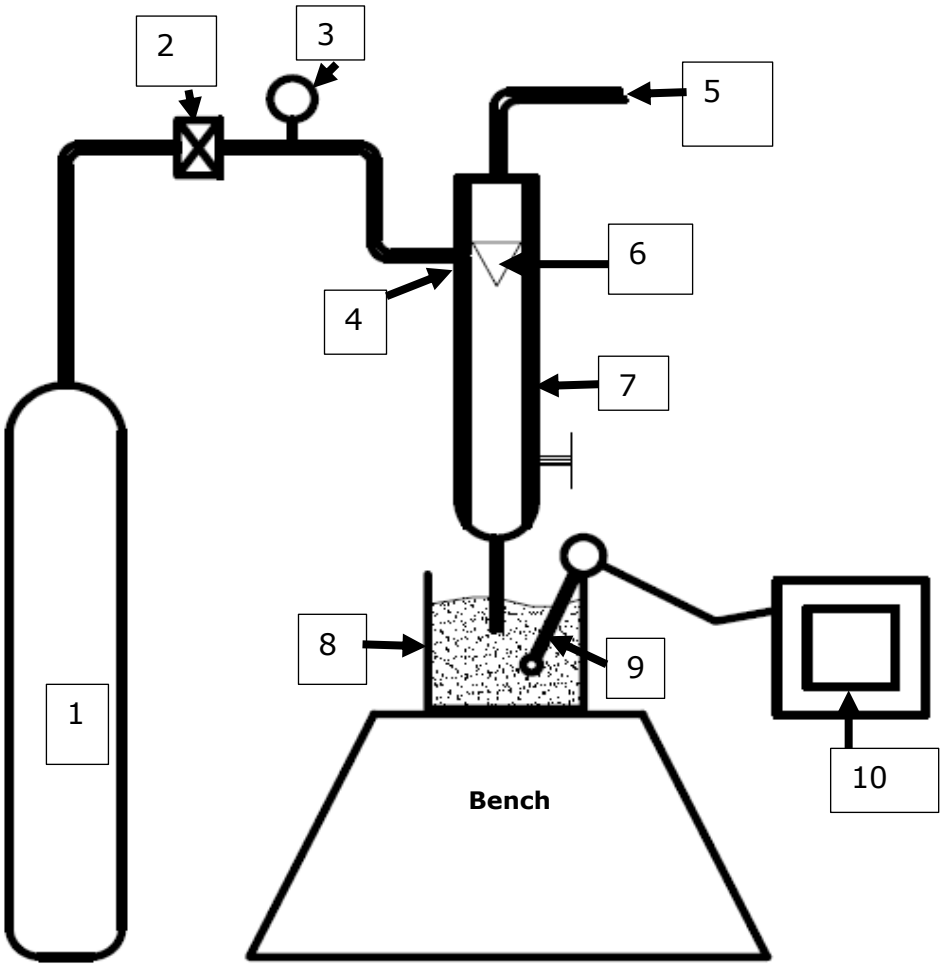

Figure 57: Schematic diagram of the fixed-bed experiment (1. Hydrogen gas, 2. Control valve, 3. Digital gauge pressure, 4. H_2 inlet port, 5. Inlet feed water source, 6. Catalyst bed, 7. Stainless-steel reactor, 8. Beaker containing water, 9. DO probe, 10. DO analyser

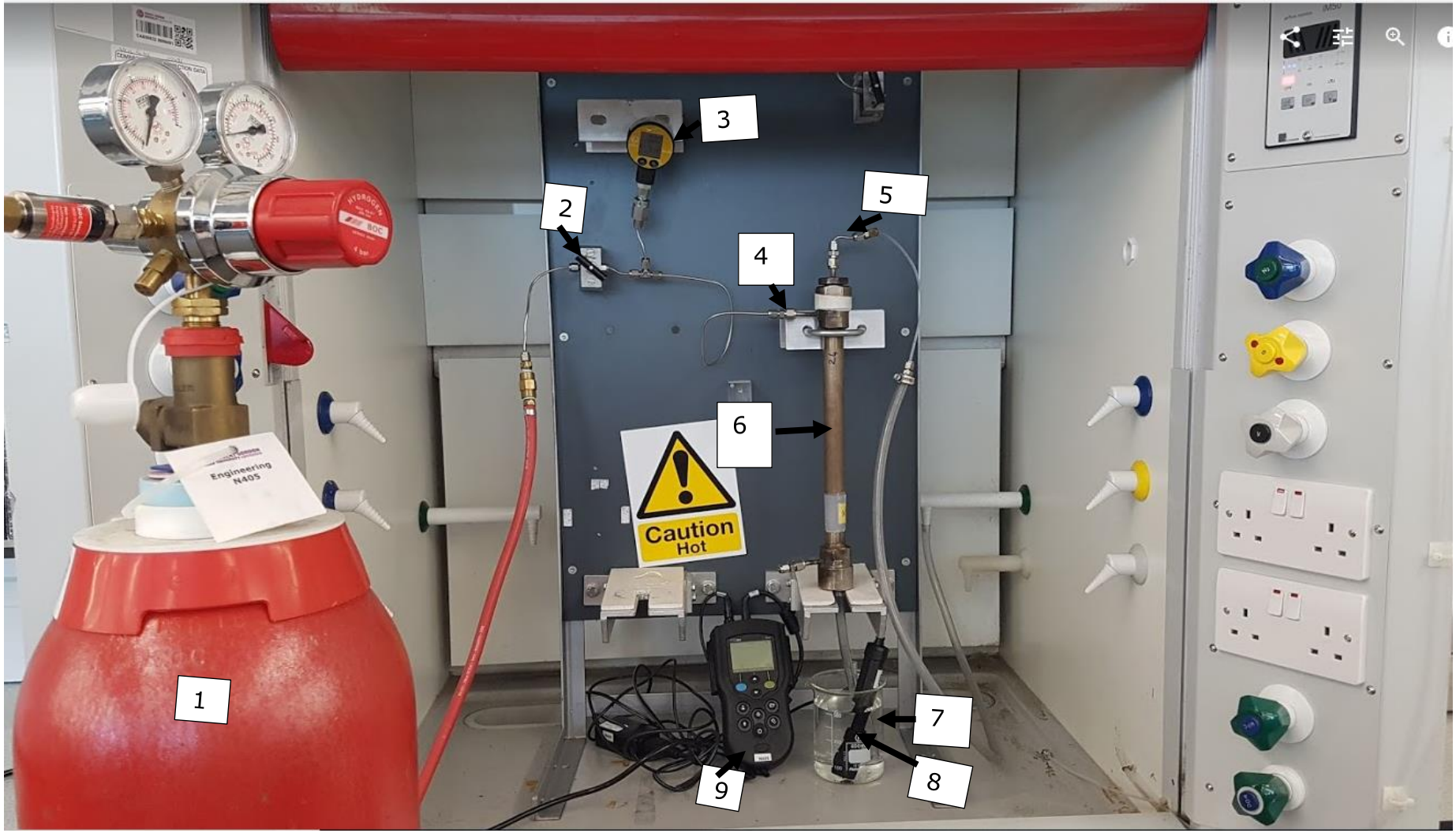

Figure 58: Pictorial diagram of the fixed-bed experiment: (1. Hydrogen gas, 2. Control valve, 3. Digital gauge pressure, 4. H_2 inlet port, 5. Inlet feed water source, 6. Stainless-steel reactor, 7. Beaker containing water, 8. DO probe, 9. DO analyser

5.5.1 Feed delivery Section

In the feed delivery section, a digital pressure gauge was connected to the control valve in which it was used to regulate the amount of hydrogen gas leaving the cylinder. This section comprises mainly of the water and hydrogen supply which from the diagrams in Figure 57 and 58 can be seen that they were fed into the reactor from different sides and this was because less resistance is experienced with the fixed-bed reactor arrangement. The plastic tubing was used to connect the water from the tap to the reactor, while stainless steel tube were used for the hydrogen gas connections. All fittings in the hydrogen connection were tested for leaks.

5.5.2 Fixed-bed catalytic reactor section

In this section, the mesh containing the catalyst pellet was suspended inside the reactor (Figure 26d section 3.1) and pushed up towards the neck closer to the entry points for both the water and hydrogen gas. The reactor was then clamped onto the rig as shown in Figure 58.

5.5.3 Analytical Section

In the analytical section, a 500 mL was used to collect the water sample exiting the fixed-bed reactor and measurement of the DO after the experiment was done by submerging the DO probe inside the collected water in the beaker and reading it off (see Figures 58 and 66).

5.5.4 Kinetic Experimental runs

The test rig was initially tested with an inert gas (helium) before carrying out the analysis with hydrogen gas. This was done to ensure that no leak was present. The hydrogen detector was clamped above the rig for safety reasons. Hydrogen gas was introduced from the top of the reactor while the tap water was introduced from the side. The volumetric water flowrates were calculated manually using a 500 mL beaker, number of turns of the tap and a stopwatch. As the tap was turned on, the timer was also started immediately, the water and hydrogen were allowed to flow through the suspended catalyst bed into a collecting beaker under the reactor until 500 mL of water was collected. After this, both the hydrogen supply, timer and tap are turned off.

Measurement of the DO before and after the experiment were taken with the use of a DO analyser while the experiment was carried out in the fume cupboard. Table 4 shows other experimental variables that were put into consideration.

Table 4: List the experimental conditions and system parameters used in the study

Parameters	**Values**	**Units**
Feed water flow rate	150-450	mL/min
Temperature	298	K
DO concentration in the feed (tap water)	9.70	ppm
Hydrogen flowrate into the mixing unit	0.1-0.8	bar
Catalyst % loading	0.16, 0.6	

CHAPTER SIX

Chapter 6

6 CATALYTIC MEMBRANE REACTOR WATER DEOXYGENATING PROCESS (Method No 2 & 3)

6.1 Introduction

Reacting oxygen with a reducing agent such as hydrogen in the presence of a catalyst to form water is an attractive method as it produces water and no by-products to contaminate the water [38]. The removal of DO was carried out experimentally using the novel catalytic membranes prepared as described in chapter 3.

The object of this chapter is therefore to design and test platinum and palladium catalytic membranes for water deoxygenation. The experiment was carried out in a continuous flow system at ambient pressure and temperature. Various operating conditions were also applied in the study.

6.2 Equipment and Apparatus

Three reactors were used and were held in place using stainless steel retort stands on which the reactors were clamped. A hydrogen detector and monitoring system was used to comply with the health and safety regulations. A three-necked round bottom flask and beakers were required for the process. The three necked flask served as the mixing units, while the beakers were used to collect deoxygenated water samples. Rubber corks were used as stoppers in the three necked round bottom flask. Digital flowmeters were used to measure and control the hydrogen gas supply into the mixing unit and also for metering the nitrogen gas when it was used as a blanket gas during the DO measurements. A DO analyser was also needed for measuring the DO levels before and after the analysis. A magnetic stirrer was used to create mixing of the hydrogen/water to enhance saturation of the hydrogen prior to being introduced into the reactor. A masterflex (Cole Parmer, UK) digital electric water pump (shown in Figure 59) was used to supply the hydrogen saturated water from the mixer to the reactor. It consists of a pump drive, with a detachable pump head connected to it. The pump head houses the tubing which serves as a source of the water from the

mixing unit into the reactor. The digital pump drive controls the speed of the pump head to provide flow rates ranging from 0.001 to 3400 mL/min.

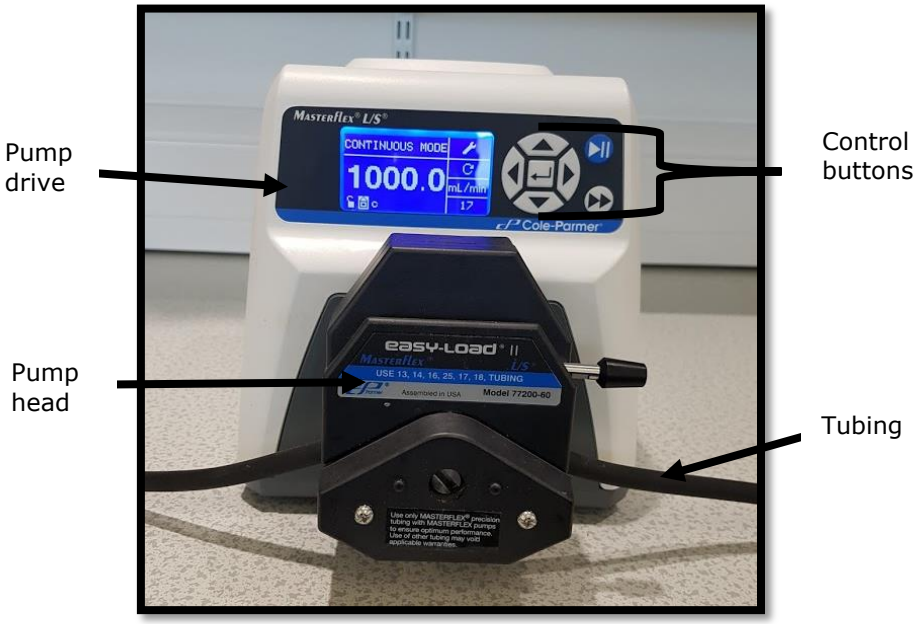

Figure 59: Electric water pump

In order to achieve maximum dissolution of hydrogen in the reactor feed-water, a stainless steel gas sparger (Figure 60) was used (Diva Envitec Pvt. India). It was used to introduce hydrogen gas into the water in very tiny numerous bubbles through its tiny pores. Introducing this gas in tiny bubbles helps in the solubility of hydrogen gas in water.

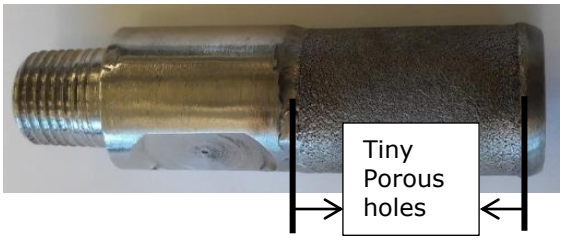

Figure 60: Stainless steel gas sparger

All experiments involving hydrogen were carried out in the fume cupboard.

6.3 Materials

Materials used for this part of the work includes the platinum impregnated membranes, palladium-coated membranes, gases (hydrogen and nitrogen) at 99% purity and tap supplied water.

6.4 Health and safety

The experiment was conducted inside the fume cupboard at all times. A hydrogen safety monitor was activated at all times due to the long duration of hydrogen gas supply. Personal protective clothing were also worn at all times. See appendix III for other health and safety measures undertaken.

6.5 Experimental Procedure

In designing the water deoxygenating process, the experimental rig was made up of 3 sections: the feed delivery, the catalytic membrane reaction and the analytical section. The experimental setup is shown schematically in Figure 61 and then represented pictorially in Figure 62.

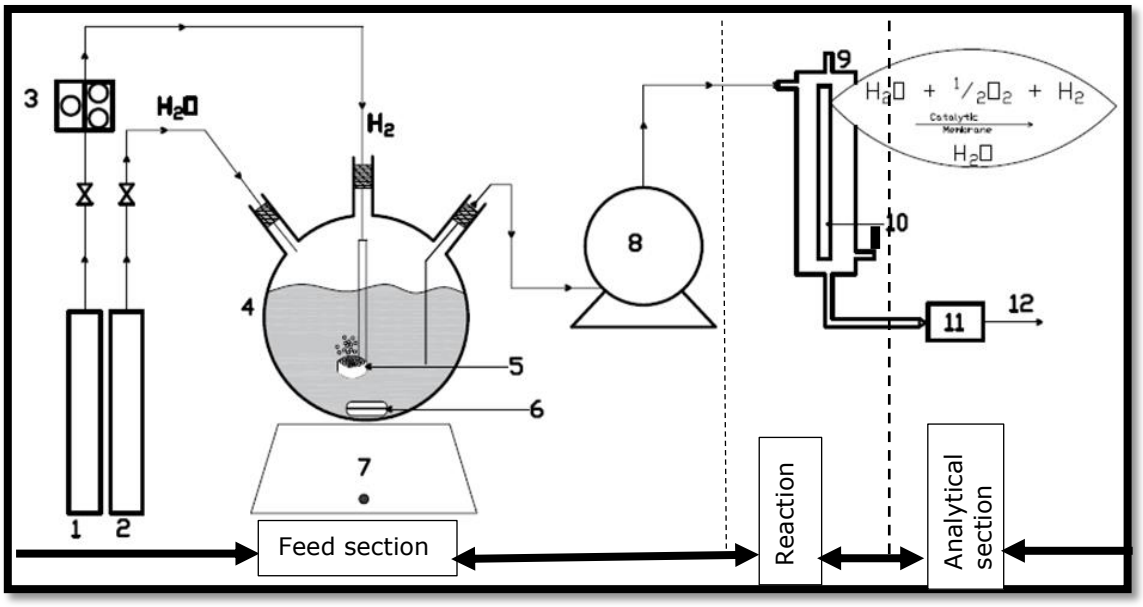

Figure 61: Schematic experimental diagram for the removal of DO in water using a catalytic membrane reactor process (1. Hydrogen cylinder, 2. Water source, 3. Flow meter, 4. Pyrex glass reactor, 5. Sparger, 6. Stirrer, 7. Magnetic stirrer plate, 8. Water pump, 9. Catalytic membrane reactor, 10. Catalytic membrane, 11. DO analyser, 12. Waste

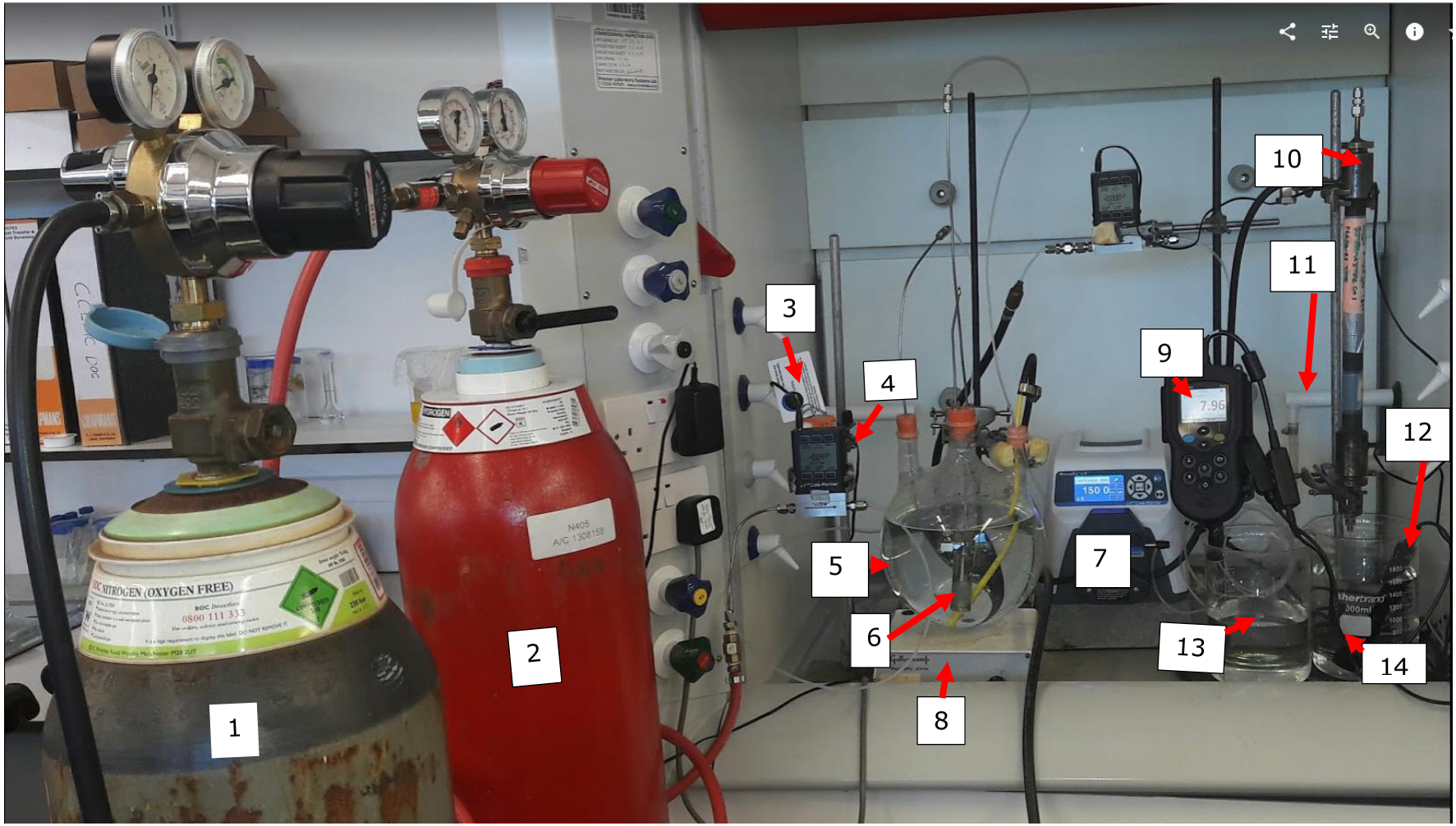

Figure 62: Pictorial representation of the experimental setup for the catalytic membrane water deoxygenating process (1. N_2 cylinder, 2, H_2 cylinder, 3. H_2 safety monitor, 4. Flowmeter for H_2 and N_2, 5. Round bottom flask, 6. H_2 sparger, 7. Cole palmer pump, 8. Stirrer, 9. DO analyser, 10. Catalytic membrane reactor, 11. Water supply, 12.DO probe, 13. Water beaker with N_2 as a blanket gas, 14. Water beaker with air as a blanket gas

6.5.1 Feed delivery Section

The feed delivery section consist of hydrogen gas supply, hydrogen safety monitor, water source (tap located in the fume cupboard), flow meter, 3-necked round bottom flask, magnetic stirrer and an electric pump with tubing. The 3 necked round bottom flask was used as a mixing unit for hydrogen and water. A stainless steel gas sparger was used to distribute the hydrogen gas in small bubbles into the water. This gas sparger was connected to a stainless steel tube (1/8 in) as shown in Figure 63 and rubber corks were used as seals both in the middle neck and at the rear sides of the flask. A vent was also created in the cork holding the sparger for the release of un-dissolved hydrogen. The rear sides of the flask were used as water inlet and outlet ports in the feed experimental arrangement as shown in Figure 61 or 62. During the experiment, a flow meter was connected to the hydrogen cylinder to measure the amount of hydrogen used at each run.

The electric pump then sends the water mixture into the reactor at various flow rates. The pump was usually calibrated on daily basis. This is done to ensure the pump is working in a good condition and also that it is pumping the required amount. The hydrogen gas safety monitor was used throughout the experiment to check and ensure that any hydrogen gas leak is detected so that it does not reach an explosive level. This monitor was located within the vicinity of the experimental setup. Leak solution (Snoop) was also used on joints on the hydrogen cylinder to ensure leak-free operation from the valves.

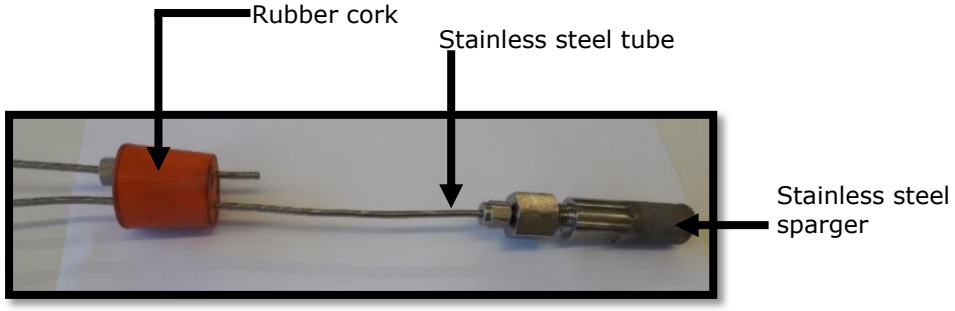

Figure 63: Connection of the gas sparger to a stainless tube and cork seal

6.5.2 Catalytic Membrane Reaction Section

In the reaction section, the catalytic membrane is inserted inside a stainless steel housing as shown in Figure 64. This is placed vertically along the reactor taking proper care to prevent any damage on the membrane. The membrane is then sealed at both ends of the reactor with the graphite 'O' rings. This is done to prevent any leakage of water mixture during the water deoxygenating experiment. The membrane reactor is then clamped and maintained vertically using a retort stand as shown in Figure 65.

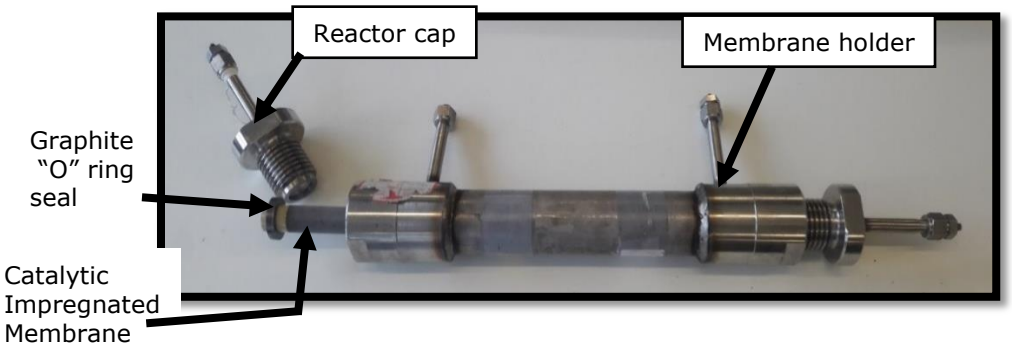

Figure 64: Pictorial representation of a Catalytic impregnated membrane inserted into the membrane holder.

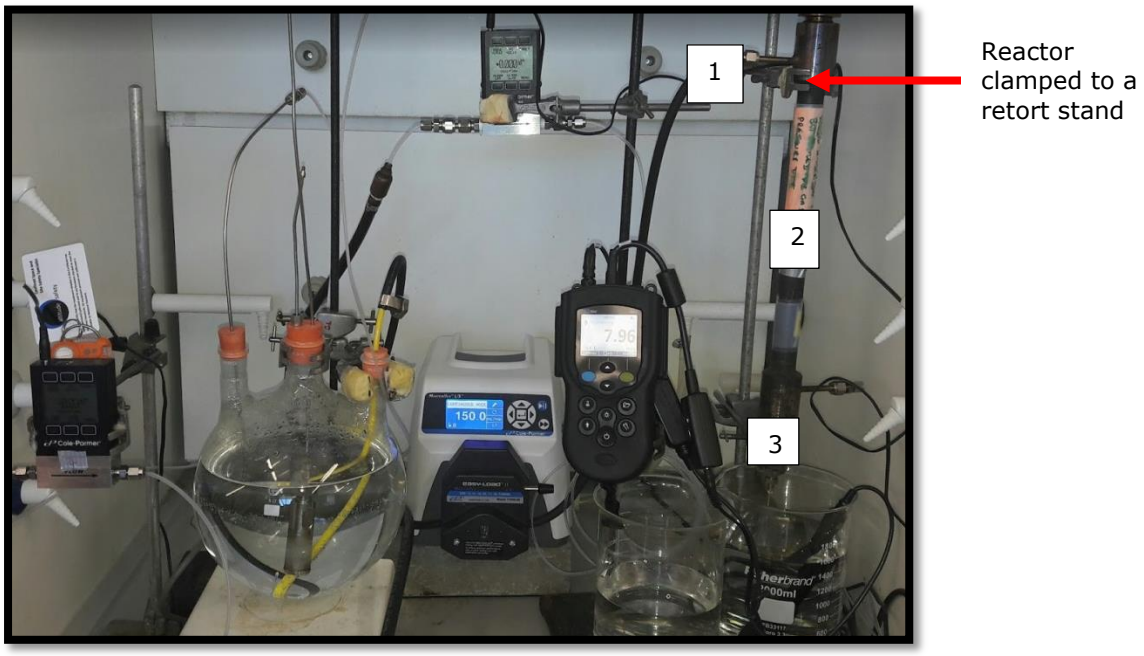

Figure 65: Picture showing the reactor clamped to a retort stand

The reaction section has 3 parts which are labelled 1, 2 and 3 as shown in Figure 65. The inlet port represented as 1, is also referred to as the feed inlet, the reaction chamber, symbolised as 2, and the permeate port, denoted as 3. The water mixture is pumped into the reaction chamber through the inlet point of the reactor using the electric pump. The water is usually allowed to flow through for a period of time, this is to allow stability of the reaction to be reached. The reaction of the hydrogenated water is expected to take place in the reaction chamber 2, which provides a suitable catalytic surface that will enhance the reaction of DO and the dissolved hydrogen [29]. The method is similar to that reported by Lebedeva et al [29].

The catalytic impregnated membrane plays a different role in the water deoxygenating process when compared to its role in gas permeation experiment. In this case, the membrane does not serve as a selective device, instead its purpose is to create a suitable surface to favour the reactions of reactants and then allowing it to permeate through the membrane.

6.5.3 Analytical Section

This section is mainly the analysis of the product permeating through the reactor using a DO analyser (HACH). A glass beaker was used to collect the product and its level of DO was measured after the inserted probe stabilized using atmospheric air as a blanket gas. Nitrogen gas was also used as a blanket gas with the aim of preventing oxygen from the atmosphere re-dissolving back into the product water. Figure 66 shows the process of measuring the level of DO in water. At each set flowrate, for example, the pump is programmed to inject a feed at 200 mL/min, that particular flowrate is allowed to run through the catalytic membrane reactor for a period of 30 minutes before readings are taken at the permeate end. Each DO measured represents the amount of DO present after the injection at that certain flowrate through the reactor.

Figure 66: Process showing measuring of DO level in water

6.5.4 Kinetic Experimental Runs

Experimental test runs were carried out in a continuous stirred flow process in which the membrane was sealed in a tubular membrane holder as explained in details in section 6.5.2. All five catalytic membranes prepared were tested in the water deoxygenating experiment. A note on the catalyst is that the catalytic loading were not altered throughout the analysis.

Hydrogen gas was introduced into the round bottom flask containing water (DO level of 9.66 ppm). The mixture was then fed into the shell-side of the catalytic membrane reactor. Because the membranes are porous with highly dispersed catalyst embedded and all over their surface and pores, it offered little resistance to water. The dissolved hydrogen and DO then reacts together in the presence of the catalyst to form water which is not a contaminant. The hydrogen gas in this experiment serves as a reducing agent, and the chemical reaction occurs in the catalytic membrane reactor leading to the oxygen level in the water at the outlet stream of the reactor to be much reduced.

Calibrations of both the electric water pump and DO analyser (HACH) were carried out and the inlet (feed) and outlet (permeate) DO levels were measured and recorded respectively. The calibration of the DO analyser was done in aerated water at room temperature and confirmed with completely

deoxygenated water by the addition of excess sodium sulphite [30]. This calibration method is also referred to as Winkler's method.

The experimental runs were carried out with variations in feed inlet flowrate, hydrogen flowrate into the mixing unit and water permeating time using the different types of membranes. A decrease in the concentration of oxygen in H_2O with time was also recorded. The final outlet level of DO was recorded after a steady state was reached. All the experiments were carried out at 25°C and ambient pressure of 1 atm. Table 5 shows the different experimental parameters.

Table 5: List the experimental conditions and system parameters used in the study.

Parameters	**Values**	**units**
Number of membranes	1	dimensionless
Membrane O.D*	10, 25, 25	mm
Membrane I.D*	7, 20, 20	mm
Length of membrane*	370, 370, 650	mm
Feed water flow rate	200-1000	mL/min
Temperature	298	K
DO concentration in the feed (tap water)	9.66	ppm
Hydrogen flowrate into the mixing unit	0.19, 0.65, 1.16,1.28, 1.55	L/min

- *dependant on which membrane being used

Figure 67 shows the catalytic membrane reactor principle for the water deoxygenating process, illustrating the arrangement of the catalyst in the pores.

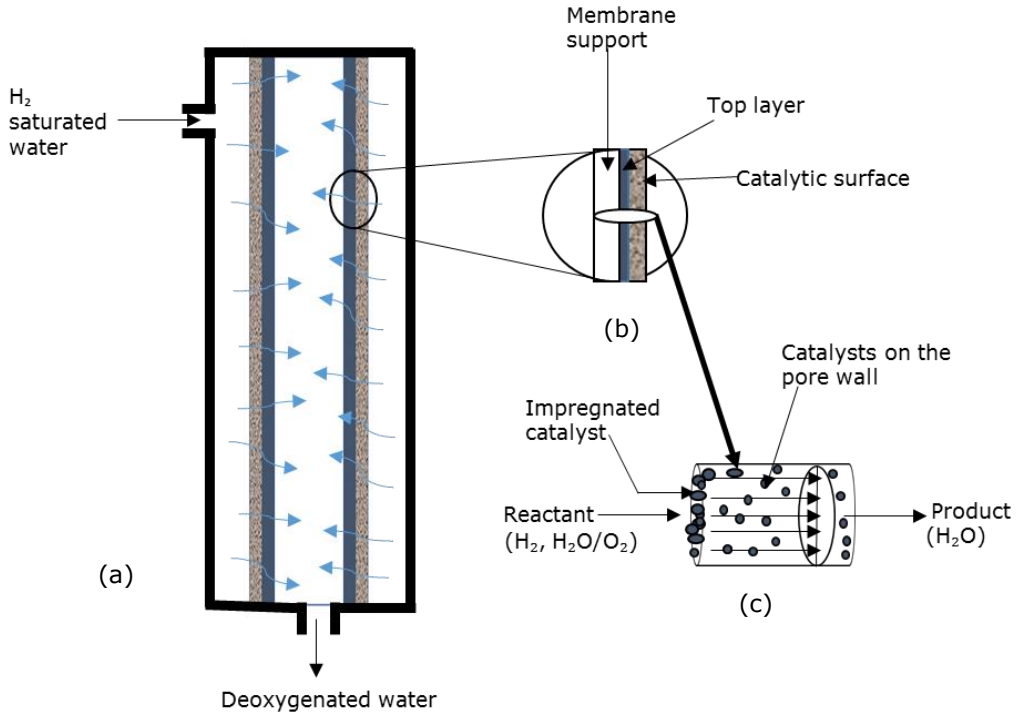

Figure 67: Schematic diagram of the reactor module (a) catalytic membrane reactor illustrating the working principle, (b) section showing the arrangement of the catalytic active phase on the tubular membrane, (c) showing a pore and how the catalyst is impregnated

CHAPTER SEVEN

Chapter 7

7 REACTOR ENGINEERING

7.1 Kinetic analysis

In the kinetic analysis of this experiment, the plug flow reactor model was used to deduce the performance equation of the reaction process considering a membrane pore in the case of the catalytic membrane or a sectional thin slice of the fixed-bed containing the catalysts. It is also important to note that the rate of reaction involves a heterogeneous catalyst. For more reliable results, the catalytic membrane and fixed-bed reactors are designed and explained as an isothermal reactor, (that is a plug flow reactor) and this design enables a better understanding of transport mechanism in a tubular reactor assuming each pore represents a cylindrical tube. Using same experimental conditions, that is, using hydrogen saturated water as the feed into the catalytic membrane or fixed-bed reactor at ambient pressure and temperature, the following assumptions will be made:

1. That the mixture is properly mixed in the mixing unit of the experiment
2. Each pore on the tubular membrane approximates a tubular fixed bed

7.1.1 Mole balance and stoichiometry

To determine the mole balance of this application, the boundaries needs be defined. Figure 68 shows the representative schematic picture of a pore or a slice of the fixed-bed section showing the direction of flow of fluid, while Figure 69 shows the x-sectional slice of the pore or section bearing the catalyst. A mole balance will be performed on reacting specie "A", where A can either be oxygen or hydrogen depending on which is termed the limiting specie. In this experiment, the concentration of oxygen at the feed was relatively constant, the concentration of hydrogen was varied.

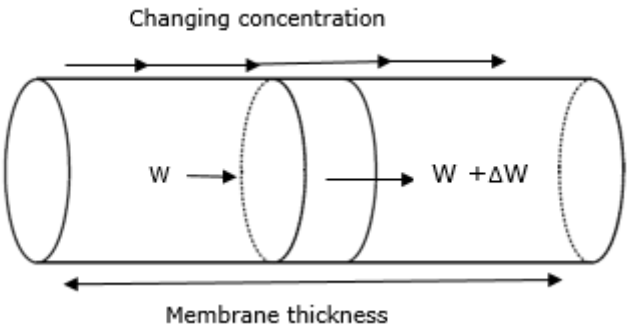

Figure 68: Schematic diagram showing the flow of water through a pore of a catalytic membrane

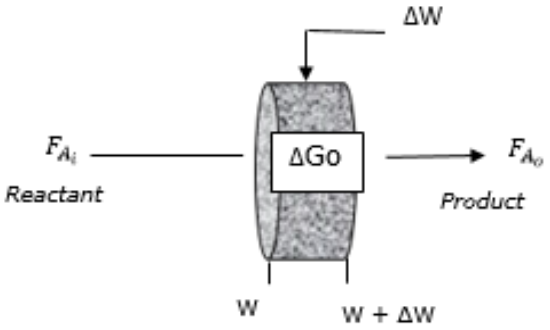

Figure 69: Cross sectional slice of the pore showing the direction of flow

Where

F_{A_i} = flowrate of oxygen inlet

F_{A_o}= flowrate of oxygen outlet

W = Weight of catalyst

At steady state, a material mole balance equation for a reactant A at any time, t, over catalyst weight ΔW is given by [98]:

Input(In) – Output(out) + Generation(G) = Accumulation (36)

In a plug flow reactor system, accumulation is zero at steady-state, so equation 36 can be rewritten as

Input(In) – Output(out) = -Generation (G) (37)

$$F_{A_i} - F_{A_o} = -G \quad (38)$$

Where

$F_{A_i} \neq F_{A_o}$ because a reaction is taking place and the reactants are continually being consumed as they flow down the length of the fixed-bed reactor or through the pore of the catalytic membrane reactor.

The generation term 'G' can be written as equation 39

$$G = (r_A)\,\Delta W \equiv \left(\frac{Moles\ of\ A}{time\ X\ mass\ of\ catalyst}\right) X\ (mass\ of\ catalyst) \equiv \frac{Moles\ of\ A}{time} \quad (39)$$

Assuming the concentration of the reactant varies continuously in the axial direction through the fixed-bed or the catalyst pore, then the reaction rate which is a function of concentration will therefore vary axially, that is, there is no special radial variation in the rate of reaction and equation 38 is rewritten as

$$F_{A_i(W)} - F_{A_o\,(W+\Delta W)} = -G \quad (40)$$

Equation 40 can also be written as

$$F_{A_i(W)} - F_{A_o\,(W+\Delta W)} = -r_A \Delta W \quad (41)$$

In the limit as $\Delta W \to 0$,

$$\Delta G = \int_0^W r_A\, dW = r_A W \quad (42)$$

Equation 41 can be rewritten as

$$dF_A = -r_A\, dW \quad (43)$$

Dividing equation 43 by dW, equation 44 is obtained and it represents the mole balance of specie "A".

$$\frac{dF_A}{dW} = -r_A \quad (44)$$

Equation 44 is then integrated and it gives equation 45 which can be used to calculate the weight of the catalyst if pressure drops in the reactor and catalyst decay are negligible.

$$W = \int_{F_A}^{F_{AO}} \frac{dF_A}{-r_A} \quad (45)$$

7.1.2 Rate law

The rate of reaction of reactant, $-r_A$ in the heterogeneous reaction involving liquid and solid catalysts can be expressed as a factor of surface area or catalyst weight. The rate of reaction $-r_A$, is therefore equal to the number of molecules of DO reacting per unit time per unit mass of catalyst (mol.s^{-1},g$^{-1}_{\text{catalyst}}$) as shown in equation 46.

$$r_A = \frac{X}{W/F_{A_i}} \quad (46)$$

Where X is DO conversion, W is the weight of the catalyst and F_{A_i} is the feed flow rate in mol/s.

To work out the rate of forming a product (in this case, H_2O), the rate of reaction will be dependent on the reacting species (oxygen and hydrogen) and reaction conditions such as reaction temperature, catalyst type and concentration of the reacting species. This process would have been totally independent on the type of reactor the reaction is taking place in, but because the catalytic membrane process and the fixed-bed reactor were operated as a differential reactor, the rate of reactions will be assumed to remain constant throughout the membrane's thickness and the bed length respectively.

The order of reaction of oxygen with hydrogen is a second order reaction, where [DO] ≠ [hydrogen]. The rate equation of this reaction can be cumbersome, there for, it will be handled as pseudo-first order reactions since hydrogen is supplied in great excess [5].

A generalized equation is given by equation 47, where A is DO and B is hydrogen, and the rate of reaction is given by equation 48

$$A + B \longrightarrow \text{Product} \quad (47)$$

$$\text{Rate} = k [A]^h [B]^f \quad (48)$$

Where, h is the order with respect to concentration of DO ([A]), and f is the order with respect to concentration of hydrogen ([B]). The total order with is then given by equation 49

$$n = h + f \quad (49)$$

If the effect of hydrogen [B] on the rate is kept constant, then, the effect of DO [A] on the rate could be studied independently of [B] and vice versa. This means that hydrogen [B] in the reaction was kept in excess and effectively constant throughout the reaction. If this is the case, then $[B]^f$ is constant and k' can represent $k[B]^f$. K' is called a pseudo-rate constant. Equation 48 can then be written as

$$\text{Rate} = k'[A]^h \quad (50)$$

Where $k' = k[B]^f$

The water chemistry can also be modelled by simple power law equations where the partial pressures of oxygen and hydrogen are considered. Equation 48 can then be written as

$$-r_A = k P_{O_2}^h P_{H_2}^f \quad (51)$$

Where k is the rate constant, P_{O_2} and P_{H_2} are partial pressures of oxygen and hydrogen. h and f are the reaction orders of oxygen and hydrogen respectively. If h with respect to oxygen is 1.0, equation 51 can be simplified to give

$$-r_{O_2} = k' P_{O_2} \quad (52)$$

Where $k' = kP_{H_2}$

If equation 52 is linearized, it yields

$$\ln(-r_{O_2}) = In\, k' + h\, In\, P_{O_2} \quad (53)$$

Equation 46 and equation 50 can also be used to calculate the rate of reaction. Combining these equations will yield

$$\frac{X_A}{W/F_{A_i}} = k'[A]^h \quad (54)$$

If equation 54 is linearized, it yields

$$\ln\left[\frac{X_A}{W/F_{A_i}}\right] = ln\, k' + h\, ln\, [A] \quad (55)$$

CHAPTER EIGHT

Chapter 8

8 RESULTS AND DISCUSSIONS

The result section is divided into three main parts:

1. Results showing the effect of catalytic loading on the membranes on the DO removal;
2. Results on fixed-bed catalyst characterization (SEM-EDAX) and membrane characterization: gas permeation, SEM-EDAX and liquid nitrogen analysis.
3. Evaluation of DO removal utilizing methods No.1, 2 and 3 in water deoxygenation.

8.1 Catalytic Loading on Membranes

After the process of membrane preparation, the catalyst loadings on the membranes were calculated and are presented in Table 6 for palladium and Table 7 for platinum membranes. It should also be noted that the dipping process was done just once, that is a single dipping. Single dipping of the support into the precursor solution or coating in the case of palladium was done to optimize the catalytic performance. This is because having a high catalytic loading may generate problems of internal diffusional resistance and also reduce dispersion hence affect the efficiency of hydrogen and oxygen recombination process. The amount of catalyst deposited on the membranes were estimated from their weight gain, that is, the change in weight between the fresh support and the activated membrane.

Table 6: Showing the catalyst loading of the palladium metal

	Membrane A	Membrane B
Weight of fresh support w_1 (g)	48.6	273.4
Weight of support after soaking in water (g)	55.3	312.3
Weight after conventional Pd-Sn activation and air drying (g)	48.7	273.5
Weight after Palladium chloride plating w_2 (g)	49.0	276.1
Weight of Palladium metal deposited w_3 (g)	49.0	276.1
Weight of catalyst deposited w_4 (g)= w_3-w_1	0.4	2.7
Catalyst loading wt. % $\left[\frac{w_4}{w_1} \right]$ x100	0.8	1

Table 7: Showing the catalyst loading of the platinum metal

	Membrane A	Membrane B	Membrane C
Weight of fresh support w_1 (g)	49.0	274.8	482.2
Weight of support after soaking in water (g)	55.8	312.7	497.2
Weight after platinum chloride deposition w_2 (g)	49.1	275.9	484.6
Weight of Platinum metal deposited w_3 (g)	49.1	275.9	484.6
Weight of catalyst deposited W_4 (g)= w_3-w_1	0.1	1.1	2.4
Catalyst loading % $\left[\frac{w_4}{w_1} \right]$ x 100	0.2	0.4	0.5

From the parameters listed in tables 6 and 7, it can be observed that the first 2 steps involved in the palladium membrane preparation showed little weight gain unlike in the plating itself. It further shows that the weight gain in the palladium membranes was as a result of the plating which forms a film on the surface and pores of the support [18].

8.2 Membrane characterisation

By characterizing a membrane, investigation on the influence of the catalyst on the performance can be carried out. The membranes were characterised by gas permeation, scanning electron microscopy and BET surface area measurements. The catalytic activities of the deposited catalysts were compared to that of the fresh support.

8.2.1 Gas Permeation

To investigate the influence of the catalyst deposition on gas transport mechanisms, permeation measurements were carried out before and after catalyst introduction. Smart et al [50] stated that the permeation measurement methods are the most reliable method for proposing a membranes' performance. The gases used were single gases: hydrogen, oxygen, nitrogen and helium. Table 8 shows the molecular weights and their individual kinetic diameters.

Table 8: Shows the molecular weights and kinetic diameter of gases

Gases	Molecular weights (g)	Kinetic diameter (Å)
Hydrogen	2	2.89
Oxygen	32	3.0
Nitrogen	28	3.64
Helium	4	2.6

8.2.1.1 Gas permeation through supports

Figures 70a and 70b show the effect of transmembrane pressure drop on the flow rates of the gases across the supports at room temperature of 298 K. It was observed that hydrogen having the lowest molecular weight permeated faster, followed by helium gas. Nitrogen and oxygen permeated at similar flow rates. Comparing Figure 70a and 70b, it will be seen that the gases exhibit similar gas transport mechanisms across the support. Viscous flow mechanism can be said to be responsible for the transport of H_2 and He, because, the increase in gauge pressure led to increase in flow rate. This is unlike nitrogen and oxygen, where they exhibited an initial increase in flowrate and then maintained constancy as the pressure was increased. This signifies Knudsen gas mechanism was responsible for the flow of oxygen and nitrogen gas.

Higher gas permeations were observed in the 6000nm pore sized support when compared to the 15 nm support. This difference in the permeation variation could be attributed to the larger pore size present in 6000nm support.

Taking a look at the trend of the gas permeation, it may be presumed that the transport mechanism is also dependent on molar weight of the gas, that is, the order of permeation is $H_2 > He > N_2 > O_2$. Oxygen permeated less having the heavier molecule weight. According to Li K. [46], some of the gas transport mechanism also considers the molecular mass of the gases and or their kinetic diameters. In this case, the molar mass was considered.

Knudsen flow transport is sufficient for separation but there is the need for catalytic deposition on the support to facilitate chemical reaction by combining other activation mechanism.

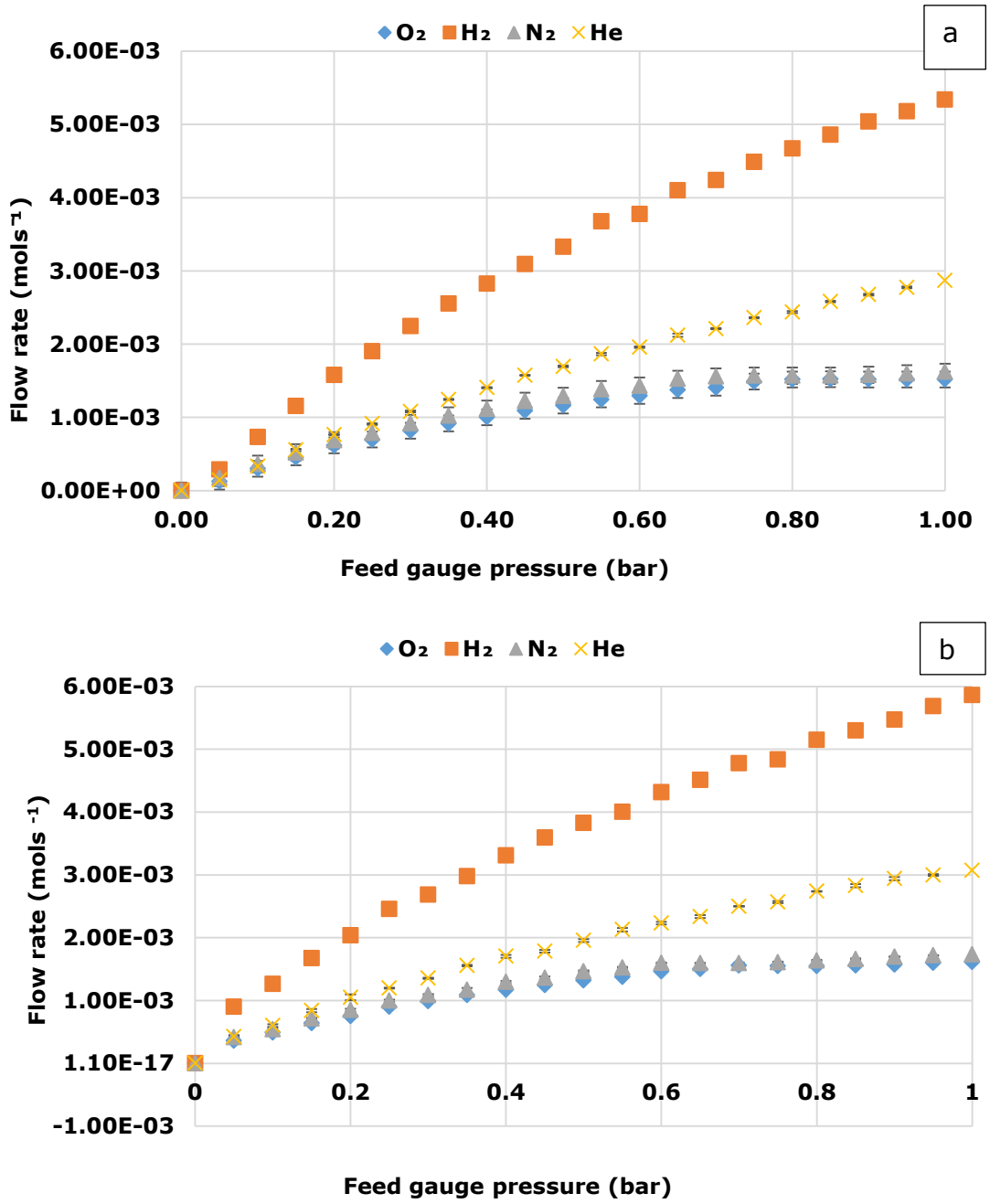

Figure 70: Effect of flow rate on the feed gauge pressure of support material (a) 15nm-support A and (b) 6000nm-support B at 298 K

Figure 71 confirms that the kinetic diameter does not contribute to the transport mechanism, but the molar mass. In this case, influence of the kinetic diameter was negligible.

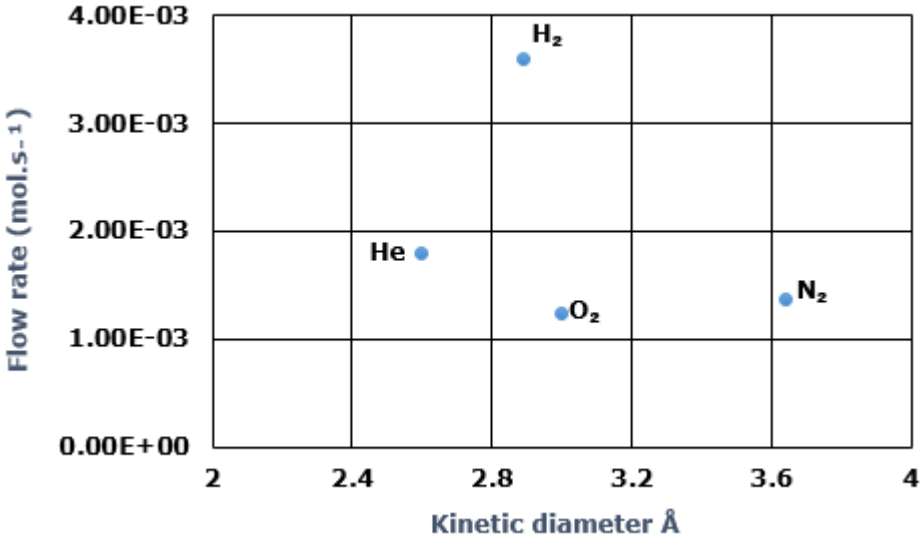

Figure 71: A plot of kinetic diameter of permeating gases against flow rate at 0.5 bar

8.2.1.2 Gas permeation through support and catalytic membranes

Figure 72 shows the flow rate of H_2 through support, platinum and palladium deposited membranes at 573 K in comparison with the fresh support. By comparing the three plots, it shows clearly that the flow rate of hydrogen was decreased by the effect of the catalyst deposition. This is due to a reduction in the pore size of the support as a result of catalytic deposition. This is similar to results presented by Lebedeva et al. [29]. Where they used nitrogen gas for permeation test, and a reduction in nitrogen flowrate in the Pd membrane was observed as a result of blockage of the small pores by palladium particles when compared with the fresh support. The flow of other gases through the catalytic membranes indicated that they were defects present and this defect would only have been of concern if a dense membrane was to be fabricated. In this work, there is no need for the layer to be dense since separation will not be effected.

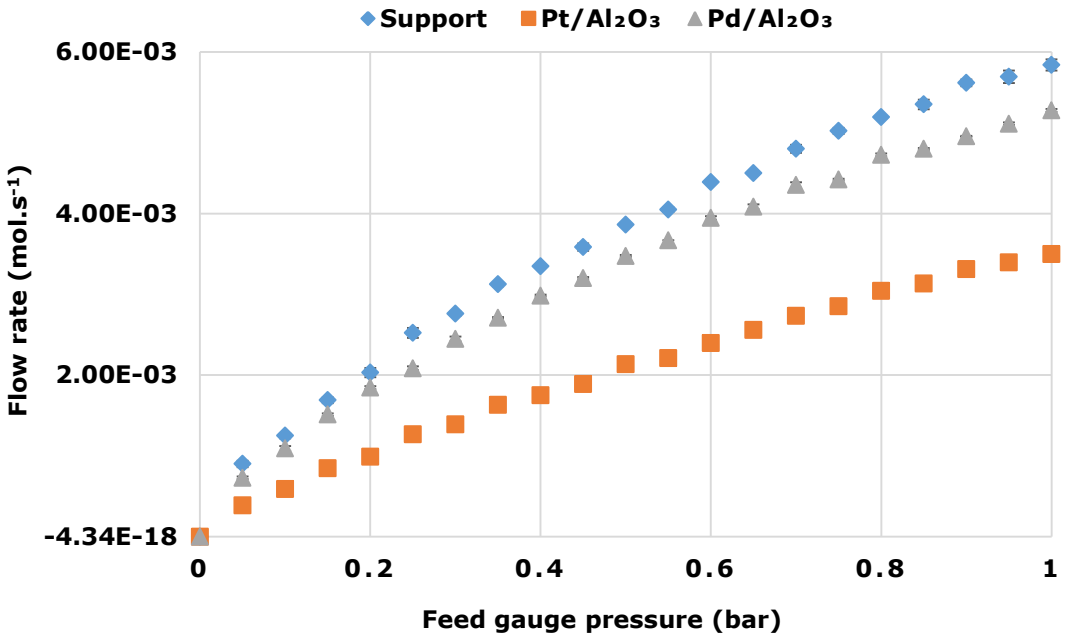

Figure 72: A graph showing the effect of hydrogen feed gauge pressure against flow rate of support, palladium and platinum deposited membranes at 573 K

Permeation of gases through the catalytic membrane is not only influenced by molecular weight, the kinetic diameter of the gases can also be a determinant. Figure 73 shows a graph of kinetic diameter verses flowrate at 0.5 gauge bar for the platinum deposited membrane carried out at a temperature of 573 K. The permeation of the various gases were investigated and it was observed that the kinetic diameter of the gases played a part in the rate of permeation as opposed to Figure 71 in which flow through the support did not show any dependence on the kinetic diameter. In Figure 73, it is seen that the order of gas permeation was $H_2 > He > O_2 > N_2$ and not $H_2 > He > N_2 > O_2$ as was observed in Figure 71 for fresh support.

It can therefore be summarized that both molecular weights and kinetic diameter contribute to the final gas transport mechanism of the catalytic membranes and the extent of this effect depends on at what pressure the test are carried out.

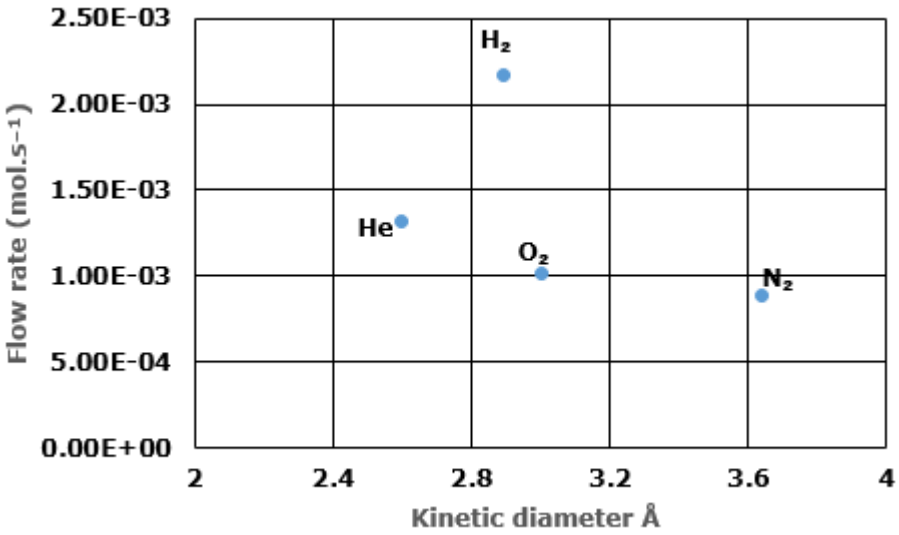

Figure 73: A plot of kinetic diameter of permeating gases through a Pt deposited membrane at 0.5 bar

8.2.2 Scanning electron microscopy coupled with Energy Dispersive Analytical X-ray analysis

8.2.2.1 Method No 1

The morphology of the outer surface of the catalyst pellet used for the fixed-bed catalyst test showed a rough appearance, dense and well dispersed coverage of the platinum metal as seen in Figure 74. To view the edge, the sample was cut into half and Figure 75 shows the inside and the platinum surface coating. The inside is full of asymmetric structures which shows the mesoporous support layer supporting the top catalytic layer.

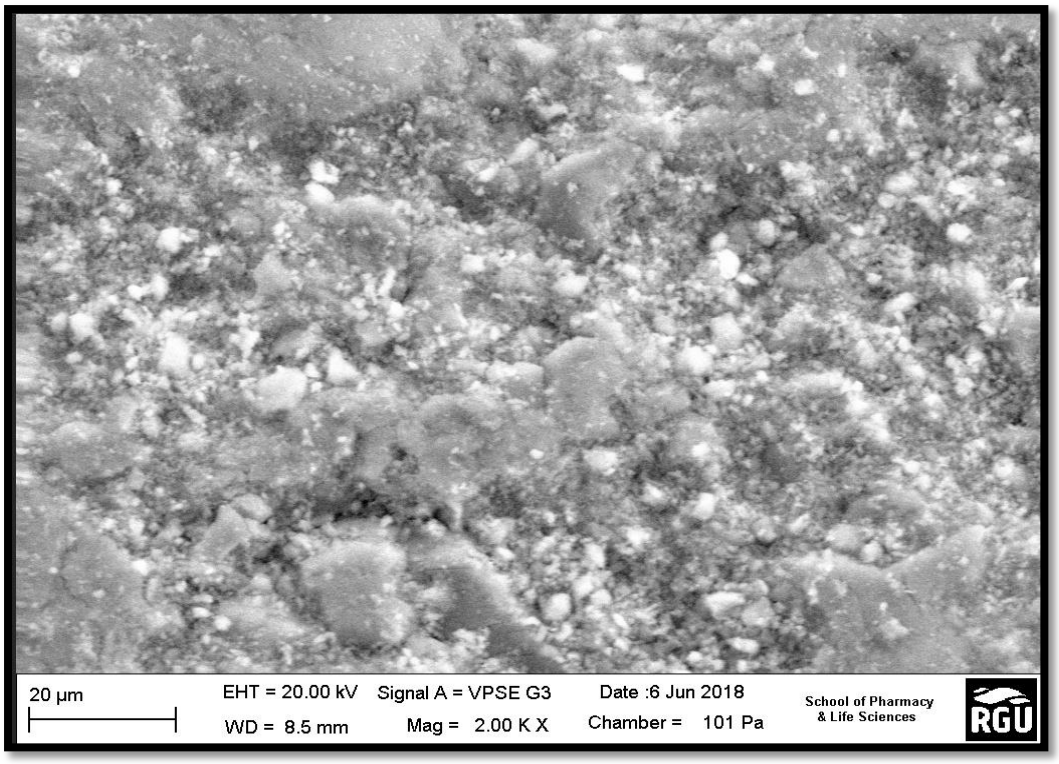

Figure 74: Micrograph showing the outer surface of the catalyst pellet

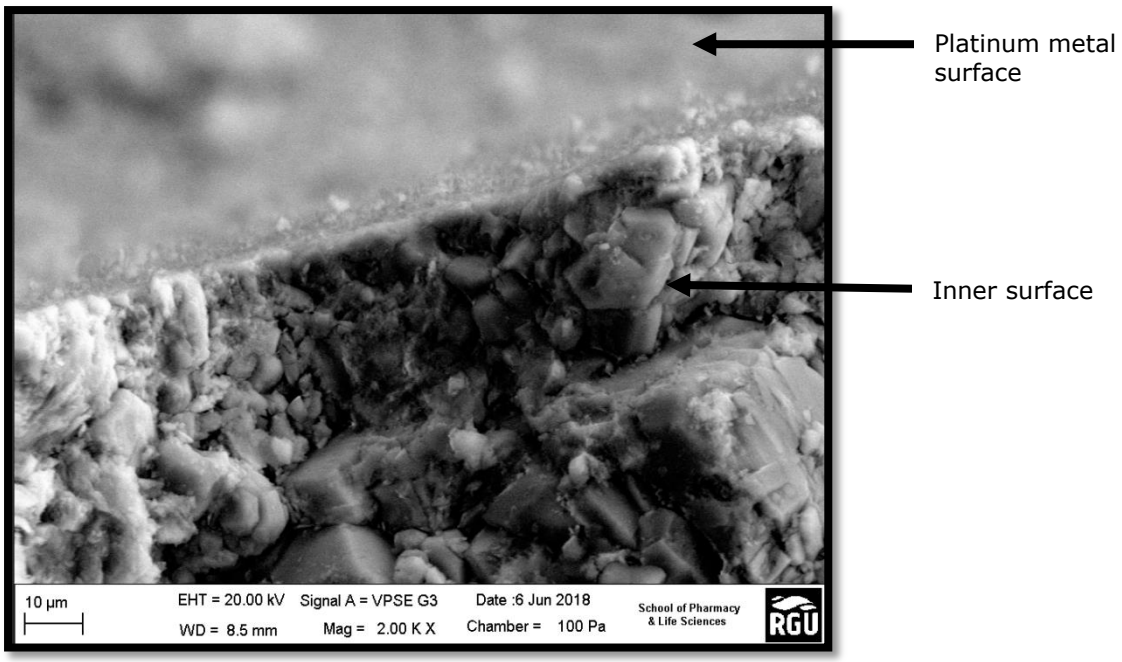

Figure 75: Micrograph showing the edge of the catalyst pellet

Figure 76 shows the EDAX of the outer surface showing very strong peaks of platinum and alumina present. It is also observed that some elements such as Cl, C and Ag are present and may be as a result of contaminations during manufacturing.

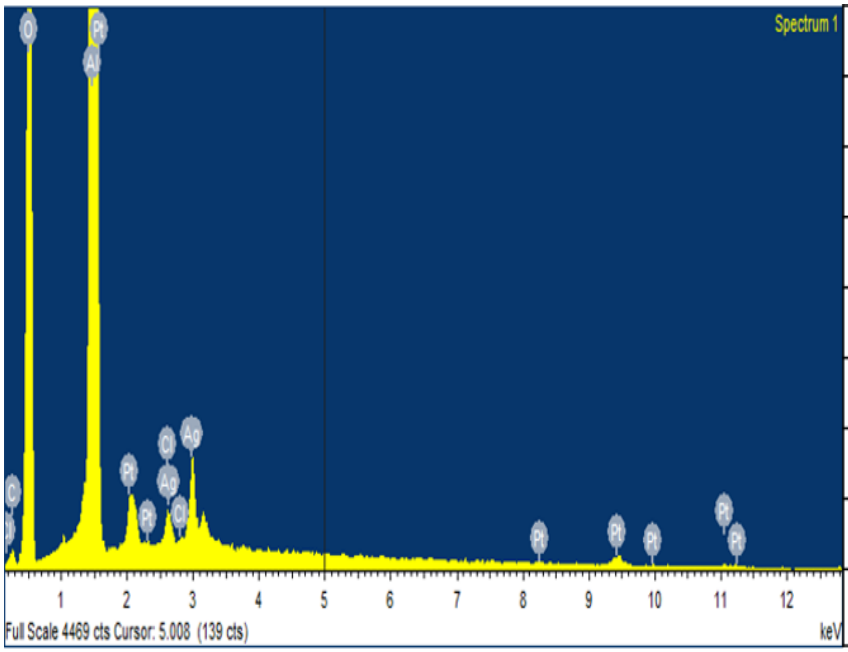

Element	Weight%
C	5.30
O	58.85
Al	57.97
Cl	0.72
Ag	5.25
Pt	3.60
Totals	131.70

Figure 76: EDAX showing the chemical compositions of the outer surface

8.2.2.2 Methods No 2 and No 3

The following sections present the SEM images obtained using the backscattering techniques across the inner and outer surfaces of the different types of supports and catalytic membranes used. The supports and catalytic membranes were examined under scanning electron microscope at 2000X magnification. The corresponding EDAX analysis of their surface areas were also reported. The micrographs of the catalytic membranes were all taken after activation of the catalytic metal.

Figures 77 and 78 present the morphological features of a 15 and 6000 nm pore sized supports focused on 2000X magnifications. The inner and outer surfaces show and confirms the support materials are indeed porous, with pores shapes of different geometries and sizes present. Figure 78a and 78b exhibits larger pore when compared to Figure 77a and 77b. The structures are not uniform and do not have a smooth appearance.

The EDAX analysis of the supports' outer surfaces are given in Figure 77c and 78c. The various elements present with their percentage compositions are identified.

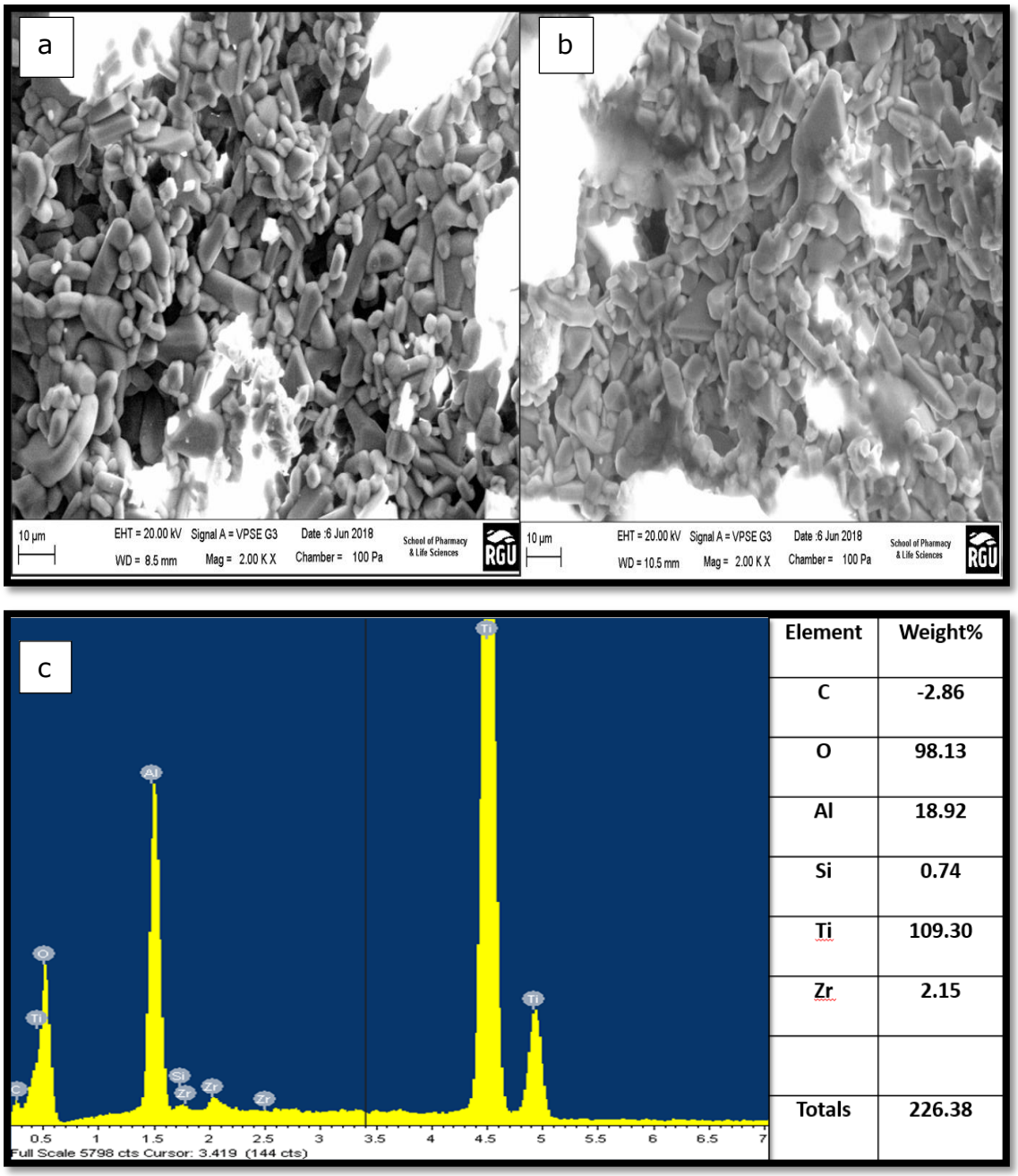

Element	Weight%
C	-2.86
O	98.13
Al	18.92
Si	0.74
Ti	109.30
Zr	2.15
Totals	226.38

Figure 77: Micrographs for 15 nm α-Al_2O_3 support: (a) inner surface, (b) outer surface and (c) EDAX showing the chemical compositions of the outer surface.

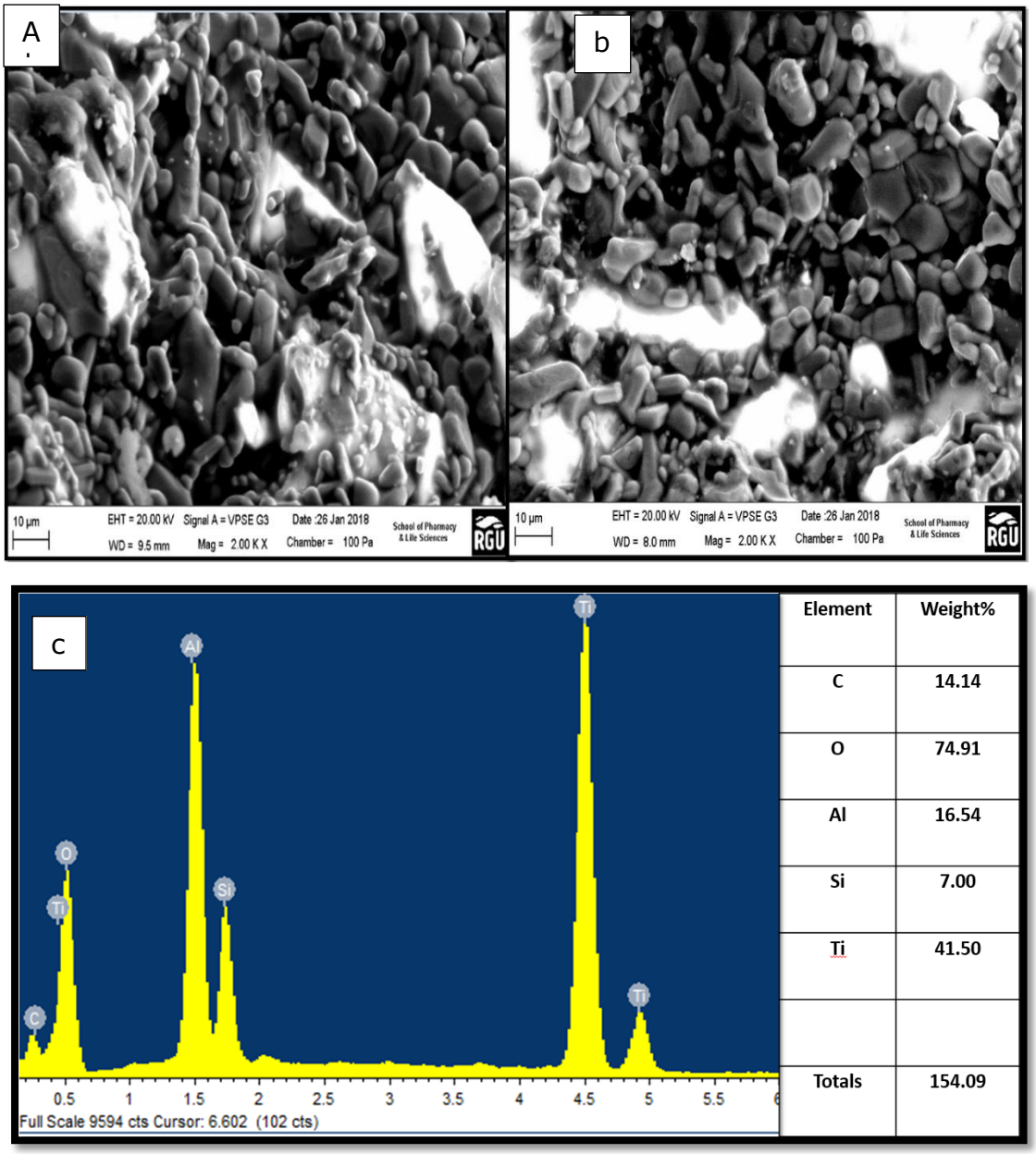

Element	Weight%
C	14.14
O	74.91
Al	16.54
Si	7.00
Ti	41.50
Totals	154.09

Figure 78 : Micrographs for 6000 nm α-Al_2O_3 support: (a) inner surface, (b) outer surface and (c) EDAX showing the chemical compositions of the outer surface.

Figures 79 and 80 show the SEM/EDAX of the palladium-coated membranes both at 2000X magnifications. Looking at the morphology of the outer surfaces presented in Figures 79b and 80b, one can easily visualize the structural change as a result of the metallic deposition when compared to that of the support shown in Figures 77b and 78b. Images of the outer surfaces (79b and 80b) show the palladium metal being deposited as clusters and not as a continuous coating. This is exactly what is required in the deoxygenation of water. The morphology of the outer surface is neither smooth nor uniform. This SEM micrograph makes it possible to view the areas and nature of the palladium's deposition. There is

no direct proportionality between the concentrations of the plating solution with the palladium occupied surface area.

It can also be observed that virtually all the pores were covered with the palladium metal aggregates. This creates phases of irregular shapes and reduced pores. The presence of the palladium clusters on the surface is a surface treatment which results in the following three factors: an increase in the surface's roughness, formation of active metallic sites and development of adlayers based on palladium nanoparticles. According to Volkov [1], the first factor, which is the increase in surface roughness promotes an increase in hydrophobic contact angle and this creates suitable surfaces for the occurrence of enhanced chemical reactions, whereas, the other two factors leads to an increase in surface energies. Measurements of the different clusters were impossible, but their presence led to the overall weight of the palladium deposition reported in chapter 3.

The micrograph of the inner surfaces show that the deposition of the palladium metal was only restricted to the outer surface. The inner sections of the membranes did not show any presence of palladium coating. This further proves that there was no penetration of the coating solution, all the palladium was localized on the outer and pore surfaces of the membranes.

The EDAX analysis of the $\gamma - Pd/Al_2O_3$ outer surfaces are given in Figure 79c and 80c. The surface composition of the palladium deposited in the outer and pore surface of the membranes showed very high peak of palladium metal. The EDXA tables also reconfirms their presence in a high concentration.

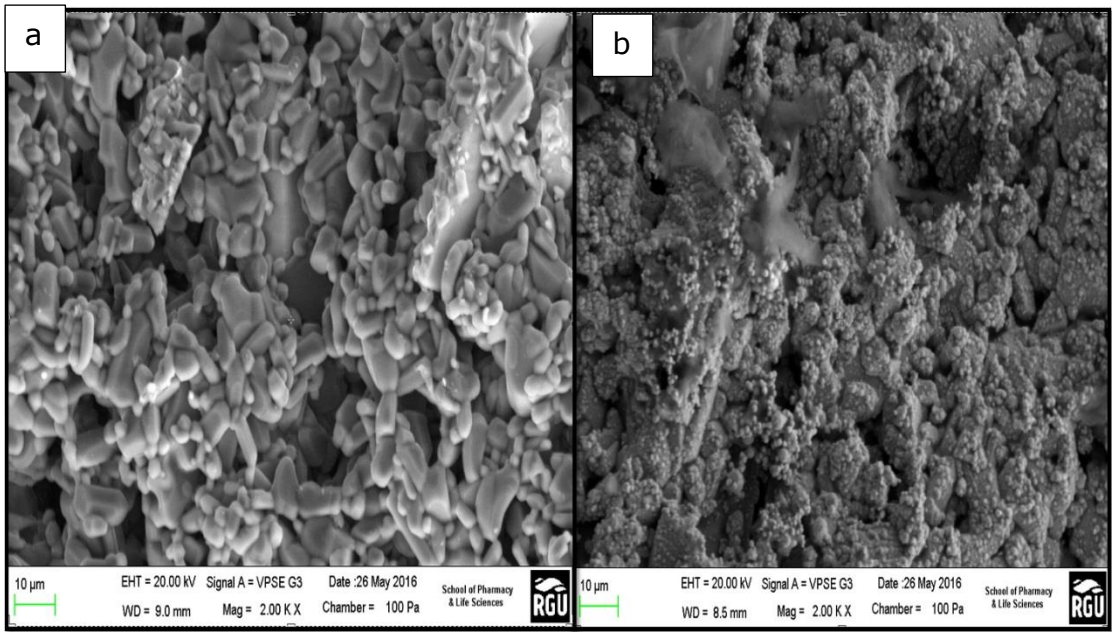

c

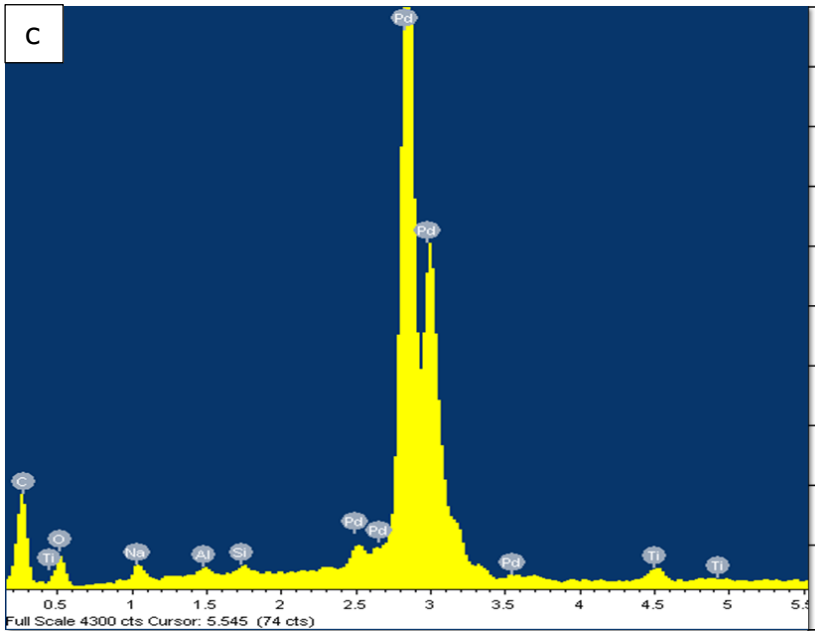

Element	Weight%
C	12.75
O	11.28
Na	1.10
Al	0.29
Si	0.26
Ti	1.17
Pd	73.15
Totals	100.00

Figure 79: Micrographs for the 15 nm γ-Pd/Al_2O_3 membrane: (a) inner surface, (b) outer surface and (c) EDAX showing the chemical compositions of the outer surface.

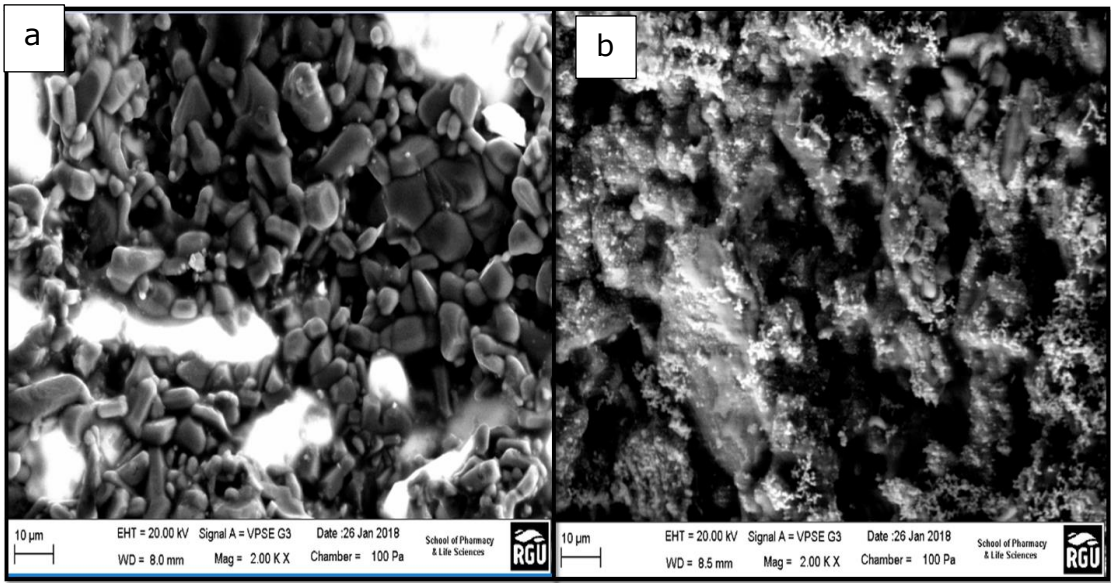

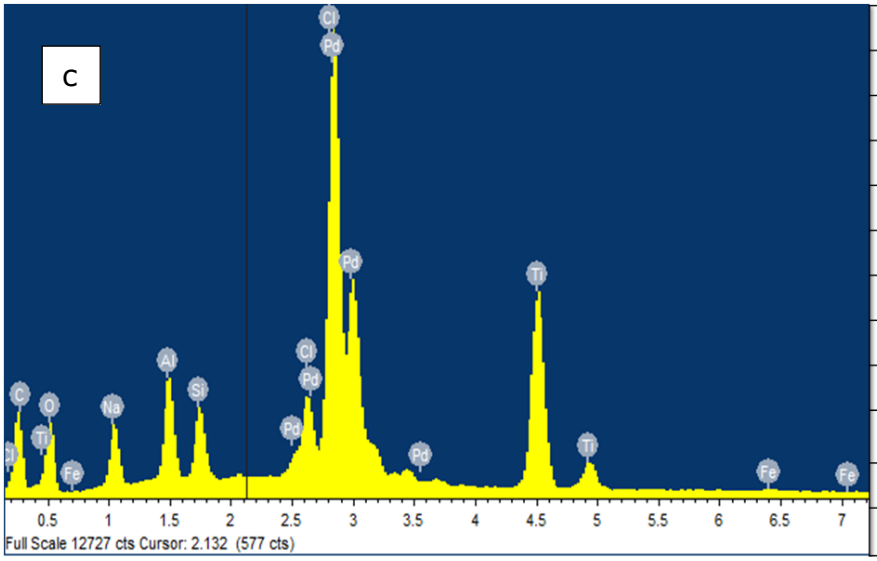

Element	Weight%
C	26.40
O	28.68
Na	4.22
Al	4.10
Si	2.77
Cl	3.54
Ti	18.36
Fe	0.32
Pd	53.38
Totals	141.77

Figure 80: Micrographs for the 6000 nm γ-Pd/Al_2O_3 membrane (a) inner surface, (b) outer surface, and (c) EDAX showing its elemental composition

Figures 81 and 82 show the SEM/EDAX micrographs of the platinum deposited membrane both at the inner and outer surfaces at 2000X magnifications, as well as their EDAX representations. The surface morphologies of Figure 81b and 82b are quite similar, but with Figure 82b showing a higher deposition of platinum metal. The platinum deposition does not appear as clusters when compared to the palladium coatings, but can be seen as dispersed on the surface as white specs. This is because the platinum precusor solution used was only 8 % weight platinum in water.

From the EDAX table representation in Figures 81c and 82c, it could be seen that platinum metal was deposited in both membranes but with the 6000nm membrane having a higher percentage of platinum metal because it has larger pores. Platinum peaks were also seen in both EDAX graphs.

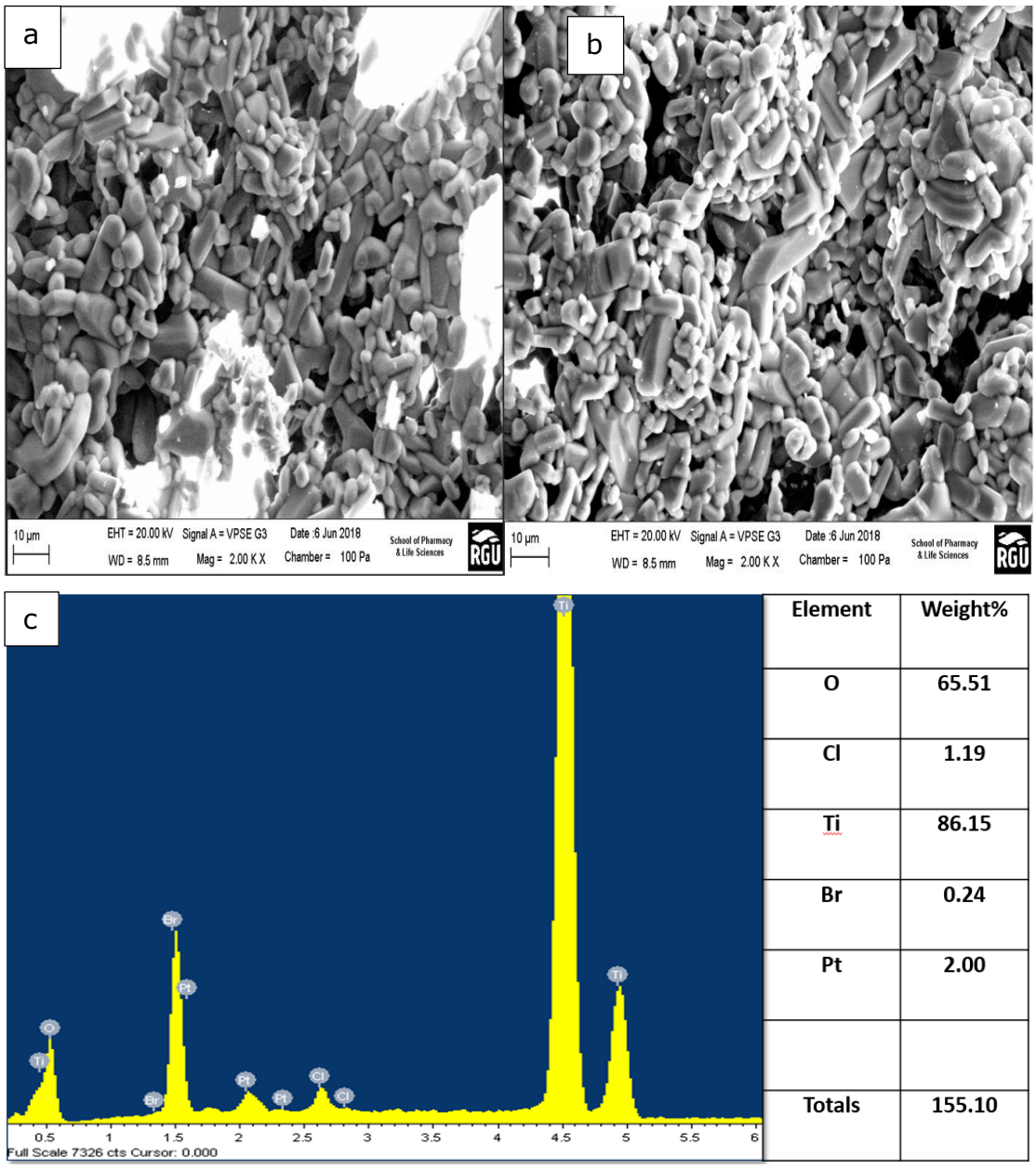

Element	Weight%
O	65.51
Cl	1.19
Ti	86.15
Br	0.24
Pt	2.00
Totals	155.10

Figure 81: Micrographs for the 15 nm γ-Pt/Al_2O_3 membrane: (a) inner surface, (b) outer surface and (c) EDAX showing the chemical compositions of the outer surface.

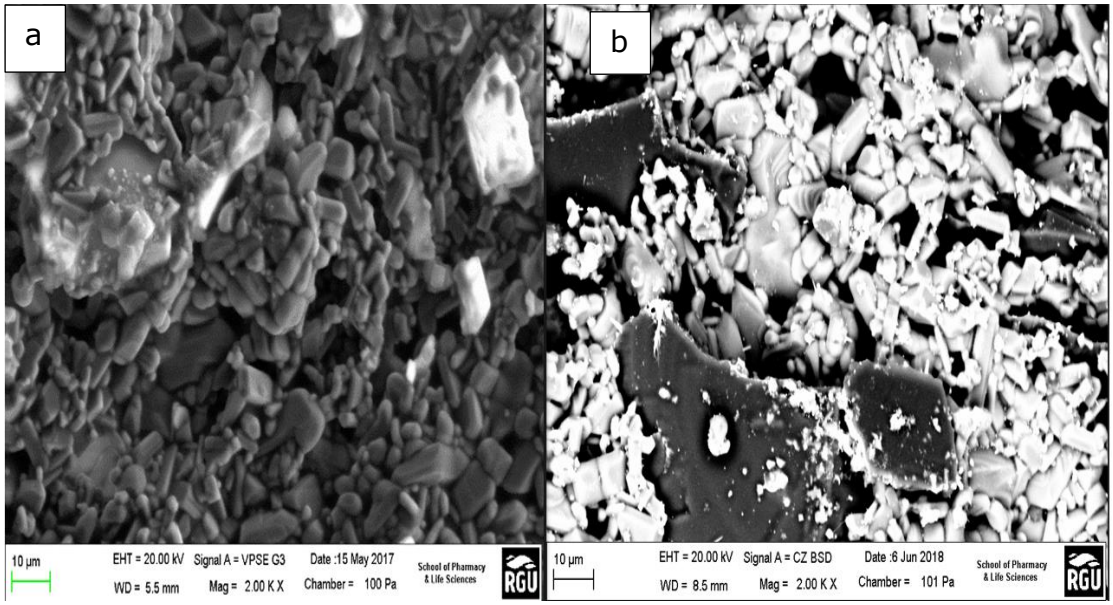

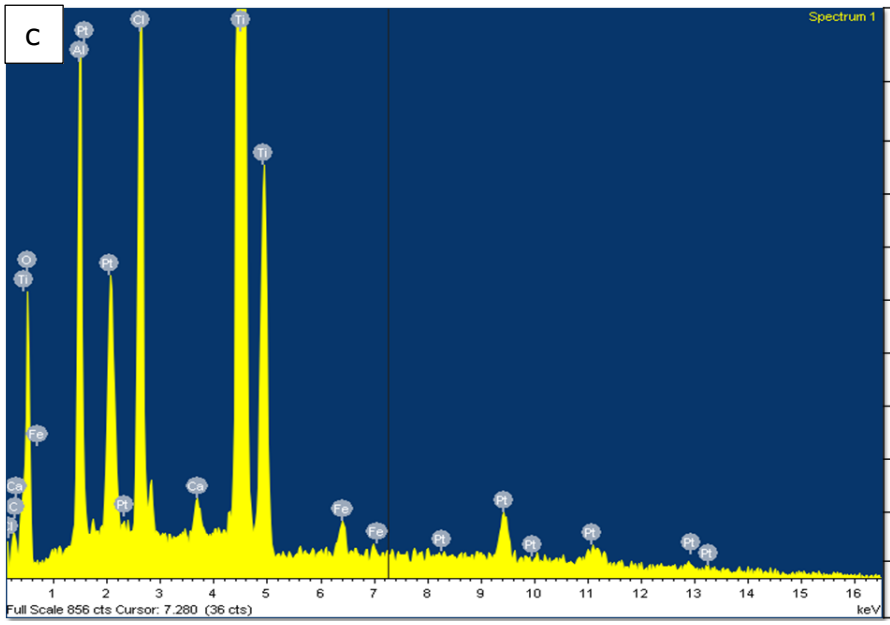

Element	Weight%
C	-0.92
O	28.92
Al	4.82
Cl	6.06
Ca	0.46
Ti	52.49
Fe	1.27
Pt	6.90
Totals	100.00

Figure 82: Micrographs for the 6000 nm γ-Pt/Al_2O_3 membrane: (a) inner surface, (b) outer surface and (c) EDAX showing the chemical compositions of the outer surface.

8.2.3 BET Liquid nitrogen analysis

The liquid nitrogen adsorption and desorption isotherms for the supports and catalytic membranes were determined from analysis carried out at a liquid temperature of 77K.

Figures 83 and 84 show the physisorption isotherms for the 15nm and 6000nm supports respectively. From the isotherms, it was concluded that they corresponded to the type IV and V isotherms as explained by Li [18]. They

showed hysteresis on their curves which signifies a membrane undergoing capillary condensation in the mesoporous region [99]. In the physisorption linear isotherms, the volume adsorbed are plotted against relative pressure P/Po, where P is the applied pressure and Po is the saturated pressure respectively.

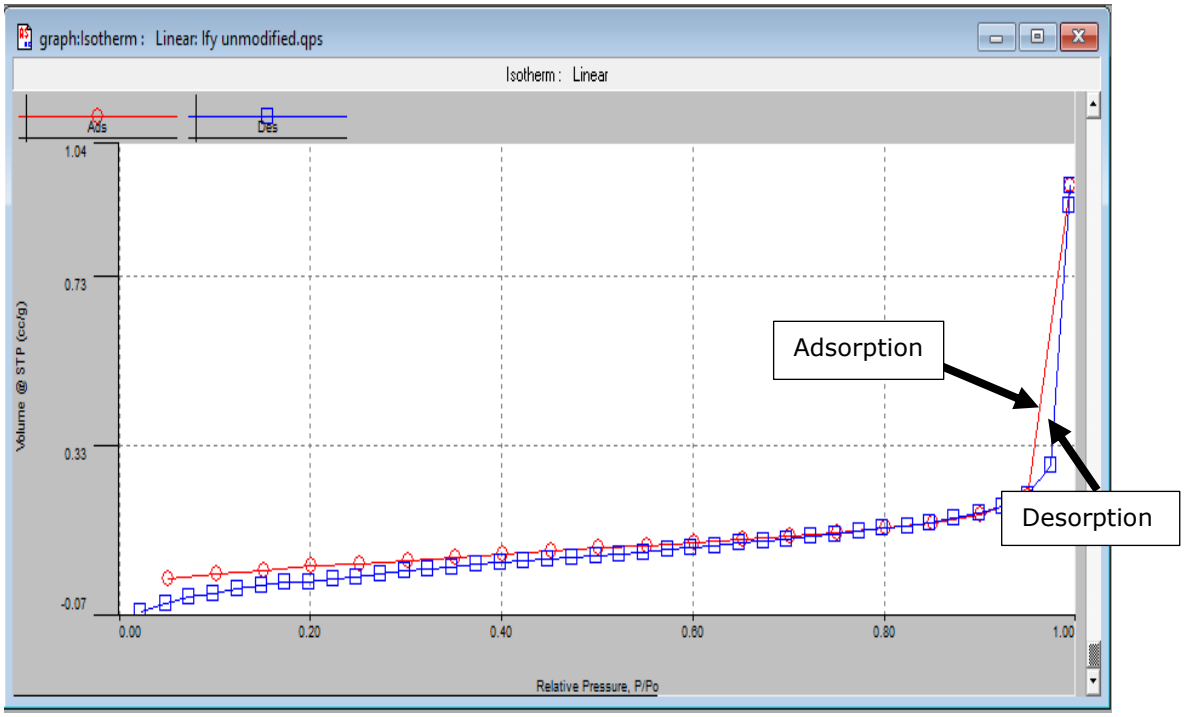

Figure 83: Physisorption isotherm of the 15nm support

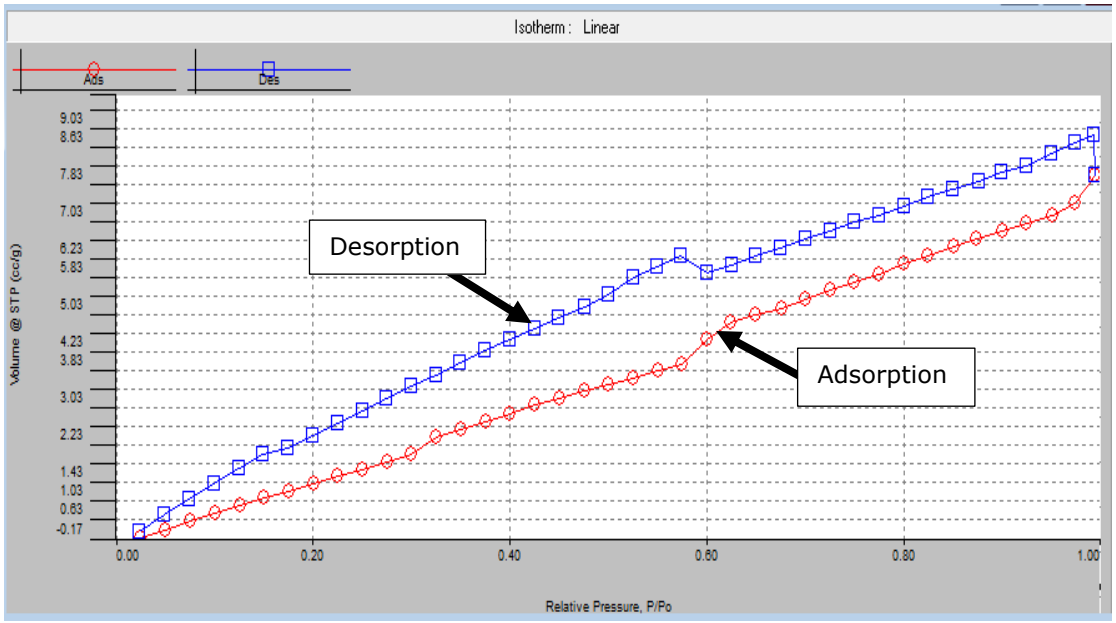

Figure 84: Physisorption isotherm of the 6000nm support

From the physisorption linear isotherms plots, Brunauer, Emmett and Teller (BET) model was used to generate a t-plot from which the specific surface areas of the supports/catalytic membranes were calculated. The Barrett, Joyner and Halenda (BJH) model was similarly used to generate the pore size distribution, pore diameter and pore volume of both the supports and catalytic deposited membranes.

Figure 85 shows the t-plot of the 15nm support, while Table 9 presents the BJH results of pore diameter and pore volume and Figure 86 shows the graph representation. The parameters characterising the porosity of 15nm support, 15nm palladium (Pd/Al_2O_3) and 15nm platinum (Pt/Al_2O_3) membranes are the specific surface area, pore volume and pore diameter. There are presented in Table 10.

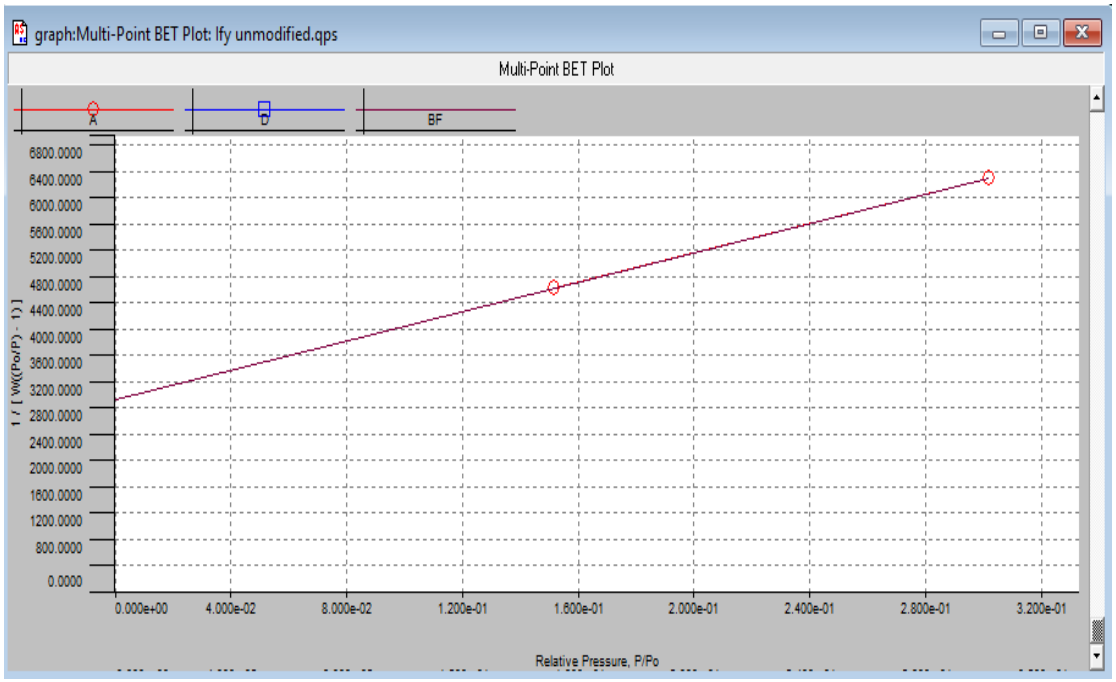

Figure 85: T-plot for a 15 nm pore sized support

Table 9: Details obtained from the BJH method on the 15nm support

BJH method Desorption dV(log d)

Quantachrome® ASiQwin™- Automated Gas Sorption Data Acquisition and Reduction
© 1994-2012, Quantachrome Instruments
version 3.0

Analysis				**Report**			
Operator:	rgu	Date:	2014/11/20	Operator:	lfy	Date:	2018/05/04
Sample ID:	I.O unmod 01	Filename:		lfy unmodified.qps			
Sample Desc:		Comment:					
Sample Weight:	0.6 g	Instrument:		Autosorb iQ Station 1			
Outgas Time:	0.0 hrs	Outgas Temp.:		0 °C			
Analysis gas:	Nitrogen	Non-ideality:		6.58e-05 1/Torr		CellType:	12mm
Analysis Time:	3:50 hr:min	Bath temp.:		77.35 K			
Analysis Mode:	Standard					VoidVol Remeasure:	off
VoidVol. Mode:	He Measure	Cold Zone V:		1.10009 cc		Warm Zone V:	6.99038 cc
	Thermal Transpiration: on			**Data Reduction Parameters**			
				Eff. mol. diameter (D):	3.54 Å	Eff. cell stem diam. (d):	4.0000 mm
t-Method	Calc. method:	de Boer					
BJH/DH method	Moving pt. avg.:	off		Ignoring P-tags below 0.35 P/Po			
Adsorbate	Nitrogen			Temperature	77.350K		
	Molec. Wt.:	28.013		Cross Section:	16.200 A²	Liquid Density:	0.806 g/cc
				BJH desorption summary			
				Surface Area =	0.192 m²/g		
				Pore Volume =	0.001 cc/g		
				Pore Diameter Dv(d) =	3.305 nm		

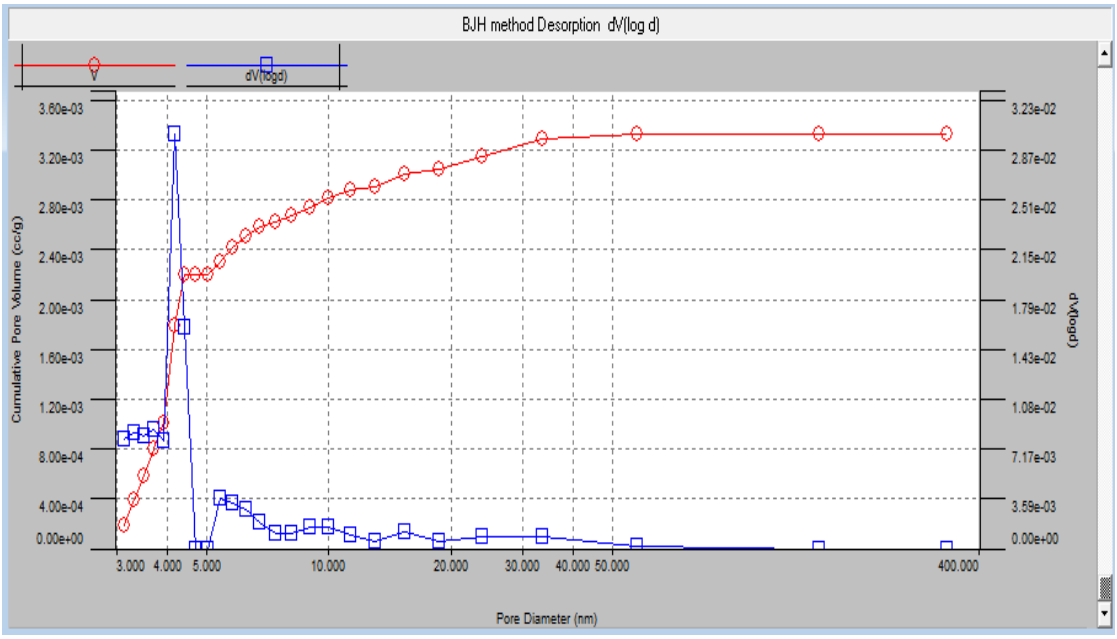

Figure 86: BJH graph showing the pore size distribution and pore diameter for 15nm support

Table 10: Results showing parameters obtained for 15nm support and catalytic deposited membranes

Parameters	$\alpha - Al_2O_3$	$\gamma - Pt/Al_2O_3$	$\gamma - Pd/Al_2O_3$
Specific surface area S_{BET}, m^2/g	0.247	7.232	9.660
Pore volume Vp, cc/g	0.001	0.031	0.212
Pore diameter BJH, nm	3.305	3.316	2.973

Figure 87 shows the t-plot of the 6000nm support, while Table 11 presents the BJH results of pore diameter and pore volume, Figure 88 shows the graph representation to this support. The parameters characterising the porosity of 6000nm support, 6000nm palladium (Pd/Al_2O_3) and 6000nm platinum (Pt/Al_2O_3) membranes, that is, the specific surface area, pore volume and pore diameter are presented in Table 12.

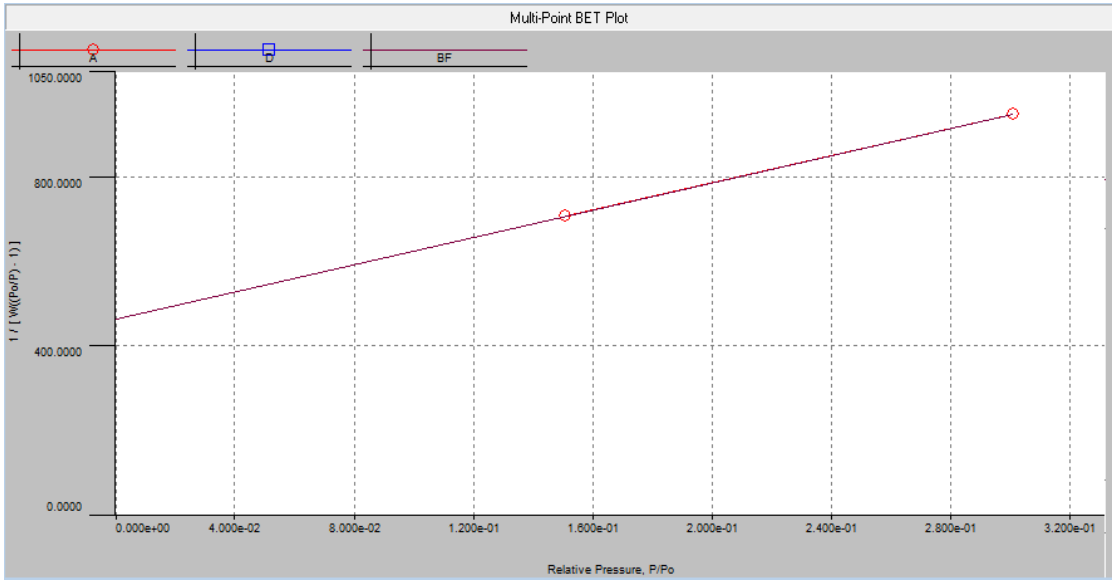

Figure 87: T-plot for a 6000 nm pore sized support

Table 11: Details obtained from the BJH method on the 6000nm support

BJH method Desorption dV(log d)

Analysis			**Report**		
Operator:	rgu	**Date:**2017/05/17	**Operator:**	lfy	**Date:**2018/05/15
Sample ID:	lfy S 6000	**Filename:**	lfy 6000 S.qps		
Sample Desc:		**Comment:**			
Sample Weight:	0.1 g	**Instrument:**	Autosorb iQ Station 1		
Outgas Time:	0.0 hrs	**Outgas Temp.:**	0 °C		
Analysis gas:	Nitrogen	**Non-ideality:**	6.58e-05 1/Torr	**CellType:**	9mm w/o rod
Analysis Time:	5:03 hr:min	**Bath temp.:**	77.35 K		
Analysis Mode:	Standard			**VoidVol Remeasure:**	off
VoidVol. Mode:	He Measure	**Cold Zone V:**	8.60405 cc	**Warm Zone V:**	14.1088 cc
		Data Reduction Parameters			
	Thermal Transpiration: on	**Eff. mol. diameter (D):**	3.54 Å	**Eff. cell stem diam. (d):**	4.0000 mm
t-Method	**Calc. method:** de Boer				
BJH/DH method	**Moving pt. avg.:** off	**Ignoring P-tags below 0.35 P/Po**			
Adsorbate	**Nitrogen**	**Temperature**	77.350K		
	Molec. Wt.: 28.013	**Cross Section:**	16.200 Å²	**Liquid Density:**	0.806 g/cc
		BJH desorption summary			
		Surface Area =	8.243 m²/g		
		Pore Volume =	0.012 cc/g		
		Pore Diameter Dv(d) =	4.176 nm		

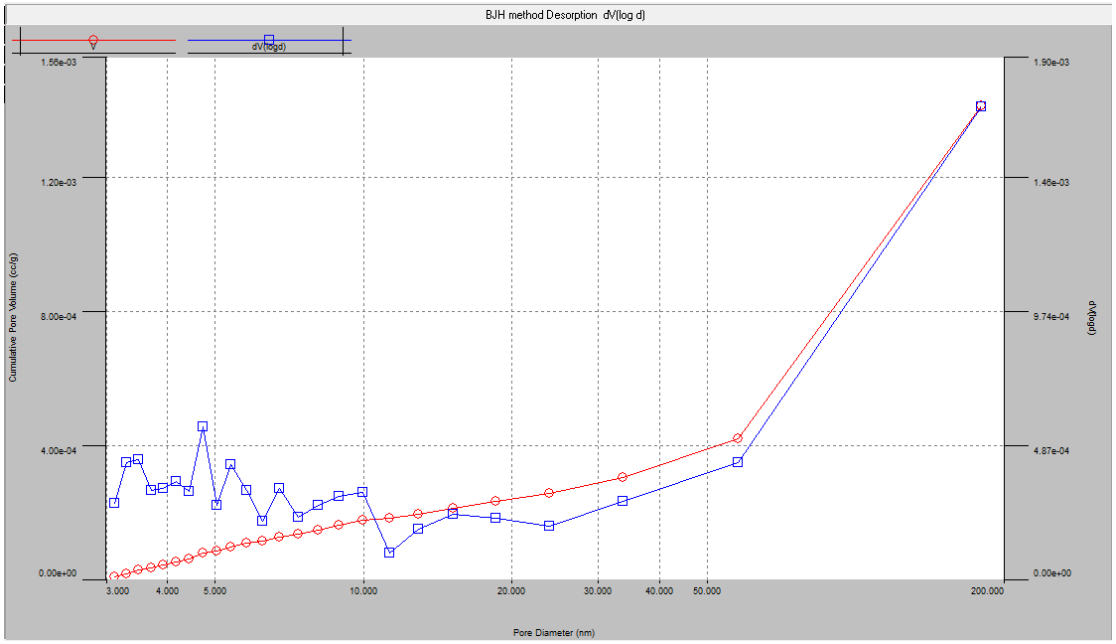

Figure 88: BJH graph showing the pore size distribution and pore diameter for 6000nm support

Table 12: Results showing parameters obtained for 6000nm support and catalytic deposited membranes

Parameters	$\alpha - Al_2O_3$	$\gamma - Pt/Al_2O_3$	$\gamma - Pd/Al_2O_3$
Specific surface area S_{BET}, m^2/g	1.676	13.477	10.680
Pore volume Vp, cc/g	0.012	0.003	0.009
Pore diameter BJH, nm	4.176	4.173	3.139

From the liquid nitrogen analysis, the catalyst deposited membranes showed very high specific surface areas when compared to that of their supports. This feature of having a higher surface area was of an advantage because it shows that the catalytic membranes had the tendency of adsorbing a greater amount of gas in their pore structure. The higher the amount of gas adsorbed by a membrane, the better in enhancing a chemical reaction. This result was attributed to nano-dispersed catalytic particles present.

There was an observed decrease in pore diameter of both Pt/Al_2O_3 and Pd/Al_2O_3. This could be as a result of deposition of the catalyst into the pores of the membranes. The pore diameter of the palladium coated membranes showed a

greater decrease in size, possible due to the formation of palladium clusters seen in the SEM images.

8.3 Catalytic performance measurement/ Efficiency and evaluation in water deoxygenating process

The following sections discuss both the fixed-bed and the catalytic membrane reactor results. The efficiency of the catalytic reactor was investigated as a function of the concentration of DO at the membrane reactor outlet. The conversion, X_o, is the number of moles of DO that have reacted per mole of inlet DO through the reactor and is given by equation 56. The % conversion (%X_o), gives the percentage efficiency of the catalyst and can then be calculated from equation 57 [7].

$$\text{Conversion}X_o=\frac{Moles\ of\ Dissolved\ oxygen\ reacted}{Moles\ of\ Dissolved\ oxygen\ at\ the\ inlet\ feed} \quad (56)$$

$$\%\text{Conversion}(\%X_o)=\left[\frac{C_{in}-C_{out}}{C_{in}}\right]X100 \quad (57)$$

Where, C_{in} is the concentration of DO in the tap water feed (ppm) and C_{out} is the concentration of DO of the water exiting the membrane reactor (ppm), which is, at the outlet/permeate end.

8.3.1 Fixed-bed reactor experiment

The following results demonstrate the efficacy of the catalytic fixed bed reactor in the removal of DO from water.

8.3.1.1 Effect of varying the amount of catalyst and hydrogen pressure

Figure 89 illustrates the effect of catalyst weight and hydrogen pressure on the removal of DO in a fixed-bed reactor experiment. 0.8 (16 wt.%) and 3g (60 wt.%) of catalyst pellet were used in the fixed-bed reactor at feed flowrate range of 400-450 mL/min and hydrogen pressure range of 0.1 to 0.7 bar. Generally, it could be seen that the higher the catalyst weight and hydrogen pressure in the system, the more effective the DO removal. The higher the

hydrogen pressure, the more soluble hydrogen is present in the water system to react with DO. The dissolution of hydrogen in water is a function of the pressure based on Henry's law [88]. The initial DO level in the feed water was 9.7 mg/L, and it was reduced to 5.62 mg/L with the 3.0g of catalyst, while 7.74 mg/L was achieved for 0.8g catalyst (See appendix V, Table 16 for experimental values). Further explanation of the effect of increased catalyst loading and hydrogen pressure will also be given in the catalytic membrane reactor section (see sections 8.3.2.1, 8.3.2.2 and 8.3.2.6).

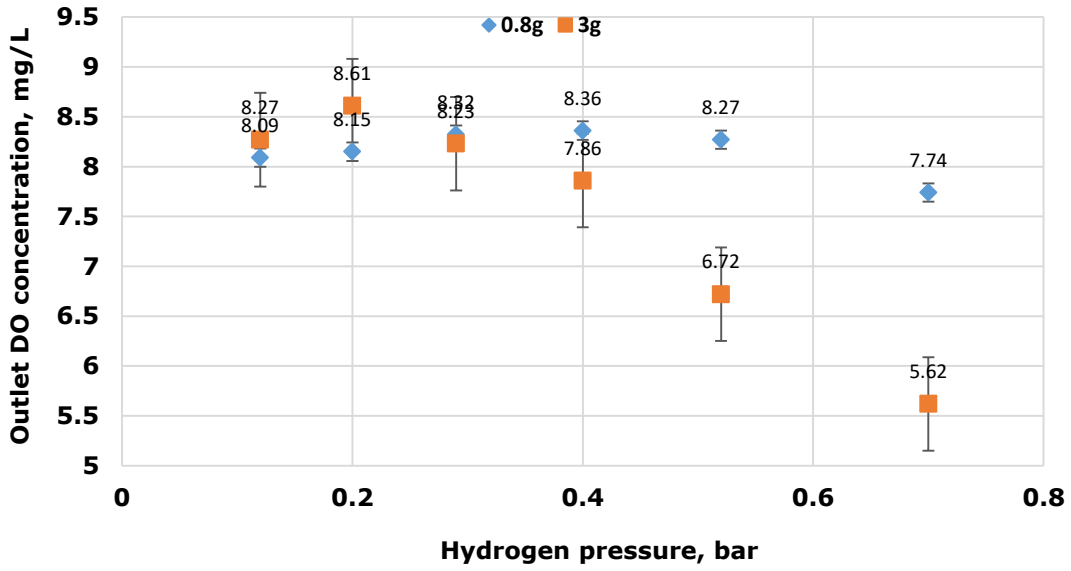

Figure 89: Graph showing the effects of catalyst weight and hydrogen pressure on the removal of DO in the fixed-bed

8.3.1.2 Effect of varying feed water flowrate

The feed water flowrate (DO:9.7 mg/L) was varied in the range from 140 to 450 mL/min to evaluate the effect on the level of DO removal in a fixed bed having 3g of catalyst pellet as shown in Figure 90. At a fixed hydrogen pressure of 0.8 bar, it was observed that the amount of DO removed decreased with increasing water flow rate. The lowest water flow rate gave a higher DO removal. This can be attributed to the fact that, at lower flowrate, the residence time of the water and hydrogen is longer on the catalyst, consequently, most of the active sites are accessed for the catalytic combination of hydrogen and dissolved oxygen.

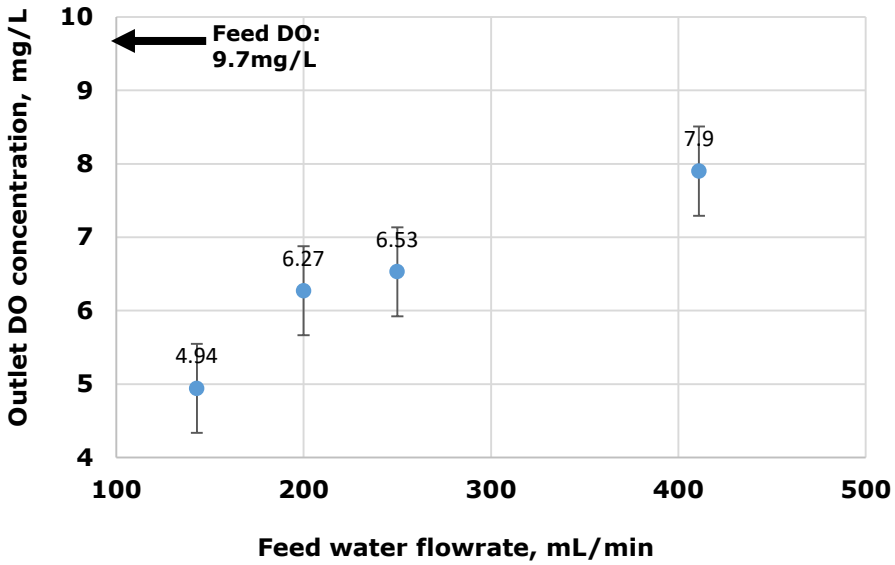

Figure 90: Graph showing the effect of water flowrate on the outlet DO concentration

From Figure 90, the percentage efficiency of the 3.0g fixed-bed catalytic reactor was evaluated using equation 57 section 8.3. It was observed that 49% DO reduction was achieved through the run as seen in Figure 91 (See appendix V, Table 17 for experimental values).

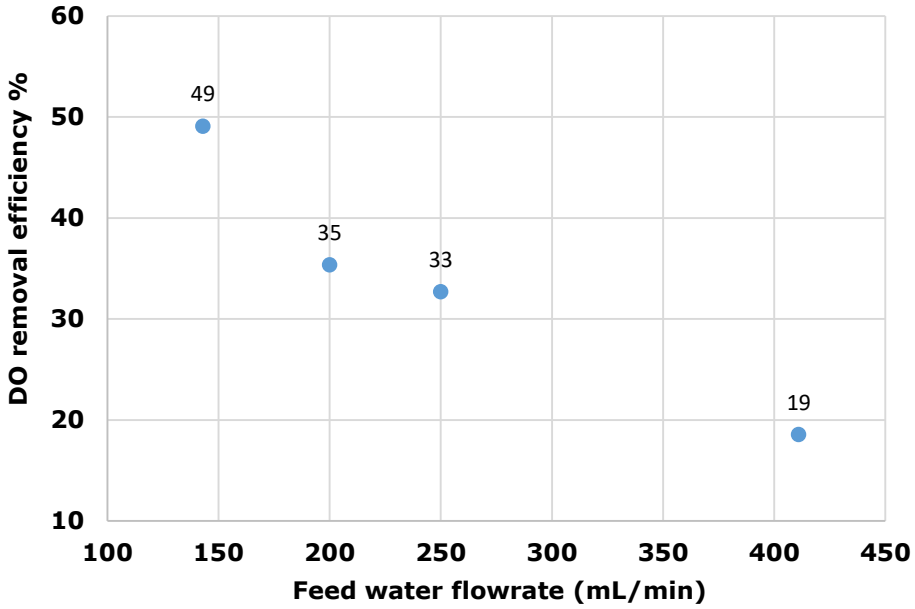

Figure 91: A plot of DO removal efficiency against water flow rate of the 3.0g fixed–bed reactor

8.3.2 Membrane Reactor Experiments

To study and compare the operational efficacy of the different catalyst synthesized by different methods, laboratory scale experiments were carried out in the CMR design operated in the plug flow model at different operating conditions. The readings (results) were taken in triplicates at each investigation.

The effect of metal: palladium and platinum catalyst, membrane pore size, catalytic membrane areas, hydrogen flowrate into the water mixing unit and the flowrate of the feed water on the conversion of the reactants (DO and H_2) into products were studied.

8.3.2.1 Effect of membrane pore size on outlet DO level using palladium membranes

To evaluate the effects of difference in pore sizes, palladium-coated 15nm pore-sized membrane (APd) and 6000nm pore-sized membrane (BPd) were tested side by side and results compared. The catalytic membrane performance was characterized in terms of the DO concentration in the inlet and outlet water stream. The DO level in the inlet stream at the point of measurement was 9.7 ppm. Figure 92 shows the variation of outlet DO with the different pore sized palladium membranes at water flow rate range of 200-1000 mL/min. It was observed that for a specific feedrate the DO concentration decreased more with the membrane BPd. For example, at water feed flowrate of 200 mL/min, membrane APd gave a DO of 2.13 ppm, while a DO of 0.31 ppm was achieved with membrane BPd. See appendix VI, Table 18 for experimental values.

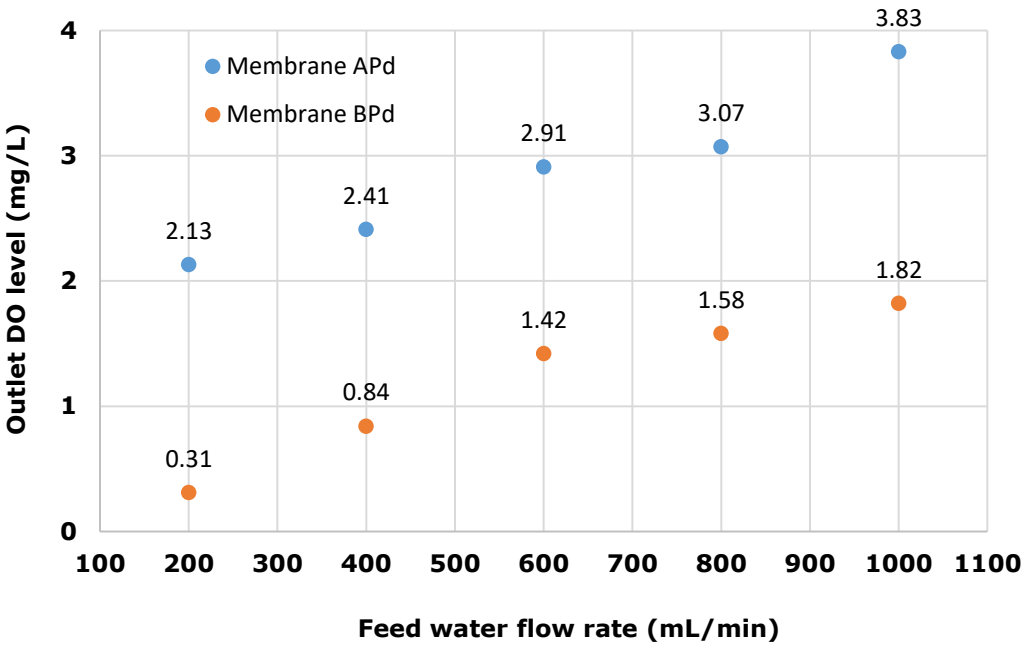

Figure 92: Graph showing the effects of membrane pore size on outlet DO concentration using palladium coated membranes

The results further indicate that the pore size of the membrane is a key factor to DO removal. Membrane B is macro porous (6000nm pore size), thereby, the amount of catalyst deposited in membrane B which is 1% wt.Pd is higher than that of membrane A (15nm pore size) which was 0.8% wt.Pd. The higher the amount of catalyst, the higher the deoxygenating property as a result of increased chemical reaction [30].

A similar observation was made when using platinum membranes A and B as shown in Figure 93. Figure 93 shows a similar graph plotted on the different pore sized platinum deposited membranes. From the BET results, platinum impregnated 6000nm pore-sized membrane (BPt) had a higher surface area (13.477 m^2/g) compared to platinum impregnated 15nm pore-sized membrane (APt) (7.232 m^2/g). It is therefore thought that this high surface area also results in higher metal dispersion which facilitates the shift of equilibrium towards the product side, that is, deoxygenation (see appendix VI, Table 19 for experimental values).

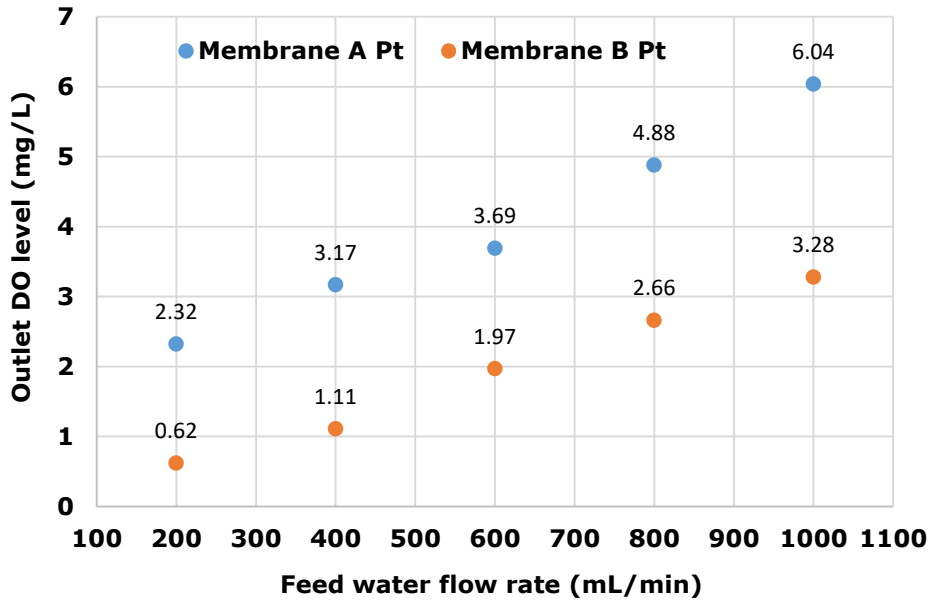

Figure 93: Graph showing the effects of membrane pore size on outlet DO concentration using platinum deposited membranes

8.3.2.2 Effect of membrane area on outlet DO level using platinum membrane

Figure 94 shows the effect of catalytic membrane surface area on the removal of DO at H_2 saturated feed water flow rate of 200 – 1000 mL/min. Membrane A (370mm in length) and C (650mm in length) are both 15 nm pore sized but of different outside surface areas as described in appendix II. Same operating conditions were used for the two different membranes. The DO efficiency increased with an increase in catalytic membrane area. For example, at flow rate of 1000 ml/min, the DO was 6.04 ppm for membrane A having membrane outside surface area of 0.008m^2 with a catalytic loading of 0.2% wt. Pt, while it gave a DO of 1.59 ppm for membrane C which had an outside surface area of 0.045m^2 with a catalytic loading of 0.5% wt. Pt. The difference in DO removal could be explained by the fact that a larger membrane outside surface area obviously has a higher catalytic loading and hence a larger catalytic surface contact area available for the chemical reaction to occur. This is similar to results reported by Shi et al. [38], where they carried out experiment on different catalytic bed height. The highest bed height gave a better conversion. This therefore implies that the membrane outside surface area plays an important role in water deoxygenation.

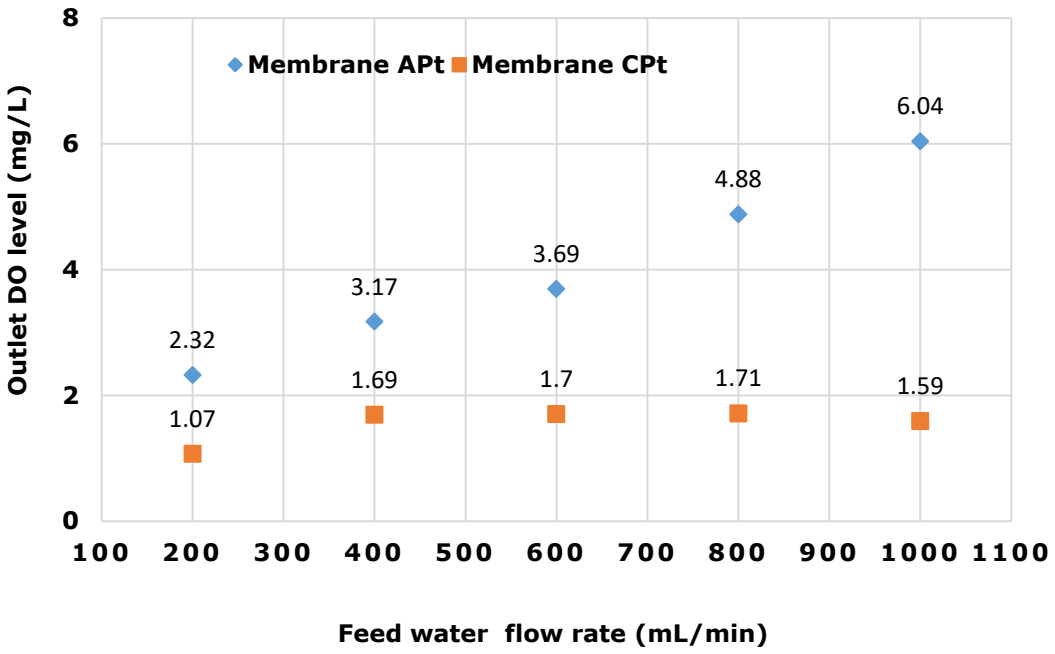

Figure 94: Effect of water flowrate on the outlet DO concentration comparing membrane areas

An observation was also made on membrane C in which the level of dissolved oxygen reduction as the water flowrate increased remained almost constant. Ito et al. [39] explained that such a pattern of result could be attributed to the absence of liquid-phase resistance. Their model [39] predicted a small effect of varying flowrate on the outlet DO. They further stated that, the membrane's length was long enough for the feed flow to reach an equilibrium concentration with the permeate end. With the membrane A, there exist liquid-phase resistance and that way, the higher the feed water flowrate, the less the removal of DO achieved. The presence of liquid-phase resistance makes the hydrogen not to dissolve properly unlike in the case of membrane C, where there is little or no liquid phase resistance. In this case, the dissolution of hydrogen into the water stream on the catalytic surface is highly efficient. It goes further to emphasise on the membrane length and area as an added advantage in the CMR process. Figure 95 shows the DO removal in relation to the presence or absence of liquid-phase resistance. The dotted line shows the calculated DO concentration in a case without liquid-phase resistance

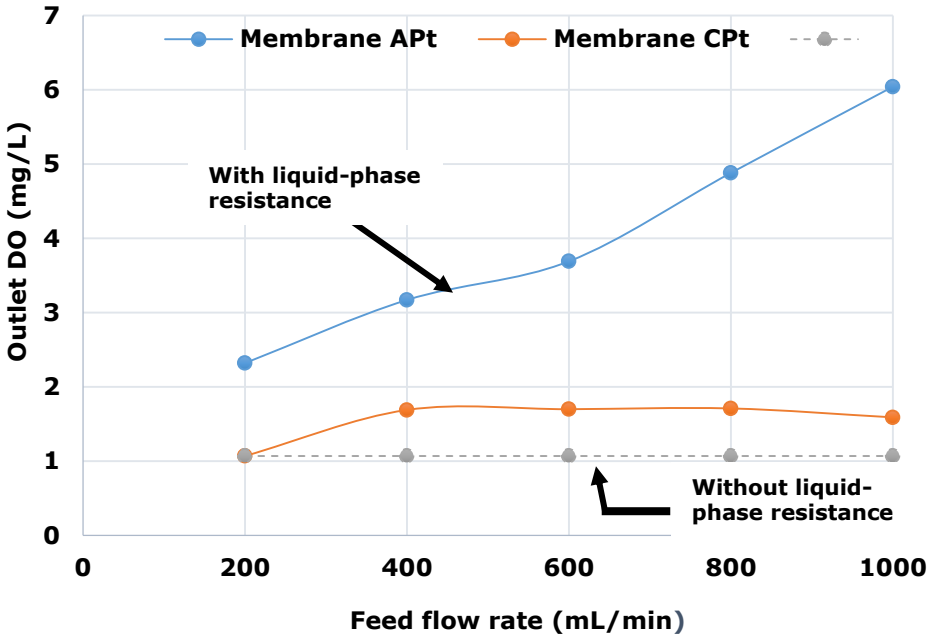

Figure 95: Effect of liquid phase resistance on the DO removal

8.3.2.3 Effect of feed water flow rate on the outlet DO level

Feed water flow rate is a key operational variable in process applications. The feed flow rates of water containing saturated hydrogen gas were varied from 200 to 1000 mL/min to establish the effect on the level of DO removal in the 6000 nm Pd/Al_2O_3 (BPd) membrane as shown in Figure 96. At a fixed hydrogen flow rate of 1.55 L/min, it was observed that the amount of DO removed decreased with increasing feed water flow rate. The lowest feed water flow rate of 200 mL/min gave a higher DO removal. Similar observations was also reported by Sinja et al. [30]. Our observation can be explained by the fact that a reduction in the contact time between the DO and the catalytic surface area results in a shortened reaction time as the flow rate increases. For example, the initial DO on the day of the experiment was 9.66 mg/L in the feed water, an exit DO of 0.31 ppm was achieved at 200 mL/min, while at 1000 mL/min the exit DO was 1.82 ppm. The residence time for the reaction was shortened with an increase in the feed water flow rate from 200 to 1000 mL/min. Shi et al. [38] suggested that in such a scenario where there exist a fixed catalytic loading and a fixed hydrogen flow rate, the feed water flowrate will then have to be controlled or adjusted to an optimal level so as to achieve the maximum conversion needed.

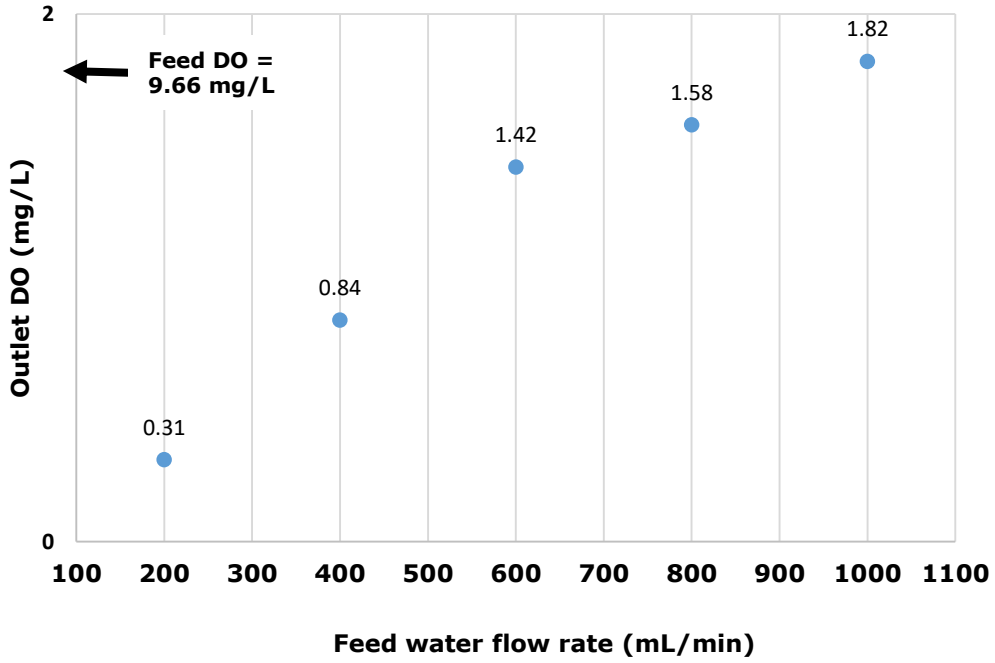

Figure 96: Effect of feed water flow rate on the DO removal

8.3.2.4 Percentage efficiency of the catalytic membranes

The results shown in Figure 97 indicates that the efficiency of water deoxygenation depends both on the pore size and outside surface area of the catalytic membrane. Both factors actually enhance more catalytic loading and therefore largely control the rate of DO removal. Figure 97 also includes similar plots of all the 5 different catalytic deposited membranes. These plots were presented to show the effects of platinum and palladium catalyst in the removal of DO. Using equation 57 in section 8.3, DO removal efficiency in excess of 80% over the range of feed water flow rates was achieved with the 6000 nm palladium deposited membrane (BPd), achieving 97% removal at the lowest applied feed flow rate. The initial DO was 9.7 ppm (see Appendix VI, Table 20 for experimental values).

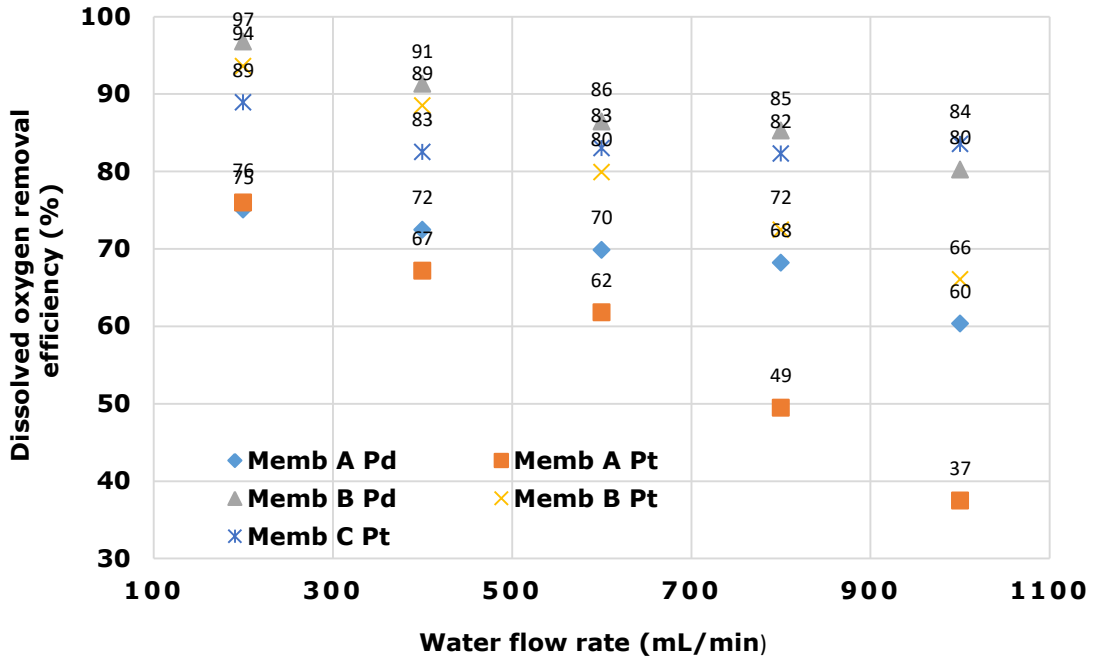

Figure 97: A plot of DO removal efficiency against water flow rate for the different catalytic deposited membranes. H_2 flow rate was 1.55 L/min. Membrane areas: Memb A= 0.0008m^2, Memb B=0.023m^2, Memb C=0.045m^2

8.3.2.5 Effect of time on DO concentration

Figure 98 shows a plot of DO concentration against deoxygenating on-stream reaction time at ambient temperature and pressure. The lowest DO concentration was recorded as the on-stream reaction time approached 30 min. This trend in deoxygenating on-stream reaction time was also similar to the results reported by Volkov et al. [1] and Shi et al. [38]. The results obtained also confirms that the on-stream reaction time plays an important role in water deoxygenation [73]. As a result of the observations from this graph, each change in flow rate was given at least 30 min on-stream time before measuring the final DO concentration. This length in time could be explained as the time required for all the active sites on the catalytic surface to be saturated with the adsorbed species. Only when this is achieved will there be efficient chemical reaction between the desorbed species for an effective reduction or removal in the level of DO present [38]. This is a typical procedure in process applications where variables are allowed to run for a certain amount of time before stability in results are obtainable. See Appendix VI, Table 21 for experimental values.

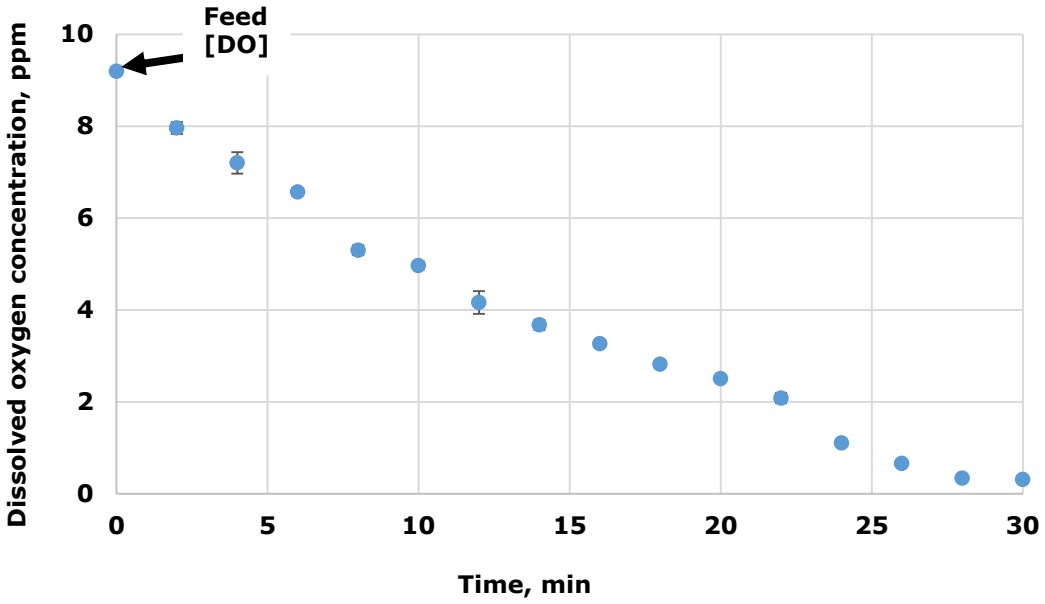

Figure 98: Effect of time on the removal of DO on 6000nm Pd coated membrane

8.3.2.6 Effect of the hydrogen gas flow rate on water deoxygenation in catalytic membrane

Figure 99 illustrates the effect of hydrogen gas flow rate on the removal of DO carried out in a 15nm platinum membrane at 200 mL/min water feed flow rate and hydrogen flow rate range of 0.19 to 1.55 $L.min^{-1}$ (see appendix VI, Table 22 for experimental values). From this graph, it is observed that, the higher the flow rate of hydrogen gas introduced, the higher the amount of DO removed. For example, at H_2 flow rate of 0.19 L/min, 67% of DO was removed; increasing the H_2 flow rate to 1.55 L/min gave above 78% DO removal. Increasing the flow rate of H_2 gas into the water mixing unit results in an increase in the partial pressure of hydrogen gas in the water mixing unit. From Henry's law, increasing the flow rate of hydrogen will automatically increase hydrogen partial pressure thereby resulting in an increase in the driving force of hydrogen dissolved into the water. This will result in having a higher concentration of hydrogen in the water. The higher the concentration of hydrogen in the water will lead to a higher reaction of H_2 and DO on the catalyst [5]. From the results shown in the graph of Figure 99, it is possible to attain 100% DO removal with sufficient increment in the H_2 flow rate to about 4.6L/min, but due to safety concerns, the flow rate was not increased beyond 1.55 L/min. It also shows that the removal of DO from water

depends on the DO concentration where the hydrogen gas is supplied in excess. This observation was similar to findings reported by Shi et al [38]. They too achieved a higher conversion of DO with increase in H_2 flow rate.

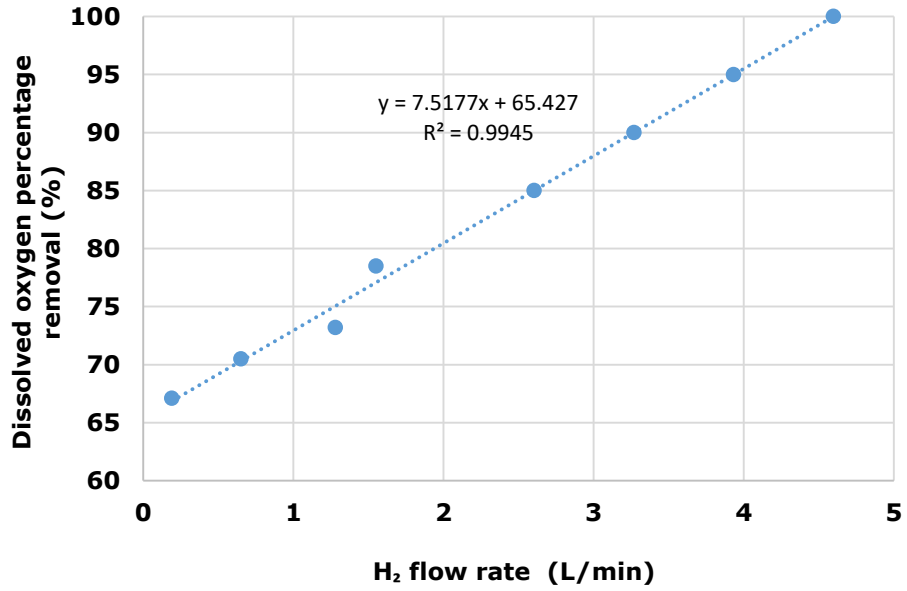

Figure 99: Effect of H_2 gas flow rate and H_2 pressure on water deoxygenation in catalytic membranes

8.3.2.7 Effect of blanket gases in DO measurement

The effect of blanket gas is being discussed because, an open glass beaker was used in collecting the water permeating through the catalytic membrane. Air or nitrogen was used as blanket gases during the actual measurement of the dissolved oxygen in the beaker. The air was sourced from the atmosphere, while nitrogen gas was supplied from a cylinder sourced from BOC, UK. At a constant feed water flowrate of 150 mL/min for example, the DO was reduced from 9.66 ppm in the feed water to 3.08 ppm at the permeate end when the DO was measured using air as a blanket gas (that is, taking the measurement without covering the beaker). The DO was then measured by flowing the nitrogen gas at 0.5 L/min above the glass beaker as it collected the permeated water. The DO measurement this time read 2.85 ppm. The explanation to the lower amount of DO removed under the air blanket gas is that, oxygen tends to re-dissolve from the air/atmosphere above the water surface into the water containing the DO probe, thereby increasing the concentration of DO while nitrogen gas prevents any oxygen gas re-dissolution by forming a blanket over the beaker. Figure 100 illustrates the different plots to the effect of blanket gases.

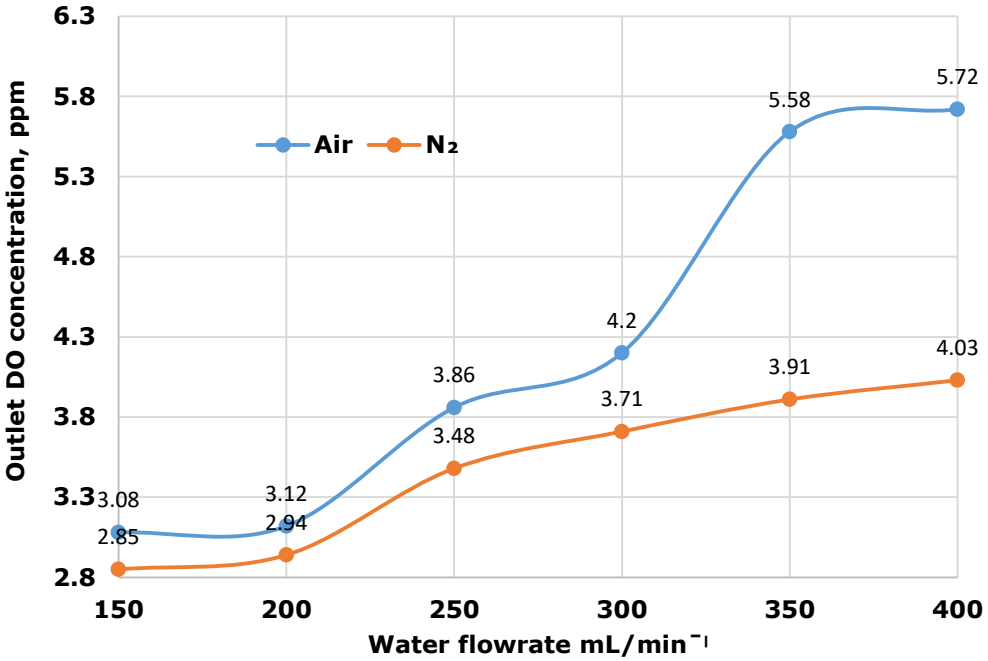

Figure 100: Effect of air and N_2 being used as blanket gases

8.3.3 Comparison of Fixed-Bed and Membrane Catalytic Deoxygenation

8.3.3.1 Catalyst weight and efficiency

Figure 101 shows a graph comparing the effect of the platinum catalyst loading on both the fixed-bed and catalytic membrane reactor at a feed flowrate of 200 mL/min with an initial feed DO of 9.7ppm. It has to be noted that the conditions of experiment were not the same (different methods of feeding in hydrogen into the system), but this results will give a rough idea of the process' efficiency. Ordinarily it will be expected that a system that has a higher catalyst loading should give a higher DO removal but that is not the case. The CMR contained 0.2 wt.% for membrane APt and 0.5 wt% for membrane CPt, while for the fixed-bed reactor, 60 wt.% of Pt catalyst was contained in the 3g of pellet used.

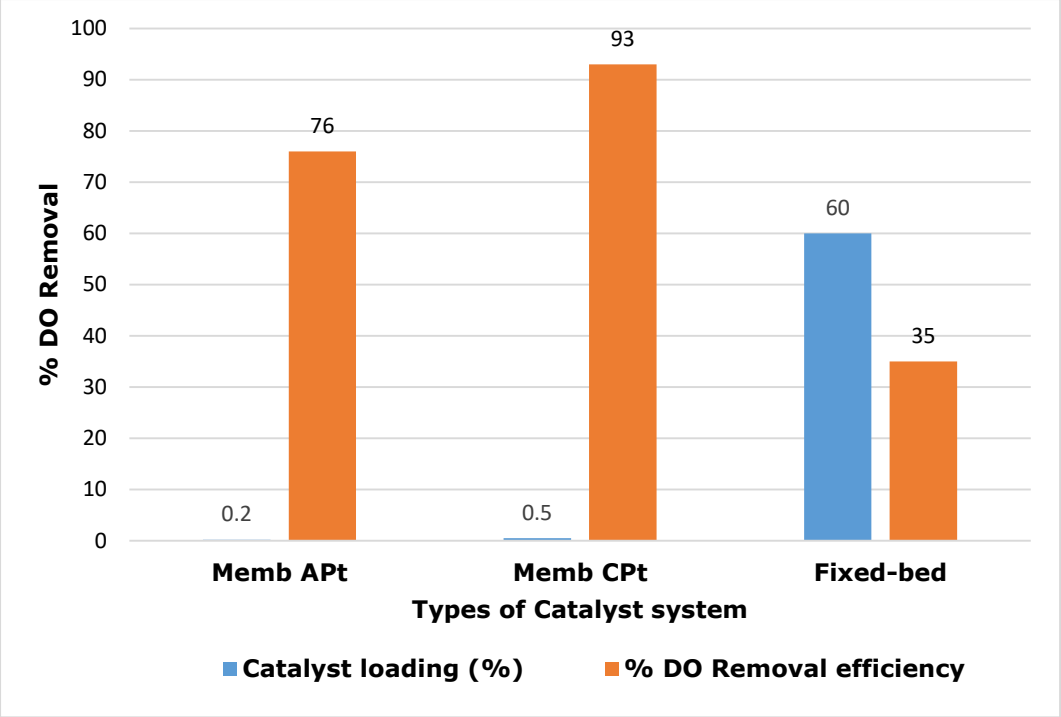

Figure 101: A plot of DO removal efficiency comparing % wt of Pt catalyst on fixed-bed and catalytic membrane reactor

For the fact that the catalyst is placed inside and around the pore walls of the membrane and with the flow of the reactants through it, this results in an intensive contact between the reactants and catalyst thereby resulting in a higher catalytic activity which is proven with the higher DO removal. It is therefore proven that for a lower DO to be achieve with the fixed-bed, more catalyst will be needed unlike the catalytic membrane reactor where a small amount is sufficient.

8.3.3.2 Rate of reaction

The dependence of the rate of reaction on the concentration of the species can be determined by experimental observations. It has been proven that the reaction between the dissolved hydrogen and DO takes place on the catalytic surface, and that when the dissolved hydrogen present in the water mixture is in excess to the stoichiometric requirement, the order of reaction with respect to the dissolve oxygen concentration is approximately 1.0 [5], therefore at steady state, equation 55 in section 7.1.2 present the rate of reaction.

Plotting a graph of $\ln\left[\frac{X_A}{W/F_{Ai}}\right]$ against $\ln[A]$ for fixed-bed reactor (Figure 102) and CMR (Figure 103), where "*A*" is denoted as oxygen gave a straight line with a slope of approximately 1. The experiment has confirmed the proposed theory. This shows a reaction of first order with respect to oxygen. Both reactors are in agreement of the first order reaction. See appendix VII, Tables 23 and 24 for experimental values.

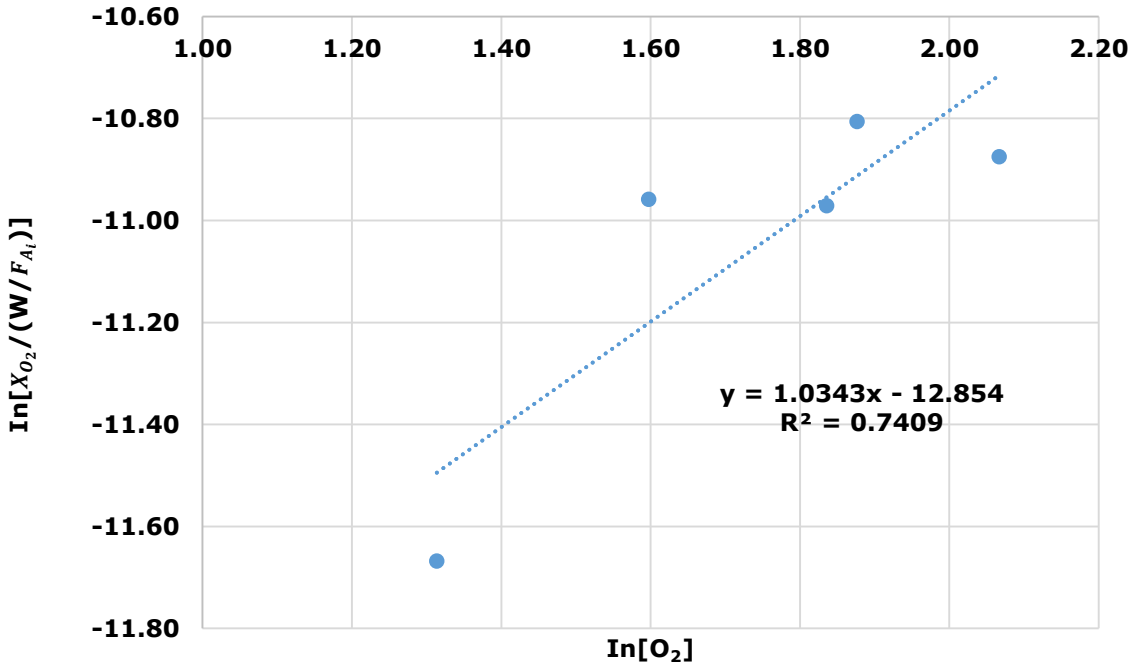

Figure 102: A plot of $\ln[XO_2/(W/F_{Ai})]$ against $\ln[O_2]$ for oxygen reaction in the fixed-bed reactor

The reaction rate constant, k, is independent of the concentrations of the species involved in the reaction. From Figure 102, the k value is so small and negligible.

$\log k_1 = -12.854$

$k_1 = e^{-12.854} = 2.6\,X\,10^{-6}$ (mol.s^{-1}.g$^{-1}_{catalyst}$.mg^{-1}.L)

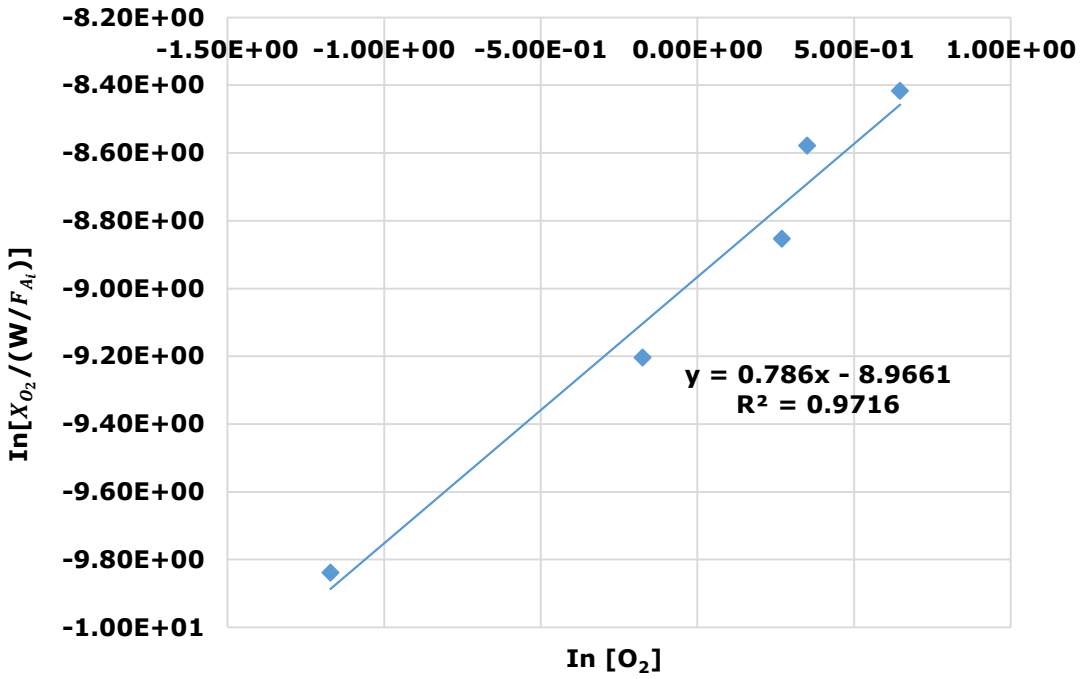

Figure 103: A plot of In[XO_2/(W/F_{Ai})] against In[O_2] in the catalytic membrane reactor

From Figure 103, the k value is so small and negligible.

$$\log k_2 = -8.9661$$

$$k_2 = e^{-8.9661} = 1.3\,X\,10^{-4}\ (\text{mol.s}^{-1}.\text{g}^{-1}_{\text{catalyst}}.\text{mg}^{-1}.\text{L})$$

Figure 104 shows a plot of the dependence of the feed hydrogen pressure on the rate of reaction of oxygen. Equation 60 was proposed to this effect and is as shown below being that the feed oxygen partial pressure was constant through out the process.

$$r_{O_2}\,\alpha\quad P_{H_2}^{n}\ .\ P_{O_2}^{f} \tag{58}$$

$$r_{O_2} = k' P_{H_2}^{n}\ P_{O_2}^{f} \tag{59}$$

Where $k_3 = k' P_{O_2}^{f}$

Substituting k in equation 59, equation 60 is generated

$$r_{O_2} = k_3 P_{H_2}^n \quad (60)$$

Where

r_{O_2} = the rate of reaction of oxygen (mol.s^{-1}.g$_{catalyst}$$^{-1}$)

k_3 = constant,

n = an order with respect to the hydrogen pressure

P_{H_2} = Feed absolute pressure (atmospheric pressure + gauge pressure), atm

P_{O_2}= Feed partial pressure of oxygen

Taking natural log of both sides of equation 60, and plotting $In\left(r_{O_2}\right)$ against $In\, P_{H_2}$ gives:

$$In\left(r_{O_2}\right) = In\, k_3 + In\, P_{H_2}$$

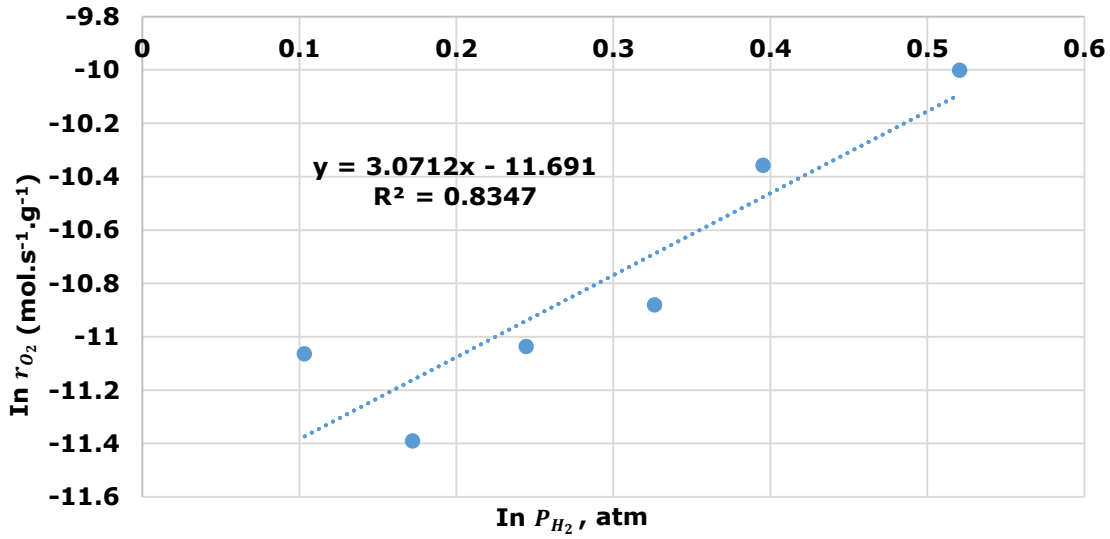

Figure 104: A plot of In(Rate of reaction of oxygen) against In(feed pressure of H_2) in the fixed-bed reactor

The feed pressure of hydrogen has dependence on which oxygen reacts and from the plot shown in Figure 104

$$\log k_3 = -11.691$$

$$k_3 = e^{-11.691} = 8.4\, X\, 10^{-6}\ (\text{mol.s}^{-1}.\text{g}^{-1}_{\text{catalyst}}.\text{atm}^{-3})$$

k_3 value is very small therefore the dependence of the constant on hydrogen pressure is weak. A value for n is 3 was obtained, showing an order of 3 for the hydrogen pressure with respect to the rate of reaction of oxygen.

It was however impossible to calculate the rate of reaction dependence on hydrogen pressure in the CMR because in this case the hydrogen was introduced into the water mixture using the gas sparger to enhance the hydrogen dissolution. Increasing the hydrogen pressure above atmospheric pressure was deemed unsafe because the saturator was made of ordinary glass. So instead a flow meter was therefore used to monitor the hydrogen inflow.

CHAPTER NINE

Chapter 9

9 CONCLUSION AND RECOMMENDATION FOR FUTURE WORK

9.1 Conclusion and significance

Hydrogenation of oxygen for the purpose of water deoxygenation is an interesting and widely applied method that is being applied industrially. The most advanced industrial process is the Seaject method that utilizes a fixed-bed catalyst with hydrogen. In this work, the removal of DO from water has been experimentally studied in a novel catalytic membrane reactor and compared with the fixed-bed process using hydrogen gas. The hydrogen gas needed was introduced into the mixing unit in very fine bubbles using a stainless steel gas sparger in the case of the catalytic membrane while for the fixed-bed the hydrogen was introduced from the reactor's side (less resistance as a result of the arrangement of the catalyst bed in the fixed-bed reactor and hence that affected the nature of adding hydrogen into the water). An appropriate mixer which ensured the complete dissolution of these tiny hydrogen bubbles in water was used in the membrane reactor process.

Based on the experimental results obtained, the following conclusions have been arrived at:

1. A design and methodology for the utilization of commercially available alumina ceramic microfiltration supports with the incorporation of low content precious metal catalytic material has been developed for water deoxygenating purposes.

2. The catalytic membranes have been characterised using gas permeation, scanning electron microscopy (SEM) with energy dispersive X-ray (EDAX) and nitrogen adsorption desorption (BET, BJH) analysis respectively. They all show the effect of the presence of the catalytic metal.

3. The results obtained from the nitrogen adsorption analysis revealed that the membranes contained a significant level of micropores based on the pore size, pore size dustribution and BET surface area. This is a very good

result because micropores are very important since they enhance the entrapment of the catalysts in the membrane and hence prevent the catalysts from being washed away by the water during the deoxygenation process. It was therefore both useful and necessary to confirm using single gas transportation that the catalyst modified membranes have not created any additional limitation in terms of flow and mechanistic aspects. The single gas transport therefore provided valuable additional information regarding the flow-through behaviour of the membranes which the Nitrogen adsorption equipment could not provide because by its very nature nitrogen adsorption does not involve a flow-through process.

4. The amount of palladium metal deposited was more than that of the platinum metal and it was concluded that this was based on the type of precursor used for each of the catalyst. The platinum and palladium membranes displayed a lesser permeation of hydrogen when compared to the fresh supports. The EDAX are rather qualitative and not quantitative analysis. They are a representative of the elements present in the entire membranes.

5. The geometry of the support (either 15nm or 6000nm porous ceramic alumina) is a determining factor in the performance of the catalytic membrane reactor. The larger the pores and the surface area of the support, the more the catalytic loading and consequently the more productive is the method.

6. Platinum and palladium catalytic membranes can be used for water deoxygenation using hydrogen gas. The choice of the catalytic metal is a crucial factor in determining the yield of the product which in this case is water.

7. The method used for palladium plating to achieved very thin coatings which help minimize diffusional problems which are experienced with thicker coatings. The electroless plating also creates a surface which is

uniformly metallized and all of the palladium is involved in the reduction of oxygen with hydrogen.

8. The method of catalyst impregnation was also carried out to favour high dispersion of the catalyst. The platinum impregnated membranes gave high affinity for DO and therefore requires no regeneration. The ceramic support has highly dispersed metals incorporated into their pores, which promotes the efficient distribution of hydrogen thereby enhancing the catalytic recombination of hydrogen and DO in water.

9. At low operating feedwater flowrate, optimum contact of the reactants with the catalytic surface were achieved.

10. The porous catalytic membranes are well suited for the purpose of water deoxygenation as they readily allow the penetration of the reactants into the porous matrix containing the catalyst.

11. The results showed reduction in DO concentration with increase of hydrogen flowrate and also reduction of the water feed flow rate. The overall reduction or reaction was achieved at either higher hydrogen flowrate or lower feed flowrate.

12. Extra precaution had to be taken when hydrogen gas was in used. Steps were taken to ensure that there were no leakage of hydrogen as it can form an explosion on contact with oxygen in the atmosphere.

13. A membrane reactor involves the additional expenditure on the catalyst, but its performance with respect to the outlet DO levels achieved is best on the long run.

14. The catalytic membrane process showed a higher efficiency in the removal of DO when compared with the fixed-bed reactor, because the catalytic membranes are applied in dead-end mode thereby forcing the reactants to flow through the membrane. The function of the catalytic membrane reactor is therefore to provide a reaction space with controlled residence time and high catalytic activity.

15. In the case of the fixed-bed reactor, the reaction of the H_2 and H_2O/O_2 is achieved with a greater amount of catalyst because it needs a greater catalytic surface to enhance the chemical reaction. This also implies on additional cost of the precious metals and limitations as a result of pore diffusion will be consequently increased.

16. From the design equations, it can be concluded that the same equation is applicable to both the fixed-bed and membrane reactor. However but for the fact that the catalyst is highly dispersed and in flow-through pore mode in the membrane reactor it functions far better than the fixed-bed.

17. Experimental results obtained from both fixed-bed and CMR are in satisfaction agreement of the first order reaction with respect to oxygen.

18. A rate of reaction in relation to the effect of hydrogen pressure was also proposed. An order of 3 was obtained.

9.2 Recommendations for future work

This study has proven the ability of the removal of DO utilizing low catalytic deposited tubular ceramic membranes. This research could be said to be a good basis for a better understanding for developing a system that will be compact and serve the purpose of water deoxygenation for down-hole water injection and process applications.

The followings are thought to further make this process applicable in near future.

1. It will be a great idea to test this novel method on other water sources, for example actual sea water. By doing this, comparisons can be made, leading to a more robust and efficient technology.

2. Investigation on effects of different catalytic loadings and water temperatures on the water deoxygenation rate of reaction. This will also include establishing proper mass flow

3. The use of a commercial deposited catalytic membrane with known catalytic loading to serve as reference for this process.

4. Additional membrane characterisation techniques will be of advantage, such as X-ray fluorescence spectrometry (XFS), inductively coupled plasma mass spectrometry (ICP-MS) and atomic absorption spectrometry (AAS) respectively.

5. Construct a pilot plant where the permeate will be collected in an enclosed system to avoid re-dissolution of oxygen from the atmosphere into the deoxygenated water.

6. Stability test also to be done to see the effect of long term stability of the catalysts.

7. Detailed reaction rate expressions should be proposed by carrying out thermodynamic analysis such as activation energies and enthalpies of adsorption on the reacting species and reaction rate constants.

8. A mathematical model should be developed which will be able to predict the performance of a reactor for the optimization of water deoxygenation. The model should be able to predict the membrane's area, catalytic loading and feed flow rate that will give optimum conversion depending on the process' requirement on limit of allowed level of DO.

9. An extensive market assessment to ascertain the cost implications.

CHAPTER TEN

Chapter 10

REFERENCES

[1] Volkov V, Lebedeva V, Petrova I, Bobyl A, Konnikov S, Roldughin V et al. Adlayers of palladium particles and their aggregates on porous polypropylene hollow fibre membranes as hydrogenization contractors/reactors. *Advances in Colloid and Interface Science.* 2011; 164(1-2):144-155.

[2] Palsson B, Davies DR, Todd AC, Somerville JM. The Water Injection Process: A Technical and Economic Integrated Approach. *Chemical Engineering Research and Design.* 2003; 81(3):333-341.

[3] Available from: **http://www.liquicel.com/applications/O_2.cfm**. Assessed 22/9/2015.

[4] Deuel CL. Compact Seawater Deoxygenation System Improvements for Floating Production Facilities. Compact Seawater Deoxygenation System Improvements for Floating Production Facilities. *SPE International Petroleum Conference and Exhibition in Mexic*o: Society of Petroleum Engineers; 2002.

[5] Tan X, Li K. Investigation of novel membrane reactors for removal of dissolved oxygen from water. *Chemical Engineering Science.* 2000; 55(7):1213-1224.

[6] Available from: http://petrowiki.org/Surface_water_treatment_for_injection. Assessed 22/9/2015.

[7] Suppiah S, Burns D, Aelick C. Catalytic Removal of Dissolved Oxygen for Nuclear and Non-Nuclear Applications.

[8] Gross MS, Pisarello ML, Pierpauli KA, Querini CA. Catalytic deoxygenation of water: Preparation, deactivation, and regeneration of palladium on a resin catalyst. *Industrial & Engineering Chemistry Research.* 2009; 49(1):81-88.

[9] De-oxygenation system eases congestion on cluttered process bays. (1999). Available from: https://www.offshore-mag.com/articles/print/volume-59/issue-11/news/production/de-oxygenation-system-eases-congestion-on-cluttered-process-bays.html. Assessed 11/02/2018

[10] Mengers H, Benes NE, Nijmeijer K. *Multi-component mass transfer behaviour in catalytic membrane reactors.* 2014ID: 271348.

[11] Usman MR. *Advanced Chemical Reaction Engineering-Part-1-10-Apr-2016.* Available from: https://www.slideshare.net/MuhammadRashidUsman1/advanced-chemical-reaction-engineeringpart110apr2016. Assessed 02/05/2018

[12] Coronas J, Santamaŕia J. Catalytic reactors based on porous ceramic membranes. *Catalysis Today.* 1999; 51(3–4):377-389.

[13] Zhang Z, Zhu Y, Asakura H, Zhang B, Zhang J, Zhou M, et al. Thermally stable single atom Pt/m-Al_2O_3 for selective hydrogenation and CO oxidation. *Nature Communications.* 2017; 8:16100.

[14] Kajama MN, Shehu H, Okon E, Orakwe I, Gobina E. VOC oxidation in excess of oxygen using flow-through catalytic membrane reactor. *International Journal of Hydrogen Energy.* 2016; 41(37):16529-16534.

[15] Uzio D, Miachon S, Dalmon J. Controlled Pt deposition in membrane mesoporous top layers. *Catalysis Today.* 2003; 82(1–4):67-74.

[16] Kajama MN, Nwogu NC, Okon EO, Shehu H, Orakwe I, Gobina E. Hydrogen Separation Using Pt-Alumina Impregnated Membrane. *Energy and Power Engineering.* 2015; 7(09):412.

[17] Melendez J, Fernandez E, Gallucci F, van Sint Annaland M, Arias PL, Pacheco Tanaka DA. *Preparation and characterization of ceramic supported ultra-thin (~1μm) Pd-Ag membranes.* 2017ID: 271357.

[18] Li A, Liang W, Hughes R. Fabrication of dense palladium composite membranes for hydrogen separation. *Catalysis Today.* 2000; 56(1–3):45-51.

[19] Abate S, Centi G, Melada S, Perathoner S, Pinna F, Strukul G. *Preparation, performances and reaction mechanism for the synthesis of H_2O_2 from H_2 and O_2 based on palladium membranes.* 2005ID: 271364.

[20] Yuranov I, Moeckli P, Suvorova E, Buffat P, Kiwi-Minsker L, Renken A. Pd/SiO_2 catalysts: synthesis of Pd nanoparticles with the controlled size in mesoporous silicas. *Journal of Molecular Catalysis A: Chemical.* 2003; 192(1-2):239-251.

[21] Wang HY, Ruckenstein E. *Carbon dioxide reforming of methane to synthesis gas over supported rhodium catalysts: the effect of support.* 2000ID: 271346.

[22] Li K, Chua I, Ng W, Teo W. Removal of dissolved oxygen in ultrapure water production using a membrane reactor. *Chemical Engineering Science.* 1995; 50(22):3547-3556.

[23] Li K, Tan X. Development of membrane–UV reactor for dissolved oxygen removal from water. *Chemical engineering science.* 2001; 56(17):5073-5083.

[24]**http://www.mymobilebay.com/stationdata/whatisDO.htm**. Assessed 11/12/2017

[25] *Fundamentals of environmental measurements.* Available from: **http://www.fondriest.com/environmental-measurements/parameters/water-quality/dissolved-oxygen/**. Assessed 15/06/2015

[26] Abdi A, Karimi A, Razzaghi M. *Continuously deoxygenation of water in a reactor packed with glucose oxidase immobilized in MnO_2/calcium alginate composite.* 2016ID: 282892.

[27] *Chapter 11 - Preboiler and Boiler Corrosion Control.* Available from: https://www.scribd.com/document/356746178/Ch-11-Corrosion-Tendencies-of-Boiler-System-Components-pdf. Assessed 02/05/2018

[28] Stipanicev M, Turcu F, Esnault L, Rosas O, Basseguy R, Sztyler M, et al. Corrosion of carbon steel by bacteria from North Sea offshore seawater injection systems: Laboratory investigation. *Bioelectrochemistry.* 2014; 97:76-88.

[29] Lebedeva V, Gryaznov V, Petrova I, Volkov V, Tereshchenko G, Shkol'nikov E, et al. Porous Pd-containing polypropylene membranes for catalytic water deoxygenation. *Kinetics and catalysis.* 2006; 47(6):867-872.

[30] Sinha V, Li K. Alternative methods for dissolved oxygen removal from water: a comparative study. *Desalination.* 2000; 127(2):155-164.

[31] Li K, Tan T, Sinha V, Teo W. Simulation of a novel glass reactor for dissolved oxygen removal from water. *Water research.* 2000; 34(7):2011-2024.

[32] Karimi A, Mahdizadeh F, Salari D, Niaei A. *Bio-deoxygenation of water using glucose oxidase immobilized in mesoporous MnO_2.* 2011ID: 271370.

[33] Available from: https://chemengineering.wikispaces.com/Henry%27s+Law. Assessed 02/05/2018

[34] Papavinasam S. Chapter 2 - Oil and Gas Industry Network. In: Papavinasam S, editor. *Corrosion Control in the Oil and Gas Industry.* Boston: Gulf Professional Publishing; 2014. p. 41-131.

[35] Brinn M. Compact Oxygen Removal for Waterflood Projects. Compact Oxygen Removal for Waterflood Projects. *Offshore Technology Conferenc*e: Offshore Technology Conference; 2013.

[36] Mode R and Haas W. Reduction in Feed Water System Corrosion Utilizing Dissolved Oxygen Reduction by Membrane Technology. Reduction in Feed Water System Corrosion Utilizing Dissolved Oxygen Reduction by Membrane Technology. *CORROSION 200*5: NACE International; 2005.

[37] *Minox Technology*. **http://www.minox.no/index.php/products**. Assessed 22/9/2015

[38] Shi W, Cui C, Zhao L, Yu S, Yun X. Removal of dissolved oxygen from water using a Pd-resin based catalytic reactor. *Frontiers of Chemical Engineering in China.* 2009; 3(1):107-111.

[39] Ito A, Yamagiwa K, Tamura M, Furusawa M. Removal of dissolved oxygen using non-porous hollow-fiber membranes. *Journal of Membrane Science.* 1998; 145(1):111-117.

[40] De Wit P, Van Daalen FS, Benes NE. The effect of the production method on the mechanical strength of an alumina porous hollow fiber. *Journal of the European Ceramic Society.* 2017; 37(10):3453-3459.

[41] Li H, Schygulla U, Hoffmann J, Niehoff P, Haas-Santo K, Dittmeyer R. Experimental and modeling study of gas transport through composite ceramic membranes. *Chemical Engineering Science.* 2014; 108(0):94-102.

[42] He X, Hägg M. Membranes for environmentally friendly energy processes. *Membranes.* 2012; 2(4):706-726.

[43] Benito JM, Conesa A, Rubio F, Rodríguez MA. Preparation and characterization of tubular ceramic membranes for treatment of oil emulsions. *Journal of the European Ceramic Society.* 2005; 25(11):1895-1903.

[44] Basile A, De Falco M, Centi G, Iaquaniello G. *Membrane Reactor Engineering: Applications for a Greener Process Industry.* John Wiley & Sons; 2016.

[45] Zeynali R, Ghasemzadeh K, Sarand AB, Kheiri F, Basile A. *Performance evaluation of graphene oxide (GO) nanocomposite membrane for hydrogen separation: Effect of dip coating sol concentration.* 2018ID: 271948.

[46] Abdel Halim KS, Ramadan M, Shawabkeh A, Abufara A. *Synthesis and characterization of metallic materials for membrane technology.* 2013ID: 305631.
[47] Westermann T, Melin T. *Flow-through catalytic membrane reactors—Principles and applications.* 2009ID: 271349.

[48] Cardoso SP, Azenha IS, Lin Z, Portugal I, Rodrigues AE, Silva CM. Inorganic Membranes for Hydrogen Separation. *Separation & Purification Reviews.* 2018; 47(3):229-266.

[49] Li K. *Ceramic membranes for separation and reaction.* John Wiley & Sons, Ltd; 2007.

[50] Smart S, Liu S, Serra JM, Diniz da Costa JC, Iulianelli A, Basile A. 8 - Porous ceramic membranes for membrane reactors. In: Basile A, editor. *Handbook of Membrane Reactors.* : Woodhead Publishing; 2013. p. 298-336.

[51] Hubadillah SK, Othman MHD, Matsuura T, Rahman MA, Jaafar J, Ismail AF, et al. *Green silica-based ceramic hollow fiber membrane for seawater desalination via direct contact membrane distillation.* 2018ID: 271948.

[52] Rezakazemi M, Maghami M, Mohammadi T. High loaded synthetic hazardous wastewater treatment using lab-scale submerged ceramic membrane bioreactor. *Periodica Polytechnica Chemical Engineering.* 2018; 62(3):299-304.

[53] Samaei SM, Gato-Trinidad S, Altaee A. *The application of pressure-driven ceramic membrane technology for the treatment of industrial wastewaters – A review.* 2018ID: 271948.

[54] Mistry VV, Maubois J. *Chapter 27 - Application of Membrane Separation Technology to Cheese Production.* San Diego: Academic Press; 2017ID: 315881.

[55] Simão L, Montedo ORK, Paula, Marcos Marques da Silva, Silva Ld, Caldato RF, Innocentini, Murilo Daniel de Mello. Structural and fluid dynamic characterization of calcium carbonate-based porous ceramics. *Materials Research.* 2013; 16(6):1439-1448.

[56] Mulder M. *Basic principles of membrane technology.* Springer Science & Business Media; 1996.

[57] Saleh TA, Gupta VK. Chapter 1 - An Overview of Membrane Science and Technology. In: Saleh TA, Gupta VK, editors. *Nanomaterial and Polymer Membranes.* : Elsevier; 2016. p. 1-23.

[58] Li X, Liang B. Permeance of pure vapours in porous γ-Al_2O_3/α-Al_2O_3 ceramic membrane. *Journal of the Taiwan Institute of Chemical Engineers.* 2012; 43(3):339-346.

[59] Carlos Finol JC. Permeation of gases in asymmetric ceramic membranes. 1999; (Chemical Engineering Education):58-60.

[60] Lee D, Oyama ST. Gas permeation characteristics of a hydrogen selective supported silica membrane. *Journal of Membrane Science.* 2002; 210(2):291-306.

[61] Pandey P, Chauhan R. Membranes for gas separation. *Progress in Polymer Science.* 2001; 26(6):853-893.

[62] Rahimpour M, Samimi F, Babapoor A, Tohidian T, Mohebi S. Palladium membranes applications in reaction systems for hydrogen separation and purification: A review. *Chemical Engineering and Processing: Process Intensification.* 2017; 121:24-49.

[63] Jones L, Atkins P. *CHEMISTRY: Molecules, Matter, and Change.* Fourth ed. New york: W. H. Freeman and Company; 2000.

[64] Available from: https://www.ck12.org/book/CK-12-Chemistry-Second-Edition/r9/section/18.4/. Assessed 29/03/2018

[65] Julbe A, Farrusseng D, Guizard C. Porous ceramic membranes for catalytic reactors — overview and new ideas. *Journal of Membrane Science.* 2001; 181(1):3-20.

[66] Johansson Å, Försth M, Rosén A. The H_2/O_2 reaction on a palladium model catalyst studied with laser-induced fluorescence and microcalorimetry. *International Journal of Molecular Sciences.* 2001; 2(5):221-229.

[67] Hellsing B, Kasemo B, Zhdanov V. Kinetics of the hydrogen-oxygen reaction on platinum. *Journal of catalysis.* 1991; 132(1):210-228.

[68] Yun S, Oyama ST. Correlations in palladium membranes for hydrogen separation: a review. *Journal of Membrane Science.* 2011; 375(1):28-45.

[69] Okazaki J, Ikeda T, Tanaka DAP, Sato K, Suzuki TM, Mizukami F. An investigation of thermal stability of thin palladium–silver alloy membranes for high temperature hydrogen separation. *Journal of Membrane Science.* 2011; 366(1):212-219.

[70] Collins JP, Way JD. Preparation and characterization of a composite palladium-ceramic membrane. *Industrial & Engineering Chemistry Research.* 1993; 32(12):3006-3013.

[71] Ghasemzadeh K, Aghaeinejad-Meybodi A, Basile A. *Hydrogen production as a green fuel in silica membrane reactor: Experimental analysis and artificial neural network modeling.* 2018ID: 271496.

[72] Zhang J, Zhao Z, Xia Z, Dai L. A metal-free bifunctional electrocatalyst for oxygen reduction and oxygen evolution reactions. *Nature nanotechnology.* 2015; 10(5):444.

[73] Ghasemzadeh K, Ahmadnejad F, Aghaeinejad-Meybodi A, Basile A. *Hydrogen production by a PdAg membrane reactor during glycerol steam reforming: ANN modeling study.* 2018ID: 271472.

[74] Michaelides A, Hu P. Catalytic water formation on platinum: A first-principles study. *Journal of the American Chemical Society.* 2001; 123(18):4235-4242.

[75] Verheij LK. Kinetic modelling of the hydrogen-oxygen reaction on Pt (111) at low temperature (< 170 K). *Surface Science.* 1997; 371(1):100-110.

[76] Available from: https://www.thoughtco.com/printable-periodic-tables-4064198. Assessed 26/03/2018

[77] Gómez-Marín AM, Feliu JM. *Thermodynamic properties of hydrogen–water adsorption at terraces and steps of Pt(111) vicinal surface electrodes.* 2016ID: 271619.

[78]**http://www.greencarcongress.com/2004/11/milestone_for_h.html** . Assessed 08/05/2018

[79] Den Exter M. The use of electroless plating as a deposition technology in the fabrication of palladiumbased membranes. *Palladium Membrane Technology for Hydrogen Production, Carbon Capture and Other Applications.* 2014;:43-67.

[80] Li A, Liang W, Hughes R. Characterisation and permeation of palladium/stainless steel composite membranes. *Journal of Membrane Science.* 1998; 149(2):259-268.

[81] Perez V, Miachon S, Dalmon J, Bredesen R, Pettersen G, Ræder H, et al. Preparation and characterisation of a Pt/ceramic catalytic membrane. *Separation and purification technology.* 2001; 25(1):33-38.

[82] Pina M, Irusta S, Menéndez M, Santamaria J, Hughes R, Boag N. Combustion of volatile organic compounds over platinum-based catalytic membranes. *Industrial & Engineering Chemistry Research.* 1997; 36(11):4557-4566.

[83] Rojas S. *Preparation of catalysts Heterogenous Catalyst.* Available from: https://www.carenafp7.eu/index.php?option=com_docman&task=doc...gid. Assessed 18/08/2018

[84] Bodke A, Bharadwaj S, Schmidt L. The effect of ceramic supports on partial oxidation of hydrocarbons over noble metal coated monoliths. *Journal of catalysis.* 1998; 179(1):138-149.

[85] Merati Z, Basiri Parsa J. *Enhancement of the catalytic activity of Pt nanoparticles toward methanol electro-oxidation using doped-SnO_2 supporting materials.* 2018ID: 271533.

[86] *Why does combining hydrogen and oxygen typically produce water rather than hydrogen peroxide?* Scientific American; Available from: https://www.scientificamerican.com/article/why-does-combining-hydrog/. Assessed 28/04/2018

[87] Kotz JC, Treichel PM, Townsent JR. *Chemistry & Chemical Reactivity.* SEVENTH ed. Canada: Thomson Brooks/Cole; 2009.

[88] Moradian A, Delijani F, Koshky FE. The Effect of Different Parameters on the Efficiency of the Catalytic Reduction of Dissolved Oxygen. *Thermal power plants-advanced applications.* 2013; :143.

[89] Henriksen N, Nord L and Kjolberg S. Efficient New Processing System for Water Deoxygenation. Efficient New Processing System for Water Deoxygenation. *Proceedings of the 19th Annual Offshore Technology Conferenc*e; 1987.

[90] Sykora A. Kitco News; USA: 2017. Available from: **http://www.kitco.com/news/2017-09-28/Palladium-Prices-Top-Platinum-For-First-Time-Since-2001-May-Not-Last.html**. Assessed 30/03/2018

[91] Yeung K, Christiansen S, Varma A. Palladium composite membranes by electroless plating technique: relationships between plating kinetics, film microstructure and membrane performance. *Journal of Membrane Science.* 1999; 159(1):107-122.

[92] Basile A. *Handbook of membrane reactors.* Cambridge, UK ; Philadelphia, PA: Woodhead Publishing; 2013[electronic resource]. Vol. 2, Reactor types and industrial applications / edited by Angelo Basile.; 1 online resource (xxxv, 936 pages) : illustrations; text txt; computer c; online resource cr; 2044-9364; Includes bibliographical references and index.; Description based on print version record.; Woodhead Publishing in energy ; vol. 56.

[93] Gobina E, inventor. *Apparatus and method for separating gases.* Washington, DC: US. Patent and Trademark Office 7,048,778. 2006

[94] https://www.lucideon.com/testing-characterization/techniques/sem-edx. Assessed 09/01/2018

[95] Othman M, Mukhtar H, Ahmad A. Gas permeation characteristics across nano-porous inorganic membranes. *IIUM Engineering Journal.* 2004; 5(2).

[96] Afandizadeh S, Foumeny E. Design of packed bed reactors: guides to catalyst shape, size, and loading selection. *Applied Thermal Engineering.* 2001; 21(6):669-682.

[97] Nemec D, Levec J. *Flow through packed bed reactors: 1. Single-phase flow.* 2005ID: 271348.

[98] Scott Fogler H. *Essentials of Cemical Reaction engineering.* Boston: Prentice Hall International Series in the Physical and Chemical Engineering Sciences; 2010.

[99] Okon E, Shehu H, Gobina E. Evaluation of the performance of α-alumina nano-porous ceramic composite membrane for esterification applications in petroleum refinery. *Catalysis Today.* 2017

[100] Gao W, Liang H, Ma J, Han M, Chen Z, Han Z, et al. *Membrane fouling control in ultrafiltration technology for drinking water production: A review.* 2011ID: 271370.

[101] Huang X, Wei C, Yu K. *Mechanism of membrane fouling control by suspended carriers in a submerged membrane bioreactor.* 2008ID: 271357.

[102] Guo W, Ngo H, Li J. *A mini-review on membrane fouling.* 2012ID: 271433.

[103] Seidel A, Elimelech M. *Coupling between chemical and physical interactions in natural organic matter (NOM) fouling of nanofiltration membranes: implications for fouling control.* 2002ID: 271357.

[104] Vrijenhoek EM, Hong S, Elimelech M. *Influence of membrane surface properties on initial rate of colloidal fouling of reverse osmosis and nanofiltration membranes.* 2001ID: 271357.

[105] Salehi E, Madaeni SS, Shamsabadi AA, Laki S. *Applicability of ceramic membrane filters in pretreatment of coke-contaminated petrochemical wastewater: Economic feasibility study.* 2014ID: 271590.

[106] Ciardelli G, Corsi L, Marcucci M. *Membrane separation for wastewater reuse in the textile industry.* 2001ID: 271808.

CHAPTER ELEVEN

Chapter 11

APPENDIX I: Experimental

The experimental section comprises of equipment and apparatus used during the whole process.

i. Tubular membrane holder: These are stainless steel materials having a tube and shell arrangement used in the housing of the membranes during experiments. It served as the reaction chamber.

ii. Spanners: Both large and small stainless steel spanners were needed during the experimental process. The larger spanners were used for locking and unlocking of the membrane reactors, while the smaller ones were used for tightening and loosening of connections.

iii. Graphite rings: Geegraf moulded graphite "O" rings, 1.6g/cc density, 98% purity as shown in Figure 105 were used as seals in the reactors. They are about 7mm thick with different outer and inner diameters to fit the different reactors. These seals help in making sure that the membranes remain in position and also to ensure no leak from the reaction chamber occurs.

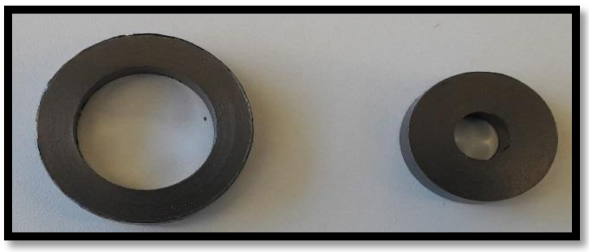

Figure 105: Graphite "O" rings

iv. Experimental rig: These are laboratory designed experimental rigs in which holes are bore and fittings are fitted for supporting the reactors and other connections such as values during experiments. They are usually heat resistant.

v. Retort stand: this was used to clamp reactors in the fume cupboard as the experimental rigs were too large to fit

vi. Power regulators (Barnstead Electro Thermal): the power regulators are connected to the heating tapes and it works by controlling the heating on the reactors by either turning it clockwise to either increase or anticlockwise to decrease the temperature showing on the thermometer.

vii. Heating tape: Heating tapes purchased from RS component were used for heating up the reactors to required temperatures. They are usually not reusable in a case the heating tapes are taken off.

viii. Thermocouple purchased from RS component were used.

ix. Thermometer (ExiaIICT4) was used for monitoring and measuring the temperature of the reactors during gas permeation analysis that required variations in working temperature. It was also used for monitoring the plating bath during palladium membrane preparation.

x. Fine stainless steel mesh: This mesh was used as a suspended for the catalyst bed.

xi. Mass flow meters: These flow meters are devices purchased from Cole-Parmer, which were used during gas permeation test to measure the gas flow at which the gas is permeating through the reactors. It gives measurement in L/min and have various settings to go with different gases. Hence during the permeation test, the flow meters are set accordingly with the permeating gas or else, wrong flow rates will be recorded. Figure 106 shows the picture of the flow meter used at a closer range.

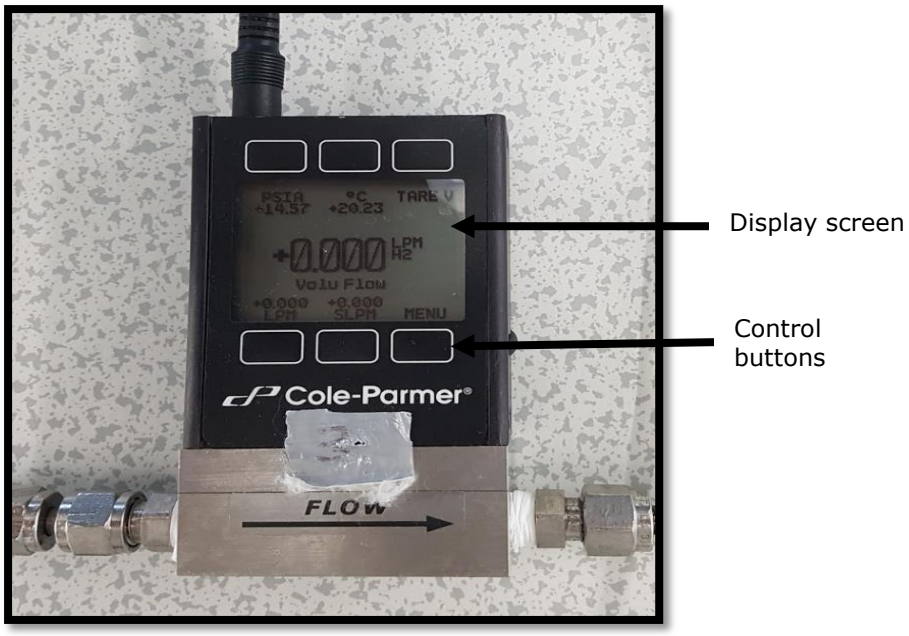

Figure 106: Picture showing a Cole-Parmer gas flow meter

xii. Vernier calliper and ruler: Vernier calliper was used for measuring the inner and outer diameters of the ceramic support materials while the ruler was used for measuring the membrane's length.

xiii. Mortar and pestle: Used for grinding membrane fragments for further analysis. For example, samples needed for liquid nitrogen adsorption desorption analysis has to been in a powered form.

xiv. Gas safety monitor: Two types of gas safety monitors were used. One is an oxygen detector which should alert those around in a case of oxygen depletion. It was mostly used when gases were been transported to and fro while using lifts and entering the gas compound cage. The other safety monitor is specifically for hydrogen as shown in Figure 107 and it was used when experiments involving hydrogen gas were being carried out. It works by alerting one if there is a hydrogen leak. Hydrogen gas has invisible flames and explosive so extra caution was necessitated.

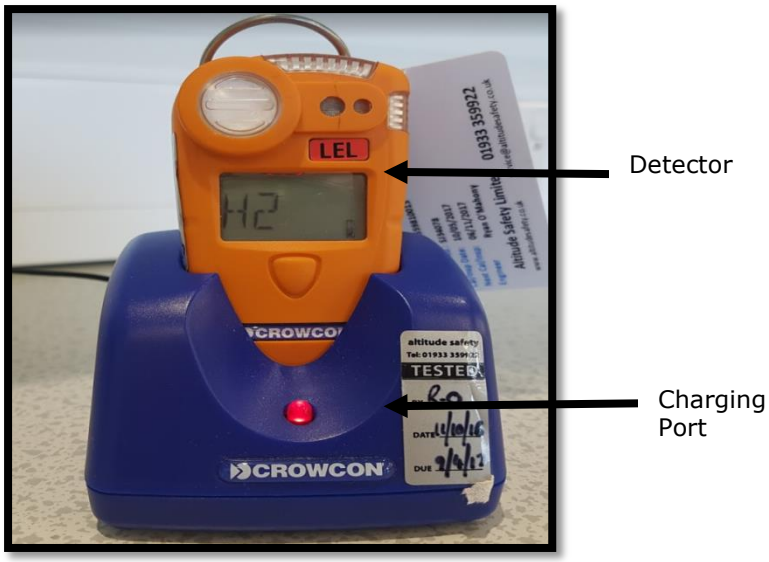

Figure 107: Picture of a H_2 safety monitor

xv. Weighing balance: this was used to measure all solid chemicals and initial and final weights of all membranes. In general, it was used for weighing all that their weights mattered in the experimental procedure.

xvi. Glass wares: these were majorly measuring cylinders, beakers and conical flasks. Some of the measuring cylinders used in sample preparation were customised in a way to allow the insertion of membrane without excess room left around it, thereby reducing the amount of chemical required. These customised glass cylinders could container around 400ml of solution and perfectly house the inserted membrane with its witness sample. In a nut shell, 1 litre measuring cylinder were avoided where the need to minimize the amount of chemicals were advisable, thereby minimizing cost. Both palladium and platinum catalyst are very expensive, so ways of achieving catalytic deposition of required percentages were still achieved working by proportions.

xvii. Magnetic stirrer: The magnetic stirrer played an important role in all processes involving mixing of chemicals. This was necessitated in order to achieve uniformity of the solution mixtures.

xviii. Digital Pressure gauges (Omni Instrument, UK) shown in Figure 108. They were used for noting down inlet feed pressures during permeation text. It gave readings in bar unit.

Figure 108: Picture of a pressure gauge

xix. Electric powered Water bath: the water bath was used to heat up water which was used during palladium plating process. The plating solutions needed to be heated to a certain temperature. This water bath has a temperature regulator and could actually heat up water contained in it up to 100^{o}C.

xx. Oven: Purchase from Carbolite, UK and was used for drying of membranes during membrane preparatory stages in cases complete drying was necessitated. It was also used for drying of glass cells used for liquid nitrogen analysis.

xxi. Fume cupboard: the fume cupboard is constructed in a way that it has an extractor which vents off waste into the external atmosphere. The vent of the gas permeation test were connected into the fume cupboard whose door was always shut during analysis. The mixing and weighing of hazardous chemicals were carried out in the fume cupboard too, this was done to prevent inhaling fumes from these chemicals.

xxii. Stainless steel fittings, Swagelok. U.K: this consist of 1/8 in stainless steel tubes, ferrule sets, bolts and screws.

xxiii. Deionised water dispenser shown in Figure 109. It was used to supply all the deionised water required at each point in time.

Figure 109: Deionised water dispenser

APPENDIX II: Materials

These materials include pellets for fixed bed reactor, ceramic supports for method no 2 and no 3, gases and chemicals. These are discussed below:

II.1 Ceramic supports

Commercially available ceramic supports purchased from Ceramiques Techniques et Industrielles (CTI SA) France were used for the study. These membranes are tubular in shape and have different membrane areas. They are made majorly of alumina material with a wash-coat of titania. Their actual composition is 77% alumina and 23% TiO_2, and are 45% porosity. Table 13 shows the dimensions of the 3 different supports used in this study.

Table 13: Ceramic supports used and their parameters

	Membrane A	Membrane B	Membrane C
Outer diameter d_2, m	0.01	0.025	0.025
Inner diameter d_1, m	0.007	0.02	0.02
Total Length (l), m	0.37	0.37	0.65
Grazed ends, m	0.05	0.05	0.05
Permeable length (l_o), m	0.32	0.32	0.645
Membrane Area, m^2	$0.008m^2$	$0.025m^2$	$0.045m^2$
Pore size, nm	15	6000	15

Figures 110 and 111 show the measurements of the support's outer and inner diameters using a Vernier calliper. The figures on a, b, c corresponds to membrane A, membrane B and membrane C shown in figure 112.

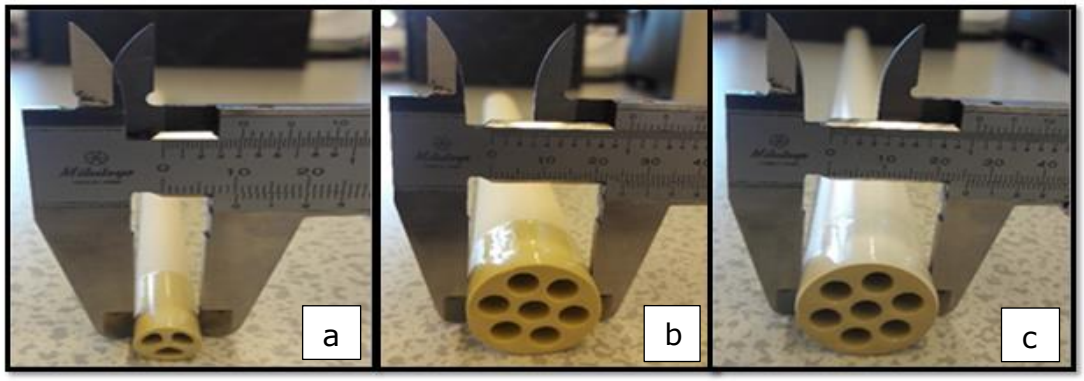

Figure 110: Measurement of the outer diameter of the 3 different supports

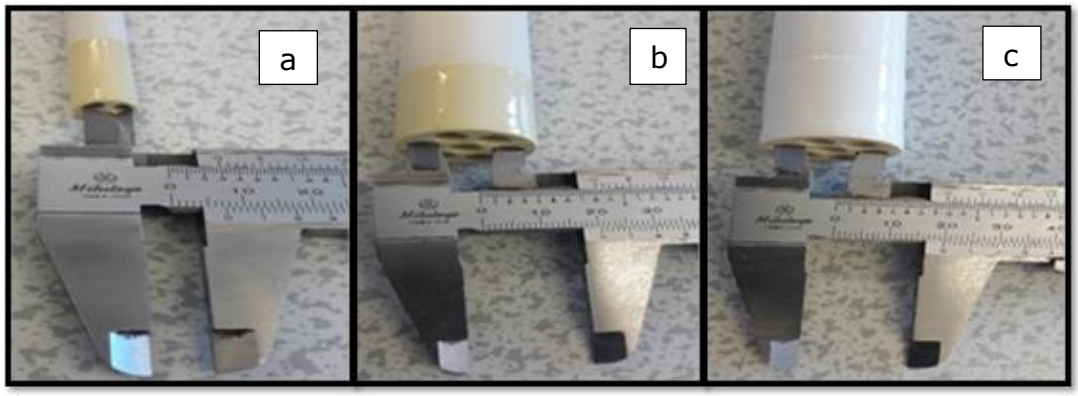

Figure 111: Measurement of the inner diameter of the 3 different supports

Figure 32 shows the pictorial representation of the 3 supports showing their variation in length and width.

Figure 112 Pictures of the 3 different supports used showing their variation in length and width

II.2 Chemicals

The following chemicals were used for the catalytic deposition stages in the membrane preparatory section.

i. Palladium II chloride ($PdCl_2$) 99.999% was supplied by Sigma Aldrich in glass containers, CAS No: 7647-10-1. They were used during the palladium seeding and plating phases.

ii. Platinum on alumina (Pt/Al_2O_3) extent of labelling: 1 wt. % loading, 3.2 mm, pellets supplied by Sigma Aldrich in glass container, CAS No: 232114. This was used in the fixed bed water deoxygenating experiment.

iii. Chloroplatinic acid solution 8wt. % in water (H_2PtCl_6) was supplied by Sigma Aldrich in glass containers, CAS No: 16941-12-1. This was used for the platinum metal deposition.

iv. Tin II chloride ($SnCl_2$) ≥99.99% was supplied by Sigma Aldrich in plastic container, CAS No: 7772-99-8. This chemical was used during the sensitization phase of the initial palladium deposition process.

v. Ethylenediaminetetraacetate acid disodium salt dihydrate (Na_2EDTA) 99.0-100.0% was supplied by Sigma Aldrich in plastic container, CAS No: 6381-92-6. This was used as a stabilizing reagent in the palladium plating solution.

vi. Ammonium hydroxide 28-30wt% solution in water (NH_4OH) was supplied by Fisher scientific in glass bottles. CAS No 1336-21-6. It made up part of the palladium plating solution.

vii. Hydrazine hydrate 50-60% in water ($NH_2NH_2.xH_2O$) was supplied by Sigma Aldrich in glass bottles, CAS No: 10217-52-4. It is the reducing agent during palladium plating.

II.3 Gases

All the gases listed below were used in this study and were supplied by BOC, Aberdeen, United Kingdom. Individual regulators and hoses were also purchased form BOC to go with items i-iv. Item v is in a liquid form and appropriate containers (Dewar) were used in fetching it. The gases needed no additional purification as they were supplied in the required state.

i. Hydrogen: 99.9% purity, used for activation of catalysts on membranes and permeation test.

ii. Helium: 99.9% purity, used for leak testing of the reactor and permeation test.

iii. Nitrogen: 99.9% purity, used for leak testing of the reactor and permeation test.

iv. Oxygen: 99.9% purity, used for permeation test.

v. Liquid Nitrogen: 99.9% purity, used in the Quantachrome analyser for membrane characterization analysis.

APPENDIX III: Health and Safety

The following discusses the risk and safety procedures carried out in the whole experimental process while handling gases, membrane reactors and chemicals. The use of Personal Protective Equipment (PPE) such as Rigger Gloves, safety glasses, safety footwear and lab coats were observed at all times.

III.1 Gases

These gases could be classified as flammable and non-flammable. Table 14 summarises the hazard, risk and safety of using these gases.

Table 14: List of gases with their risk and safely measures

	Gases	Hazards	Risk	Safety
i	Hydrogen	Extremely Flammable Burns with an invisible flame	Asphyxiation if inhaled in large concentration.	The cylinder kept away from ignition sources Fire extinguishers located at both ends of the corridor outside the lab. Use of Hydrogen Detector when in use Leak testing is mandatory Lab area is well ventilated
ii iii iv	Helium Nitrogen Oxygen	Non-flammable	Asphyxiation if inhaled in large concentration.	Leak testing is mandatory Lab area is well ventilated
v	Liquid nitrogen	Non-flammable	Risk of burns Asphyxiation if inhaled in large concentration	Visual check of Dewar Lab area is well ventilated

Others hazards includes trips and slips that could happen when manual moving and handling of the gas cylinders from the gas cage to the lab and back. The use of appropriate trolleys in transporting the gas cylinders is always practised.

The use and handling of gas and liquid nitrogen certification was achieved before handling any of these gases. There was also a biannual training during the course of my research. I (Ifeyinwa Orakwe) had to be gas safe trained/certified as well as being up to date with my training at each point in time.

III.2 Membrane Reactors

The risk involved with using the membrane reactors is that they are sometimes heated to very high temperatures of 350^0C. This could cause severe burns. The safety measures carried out here is the wrapping of the reactors with fibre materials or thermal jackets. This helps in preventing accidental contact. Skin irritation can also be experienced from the heating and conducting material used in wrapping around the reactors. Appropriate personal, protective equipment (PPE) are worn at all times when removing membranes from the reactors. In addition, as a result of several heating and cooling taking place on the membrane reactors, there could be expansion of the stainless steel materials making it difficult to unscrew. Care must be taken in such an instance and the use of bench mounted vice to hold the reactors was recommended.

The risk of gas leak from the reactor occurring during experiments being that the reactor can be pressurised up to 2 bar. All connections are leak tested with snoop solutions at all times. These snoop solutions are the most appropriate solutions that should be used and not soapy water.

The risk of membrane reactor falling off its holder, manual handling of ceramic membranes and membrane reactors can also be an issue. The safety employed is that membrane reactors are fixed on appropriate support frames and assistance is always there when moving the reactors as the case may be.

III.3 Chemical:

Table 15 summarizes the chemicals with their hazards, risk and safety measures.

Table 15: show the chemicals and their health and safety measures

	Name of chemical	Risk	Safety
i	Palladium II chloride ($PdCl_2$)	Toxic if swallowed, may cause skin allergic reaction	Rinse mouth with plenty water. Take off contaminated clothing and shoes immediately. Rinse thoroughly with plenty of water
ii	Platinum on alumina	The substance contains no component considered to be toxic. In summary, none	None
iii	Chloroplatinic acid solution 8wt.% in water (H_2PtCl_6)	Harmful if swallowed, causes severe skin burns and eye damage, may cause skin allergic reaction, harmful if inhaled	Rinse mouth with plenty water. Take off contaminated clothing and shoes immediately. Wash off with soap and plenty water. Move person into fresh air
iv	Tin II chloride ($SnCl_2$)	Severe skin burns and eye damage, allergic skin reaction, harmful if inhaled, toxic if swallowed, toxic to aquatic life	Take off contaminated clothing and shoes immediately. Wash off with soap and plenty water. Rinse mouth with plenty water. Move person into fresh air. Disposal through licensed disposal company.
v	Ethylenediaminetet-raacetate acid disodium salt dihydrate (Na_2EDTA)	Harmful if inhaled	Move person into fresh air.
vi	Ammonium hydroxide 28-30wt% solution in water (NH_4OH)	May cause respiratory irritation, very toxic to aquatic life, causes severe skins and eye damage	Move person into fresh air. Take off contaminated clothing and shoes immediately. Wash off with soap and plenty water Disposal through licensed disposal company.
vii	Hydrazine hydrate 50-60% in water ($NH_2NH_2.xH_2O$)	Toxic if swallowed, severe skin burns and eye damage, skin allergic reaction, carcinogenic, toxic to aquatic life	Rinse mouth with water. Take off contaminated clothing and shoes immediately. Wash off with soap and plenty water Disposal through licensed disposal company.

APPENDIX IV: Calculation

Calculation of Area of membranes

Area of membrane was calculated from equation 61

$$A = 2\pi l_o \left[\frac{r_2 - r_1}{\ln\left[\frac{r_2}{r_1}\right]}\right] \quad (61)$$

Where:

A= Area, l_o= permeable length, r_1= outer radius, r_2 = inner radius, r=$\frac{d}{2}$

Calculation of %wt of platinum metal on catalyst pellet

Each catalyst pellet weighs = 0.05g weight = 1 % wt. of Pt = 0.01g of Platinum metal

For 0.8g of pellets = $\frac{0.8g\ weight\ X\ 0.01\ g\ Pt}{0.05g\ weight}$ = 0.16g Pt = 16% wt. Pt

For 3.0 g of pellets = $\frac{3.0g\ weight\ X\ 0.01g\ Pt}{0.05g\ weight}$ = 0.6g Pt = 60% wt. Pt

APPENDIX V: Results for Fixed-bed Deoxygenating Processes

Table 16: results showing effects of catalyst loading and hydrogen pressure in the removal of DO in the fixed-bed reactor

Runs	Hydrogen pressure	Outlet DO, ppm 0.8g catalyst	Outlet DO, ppm 3.0g catalyst
1	0.12	8.09	8.27
2	0.2	8.15	8.61
3	0.29	8.32	8.23
4	0.4	8.36	7.86
5	0.52	8.27	6.72
6	0.7	7.74	5.62

Table 17: Results for water deoxygenation using 3.0g of catalyst pellet in the fixed-bed reactor

Initial DO: 9.7mg/L, 0.8 bar H_2		
Flowrate mL/min	3.0g [DO]	%Xo
143	4.94	49.07
200	6.27	35.36
250	6.53	32.68
411	7.9	18.56

APPENDIX VI: Results for Catalytic Membrane Deoxygenating Process

Table 18: Results showing the effects of membrane pore size on outlet DO concentration using platinum deposited membranes

FLOWRATE(mL/min)	Membrane APd	Membrane BPd
200	2.14	0.33
400	2.52	0.88
600	2.97	1.30
800	3.14	1.53
1000	3.84	1.90

Table 19: Results showing the effects of membrane pore size on outlet DO concentration using platinum deposited membranes

Initial DO: 9.7mg/L			
FLOWRATE(mL/min)	Membrane A Pt	Membrane B Pt	Membrane C Pt
200	2.32	0.62	1.07
400	3.17	1.11	1.69
600	3.69	1.97	1.70
800	4.88	2.66	1.71
1000	6.04	3.28	1.59

Table 20: Table showing the DO removal efficiency against water flow rate for the different catalytic deposited membranes. H_2 flow rate was 1.55 L/min. Membrane areas: Memb A= 0.0008m^2, Memb B=0.023m^2, Memb C=0.045m^2

Water flow rate (mL/min)	Memb A Pd	Memb A Pt	Memb B Pd	Memb B Pt	Memb C Pt
200	75	76	97	94	89
400	72	67	91	89	83
600	70	62	86	80	83
800	68	49	85	72	82
1000	60	37	80	66	84

Table 21: Results showing the effect of time on the removal of DO concentration in Pd coated 6000nm membrane

Time, min	Dissolved oxygen concentration, ppm
0	9.195
2	7.96
4	7.2
6	6.565
8	5.3
10	4.965
12	4.16
14	3.675
16	3.265
18	2.815
20	2.505
22	2.08
24	1.1
26	0.655
28	0.335
30	0.31

Table 22: Extrapolated values for the effect of H_2 gas flow rate and H_2 pressure on water deoxygenation in catalytic membranes

H_2 flowrate (L/min)	Dissolved oxygen percentage removal rate
0.19	67.1
0.65	70.5
1.28	73.2
1.55	78.5
2.60	85
3.27	90
3.93	95
4.60	100

APPENDIX VII: Results used for rate of reaction

Table 23: Showing the values drawn for rate of reaction for oxygen in the fixed-bed reactor

	Initial DO: 9.70ppm						
F_{Ai} (mol/s)	W(g)	W/F_{Ai}	X	$X/(W/F_{Ai})$	$\ln[X/W/F_{Ai}]$	$\ln[O_2]$	$[O_2]$
4.17E-05	3	7.20E+04	6.16E-01	8.56243E-06	-11.67	1.31	3.72
1.06E-04	3	2.82E+04	4.91E-01	1.74041E-05	-10.96	1.60	4.94
1.46E-04	3	2.06E+04	3.54E-01	1.71893E-05	-10.97	1.84	6.27
1.86E-04	3	1.61E+04	3.27E-01	2.02632E-05	-10.81	1.88	6.53
3.06E-04	3	9.81E+03	1.86E-01	1.89157E-05	-10.88	2.07	7.9

Table 24: Showing the values drawn for rate of reaction for oxygen in for CMR

Initial DO: 9.66mg/L							
F_{Ai} (mol/s)	W (g)	W/F_{Ai}	X	$X/(W/F_{Ai})$	$\ln[X/W/F_{Ai}]$	$\ln[O_2]$	$[O_2]$
1.49E-04	2.7	1.81E+04	9.68E-01	5.33E-05	-9.84E+00	-1.17E+00	0.31
2.98E-04	2.7	9.07E+03	9.13E-01	1.01E-04	-9.20E+00	-1.74E-01	0.84
4.46E-04	2.7	6.05E+03	8.64E-01	1.43E-04	-8.85E+00	2.70E-01	1.31
5.95E-04	2.7	4.54E+03	8.53E-01	1.88E-04	-8.58E+00	3.51E-01	1.42
7.44E-04	2.7	3.63E+03	8.02E-01	2.21E-04	-8.42E+00	6.47E-01	1.91

Table 25: Results drawn from the dependency of hydrogen pressure on the rate of reaction of oxygen in the fixed-bed reactor

	Initial DO: 9.70ppm	Weight of catalyst: 3g				
H_2, atm	Outlet DO, ppm	Xo	F_{Ai}	$X/W/F_{Ai}$	$\ln (X/W/F_{Ai})$	$\ln H_2$
1.11	8.27	0.147423	3.19E-04	1.57E-05	-11.064	0.103278349
1.19	8.61	0.112371	3.02E-04	1.13E-05	-11.391	0.172271221
1.28	8.23	0.151546	3.19E-04	1.61E-05	-11.036	0.244591883
1.39	7.86	0.189691	2.98E-04	1.88E-05	-10.881	0.326421901
1.49	6.72	0.307216	3.10E-04	3.17E-05	-10.358	0.395414772
1.68	5.62	0.420619	3.23E-04	4.54E-05	-10.001	0.520577915

APPENDIX VIII: Other Conferences

During the course of my research, I was a research assistant on a project founded by CCEMC (Climate Change and Emissions Management Corporation) now known as ERA (Emissions Reduction Alberta). The research was on dry reforming of methane using catalytic membrane reactor and was carried out at centre for process intergration of membrane technology, RGU. During this period, I attended a number of conferences on a project.

2018

Orakwe, I, Shehu, H and Gobina, E. "Preparation and characterization of palladium ceramic membrane for hydrogen production". *9th International conference on hydrogen production*. Zagreb, Croatia July 16-19th 2018. Full paper has been submited for publication review in journal of hydrogen energy.

Orakwe, I., Shehu, H., Okon, E. and Gobina, E "Fabrication and characterization of Rhodium impregnated ceramic alumina membrane for dry reforming of methane". *9th International conference on hydrogen production.* Zagreb, Croatia July 16-19th 2018. Full paper has been submited for publication review in journal of hydrogen energy.

2017

Ifeyinwa Orakwe, Edward Gobina, Edidiong Okon and Habiba Shehu "Integrated catalytic membrane reactor process for CO_2 reforming of methane". 7th World Congress on Petrochemistry and Chemical engineering, November 13-14, 2017, Atlanta, Georgia, USA

Orakwe I, Gobina E, Shehu H and Okon E. "Study of the preparation and characterization of Rh catalyst on an alumina ceramic membrane for CO_2 reduction from flue gas". International Conference & Exhibition on Advanced & Nano Materials 2017 Proceeding August 7-9, 2017, Toronto, Canada. Pp 133-139. *http://iaemm.com.*